Universidade do Minho
Escola de Ciências da Saúde

Caroline Jeya Sheeba Daniel Sunder Singh

Molecular parallelisms between vertebrate limb development and somitogenesis
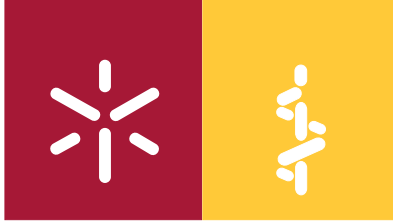
Universidade do Minho
Escola de Ciências da Saúde

Caroline Jeya Sheeba Daniel Sunder Singh

Molecular parallelisms between vertebrate limb development and somitogenesis

Tese de Doutoramento em Ciências da Saúde

Trabalho efectuado sobre a orientação da
Doutora Isabel Palmeirim
Professora Auxiliar, Departamento de Ciências Biomédicas
e Medicina, Centro de Biomedicina Molecular e Estrutural,
Universidade do Algarve, Faro, Portugal
e do
Doutor Jorge Manuel Nunes Correia Pinto
Professor Catedrático Convidado, Escola de Ciências da Saúde
Universidade do Minho
Braga, Portugal

Novembro de 2011

DECLARAÇÃO

Nome: Caroline Jeya Sheeba Daniel Sunder Singh

Endereço electrónico: sheeba@ecsaude.uminho.pt

Telefone: +351960061683

Número do Bilhete de Identidade: J6679656

Título dissertação:

Molecular parallelisms between vertebrate limb development and somitogenesis

Orientadores:

Professora Doutora Isabel Palmeirim

Professor Doutor Jorge Manuel Nunes Correia Pinto

Ano de conclusão: 2011

Designação do Ramo de Conhecimento do Doutoramento:

Ciências da Saúde

Universidade do Minho, ___/___/_____

Assinatura: _____

ACKNOWLEDGEMENTS

I want to express my gratitude and deepest respect for all those who helped me during this wonderful phase of my life.

My first thanks are dedicated to Isabel, my beloved supervisor, for giving me the opportunity to pursue my PhD studies in her laboratory, for training me, giving me independence and freedom to develop my own ideas. Thanks for putting me back on track when I was getting lost and for your support during all these years. I must acknowledge that I learnt almost everything from your lab and what I am now is because of you. Isabel, I would also like to thank you for being a fantastic person packed with energy, enthusiasm and compassion. Thanks a lot.

I am grateful to Jorge, my co-supervisor for being kind and supportive throughout the course of my work. Your co-supervision gave me a feeling of strength. Thanks for all your timely help that provided me confidence and strength to accomplish this work at the ICVS.

Raquel, I owe you special thanks for your all time support right from the beginning I join the group. Your support and wonderful talks molded me into an independent researcher skilled in many molecular biology techniques. I learnt many vital tools that made me efficient to do my work in an effective manner. Whenever, I approached, you helped me cheerfully. Thanks for your time and participation in this project and providing wonderful insights which made my research reach new heights.

I would like to express my sincere gratitude to Professor Cecília Leão, President of the ICVS, University of Minho, for allowing me to perform this research in this esteemed institute. I would like to acknowledge her constant commitment and hard work to make ICVS an excellent institute. Professor, I thank you for your kind gesture, willingness to help and concern whenever I met you. I would also like to express my gratefulness to Prof. Jorge Manuel Rolo Pedrosa, Director of the ICVS, University of Minho, for accepting me as a PhD student. I truly appreciate this wonderful opportunity.

SUMMARY/ SUMÁRIO

SUMMARY

Limbs emerge from the embryo flank as a mass of mesenchymal cells within an ectodermal jacket that will give rise to skeletal elements and connective tissues, structured along the dorsal-ventral (DV), anterior-posterior (AP) and proximal-distal (PD) axes. The apical ectodermal ridge (AER) and the zone of polarizing activity (ZPA) are limb signalling centres that drive the establishment of PD and AP axis, respectively (Zeller et al., 2009). Development of all embryo structures requires precise orchestration of cell proliferation and differentiation in both space and time. However, how cells measure time was puzzling until the first evidence for a time counting mechanism was provided by Palmeirim et al. (1997) in chick presomitic mesoderm (PSM). In a decade, the existence of a limb molecular clock by unveiling cyclic *hairy2* gene expression in limb chondrogenic precursor cells was demonstrated (Pascoal et al., 2007). The discovery of the limb clock raises the exciting possibility that parallelisms could be established between somitogenesis and limb development. This PhD work has been designed to establish parallelisms between limb and trunk development. In order to do this analysis, first, we have established the existing parallelisms from the available literature and further extended the list by focusing on limb *hairy2* oscillation´s biological significance.

So as to comprehend the biological significance of *hairy2* oscillations, two main approaches have been taken. One is to understand its regulatory pathways; the second is to analyse the functional relevance of *hairy2* cycles and to assess the existence of a wavefront in limb. In the light of the first part, we have found the involvement of the two major limb signaling centers and their signaling molecules, the AER/FGFs and the ZPA/SHH in *hairy2* regulation. This regulatory network was identified based on in-ovo ablation and bead implantation experiments to overexpress or downregulate signalling molecules in both the *hairy2* positive (Posterior positive domain: PPD and Distal Cyclic Domain: DCD) and negative (Anterior and Posterior Negative Domains: AND and PND) limb domains. Analysis on the intracellular pathways by immunoblot revealed that FGF mediated Erk and Akt phosphorylation and SHH mediated modulation of Gli3 activity levels is responsible for this effect. We have further established the difference in the mechanisms employed by the AER/FGFs and ZPA/SHH to regulate distal limb mesenchymal *hairy2* expression. The AER-FGFs provide a short-term, short-range instructive signal while, the ZPA-SHH deliver a long-term, long-range permissive signal for limb *hairy2*

expression. The AER/FGFs were only able to execute their inductive role on *hairy2* expression when the tissue is in a ZPA/SHH-created permissive state defined as Gli3-A/Gli3-R≥1. In accordance with the ZPA/SHH reliant posteriot-anterior Gli3-A/Gli3-R ratio gradient, *hairy2* is persistently expression in the PPD and absent from the AND. However, in the absence of the inductive AER/FGF signal, SHH cannot induce *hairy2* expression suggesting a mutual dependency existing between AER/FGF and ZPA/SHH for limb *hairy2* expression regulation. Importantly, we demonstrate that this joint requirement is not a signaling relay but a convergence of both signals at the level of *hairy2* expression making *hairy2* a readout of AER/FGF and ZPA/SHH signals at both time and space.

Additional analysis on the participation of RA and BMP4 signals in limb *hairy2* expression suggests RA as a positive regulator and BMP4 as a negative regulator of its expression. Interestingly, the inductive effect of RA-bead is also found to be via Gli3 activity modulation.

Finally, we have proposed a model defining the combinations of signals laying down the distinct expression domains of *hairy2* in the limb distal mesenchyme. The PPD is defined by high AER/FGF and ZPA/SHH signal mediated Gli3-A/Gli3-R≥1 (higher than 1); the DCD with high AER/FGF and moderate ZPA/SHH derived Gli3-A/Gli3-R≥1 (tending towards 1) and the AND possesses no SHH signal and so Gli3-A/Gli3-R<1 (less than 1) and high BMP4 activity.

The functional relevance of cyclic gene expression in limb development/patterning will be assessed by perturbing *hairy2* oscillations in limb mesenchymal cells by infecting them with retrovirus carrying either *hairy2* gene or *hairy2* specific siRNAs. At present we are performing this task and the results are promising. Since *hairy2* expression is tightly regulated by the PD patterning AER/FGFs and the AP pattering ZPA/SHH signals, we expect to obtain limb elements displaying both PD and AP defects upon Hairy2 misexpression. Supporting our analysis of molecular parallelisms among somitogenesis and limb development, the existence of a limb wavefront (Differentiation Front: DF) reminiscent to the PSM Determination Front (DetF) has also been evaluated. Experiments aiming to shift the limits of FGF or RA signaling along the PD limb axis is affecting the limb skeletal element size, reinforcing the similarity with somitogenesis. However, the results are not yet conclusive.

The parallelisms identified from our work and the ones established from the literature point to enormous resemblance among limb and trunk development at the level of gene

expression and their function. This brings great insight on the molecular mechanisms operating in both systems and enriches our understanding of how a pool of undifferentiated cells acquires spatial/temporal information to form a defined structure.

SUMÁRIO

Os membros dos embriões vertebrados começam a formar-se à medida que uma massa de células mesenquimais rodeada de tecido epitelial cria uma protuberância nos flancos do embrião, mais tarde originando os elementos ósseos, músculos e tecido conjuntivo, estruturados ao longos dos eixos dorsal-ventral (DV), anterior-posterior (AP) e proximal-distal (PD). A *apical ectodermal ridge* (AER) e a *zone of polarizing activity* (ZPA) são centros sinalizadores que orquestram o estabelecimento dos eixos PD e AP do membro embrionário, respectivamente (Zeller et al., 2009). O desenvolvimento de todas as estruturas embrionárias requer uma coordenação espacial e temporal precisa de proliferação e diferenciação celulares. No entanto, não se sabia como medem a células o tempo até se obter a primeira evidência da existência de um relógio molecular embrionário, providenciada por Palmeirim *et al.* (1997). Uma década depois foi demonstrada a existência de um um relógio molecular no membro através daidentificação da expressão cíclica do gene *hairy2* nas células precursoras de condrócitos (Pascoal et al., 2007). A descoberta de um relógio no membro sugere a forte possibilidade de ser possível estabelecer paralelismos moleculares entre o processo de somitogénese e o desenvolvimento do membro. Esta tese de doutoramento foi projectado de modo a estabelecer os paralelismos entre o desenvolvimento do membro e do tronco. Para tal, começamos por estabelecer os paralelismos já existentes na literatura e aumentámos esta lista concentrando a atenção no significado biológico das oscilações de *hairy2* no membro.

Com o objectivo de melhor compreender o significado biológico das oscilações de *hairy2* no membro em desenvolvimento, aplicámos duas abordagens distintas. Primeiramente, procurámos identificar as vias de sinalização envolvidas na regulação da sua expressão. Posteriormente analisámos a relevância funcional do relógio no desenvolvimento do membro. Relativamente ao primeiro objectivo, descrevemos o envolvimento dos centros sinalizadores do membro e as suas moléculas de sinalização, o AER/FGF e o ZPA/SHH, na regulação da expressão de *hairy2*, utilizando experiências de ablação e/ou de implantação de micro-esferas *in ovo* com o objectivo de sobre- ou sub-expressar estas as moléculas sinalizadoras nos domínios *hairy2* positivo (Posterior positive domain: PPD e Distal Cyclic Domain: DCD) e *hairy2* negativo (Anterior and Posterior Negative Domains: AND e PND) do membro. Análise das vias intracelulares por *immunoblot* mostraram que a fosforilação mediada por Erk e Akt e a modulação dos níveis de

actividade de Gli3 por SHH são responsáveis por este efeito. Também descobrimos que os AER/FGFs e o ZPA/SHH utilizam diferentes mecanismos para regular a expressão de *hairy2* no membro distal Os resultados obtidos indicam que os AER-FGFs são sinais reguladores da expressão de *hairy2* com curto alcance e de curta duração, enquanto o ZPA-SHH é um morfogene com uma acção permissiva de longo alcance e duração sobre *hairy2* no membro.

A AER/FGFs foram apenas capazes de executar a sua função indutiva quando os tecidos estavam num estado permissivo criado pela ZPA/SHH, definido como Gli3-A/Gli3-R≥1. Em sintonia com o gradiente AP do ratio Gli3-A/Gli3-R≥1, *hairy2* apresenta expressão na PPD e não na AND. No entanto, na ausência de sinal indutivo da ERA/FGF, SHH não é capaz de induzir expressão de *hairy2*, o que sugere uma dependência mútua entre o AER/FGF e o ZPA/SHH na regulação da expressão de *hairy2* no membro. De forma importante demonstramos que este necessidade conjunta não é uma passagem de sinal, mas uma convergência de ambos os sinais ao nível da expressão de *hairy2*, o que torna esta expressão uma leitura dos sinais do AER/FGF e do ZPA/SHH no tempo e no espaço.

Uma análise adicional da contribuição dos sinais RA e BMP4 para a expressão de *hairy2* sugere que o RA seja um regulador positivo e que o BMP4 seja um regulador negativo. É também de notar de forma interessante que o efeito de uma micro-esfera de RA também pode obter através da modulação da actividade de Gli3. Finalmente, propomos um modelo que define a combinação dos sinais que ditam a expressão de domínios distintos de *hairy2* no mesênquima distal do membro. A PPD é definida por altos níveis de Gli3-A/Gli3-R≥1 (maiores que 1) mediados por sinalização da AER/FGF e ZPA/SHH; A DCD por altos níveis de FGF e níveis moderados de Gli3-A/Gli3-R≥1 (tendendo para 1) derivado de ZPA/SHH e a AND por não possuir sinalização SHH e, portanto, Gli3-A/Gli3-R<1 (menor que 1), para além de alta actividade de BMP4.

No sentido de estabelecer a relevância funcional da expressão cíclica de *hairy2* no crescimento e padronização do membro em desenvolvimento, propomo-nos a perturbar a expressão de *hairy2* nas células distais do mesênquima do membro, recorrendo a infecção por retrovírus, expressando o gene *hairy2* ou siRNAs específicos para o gene De momento estamos a realizar esta tarefa e os resultados são promissores. Sabendo que a expressão de *hairy2* é fortemente regulada pelos sinais padronizantes da AER/FGF e da ZPA/SHH, esperamos obter elementos do membro com defeitos nos eixos PD e AP após desregulação da expressão de

Hairy2. De modo a apoiar a nossa tese da existência de paralelismos entre a somitogénese e o desenvolvimento do membro, avaliámos ainda a existência de uma frente de diferenciação no membro (DF) reminescente da frente de determinação na PSM (DetF). Verificamos também se a alteração dos limites de sinalização de FGFs ou RA ao longo do eixo PD tem efeito sobre o tamanho dos elementos ósseos do membro, reforçando as semelhanças com a somitogénese. No entanto estes resultados não foram até agora conclusivos.

Tanto os paralelismos identificados no nosso trabalho, como os recolhidos a partir da literatura apontam para uma grande semelhança entre o desenvolvimento membro e do tronco ao nível funcional e de expressão génica. Todo o trabalho desenvolvido tem como objectivo global a aplicação dos conhecimentos adquiridos no processo da somitogénese para uma melhor compreensão de como as células indiferenciadas do membro em desenvolvimento adquirem informação espacial/temporal e se diferenciam de forma coordenada ao longo do tempo, formando um membro correctamente segmentado e inteiramente funcional.

CONTENTS

CONTENTS

ABBREVIATIONS LIST

ABBREVIATIONS LIST

AER	Apical Ectodermal Ridge
Akt	Protein kinase B
AND	Anterior Negative Domain
AP	Anterior-Posterior
AP2	Transcription Factor Gene AP-2
BMP	Bone Morphogenetic Protein
BmpR1	Bone morphogenetic protein Receptor, type I
Cyp26b1	Cytochrome P450 26b1
DCD	Distal Cyclic Domain
DetF	Determination Front
DF	Differentiation Front
Dll1	Delta-like 1
DMSO	Dimethyl Sulfoxide
Dusp6	Dual specificity phosphatase 6
DV	Dorsal-Ventral
E11.5	Embryonic day 11.5
ECM	Extracellular Matrix
EN-1	Homeobox protein Engrailed-1
Erk	Extracellular-signal-regulated kinase
ESC	Embryonic Stem Cells
FGF	Fibroblast Growth Factor
FgfR	Fibroblast growth factor Receptor
Gli-A	Glioma Activator
Gli-R	Glioma Repressor
GREM1	Gremlin1
HAND2	Heart And Neural crest Derivatives expressed 2
HES	Hairy/Enhancer-of-Split
HH24	Hamburger-Hamilton 24
Hox	Homeobox protein
IM	Intermediate Mesoderm
KO	Knockout
LEF1	Lymphoid Enhancer-binding Factor-1
Lfng	Lunatic fringe
Lmx1b	LIM homeobox transcription factor 1-beta
LPM	Lateral Plate Mesoderm
MAPK	Mitogen Activated Protein Kinase
Meis	Myeloid ecotropic viral integration site
Mesp2	Mesoderm posterior protein 2
Msx1	Msh homeobox 1
NICD	Notch-Intracellular Domain
No	Notochord
ozd	chick oligozeugodactyly mutant that lacks SHH function in the limb
PD	Proximal-Distal
PI3K	Phosphatidylinositol-3-kinase

Pitx1	Pituitary homeobox 1
PND	Posterior Negative Domain
PPD	Posterior Positive Domain
Prx1	Paired-related homeobox gene 1
PS	Primitive Streak
PSM	Presomitic Mesoderm
PTC	Patched
PZ	Progress Zone
RA	Retinoic Acid
Raldh2	Retinaldehyde dehydrogenase 2
RAR	Retinoic Acid Receptor
RARE	Retinoic Acid Response Element
RBP-jk	Recombination signal Binding Protein for immunoglobulin kappa J
RCAS	Replication-Competent ASLV long terminal repeat (LTR) with a Splice acceptor
Rfng	Radical fringe
SE	Surrounding Ectoderm
Shh	Sonic Hedgehog
siRNA	Small *i*nterfering RNA
SMO	Smoothened
Tbx	T-box transcription factor
TCF1	HMG-box Transcription Factor-1
UZ	Undifferentiated Zone
vt	*wnt3a* hypomorphic mutant Vestigial Tail
WNT	Wingless-wint
ZPA	Zone of Polarizing Activity

CHAPTER I:

GENERAL INTRODUCTION

1. GENERAL INTRODUCTION

1.1. AN OVERVIEW ON VERTEBRATE LIMB PATTERNING

Vertebrate appendages have undergone tremendous diversification, ranging from fin folds or pectoral and pelvic fins to wings, hands and legs. However, the fundamental arrangement and pattern of the developing tetrapod limb has been preserved in phylogeny (Shubin et al., 1997). Tetrapods have a pair of both fore and hind limbs, which emerge at defined somite positions perpendicular to the primary body axis (Figure 1.1). At presumptive limb levels, lateral plate mesoderm (LPM) cells proliferate under the epidermal tissue, initiating the formation of growing buds. Later on, this mesenchyme will give rise to skeletogenic precursors, while muscle precursor cells invade the limb upon delamination from the lateral edges of the nearby somites (Figure 1.1) (Niswander, 2003). Three orthogonal axes describe the anatomy of the limb: anterior-posterior (AP), from the thumb to little finger; dorsal-ventral (DV), from the back of the hand (knuckle) to the palm and the proximal-distal (PD), from the shoulder to the fingertips.

A crucial step during the initiation of vertebrate limb development is the formation and establishment of morphogenetic signaling centers that co-ordinately control cell specification and proliferation along these three axes. Patterning of each limb axis is controlled by key signaling centres within the limb bud (Figure 1.1). Morphologically, the limb skeleton develops with three distinct sets of bones possessing a characteristic size and shape that are laid down along the PD axis of the growing limb bud. The apical ectodermal ridge (AER), which is formed by the thickening of ectoderm at the distal tip of the limb bud is responsible for the PD patterning of the limb and this axis is characterised by the most proximal stylopod (humerus and femur), the middle zeugopod (radius/ulna and tibia/fibula) and the distal autopod (metacarpals and phalanges) limb bone elements (Figure 1.1). The activities of the AER are mediated by Fibroblast Growth Factor (FGF) family of secreted proteins (Martin, 1998; Towers and Tickle, 2009) reviewed in Towers and Tickle, 2009, Martin, 1998). The zone of polarising activity (ZPA) which is located at the posterior domain of the limb bud regulates the AP axis development. Although the number of digits differs between chick and mouse, the molecular mechanism involved in their determination is almost similar (Towers and Tickle, 2009). Digit formation is instructed by ZPA secreted Sonic Hedgehog (SHH), which belongs to the Hedgehog (HH) family of signaling proteins

(Tickle, 2003). The DV axis is specified by the expression of *wnt7a* and the transcription factor *Lmx1b*, which are respectively expressed in the dorsal limb ectoderm and in the dorsal mesenchyme (Chen and Johnson, 1999; Arques et al., 2007). Expression of *wnt7a* in the ventral ectoderm is repressed by Engrailed1, a target of BMP signaling (Loomis et al., 1996).

Additionally, cell proliferation, cell movement, cell death as well as assignment and interpretation of positional information must be coordinated along all the three axes for proper limb bud development.
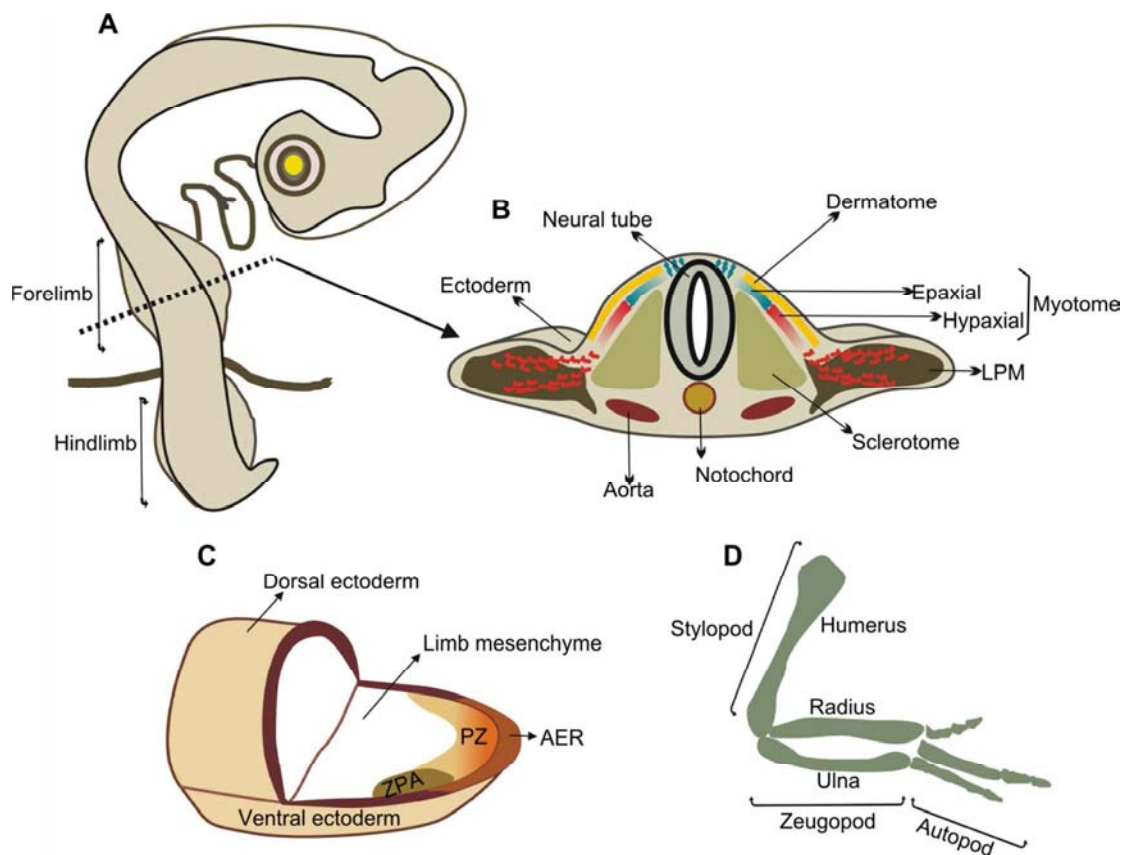
Figure 1.1: An over view of chick limb development. (A) Schematic representation of stage HH18 chicken embryo representing the forelimb and hindlimb positions in the AP body axis. **(B)** Transverse section of the embryo trunk at the forelimb level. As a result of rapid proliferation of the LPM cells under the surrounding ectoderm, the limb bud begins to be visible from stage HH17 onwards. These mesenchymal cells contain the skeletal precursors while the limb muscles are derived from the nearby differentiated somitic compartments. Somites differentiate into the ventro-medial sclerotome and the dorso-lateral dermomyotome which will further subdivide into dermotome and myotome. The precursor cells from the epaxial myotome migrate to form the back musculature (blue dots) and the precursors from the hypaxial region migrate to the newly formed limb buds (red dots). These cells take two paths to occupy the dorsal and ventral compartments, which will eventually become the extensor and flexor muscle groups of

the limb. This movement is facilitated by the surrounding structures such as the neural tube, notochord, aorta, and overlying ectoderm (reviewed in (Hawke and Garry, 2001; Niswander, 2003). **(C)** Stage HH23 limb illustrating the key limb signaling centers governing its patterning and growth along the three limb axes. The AER will direct the PD patterning through its morphogen FGFs. The distal limb mesenchymal cells directly under the influence of the AER-FGFs are maintained in a proliferative undifferentiated state and this region is called the Progress Zone (PZ). The ZPA derived SHH patterns the AP axis and the non-ridge ectoderm is responsible for DV patterning. **(D)** Schematic representation of chick limb skeleton from a 7 days incubated embryo. All the three limb segments: the stylopod, zeugopod and the autopod are represented.

1.1.1. LIMB BUD INITIATION

Limb bud begins as a mass of mesenchymal cells encompassed within the ectoderm as the LPM at specific AP axis of the embryo (forelimb between somite position 15-20 in chick and 8-12 in mouse) starts to undergo rapid proliferation compared to the rest of the LPM (Searls and Janners, 1971). These mesenchymal cells along with the ectoderm are believed to possess the cues to form a complete limb, as grafting of these cells in another location can induce ectopic limb development. Hox genes, particularly the HoxC cluster has been implicated in providing positional information to the limb forming flank, in such a way that the 3´ *HoxC* genes are expressed in the forelimb forming LPM and 5´ *HoxC* genes in the hindlimb LPM domain (Christ et al., 1998; Duboc and Logan, 2011). However, this is not conclusive, since deletion of the entire *HoxC* cluster did not alter limb position in mouse (Suemori and Noguchi, 2000).

1.1.1.1. *FGFs and WNTs in limb initiation*

FGFs in limb initiation

Numerous molecules have been proposed to be required for limb initiation program (Martin, 1998). A potential cross talk between the FGF, WNT, RA and SHH signaling has pronounced effect on this process. These signaling pathways must be sensed by appropriate tissues to get the trigger and one such tissue is the intermediate mesoderm (IM) that lies between the somites and the LPM. Active participation of IM in limb initiation has been described based on the results obtained from classical experiments, namely placing a barrier between the IM and the LPM or extirpation of the IM, that inhibited limb initiation (Stephens and McNulty, 1981; Strecker and Stephens, 1983; Geduspan and Solursh, 1992). However, irrespective of the

presence of IM all along the embryonic AP axis, the limb develops only from its presumptive territory suggesting that a signaling molecule could be expressed at this level of the IM. Eventually, this molecule was identified as FGF8 (Crossley et al., 1996; Vogel et al., 1996) (Figure 1.2). Shortly before limb bud outgrowth and during its initiation, *fgf8* is expressed at the surface ectoderm (SE) (Crossley and Martin, 1995; Mahmood et al., 1995) suggesting that the tissue located between the IM and the SE (LPM) is somehow relaying *fgf8* from the IM to the SE. The excellent candidate to mediate this event was found to be *fgf10*, which is induced by IM expressed *fgf8* (Ohuchi et al., 1997; Xu et al., 1998) (Figure 1.2). This induction occurs in parallel to the appearance of the AER. Although *fgf10* begins to be expressed in a wider domain of the presomitic mesoderm (PSM) and the LPM, at stage HH14 it becomes restricted to the presumptive limb areas (Ohuchi et al., 1997). Limbless mice generated by *fgf10* mutants emphasise the importance of FGF10 in limb initiation (Min et al., 1998; Sekine et al., 1999). Remarkably, the capability of different FGF soaked beads to produce a complete ectopic limb when implanted in the flank (Martin, 1998) and to maintain the LPM cells in proliferative state, points FGFs as the key inducers of limb formation (Cohn et al., 1995; Ohuchi et al., 1997). In addition, these experiments also show that the short window of FGF ligand activity is enough to begin a whole cascade of signaling mechanisms necessary to form a complete limb (Duboc and Logan, 2011).

All FGFs mediate their cellular responses by binding to and activating appropriate FGF receptors (FgfRs- a subclass of receptor tyrosine kinases). There are four known FgfRs (FgfR1-4). The alternative splicing within the third Immunoglobulin (Ig) like domain generates IIIb and IIIc isoforms in FgfR1-3 (Eswarakumar et al., 2005) that display different ligand specificity (Ornitz et al., 1996; Zhang et al., 2006). Similar to the FGF ligands, their receptors also have restricted spatial expression in limb (Marcelle et al., 1995; Szebenyi et al., 1995; Lizarraga et al., 1999; Havens et al., 2006; Eloy-Trinquet et al., 2009; Sheeba et al., 2010) *FgfR1* is ubiquitously expressed all over the limb mesenchyme from very early stages of its development. *FgfR1* and *FgfR2* take part in limb development right from very early stages (Orr-Urtreger et al., 1991; Xu et al., 1998) whereas, *FgfR3* and *FgfR4* are involved in later events like chondrogenesis and myogenesis through their proficient interaction with specific FGF ligands (Ornitz et al., 1996; Zhang et al., 2006; Sheeba et al., 2010). Although FgfR1-3 have splice variants, FgfR2IIIb and IIIc variants are crucial for limb initiation, since FGF8 and FGF10 signal through distinct FgfR2 splice

variants enabled by their tissue specific expression. *FgfR2IIIb* is mainly expressed in the ectoderm and *FgfR2IIIc* in limb mesenchyme (Orr-Urtreger et al., 1993). This exclusive expression profile of *FgfR2* renders a paracrine signaling loop for FGF8 and FGF10 activity, which is crucial not only for limb initiation but also for its outgrowth. Ectodermal FGF8 and mesenchymal FGF10 predominantly activate mesenchymal *FgfR2IIIc* and ectodermal *FgfR2IIIb*, respectively (Ornitz et al., 1996; Xu et al., 1998; Revest et al., 2001). Absence of FgfR2 signaling resulted in limbless mice revealing the importance of *FgfR2* expression and epithelial-mesenchymal interaction for limb initiation (Xu et al., 1998). This is because, when there is no ectodermal-*FgfR2*, the mesenchymal FGF10 could not induce *fgf8* in ectoderm including the AER, as this induction requires ectodermal-FgfR2. Since there is no FGF8 in the ectoderm to feedback to the mesenchymal FGF10, the epithelial-mesenchymal loop halts and so does the limb development. Furthermore, FGF signaling mediated by FgfR2IIIb is essential for ZPA-*shh* and AER-*fgf4* expression to be induced (Revest et al., 2001). Although FgfR1 is shown not to be required for limb initiation (Deng et al., 1997), due to its strong mesenchymal expression, it could be transducing FGF signaling in limb mesenchyme (Revest et al., 2001) along with FgfR2IIIc.

Integration of WNT signaling in limb initiation

The Wingless (WNT) family members signal through the trans-membrane frizzled receptors. There are canonical and non-canonical WNT signaling pathways. In the canonical way, WNT proteins signal via β-catenin by repressing the axin/glycogen synthase kinase-3β (GSK3β) complex that stimulates the degradation of β-catenin (Kikuchi, 2000). Hence, in WNT-activated cells, cytoplasmic β-catenin accumulates and is translocated into the nucleus. There, β-catenin along with T-cell-specific factor and lymphoid enhancer binding factor1 (Tcf/Lef1) transcription factors activates the transcription of WNT target genes. In the non-canonical way, WNT signal occurs through the release of intracellular Ca^{2+}, activator of protein kinase C (PKC) and Ca^{2+}/calmodulin-dependent kinase II (CamKII) (Sheldahl et al., 1999; Kuhl et al., 2000). In 2001, WNT signaling was introduced to the prevailing FGF based model of limb initiation, where the canonical WNT/β-catenin signaling was shown to be necessary and sufficient to induce both the fore and hind limbs in chick (Kawakami et al., 2001). At stage HH14, *wnt2b* is expressed in the LPM of the presumptive forelimb region and the IM along with *fgf8* (Figure 1.2). According to the model proposed by Kawakami et al. (2001), *fgf8* controls *wnt2b* expression in the LPM which

induces *fgf10* expression in the LPM. Similar to FGF protein beads, ectopic WNT2b in the flank was able to produce ectopic limb (Kawakami et al., 2001) enlightening the importance of this molecule in limb initiation program. Furthermore, another WNT family member, *wnt8c* is co-localized with *fgf10* in the presumptive hindlimb area and thus may be responsible for restricting *fgf10* to this area, as suggested by ectopic induction of *fgf10* by WNT8c producing cells implanted in the embryo flank. Additionally, this model also proposes that FGF10 in the LPM will in turn induce *wnt3a* in the SE along with *fgf8* and WNT3a helps in the maintenance of *fgf8* in the AER (Kengaku et al., 1997; Kawakami et al., 2001). Both WNT2b and WNT8c signal through the canonical β-catenin pathway and take part in the regulation of *fgf10* expression (Kawakami et al., 2001). However, the participation of WNT2b and WNT8c in mouse limb bud induction is questioned, since these molecules are not expressed in mouse limb (Agarwal et al., 2003). Nevertheless, the crucial WNT/β-catenin dependent transcription factors LEF1 and TCF1 have been illustrated to be required for normal *fgf10* expression and limb development in mouse (Galceran et al., 1999; Agarwal et al., 2003).

1.1.1.2. Importance of SHH and RA signaling in early limb development

The nascent limb mesenchyme prior to initial *shh* expression is pre-patterned by anteriorly expressed *Gli3* and posteriorly restricted *Hand2* (also known as *dHand*) expression (Figure 1.2)*. These two molecules inhibit each other to maintain their domain-restricted expression. Thus, HAND2 inhibits *Gli3* and *Alx4* expression in the posterior mesenchyme and enables the establishment of *shh* expression in the ZPA (te Welscher et al., 2002). Recently, the absolute need for Hox9 genes from all the four Hox clusters (HoxA, B, C, D) for the initiation of *Hand2* expression and eventually for *shh* in mouse forelimb was demonstrated (Xu and Wellik, 2011). In the absence of Hox9 genes, *Hand2* was never established in the posterior limb and *Gli3* expanded its domain to the posterior mesenchyme resulting in a skeletal phenotype similar to conditional *shh* or *Hand2* null mutant mice (Chiang et al., 2001; Kraus et al., 2001; Galli et al., 2010). The positive feedback loop between the AER-FGFs and ZPA-SHH helps to maintain their mutual expression (Laufer et al., 1994; Niswander et al., 1994) (Figure 1.2) and is crucial in all stages of limb development (Zeller et al., 2009). Accordingly, conditional *shh* mutants exhibit abrogated AER-*fgf4* and *fgf8* expression (Chiang et al., 2001; Kraus et al., 2001) and AER-*fgf8/fgf4*

mutants have no *shh* expression (Sun et al., 2002). This loop which links the mesenchymal SHH signaling with the ectodermal FGF signaling is mediated by mesenchymal expressed BMP antagonist *Grem1 (Gremlin1)* (Zuniga et al., 1999; Michos et al., 2004).

Figure 1.2: A scheme illustrating all the important interactions involved during limb bud initiation. (A) Stage HH14 chicken embryo, where the blue box represents the presumptive forelimb field between somite 15 and 20. **(A´)** Enlarged view of the presumptive forelimb region and operating molecular interactions therein. The intermediate mesoderm (IM) expresses *fgf8* in a broader domain (green bar) which induce *fgf10* expression in the lateral plate

mesoderm (LPM). This induction is regulated by *fgf8* induced *wnt2b* expression in the LPM (combination of red and blue for *fgf10+ wnt2b*). The LPM also expresses *meis2* and the forelimb identity gene *Tbx5* downstream of RA signaling (Mic et al., 2004). **(B, B´)** Representation of stage HH16 chick embryo and the enlarged presumptive limb field interactions. During this stage, FGF10 from the LPM relay *fgf8* expression from the IM to the surrounding ectoderm (SE). This happens through the induction of *wnt3a* in the SE (Kawakami et al., 2001). Both *wnt3a* and *fgf8* co-exists in the SE (navy blue and green). **(C, C´)** Scheme illustrating the molecular network underlying forelimb initiation in stage HH17 chick embryo. Initiation of *shh* (orange) expression and the emergence of the pre-AER are the key events taking place at this stage of development. **(D)** Higher magnification of stage HH17 limb bud (E9.5 in mouse) revealing the molecular cross talks involved in ZPA-*shh* establishment. The limb is pre-patterned by mutually antagonising anteriorly expressed *Gli3* (yellow gradient) and the posteriorly expressed *Hand2* (purple gradient). Positive cooperative regulations from RA, AER-FGFs and HAND2 facilitate shh induction in the ZPA, in turn, SHH induce *fgf4* expression in the posterior AER. Among the signaling modules operating between the ZPA-SHH and AER-FGFs positive loop (Benazet et al., 2009; reviewed in Zeller et al., 2009), by stage HH17, BMP induce *Grem1* expression through a fast module (2h). Eventually GREM1 will also be produced by ZPA-SHH which will relieve BMPs inhibition on AER-*fgfs* in the subsequent module (represented by dotted bars; Benazet et al., 2009). Black arrows indicate positive transcriptional interactions; black lines with blunt bars in the end represent inhibitions and dotted lines denote interaction that will occur in the subsequent stages of limb development. This image is a modification of Fig. 2 from the review Capdevila and Belmonte, 2001.

Gli3 mediated initial pre-patterning of limb mesenchyme also restricts *Grem1* to the posterior limb (te Welscher et al., 2002). This mesenchymal-epithelial interaction to establish the functional AER and ZPA consists of two loops: the initial fast loop (2h; Figure 1.2) of BMP-induced G*rem1* expression in limb mesenchyme that enables the slow loop (12h) of SHH-GREM1-FGF (Benazet et al., 2009). Recent studies suggests the presence of SHH protein and Hedgehog signaling in the limb ectoderm including the AER (Bell et al., 2005; Bouldin et al., 2010). Furthermore, Bouldin et al. have described the role of AER-SHH signaling in regulating the AER-*fgf* expression and thus the length of AER in mouse and chick (Bouldin et al., 2010). These authors have proposed that the link between AER-SHH signaling and AER-*fgfs* (*4* and *8*) expression is crucial to maintain proper mesenchymal SHH concentration (Harfe, 2011). The intensity of AER-SHH signaling is directly proportional to the level of SHH produced by the ZPA cells i.e, if the ZPA produces too much of SHH, then this leads to a corresponding increase in the AER-SHH signaling which will modulate AER length by decreasing AER-*fgf* expression. As a result, the AER-FGF/ZPA-SHH positive feedback loop will reduce the levels of SHH in the ZPA and regulate optimum concentration of SHH in the ZPA (Bouldin et al., 2010; Harfe, 2011).

Retinoic acid (RA), the active derivative of vitamin A signaling is also critical in many aspects of limb development including its initiation, since inhibition of RA synthesis or signaling prevents limb bud initiation in chick, mouse and zebrafish (Helms et al., 1996; Stratford et al., 1996; Niederreither et al., 1999; Grandel et al., 2002; Gibert et al., 2006). Recently, RA has been proposed to have two distinct yet related roles during zebrafish fin development (Grandel and Brand, 2010). Consistent with the role for RA in limb initiation, Raldh2 mutant mouse or zebrafish lacks forelimb or pectoral fins development, respectively (Niederreither et al., 1999; Mic et al., 2004; Gibert et al., 2006). These authors showed that at early gastrula stage, RA signaling specifies Tbx5 expressing fin precursors and in later stages, maintains and expands these fin precursors (Grandel and Brand, 2010). Somites express *Raldh2* and serve as a main source of RA, which has been implicated in limb initiation, through classical experiments in chick. When an impermeable foil barrier was inserted between the somites and the LPM from where forelimb will emerge, forelimb buds failed to be formed (Duboc and Logan, 2011). Although maternal dietary RA supplementation rescued forelimbs of *Raldh2/Raldh3* deficient mouse, these limbs did not possess any RA activity in both mesenchyme and presumptive LPM arguing against the need for RA for limb induction (Zhao et al., 2009). Endogenous RA synthesised in the somites and LPM is only needed in a paracrine fashion to antagonise FGF signaling in the developing trunk to provide a permissive environment for the induction of forelimbs. In agreement with these results from mouse mutants, zebrafish *Raldh2* mutants treated with SU5402 (an FgfR inhibitor) formed pectoral fins which are otherwise absent (Zhao et al., 2009). This finding suggests a permissive role for RA rather than its long accepted instructive role (Lewandoski and Mackem, 2009).

High rate of RA synthesis in the presumptive forelimb territory is demonstrated to be necessary for proper ZPA-*shh* expression and early limb development (Helms et al., 1996). In chick, RA signaling has been shown to induce ZPA-*shh* expression through its cooperative role with posterior signals like HAND2 (Niederreither et al., 1999; Tickle, 2002; Mic et al., 2004). Further, it is reported that RA deficiency prevents FGF4-SHH signaling loop (Power et al., 1999; Stratford et al., 1999). An antagonistic AER-FGF/Cyp26b1/RA module established during limb initiation even before the onset of *shh* expression in mouse forelimb development was recently identified (Probst et al., 2011). They have also demonstrated that RA beads could inhibit AER-*fgf8* and AER-*fgf4* expression. This study had postulated two potent roles for RA at different limb developmental stages: at induction stages, RA might be restricting *fgf8* expression in the flank to

mark the forelimb territory and shortly after limb bud formation, RA establish proper AER length by controlling AER-*fgf8* expression (Probst et al., 2011). This proposal is also supported by previous studies (Mic et al., 2004; Zhao et al., 2009; Probst et al., 2011).

1.1.1.3. Establishment of limb identity

Although the two pairs of tetrapod limbs look very much alike in their early stages of development, soon they begin to be morphologically and functionally different. This difference starts with the differentially expressed genes in the fore and hindlimb territories. Tissue grafting experiments performed in chick suggest that the fore and hindlimb specification area in embryonic flank is established pretty earlier than LPM budding. When presumptive forelimb LPM cells were transplanted into an ectopic location, they always induced forelimb formation indicating that the specification of limb identity resides in these cells (Zwilling, 1955).

The T-box transcription factors, Tbx5 and Tbx4, and a paired-like homeodomain factor Pitx1 play important roles in type-specific limb initiation. *Tbx5* expression starts in the presumptive forelimb region and its expression is maintained in the forelimb bud during limb development, whereas the expression of *Tbx4* and *Pitx1* is totally hindlimb bud specific (Gibson-Brown et al., 1998; Isaac et al., 1998; Logan et al., 1998; Ohuchi et al., 1998; Saito et al., 2002). Limb specific expression of *Tbx5* or *Tbx4* is evolutionarily conserved (Duboc and Logan, 2011). Tbx5 or Tbx4 have the ability to change limb identity from one to the other when introduced into the presumptive hind limb or forelimb regions, respectively (Rodriguez-Esteban et al., 1999; Takeuchi et al., 1999; Takeuchi et al., 2003). *Tbx5, Tbx4* and *Pitx1* gain-of-function and loss-of-function studies suggest that these molecules are involved in limb initiation and outgrowth process in association with members of the FGF and WNT families (Ahn et al., 2002; Ng et al., 2002; Agarwal et al., 2003; Marcil et al., 2003; Rallis et al., 2003; Takeuchi et al., 2003; Minguillon et al., 2005). Takeuchi et al. (2003), blocked *Tbx5* or *Tbx4* genes activity by misexpressing dominant negative forms of these genes in the prospective limb field and produced limbless chick embryos via downregulation of FGF and WNT components. Similarly, when they misexpressed either one of these genes in the embryo flank, an ectopic limb was formed through the induction of the limb initiation oriented genes, *fgf10, fgf8* and *wnt2b* or *wnt8c* suggesting that these T-box genes are not only involved in limb identity but also in limb initiation (Takeuchi et al., 2003).

Moreover, these results also reveal that Tbx genes function upstream of *fgf* and *Wnt* genes in limb (Duboc and Logan, 2011). Evidence for RA acting upstream of *Tbx5* expression in mice also exists (Mic et al., 2004). Although, Tbx4 and Tbx5 are thought to substitute for each other (Minguillon et al., 2005), a difference in the phenotypes observed in Tbx5 (Rallis et al., 2003) and Tbx4 (Naiche and Papaioannou, 2003) null mutants argue against this possibility. Recent evidence points to different temporal roles for *Tbx5* and *Tbx4* genes: an early role during limb initiation by involving in FGF10 based feedback loop establishment and a later role in limb morphogenesis while limb outgrowth is independent of these genes (Hasson et al., 2007; Naiche and Papaioannou, 2007; Hasson et al., 2010). Despite these evidences, the direct involvement of *T-box* genes in limb specification is still questioned and elusive (Minguillon et al., 2005; Naiche and Papaioannou, 2007). Pitx1 regulates Tbx4 expression and contributes to hindlimb initiation and morphology (Duboc and Logan, 2011). Consistent with Pitx1´s role in hindlimb identity, Pitx1 misexpression in the forelimb has the ability to transform the morphologies into hindlimb oriented at the level of the bones, muscles and tendons in chick and mouse (Logan and Tabin, 1999; Takeuchi et al., 1999; Delaurier et al., 2008).

1.1.2. LIMB OUTGROWTH

Although the molecular determination at the presumptive limb level takes place between stages HH13 to HH14 in chick, limb bud will be visible only from stage HH17 onwards. In order to obtain a proper limb, changes should occur co-ordinately in three different orthogonal axes during limb outgrowth: the PD, AP and DV axes. Growth along each axis is controlled by different signaling centers: the AER, the ZPA and the non-ridge ectoderm respectively controls the PD, AP and DV axis.

1.1.2.1. AER formation and fgf signalling in limb outgrowth
AER formation

As a consequence of the limb initiation program, certain inductive signals from the LPM will give rise to a thickening in the distal tip of the surface ectoderm structuring it like a ridge called the apical ectodermal ridge (AER). During its life span, the AER undergoes four sequential morphogenic changes namely initiation, maturation, maintenance and regression which are

denoted by changes in gene expression and cell shape (Altabef et al., 1997; Kimmel et al., 2000). In chick, the AER becomes visible from stage HH18 and it runs along the AP axis separating the dorsal and ventral sides of the limb, while in mouse, the AER is conspicuous from E10.5, although its activity can be traced back from E9.5 onwards (Wanek et al., 1989).

During limb initiation, FGF10 in the LPM relays *fgf8* expression from the IM to the AER (Ohuchi et al., 1997; Xu et al., 1998) where it will be expressed until its regression. Apart from the induction of the AER, FGF signaling through AER expressed *FgfR2* is necessary for the survival of AER cells, its maintenance and proper AER-*fgf8* expression (Lu et al., 2008). As mentioned before, the participation of WNT/β-catenin signaling in AER induction cannot be neglected. It is proposed that FGF10 will induce *wnt3a* in the SE along with *fgf8* (Kawakami et al., 2001) and *wnt3a* helps in the maintenance of *fgf8* in the AER during later stages through its persistent expression in the AER. Meanwhile, the complete absence of *fgf8* expression in the SE of WNT/β-catenin mediators *Lef-1* and *Tcf-1* knockout mice (Galceran et al., 1999), the ability of ectopic WNT3A to induce *fgf8* and the inability of FGF8 to induce *wnt3a* suggest that WNT3A lies upstream of AER-*fgf8* expression (Kengaku et al., 1998; Kawakami et al., 2001). In agreement with the importance of ectodermally expressed *wnt3a*, its inactivation caused severe limb defects (Barrow et al., 2003). Moreover, β-catenin signaling has been shown to be necessary for the formation of functional AER and for its maintenance (Barrow et al., 2003; Soshnikova et al., 2003; Lu et al., 2008).

The SE surrounding the LPM seems to be pre-patterned before limb bud induction and contains pre-AER cells (Altabef et al. 1997). These pre-AER cells migrate from the ectoderm towards the distal limb and compact themselves to form the mature AER (Loomis et al., 1998). Prior to AER induction, the DV specifying gene *Rfng* (*Radical fringe*) and the homeobox-containing transcription factor *En-1* are expressed respectively in the dorsal and ventral ectoderm of the chick limb bud (Davis and Joyner, 1988; Laufer et al., 1997; Rodriguez-Esteban et al., 1997). Eventually, AER forms right between the cells that express *Rfng* and *En-1* where EN-1 prevents the expression of *Rfng* in the ventral ectoderm (Laufer et al. 1997, Rodriguez-Esteban et al. 1997) indicating the importance of DV boundary establishment for AER induction. Bone morphogenetic proteins (BMPs) that belong to the Transforming growth factor beta (TGFβ) multigene family play a major role in determining the DV axis of limb (Ahn et al. 2001; Pizette et al. 2001). Since the interface between the dorsal and ventral ectoderm is necessary for the emergence of the AER, the importance of BMPs in AER formation is noteworthy. BMP4 and BMP7

signalling are participating in AER formation through ectodermally expressed *BmpR1a* (Ahn et al., 2001; Pizette et al., 2001; Lallemand et al., 2005). In physiological condition these major signaling pathways cooperatively function in AER formation. Emphasising this notion, the necessity of BMP and FGF receptors, *BmpR1a* and *FgfR2*, respectively for AER formation and WNT/β-catenin signaling for its maintenance has been reported (Soshnikova et al. 2003; Lu et al., 2008).

Before regression, the signals from the AER maintain the underlying distal mesenchymal cells in undifferentiated proliferative state (Dudley et al., 2002; Sun et al., 2002) and pattern the PD axis of limb (Saunders, 1948). Eventually it starts to regress through apoptosis and become a flat cuboidal epithelium (Guo et al., 2003) at stage HH33-HH35 in chick hindlimb (Pautou, 1978). Despite its role in AER initiation, BMP signaling promotes AER destruction (Pizette and Niswander, 1999). Accordingly, the AER cells are first lost in the interdigital domain with high BMP signaling and then in the distal tip leading to its complete absence at birth (Guo et al., 2003). Expression of *fgf8*, considered as the marker of AER tissue that persists until its regression, is first lost in the AER over the primordia of digit4 followed by digit2 and digit3. This correlates the loss of AER-fgf8 expression with the number of phalanges in each digit in away digits with more phalanges switch-off *fgf8* later than digits with fewer phalanxes (Sanz-Ezquerro and Tickle, 2003).

FGFs are the prime AER signaling molecules

The key signaling molecules produced by the AER are the members of the Fibroblast Growth Family (FGF) morphogenic proteins. Expression of *fgf8* marks the AER progenitors even before the morphologically distinct AER is formed (Martin, 1998). After AER establishment in mouse and chick, *fgf2, fgf4, fgf9, fgf17* and *fgf19* are also expressed in the AER, while some are expressed only in chick (*fgf2* and *fgf19*) (Fernandez-Teran and Ros, 2008). *fgf10, fgf12, fgf13* and *fgf18* are expressed in chick limb mesenchyme and *fgf2* transcripts are detected both in the ectoderm, including the AER, and in the mesenchyme (Sheeba et al., 2010 and references there in). Although initially *fgf8* begins to be expressed in patches of AER cells, soon it marks the entire AER (Crossley et al., 1996), whereas, other AER-*fgf*s (*fgf4, fgf9, fgf17*) are restricted to its posterior domain in chick and mouse (Fernandez-Teran and Ros, 2008; Mariani et al., 2008). Moreover, studies performed in mouse show that the spacio-temporal expression of *fgf4* in the AER is negatively regulated by AER-FGF8, as the absence of *fgf8* caused anterior expansion and prolonged *fgf4* expression (Lewandoski et al., 2000; Moon and Capecchi, 2000).

The reason to imply FGFs as the mediator of AER signaling is due to the ability of heparin beads soaked in different FGF proteins to substitute the major role of AER as the regulator of PD growth and patterning after AER ablation (Niswander et al., 1993; Fallon et al., 1994; Martin, 1998; Zeller et al., 2009). This property is partially attributed to their capacity to prevent distal limb mesenchymal cell death after AER extirpation (Fallon et al., 1994; Dudley et al., 2002).

After a series of classical amputation and transplantation studies from 1940s, many other experimental manipulations in chick limb contributed to our present understanding about AER-FGF signaling and its importance in limb development. Although ectopic application of FGF1, FGF2, FGF4, FGF8 or FGF10 in the flank gave rise to an ectopic limb (Cohn et al., 1995; Vogel et al., 1996; Ohuchi et al., 1997), the only gene among them that is expressed early and longer in the entire AER is *fgf8*. However, misexpression of *fgf8* in chick forelimb using retroviral vectors or by grafting cells transfected with *fgf8* constructs caused severely shortened limb structure suggesting that higher and continuous exposure of FGF8 or misexpression at wrong time has adverse effect in limb development (Vogel et al., 1996). Similarly, implantation of FGF4 soaked beads in different positions of stage HH20-21 wing bud formed thick and short limb bone elements (Akita et al., 1996). These authors accounted the formation of thicker bones to upregulation of *Bmp2* and *Bmp4* expression following FGF4 bead implantation. Whereas, another study attributed the chemoattractive nature of FGF4 soaked beads for the generation of short radius and ulna (Li and Muneoka, 1999). This work shows that FGF4 is a potent chemoattractive molecule produced by the AER and its presence in the AER, is necessary for limb distal outgrowth.

Nevertheless, the mutant studies performed in mice embryos have added substantial wealth of knowledge in this field. The mouse AER expresses *fgf4, fgf8, fgf9* and *fgf17*, where, *fgf8* is the first to be expressed and persists in the entire AER until its regression unlike the other three members (Crossley and Martin, 1995; Mariani et al., 2008). Conditional KO of *fgf8* in the AER using two different promoters, the *Msx2* that corresponds to transient *fgf8* expression in the forelimb and complete absence of *fgf8* in the hindlimb (Lewandoski et al., 2000) and *RARβ2* that render complete absence of *fgf8* in the forelimb bud (Moon and Capecchi, 2000) reveal that FGF8 is the only individual AER-FGF necessary for normal limb development. Additionally, these studies have also revealed the instructive nature of AER-FGF signal. On the other hand, the KO mice for other AER-FGFs either alone or in combination (*fgf4*: (Moon and Capecchi, 2000; Sun et al.,

2000), *fgf17*: (Xu et al., 2000), *fgf9*: (Colvin et al., 2001), triple KO for *fgf4, fgf9, fgf17*: Mariani et al., 2008), did not show any limb abnormalities indicating that *fgf8* is sufficient for normal limb patterning and growth, while the other members have redundant function. Consistent with their redundant function, FGF4 was able to replace and rescue the limb defects caused by the absence of FGF8 (Lu et al., 2005). Although conditional *fgf8* and/or *fgf4* KOs had defective limbs and normal limbs respectively, *fgf8/fgf4* double KOs failed to form hindlimbs although defective forelimbs were formed (Sun et al., 2002). This variation observed among the hind and forelimb formation is due to the difference in the *Msx2-Cre-* function which commences before and after hindlimb and forelimb initiations, respectively. Thus, hindlimb presents complete absence of *fgf8* and *fgf4* expression while forelimb has their transient expression in the AER. The loss of hindlimb was attributed to the role of AER-FGFs as cell survival factors to maintain ideal number of cells in the limb mesenchyme to form the limb elements (Sun et al., 2002; Boulet et al., 2004). However, compound triple KO mice of *fgf8/fgf4* along with other AER-*fgf* members (*fgf9*) displayed much severe forelimb phenotypes compared to *fgf8/fgf4* double KO mouse forelimbs, indicating the importance of each AER-*fgf*'s contribution for the total AER-FGF signal (Mariani et al., 2008). Since *fgf8 is* the first FGF member to be expressed and the last to disappear from the entire AER, it could contribute in a more crucial way than other FGF members to the total AER-FGF signal allowing it to account for the phenotypes resulting from individual *fgf8* inactivation.

The impact of FgfRs is also equally important to that of FGF ligands for proper FGF signaling to occur. Interaction of FGFs with FgfRs leads to the formation of receptor dimers and activation of their intracellular tyrosine kinases domain. Activated kinases phosphorylate tyrosine residues to provide a docking site for other proteins to bind. In turn, signaling complexes are formed and cause a cascade of phosphorylation events that activate downstream signal transduction pathways. Among them the more important ones are the Erk/MAPK, Akt/PI3K and the PLCγ pathways (Dailey et al., 2005; Eswarakumar et al., 2005). During limb development the Erk/MAPK and the Akt/PI3K pathways have been proposed to be essential. Corson et al. (2003) detected phosphorylated-Erk (p-Erk) in the surface ectoderm of initiating limb and in a distal to proximal gradient in the mesenchyme during limb outgrowth stages of mouse. The authors were able to inhibit p-ERK in the presence of the FgfR inhibitor SU5402 suggesting the importance of the FfgR mediated activation of Erk/MAPK pathway in limb initiation, outgrowth and patterning (Corson et al., 2003). In the same year, another study performed in chick has proposed MAPK

phosphatase 3 (Mkp3) as the effector of limb FGF signaling, which was illustrated as a target of Akt/PI3K pathway. Mkp3 functions as an anti-apoptotic agent by dephosphorylating p-Erk (Muda et al., 1996; Kawakami et al., 2003). This study also demonstrated that p-Akt and p-Erk have a complementary expression during chick limb development, the former being expressed in the distal mesenchyme and the later in the AER, thus enabling the survival of distal mesenchymal cells (Kawakami et al., 2003). Later on, Palmeirim and co-workers shown that the distal to proximal gradient of *mkp3* expression observed in chick distal limb mesenchyme is the consequence of mRNA decay (Pascoal et al., 2007b).

As the complete deletion of *FgfR1* or *FgfR2* was lethal, different approaches such as, hypomorphic mutations, isoform KOs and transgenic chimeric animals were used to access their function during limb development (Xu et al., 1999). Manipulation of ectodermal FgfR2 levels originated various phenotypes, including limbless mice, pointing to the importance of this receptor for limb initiation (Celli et al., 1998; Xu et al., 1998; Arman et al., 1999; Revest et al., 2001) and supporting the involvement of FgfR2 in the epithelial (FGF8)-mesenchymal(FGF10) loop (Sekine et al., 1999). *Shh* and *fgf4* expression were never observed in FgfR2IIIb disrupted mouse limb buds, strongly suggesting that FgfR2 ectodermal signal is required for their induction (Reveste et al., 2001). Genetic ablation of AER by conditional inactivation of *FgfR2* in the AER after its induction by *Msx2-Cre* resulted in the absence of forelimb hand-plate emphasising the novel function of AER in autopod development (Lu et al., 2008). Cell survival and proliferation experiments have shown massive cell death only in the ectoderm and not in the mesenchyme of AER-*FgfR2* KO limbs, suggesting a prematured regression of the AER in the absence of FgfR2 signal (Lu et al., 2008). Alternatively, another study utilizing similar *Msx2-Cre* mediated ectodermal specific inactivation of *FgfR2* also obtained the same phenotype and the authors compared it to the classical stage HH23 AER ablated chick limb skeleton (Yu and Ornitz, 2008). Unlike Lu et al (2008), who suggested a delay in autopod progenitor generation as a reason for the absence of forelimb handplate, Yu and Ornitz (2008) attributed this to increased cell death, decreased cell proliferation and failure to establish chondrogenic primordia along the PD axis marked by *sox9* expression for the observed phenotype. Mesenchymal-FgfR2´s role in autopod patterning was also demonstrated using an RNA interference (RNAi) approach in mouse (Coumoul et al., 2005). Yu and Ornitz also inactivated *FgfR1IIIc* and *FgfR2IIIc* either alone or in combination to ensure complete absence of mesenchymal-FgfRs in mouse. This manipulation

resulted in mild limb phenotypes for *FgfR1IIIc* and no effect for *FgfR2IIIc*, while the double KO presented severe skeletal hypoplasia suggesting that AER-FGFs signal transduction by FgfR1 and FgfR2 in the early limb mesenchyme is partially redundant and that mesenchymal-FgfR1 plays a role in distal limb patterning, compared to the mesenchymal-FgfR2 (Yu and Ornitz, 2008). This result with FgfR1IIIc is consistent with previous reports about mesenchymal FgfR1 signal in distal limb patterning and morphogenic movements (Ciruna et al., 1997; Deng et al., 1997; Partanen et al., 1998; Xu et al., 1999; Ciruna and Rossant, 2001) and suggests that FgfR1 might be the predominant candidate mediating FGF signaling in the mesenchyme as proposed by Revest et al. (2001). By taking an approach of conditionally inactivating mesenchymal FgfR1 before and after limb initiation, Li et al. (2005) emphasised the necessity of mesenchymal FgfR1 for early limb patterning events, cell survival and for proper digit formation. In this study, early inactivation caused severely truncated limb skeletal phenotypes and late inactivation affected anterior digit formation (Li et al., 2005). In the absence of mesenchymal-FgfR1, although defective, AER-*fgf8* and ZPA-*shh* expression were observed further suggesting that FgfR1 signaling is dispensable for limb initiation (Li et al., 2005). Applying a similar strategy, Verheyden et al (2005) conditionally inactivated *FgfR1* using two different *cre* promoters: *T* (*brachyury)* and *shh*, which disabled FgfR1 throughout the limb mesenchyme and in the ZPA, respectively. The results enabled the authors to propose that FgfR1 signaling is necessary in the initial phase to pattern the PD axis by regulating cell number, in the middle phase for cell survival allowing the expansion of skeletal precursors and finally in later stages for autopod patterning (Verheyden et al., 2005).

Overall, FGF signal from the AER that is transduced through FgfR1 and FgfR2 mainly functions as a cell survival factor for both the AER and mesenchymal cells. AER-FGFs also ensure that proper number of skeletal progenitors is specified for each PD segment (Reveste et al., 2001; Li et al., 2005; Lu et al., 2008). Table 1.1 summarizes all the important functional studies so far carried out to decipher the function of limb FGF signaling.

Table 1.1: A comparative analysis of the limb phenotypes, gene expression alterations and main conclusions obtained from important functional studies performed in chick and mouse FGF signaling components

Gene	Manipulation strategy		Limb phenotypes, and main conclusions	Reference
fgf4 *fgf1, Fgf2*	OE	RCAS BP(A)/ beads- **C**	Importance of AER expressed FGFs and demonstrated ectopic limb formation from the flank upon respective bead implantations.	Niswander et al., 1993; Fallon et al., 1994; Ohuchi et al.,1994

Gene	Type	Method	Description	Reference
fgF4	OE	Bead- **C**	Chemo attractive nature of FGF4 responsible for distal limb outgrowth	Li and Muneoka, 1999
fgf8			FGF8 is an AER-derived mitogen that stimulates limb bud outgrowth in chick and mouse	Mahmood et al., 1995
fgf8	OE	Bead- **C**	*fgf8* expression in IM is necessary for limb induction; FGF8 induce *shh* expression in stage HH17 limb mesenchyme	Crossley et al., 1996
fgf8	OE	RCAS BP(A)- **C**	Reduction of proximal skeletal limb structures; digit abnormalities resembling the phocomelic phenotypes- FGF8 is a key signaling molecule involved in limb initiation, outgrowth and patterning	Vogel et al., 1996
fgf10	OE	RCAS BP(A)- **C**	Mesenchymal FGF10 can induce *fgf8* expression and a complete ectopic limb; it is the endogenous inducer of limb bud formation	Ohuchi et al. 1997
fgf10	KO	KO- **M**	Perinatal lethality associated with complete absence of lungs; limb bud formation was initiated but outgrowth did not occur; *Fgfr2b* was expressed in presumptive limb region; no *fgf8* expression was detected; AER and ZPA were not established	Min et al., 1998; Sekine et al., 1999
fgf17	KO	**M**	No limb defects	Xu et al., 2000
fgf9	KO	**M**	No limb defects	Colvin et al., 2001
fgf4	C-KO	Msx2-Cre (AER) or RAR-Cre (IM, LPM & AER)- **M**	No limb defects; normal *shh, Bmp2, Bmp4, fgf8 & fgf10* expression - suggesting a combination of at least 2 AER-FGFs is needed to maintain ZPA-*shh* expression & limb development	Sun et al., 2000; Moon et al., 2000
fgf8	C-KO	Msx2-Cre or RAR-Cre **M**	Substantially shortened limb phenotype and autopod defects; late *shh* expression; anteriorly expanded AER-*fgf4* expression- suggesting AER-*fgf8´s* role in limb patterning and outgrowth	Lewandoski et al., 2000 Moon and Capecchi, 2000
fgf8/fgf4	C-KO	Lefty-Cre(early mesoderm-IM) or RAR-Cre or AP2-Cre (PZ at E10.5)- **M**	No limb defects in Lefty-Cre-*fgf8* KO; Absence of forelimb in RAR-Cre- *fgf8/fgf4* KO & expression of *shh & fgf10* were nearly abolished; Absence of both fore and hind limb in AP2-Cre-*fgf8/fgf4* KO- suggesting AER *expressed fgf8 & fgf4´s* importance in limb initiation	Boulet et al., 2004
fgf8/fgf4	C-KO	Compound-Msx2-Cre- **M**	Abnormal forelimbs and no hind limbs were generated; *Shh* expression was never initiated; presented abnormal cell death- suggesting AER-FGFs as cell survival factors regulating sufficient progenitor cell number to form limb elements	Sun et al., 2002
fgf4	C-GOF	Msx2-Cre GOF or Msx2-Cre substituting AER-fgf8 KO - mouse	Limb polydactyly & syndactyly in *fgf4* GOF mutants & expansion of *shh & Gremlin1* expression were observed; FGF4 completely rescued limb defects caused by the loss of FGF8- suggesting the need for proper AER-FGF signaling for normal limb development and FGF4´s ability to replace FGF8	Lu et al., 2005
AER-fgfs (fgf8,4,9,17)	C-KO	Compound Msx2-Cre- **M**	No limb defects & normal *shh* expression - AER-*fgf4 fgf9 & fgf17* triple KO; Mild limb defects- *fgf8/fgf17* or *fgf8/fgf9 or fgf8/fgf4* double KO; Severe limb truncations- *fgf8/fgf4/fgf9* triple KO suggesting the contribution of each AER-FGFs role for cell survival & PD patterning	Mariani et al., 2008
FgfR1	KO	Gene targeting in ES cells- **M**	Embryos die between E6.5 and E9.5 with severe growth retardation and defective mesodermal patterning.	Deng et al., 1994; Yamaguchi et al., 1994
FgfR1	KO	Chimeric embryo- **M**	Malformed limb buds-suggesting FgfR1 mediated signaling in the PZ for cellular proliferation and patterning; FgfR1 signal is dispensable for AER establishment and limb initiation	Deng et al., 1997
FgfR1	C-KO	Ap2-Cre;	Short & distorted AER; *shh, mkp3* expression was	Li et al., 2005

		Hoxb6-Cre (LPM at E8.5)- **M**	downregulated; affected autopod development- suggesting FGF/FGFR1 signaling is dispensable for limb initiation and necessary for PD patterning (anterior digit formation)	
FgfR1	C-KO	T-Cre (in all limb mesenchyme) Shh-Cre (in posterior limb mesenchyme)- **M**	T-Cre-FgfR1 mutants die at birth; present severely affected fore and hind limb skeletons with defect in all the 3 limb segments; abnormal expression of *shh, Bmps, Hox13* genes. *Shh*-Cre-FgfR1 mutants miss one digit in the autopod. Suggesting FgfR1´s role in PD patterning, cell survival and expansion of progenitor cell population.	Verheyden et al., 2005
Fgfr1IIIc	C-KO	Prx1-Cre- **M**	Mild limb skeletal defects- suggesting unique function mesenchymal- FgfR1IIIc during limb development compared to mesenchymal-FgfRIIIc	Yu and Ornitz, 2008
Fgfr2IgIII	KO	**M**	Perinatal lethality between E10.5-E11.5; no limb formation; absence of *fgf8* expression in the ectoderm and *fgf10* downregulation in limb mesenchyme-FGFR2 signal is essential for the reciprocal regulation loop between FGF8 and FGF10 during limb induction.	Xu et al. 1998
FgfR2	KO	Chimeric embryo- **M**	No limb buds form; *fgf10* and *msx1* were downregulated in presumptive limb mesenchyme; *fgf8* expression was not detected	Arman et al., 1999
FgfR2IIIb	KO	Hypomorphic mutants- **M**	Limb less mice were generated; limb bud initiates but fail to grow; *fgf8, fgf10, msx1 & Bmp4* were expressed while *shh & fgf4* were not expressed- suggesting an essential role for FgfR2IIIb in AER maintenance, limb outgrowth, and cell survival; FgfR1IIIc might be the major mesenchymal receptor	Revest et al., 2001
FgfR2	C-KO	Msx2-Cre **M**	Defective autopod; expression of *mkp3, shh & Gremlin1* was downregulated- Suggesting AER-FgfR2 is necessary for AER maintenance, autopod development by regulating the number of autopod progenitors	Lu et al., 2008
Fgfr2	C-KO	Msx2-Cre- **M**	Absence of hind limb & severely truncated (without autopod) forelimb ; also showed reduced cell proliferation- suggesting decreased cell proliferation and sustained cell death accountable for limb truncations	Yu and Ornitz, 2008
Fgfr2IIIc	C-KO	Prx1-Cre- **M**	No limb skeletal defects	Yu and Ornitz, 2008
FgfR1IIIc/FgfR2IIIc	C-KO	Prx1-Cre (both fore & hindlimb mesenchyme)- **M**	Severe skeletal hypoplasia in forelimbs and hindlimb- suggesting that AER-FGF signaling is mediated in the mesenchyme by both FgfR1 & FgfR2. This facilitates SOX9 function and ensure progressive establishment of chondrogenic primordia along the PD axis.	Yu and Ornitz, 2008

KO: Knockout; C-KO: Conditional Knockout; C-GOF: Conditional Gain of Function; OE: Overexpression; **M**: Mouse; **C**: Chick

1.1.2.2. Proximal-Distal (PD) patterning

The PD axis defines the primary direction of limb outgrowth and is governed by the AER. This axis is characterized by three limb segments: the most proximal stylopod, the middle zeugopod and the distal autopod. These skeletal elements are laid down as cartilaginous primordia in a PD sequence during limb outgrowth.

PD patterning models

The Progress Zone (PZ) model

Microsurgical experiments performed in 1940s in order to access the role of the AER in laying down the future limb tissues show that the earlier the removal of the AER, the most proximal limb elements are truncated (Saunders, 1948). These results directly revealed that the AER is necessary for normal limb outgrowth and its patterning in the PD sequence. The PZ model was built on this foundation and proposes that the positional values in the distal mesenchyme freezes after AER ablation and thus the resulting skeletal patterns reproduce the PD information already acquired by these cells. Additionally, other microsurgical manipulations were performed in which AER or AER along with the limb distal mesenchyme were swapped from younger to older and older to younger embryos (Rubin and Saunders, 1972; Summerbell et al., 1973). Limb elements developed from this transplanted tissue retained their presumptive fate, suggesting that the PD positional information is retained by the distal limb mesenchyme and that the nature of the AER signal is permissive. These conclusions led to the proposal of the `PZ model´ in 1973 (Summerbell et al., 1973; summarized in Figure 1.3). This model calls the distal mesenchymal cells corresponding to about 300 μm just beneath the AER as the PZ. These cells are under the influence of the AER and are maintained in an undifferentiated, proliferating state and keep them labile to acquire positional information about their future PD fate. The model also proposes an intrinsic timer operating in the PZ that would provide the cells the notion of time they spend in the PZ. Due to continuous cell proliferation and outgrowth of the limb, cells will be pushed out of the PZ and escape the influence of the AER. The amount of time each cell spends in the PZ will determine its positional identity. In other words, the cells that leave the PZ earlier will be incorporated in more proximal limb segment compared to the cells that leave later in development. Once cells leave the PZ, cartilage elements begin to develop in a proximal to distal sequence.

This proposal was supported by X-irradiation experiments which gave similar results in the congenital limb malformation, phocomelia or the toxicological effect induced by thalidomide where proximal limb elements are missing while the distal elements are present (Wolpert et al., 1979). The authors reasoned this phenotype through their model: PZ cells supposed to form the proximal limb segments were killed by irradiation and hence the remaining cells need to spend longer time in the PZ before they could be pushed out to be determined. This phenomenon

makes them to be a part of a more distal element while the proximal elements are left without enough or no determined cells. Recently Tabin and collaborators repeated the same X-irradiation experiments in the light of molecular data that has been accumulated during the past years (Galloway et al., 2009). Although the results were similar to that of Wolpert et al. (1979), these authors suggested that the phenotype is not due to patterning defects but the reflection of poor cell survival and differentiation (Galloway et al., 2009). This conclusion was deduced based on the expression of segment specific marker genes (*Meis1, Hoxa11* and *Hoxa13*) subsequent to irradiation. While no respecification was observed at the level of the markers, expression of *Sox9*, the earliest marker for condensing mesenchyme showed considerable absence or reduction in its expression (Galloway et al., 2009). These experimental results enabled the authors to state that the absence of proximal segments after X-irradiation is the consequence of the proximal chondrogenic precursor's elimination by cell death and not because the cells stay in the PZ longer than usual and acquire different PD identity.

However, the PZ model prevailed for around 30 years after which a new model was proposed to explain the PD patterning of limb. Moreover, the driving force of the PZ model, the distal limb mesenchymal intrinsic clock was revealed by Palmeirim and co-workers after 10 years of the discovery of the somitogenesis molecular clock (Pascoal et al., 2007).

Early specification (ES) model

The forelimb developed from the *fgf4/ fgf8* double KO mice (Sun et al., 2002) and the hindlimb developed from single *fgf8* KO mice (Lewandoski et al., 2000) lacked some proximal elements while forming the distal elements arguing against the PZ model which states that PD patterning is a progressive process where proximal structures are laid down before the distal (Summerbell et al., 1973). Although these phenotypes could be explained based on the X-irradiation experiments (Wolpert et al., 1979) in such a way that the PZ cells might have been killed by the reduced AER-FGF signaling, hence, the remaining cells need to stay in the PZ longer than usual and thus got distalized. However, this was not the case since TUNEL assay showed cell death only in the proximal zone of the limb (Sun et al., 2002). At the same time, based on fate mapping and transplantation experiments in chick limb, Dudley and co-workers (Dudley et al., 2002) came up with a new model in which they proposed that all the three limb segments are already specified in the very early limb bud as distinct domains and only further expansion occurs

during development (Figure 1.3). Cell death and cell proliferation assays revealed that the distal mesenchymal cells corresponding to the PZ suffered extensive cell death and decreased cell proliferation after AER extirpation, which emphasises these mesenchymal cells as the possible cause for the truncations resulted from AER ablation experiments which were on the basis of the proposal of the PZ model (Dudley et al., 2002). Moreover, cell labelling studies did not show the incorporation of the distal limb cells in any skeletal elements formed after AER ablation (Dudley et al., 2002; Galloway and Tabin, 2008) as it had been predicted by the PZ model. Additional fate mapping studies to identify the time or stage at which the PD segments are specified revealed that the already specified pool of progenitor cells in the early chick limb bud complete their expansion between specific developmental stages: stylopod between stage HH19-20, zeugopod between HH22-23 and the autopod progenitors continue to expand even after stage HH26 (Dudley et al., 2002). Consistent with this, another fate map study carried out in chick showed that the prospective stylopod and zeugopod limb segments were located in distinct distal domains by stage HH19 limb while considerable mixing or overlap between the future zeugopod and autopod cells was observed (Sato et al., 2007). In agreement with both the PZ and ES models, this fate map also states that the proximal elements are laid down before the distal elements.

The two signal (TS) model

Although a mechanism that renders the notion of time to the distal limb mesenchymal cells has been identified (Pascoal et al., 2007), so far no other functional or molecular data supporting neither the PZ model nor the ES model has been reported. As a result, a new model purely based on the molecular evidence such as gene expression pattern and genetic mutations was proposed (Tabin and Wolpert, 2007) (Figure 1.3). During the early and outgrowth limb developmental stages, the distal limb mesenchymal cells experience the activity of two opposing signals: RA signaling from the proximal stump and FGF signaling from the distal tip (Capdevila et al., 1999; Mercader et al., 1999; Mercader et al., 2000). However, in the early limb bud, these two signals overlap with each other. As the limb bud grows, the space between the proximal-RA and the distal-FGF signals increases and establishes three separate domains: the proximal domain under the influence of RA signal, the distal domain under the influence of FGF signal and the middle domain that is neither influenced by RA nor by FGFs. These domains also express specific genes which represent the three PD segments of the limb: the proximal *meis1* or *meis2*, the

middle portion with *Hoxa11* and the distal most with *Hoxa13* which would result in the formation of stylopod, zeugopod and autopod respectively. Except *meis1* and *meis2*, none of these segment specific markers are directly involved in segment specification (Tabin and Wolpert, 2007). This model also refers the region almost corresponding to the PZ as Undifferentiated Zone (UZ) as the cells in this region are under the influence of the AER-FGFs and maintained in a proliferating undifferentiated state (Globus and Vethamany-Globus, 1976; Tabin and Wolpert, 2007). Due to limb outgrowth and continuous proliferation in the UZ, cells are pushed out of the AER-FGFs influence and begin to enter the differentiation program. The marker gene expressed in the cell at the time of its exit from the UZ determines its fate (in which limb element the cell should be incorporated). The limb region from where cells start their differentiation program is named as the `Differentiation Front´ (DF) which represents the proximal limit of the AER-FGF signal (Tabin and Wolpert, 2007).
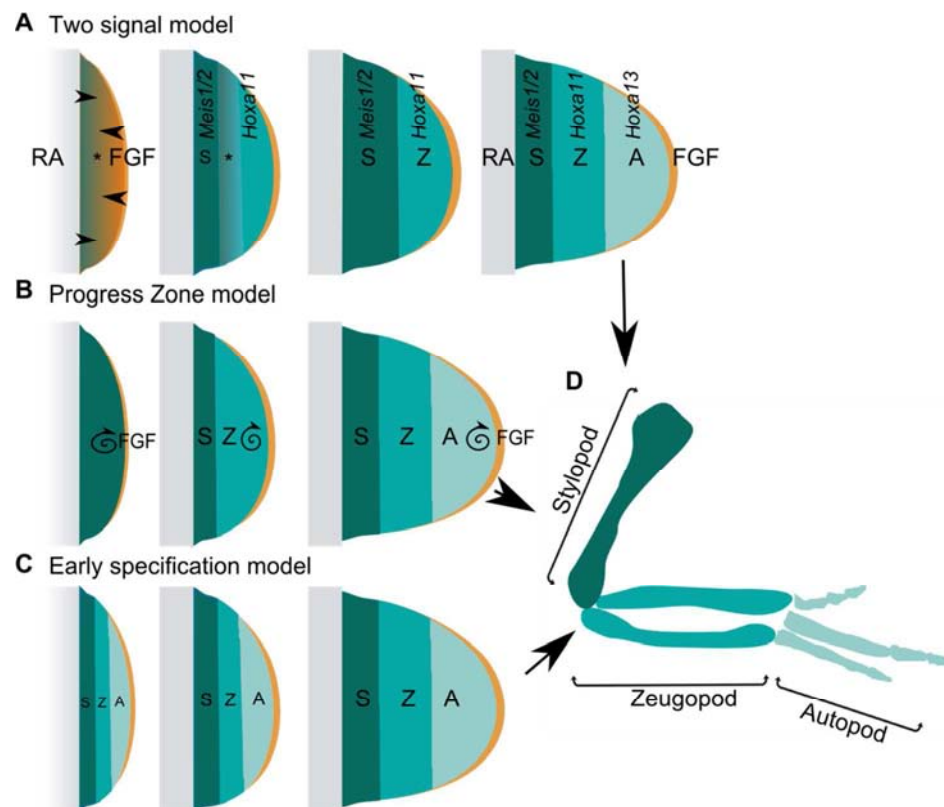

Figure 1.3: Depiction of all the three PD patterning models so for proposed. (A) The present model for PD patterning: The two-signal model. As per this model, the opposing gradients of flank RA (Proximal-Distal) and the AER-FGF (Distal-Proximal) signals pattern the limb mesenchyme based on their influence. This sequentially

establishes the proximal stylopod (S) expressing *Meis1* or *Meis2*, middle zeugopod (Z) expressing *Hoxa11* and the most distal autopod (A) with *Hoxa13* expression (reviewed in Tabin and Wolpert, 2007). The asterisks represent limb domains under the influence of both the RA and FGF signals **(B)** The very first PD patterning model: The progress zone model (Summerbell et al., 1973). Here, the distal most (~300μm) limb mesenchymal cells under the influence of the AER-FGFs called the Progress Zone (PZ) is maintained in a labile state to undergo patterning by the intrinsic clock like mechanism functioning in these cells (marked with spiral arrow). Thus, the limb segments are laid down in a PD sequence. **(C)** The early specification model proposed is based on the fate map studies which states that the limb segments are pre-patterned in the very early limb mesenchyme and they just need to proliferate and expand further in population to form the skeletal primodia (Dudley et al., 2002). **(D)** Chick wing skeleton representing all the three limb segments that (stylopod, zeugopod and the autopod) eventually form from the patterned limb mesenchymal cells. All limbs are represented anterior on top and proximal side to the left.

This model could explain the single *fgf8* and double *fgf8/fgf4* KO mouse mutant phenotypes that do not fit into the explanations of the previous PD patterning models (Mariani et al., 2008). The participation of the proximal (RA) and distal (FGF and WNT) signals in PD patterning was recently substantiated by two parallel studies in chick embryo. Cooper et al. (2011), used the in vitro system of cultured primary limb mesenchymal cells from stage HH18 embryo in the presence of WNT3A and FGF8 to maintain them in the proliferative undifferentiated state to prove the requirement of RA signaling for the expression of the proximal marker *Meis1* and the necessity of AER produced FGF8 and WNT3A for the sequential expression of *Hoxa11* and *Hoxa13* by quantitative RT-PCR. Further, the authors also utilized the recombinant limbs in association with their previous experiments (in vitro cultures of stage HH18 limb mesenchyme maintained under various combinations of FGF8, WNT3A and/or RA) to show that exposure of limb mesenchymal cells to RA signaling is enough to express *Meis1* and for their subsequent differentiation into stylopod. Similarly, FGF and WNT signaling make the cells to express the middle and distal markers, *Hoxa11* and *Hoxa13* and eventually form the zeugopod and autopod, respectively (Cooper et al., 2011). Simultaneously, another study also concluded the same through transplantation of stage HH19-20 distal leg tip to non-RA and endogenous RA containing embryonic regions and recombinant limb experimental systems in chick (Rosello-Diez et al., 2011). These experiments suggest a balance between the trunk-RA and the distal-FGF signals rather than certain level of one particular signal for PD patterning. Moreover, they also

suggest that the plasticity of limb mesenchyme to respond to the proximal RA signal is progressively lost as the limb develops (Rosello-Diez et al., 2011).

1.1.2.3. WNT and BMP signaling in limb outgrowth

WNT signaling in limb outgrowth

Several members of WNT family are expressed in the SE including the AER and in the limb mesenchyme (Loganathan et al., 2005). Apart from the importance of WNT/β-catenin signaling in AER establishment and maintenance (Fernandez-Teran and Ros, 2008), it is also required for cell proliferation, cell fate specification and differentiation (ten Berge et al., 2008). Although the AER has been implemented in maintaining the distal limb mesenchymal cells in an undifferentiated proliferative state, AER-FGFs have been demonstrated as survival factors more than proliferative signals (Reveste et al., 2001; Li et al., 2005; Lu et al., 2008). Recently, AER-WNTs were established as the proliferative signaling molecules produced by the ectoderm. While continuous exposure to FGF8 or WNT3A rendered chondrogenic or connective tissue fate, their combined application to limb micromass cultures retained the cells in undifferentiated proliferative state and upon their withdrawal cells began to differentiate. Interestingly, these signals regulate the expression of distinct target genes based on their individual or synergistic action in the limb field (ten Berge et al., 2008). Thus, a model implementing WNT/FGF signaling was proposed to explain limb development: The early limb mesenchyme experiences both the ectodermal WNT and AER-FGF/WNT signals and maintains the cells in a multipotent proliferative state. As a result of proliferation, cells start to escape the influence of the AER derived signals and begin to differentiate into chondrocytes. Since the entire limb ectoderm expresses *wnt3a,* limb periphery still undergoes proliferation. WNT signal also re-specifies the outer layer of chondrogenic cells into soft connective tissue fate. Although, proliferation takes place all over the limb margin by WNT signal, the distal proliferation dominates due to the strength of the AER-FGF/WNT signals. Thus, a distally growing (the limb also grows in other dimensions) limb with a chondrogenic core surrounded by connective tissues is sculptured by the combination of FGF and WNT signal (ten Berge et al., 2008). Moreover, Dickkopf1 (Dkk1) the negative regulator of WNT signaling also regulates limb development. Corroborating this, thalidomide induced limb truncations were attributed to enhanced Dkk1 levels, induced WNT/β-catenin signal inhibition and increased cell

death since, blocking Dkk1 or Gsk3 dramatically counteracted thalidomide-induced limb truncations (Knobloch et al., 2007).

BMP signaling in limb outgrowth

BMP signal plays a considerable role in limb development. However, its contribution to the PD patterning and outgrowth is not as highlighted as its role in early limb establishment, DV patterning, chondrogenic differentiation as well as patterning and shaping of the digits. Several members of the BMP genes are expressed throughout limb development (Geetha-Loganathan et al., 2006). Particularly, Bmp2, Bmp4 and Bmp7 are crucial for normal limb formation. Although all these three *Bmp*s are expressed in the AER and mesenchyme, *Bmp4* and *Bmp7* have stronger expression in the AER, while *Bmp2* and *Bmp7* have stronger distal limb mesenchymal expression (Geetha-Loganathan et al., 2006). Due to the absolute requirement of these BMPs for embryo development and their functional redundancy, it had been hard to decipher their precise function in limb development until the introduction of the conditional allele technique where we can inactivate or over express genes in a tissue and stage specific manner.

In the developing limb, the predominantly expressed BMP receptors are *BmpR1a* and *BmpR1b*. Among these, BmpR1a has high affinity for BMP2 and BMP4 (Yamaji et al., 1994; Robert, 2007). The ubiquitously expressed BmpR1a mutant mice present abnormalities in all the three limb segments (Ovchinnikov et al., 2006), while mutants for *BmpR1b* expressed in the mesenchymal condensations display mild defects in cartilage differentiation (Baur et al., 2000; Yi et al., 2000). Inactivation of mesenchymal-*BmpR1a* resulted in mildly affected stylopod/zeugopod and severely affected autopod. The short limb phenotype was attributed to reduced cell proliferation as *CyclinD1* and *Wnt5a* expression decreased in the mutant limbs rather than PD patterning defects (Ovchinnikov et al., 2006). But, AP and DV patterning signal related genes such as: *patched1, Hoxd11, Hoxd13* and *Lmx1b* were affected in the mutant limb buds suggesting a patterning defect in these two axes. However, these molecular changes and cell proliferation defects were traced back only from E11.5 and so the limb skeletal phenotype might be a consequence of poor mesenchymal condensation and cartilage differentiation rather than incorrect patterning (reviewed in Robert, 2007). Individual inactivation of either *Bmp7* or *Bmp4* had almost no effect to mild autopod defects with polydactyly (*Bmp7*- Luo et al., 1995; *Bmp4*-Selever et al., 2004) due to the functional redundancy between BMPs. Tabin and his group took

an approach of conditionally inactivating *Bmp2, Bmp4* and *Bmp7* either alone or in combination to gain further insights on the role of BMP signaling in limb development (Bandyopadhyay et al., 2006). This study revealed that none of these BMPs are involved in the limb mesenchymal patterning, but a certain threshold of BMP signaling is necessary to form proper chondrogenic condensations (Bandyopadhyay et al., 2006). However, the BMP antagonist GREM1 which is expressed in a complementary pattern to the *Bmp´s* in chick forelimb is important for distal outgrowth by neutralizing BMP signal (Merino et al., 1999) and by relaying SHH mediated positive feedback loop (Zuniga et al., 1999; Michos et al., 2004) to maintain a functional AER.

1.1.2.4. Role of RA and SHH signal in limb outgrowth

Role of RA signal in limb outgrowth

RA is an important signaling molecule for embryo development. Although it is difficult to detect its precise location in the embryo, detection of RA synthesising (Retinaldehyde dehydrogenases: *Raldh1-3*) and catabolising enzymes (cytochrome P450 family members: *Cyp26a1, b1, c1*) distribution is an alternative approach to locate RA. During limb development, the synthesising and catabolising enzymes are transcribed in mutually exclusive domains, where *Raldh2,* the most relevant enzyme for limb development (Niederreither et al., 1999) is expressed in the limb stump mesenchyme and *Cyp26b1* in the distal limb mesenchyme and ectoderm other than the AER (Yashiro et al., 2004) generating a graded RA activity across the limb mesenchyme (Lewandoski and Mackem, 2009). RA activity is denoted by two closely related homeobox genes, *Meis1* and *Meis2* expression. These genes are expressed in the LPM before limb initiation, in the entire nascent limb bud mesenchyme, in early phase of limb development and later in the proximal limb region, up to the humerus-radius/ulna boundary (Tabin and Wolpert, 2007). This pattern of proximal to distal RA signaling opposing the distal to proximal FGF signaling has long been believed to be an instructive signal functioning during limb initiation and patterning. These genes have been identified as determinants of proximal limb elements, since overexpression of either of these *Meis* genes leads to inhibition or truncation of the distal compartments. In addition, ectopic distal *Meis1* expression inhibits progressive distalization of PZ cells, resulting in limbs with proximally shifted identities along the P-D axis in chick and mouse (Capdevila et al., 1999; Mercader et al., 1999; Mercader et al., 2000; Mercader et al., 2009). When RA activity in

the limb mesenchyme was distally expanded by inactivation of its degrading enzyme Cyp26b1, distal limb truncated phenotypes similar to *Meis* gene overexpression were observed (Yashiro et al., 2004). Also in amphibians RA acts as a proximalizing signal during limb regeneration causing tandem duplicated PD limb structures (Maden, 1982). Indeed, the two-signal model for PD patterning has been built on the basis of the work of Mercader et al. (2000), where the authors clearly showed the proximalizing potential of RA signal denoted by *Meis* expression which is counteracted by the distal FGF signaling in chick limb (Mercader et al., 2000). As mentioned before, the proximalizing ability of RA during chick limb development has been clearly illustrated by two parallel studies (Cooper et al., 2011; Rosello-Diez et al., 2011). Furthermore, apart from the necessity of RA signal in the early phase of limb development for the induction of *Tbx5, Meis2* and *Hand2*, it is also required in later phase for proper AER formation (Mic et al., 2004). Together, these data provide a compelling evidence for the requirement of RA signaling for proper PD patterning. However, recent data based on *Raldh2/Raldh3* double KO mice argue against the instructive role of RA signal during limb development (Lewandoski and Mackem, 2009). These mice, which had a complete absence of endogenous RA production/signaling, managed to restore normal hindlimb and relatively small forelimb upon maternal RA supplementation during gastrulation (Zhao et al., 2009). Since the restored limb buds completely lacked RA activity, these authors proposed that the role of RA is only to counteract FGF signaling which will otherwise inhibit limb induction (Zhao et al., 2009). Supporting this proposal, recently, AER-FGF signal was found to positively regulate distal limb mesenchymal *Cyp26b1* expression in mouse (Probst et al., 2011).

SHH signaling in limb outgrowth

ZPA-SHH signaling is well known to govern AP limb patterning (Riddle et al., 1993). Null *shh* mutants present abnormal limb phenotype with unaffected stylopod, severely affected zeugopod and autopod (Chiang et al., 2001; Kraus et al., 2001). Moreover, expression of AER-*fgf8* was progressively lost in *shh* null limbs and restricted to the posterior AER indicating that the SHH signaling is not only important for AP patterning but also for proper PD patterning. Oligozeugodactyly (ozd) chick mutant limbs, which develop in the absence of SHH signaling, also exhibit skeletal phenotypes similar to that of *shh* null mouse mutants and show progressive loss of *fgf4* and *fgf8* expression in the AER (Ros et al., 2003). These results support the positive

signaling loop operating between AER-FGFs and ZPA-SHH via the BMP antagonist GREM1 to maintain each other's expression (Michos et al., 2004). In fact, the ZPA-SHH/GREM1/AER-FGF positive module is a self-regulatory loop allowing the propagation and termination of distal limb outgrowth (Benazet et al., 2009; Verheyden and Sun, 2008; Scherz et al., 2004) supporting the fact that SHH signaling may have a role in PD patterning. In corroboration with this, Probst et al. identified a negative AER-FGF/Cyp26b1/RA module in mouse which provided a more direct evidence for the requirement of SHH in PD patterning. These authors show that ZPA-SHH signal not only allows the propagation of the ZPA-SHH/GREM1/AER-FGF positive module, but also indirectly enables the expression of *Cyp26b1* in the distal limb mesenchyme through AER-FGFs which, in turn, establishes a RA free distal domain (Probst et al., 2011). The negative AER-FGF/Cyp26b1/RA module is crucial for distal propagation by eliminating the teratogenic activity of RA (Yashiro et al., 2004; Zhou and Kochhar, 2004). Distal mesenchymal cells have to be maintained in a proliferative and undifferentiated state for distal propagation of limb (Dudley et al., 2002). SHH also functions as a proliferative signal in the distal limb mesenchyme in chick and mouse (Towers et al., 2008; Zhu et al., 2008), further emphasising its role in distal limb outgrowth.

1.1.3. ANTERIOR- POSTERIOR (AP) PATTERNING

Limb development should also occur along the anterior to posterior (AP) axis to pattern the autopod that runs from the little finger to the thumb in the forelimb. The directions for this axis formation is provided by the posterior distal limb mesenchyme located signaling centre, the zone of polarizing activity (ZPA).

1.1.3.1. Establishment of ZPA-SHH expression

The early classical experiments in chick (Saunders and and Gasseling, 1968) lead to the discovery of the limb polarizing region, a group of mesenchymal cells located at the posterior margin of limb bud. This region has the potential to induce complete mirror image duplications of the digits when transplanted to the anterior margin of chick wing bud, revealing its function an AP limb axis organiser (Saunders and Gasseling, 1968). The number and identity of the induced digits was shown to be dependent on both the strength (Tickle, 1981) and duration (Smith, 1980)

of the polarizing signal. Based on these findings, it was proposed that the ZPA signal should be mediated by a morphogen. RA was the first chemical identified to behave as a polarizing activity morphologic signal, because of its diffusible nature and potential to establish a gradient (Tickle et al., 1982). Moreover, dose-dependent anterior digit duplications similar to the polarizing region grafts were observed, when RA-soaked beads were implanted at the anterior margins of chick wings (Tickle et al., 1985). But, now it is known that the effect of RA on AP patterning is not direct, but, through the activation of *shh* expression (Riddle et al., 1993).

Eventually, Tabin and colleagues identified sonic hedgehog (SHH) as the correct ZPA signaling molecule (Riddle et al., 1993). Several molecular networks function together to initiate *shh* expression in the ZPA. Two molecules upstream of SHH such as the basic helix-loop-helix (bHLH) transcription factor HAND2 and Gli3 are involved in the early restriction of *shh* to the posterior portion of the nascent limb bud by mutual antagonism (Zeller et al., 2009; te Welscher et al., 2002) (Figure 1.2). Functional analysis of *Hand2* in mice emphasises the role of this molecule in *shh* initiation. *Hand2* deficient limbs fail to express *shh* and have limb skeletal phenotypes similar to *shh* null limbs (Charite et al., 2000; Galli et al., 2010), whereas, over-expression of *Hand2* caused polydactyls limb (McFadden et al., 2002). This particular function of HAND2 is expected to happen through its direct interaction with the *cis*-regulatory region known as the ZPA regulatory sequence (ZRS), located about 800 Kb up-stream of the *shh* gene (Lettice et al., 2003; Liu et al., 2009; Galli et al., 2010). Similar to *Hand2,* Gli3 also restricts the expression of *5´Hoxa* and *Hoxd* genes to the posterior limb which participate in the initial establishment of *shh* expression (Zuniga and Zeller, 1999; Kmita et al., 2005; Tarchini et al., 2006) through their direct interaction with the ZRS (Capellini et al., 2006). Interestingly, Galli et al (2010) enlightened the requirement of cross interactions between HAND2, Gli3 and HoxD13 in the ZRS of mouse limb for *shh* expression in the posterior limb bud.

Many other additional pathways are also necessary for this initial organization of limb polarizing region. One such factor is RA which might be doing this in cooperation with *Hand2* or *Hoxb8* expression (Niederreither et al., 2002) (Figure 1.2). However, RA bead implanted in the anterior limb mesenchyme could only induce *shh* expression in its distal side proximal to the AER after 24h, pointing to the need of AER signal in this process (Riddle et al., 1993). Hox9 cluster is crucial for ZPA-*shh* induction through its regulation on *Hand2* expression in the posterior limb (Xu and Wellik, 2011) (Figure 1.2). Apart from establishing the PD patterning and ensuring distal

outgrowth of developing limb, AER-FGFs also maintain *shh* expression in the ZPA through the positive SHH/GREM1/FGF module operating in the distal limb (Benazet et al., 2009; Figure 1.2). This positive regulation could be evidenced by the downregulation of *shh* in the AER ablated chick and conditional *fgf8/fgf4* double knock-out mice limbs and its rescue upon implantation of FGF-soaked bead in chick limb (Laufer et al., 1994; Niswander et al., 1994; Yang and Niswander, 1995; Vogel et al., 1996; Sun et al., 2002). Moreover, Wnt7a secreted by the dorsal ectoderm is another factor required for *shh* expression (Parr and McMahon, 1995; Yang et al., 1997). Although, the entire distal limb mesenchyme is influenced by both FGF and WNT signaling, the transcription factor Tbx2 restricts *shh* expression to the posterior margin (Nissim et al., 2007). SHH can also regulate its own domain by controlling the number of *shh* expressing cells through apoptosis (Sanz-Ezquerro and Tickle, 2000). However, this auto-regulatory effect was shown to be operating through the BMPs later on (Bastida et al., 2009). As a negative regulator of SHH, BMP signaling is also participating in ZPA confined *shh* expression by interfering with FGF and WNT signaling pathways that positively regulate *shh* expression (Bastida et al., 2009).

1.1.3.2. AP patterning by ZPA-SHH signaling

During limb development, the canonical Hedgehog signaling pathway plays a major role compared to the non-canonical signalling, since all the reported effects of SHH signaling on limb development are mediated by Gli´s (Ahn and Joyner, 2004). There are three Gli´s in vertebrates each of them performing distinct transcriptional functions (Theil et al., 1999). Gli2 and Gli3 can be either in an activator or in a repressor form, whereas, Gli1 is always an activator and a target of SHH signaling. Across the limb field, Gli1 and Gli2 mediate the activator function while Gli3 contributes to the repressor activity (Ahn and Joyner, 2004). SHH signaling pathway involves two trans-membrane proteins, Patched 1 and 2 (PTC1 and PTC2) (Carpenter et al., 1998), which binds to SHH ligand and the signal transducer Smoothened (SMO). Upon ligand binding, the inhibition of PTC on SMO is released which stops the constitutive processing of full length Gli3 Activator (Gli3-A) to its repressor form (Gli3-R) (Wang et al., 2000; Varjosalo and Taipale, 2008). Both Gli-R and Gli-A are translocated into the nucleus where they function as transcriptional repressors and activators respectively, of SHH target genes *Ptc1* and *Gli1* (Yang et al., 1997).

Initially, a morphogen based French flag model was formulated (Wolpert, 1969) to explain the digit duplications caused by ectopic SHH in chick (Wolpert, 1969; Figure 1.4). According to

this model, the ZPA secretes a morphogen that diffuses and generates a spatial gradient across the limb field forming a French flag pattern depending on the morphogen threshold levels. Eventually, each threshold level will give rise to each digit of the chick forelimb. The posterior-anterior SHH concentration gradient is translated into Gli-A (Gli1 and Gli2) gradient that is opposed by the anterior-posterior Gli-R (Gli3-R) gradient (Ahn and Joyner, 2004). Consistent with the establishment of a Gli based gradient in the limb, SHH has been shown to prevent Gli3 proteolytic cleavage into its repressor form (Wang et al., 2000). Genetic analysis shows that Gli1 and Gli2 are not essential for limb bud development as revealed by the normal limb formation after their inactivation (Park et al., 2000; Bai et al., 2002). In contrast, inactivation of *Gli3* resulted in severe polydactyly (Hui and Joyner, 1993) emphasising the importance of Gli3 in specifying the number and identity of digits (Benazet and Zeller, 2009). Polydactyl limb phenotypes of both single *Gli3* and double *Gli3/shh* mutants suggest that SHH functions almost solely through Gli3 processing in limb AP patterning (Litingtung et al., 2002; te Welscher et al., 2002). The nonprocessed full length Gli3 functions as an activator as demonstrated in *shh* null background, where, the conversion of one *Gli3* allele into a *Gli3* mutant allele (activator form) was able to considerably rescue *shh* mutant limb phenotype (Wang et al., 2007). However, reduction of the SHH target gene *Gli1* expression in *Gli2* null mutants and its loss in *Gli2/Gli3* double mutants reveal that the activator function of SHH is also mediated by Gli2 (Bai et al., 2004). Fate map of SHH responding cells, as revealed by Gli1 reporter assay, clearly showed the importance of opposing Gli3-R and Gli-A gradients in the limb and enabled the proposal of an AP patterning model purely based on Gli3-R activity. As per this model, the anterior-most digit is patterned by high Gli3-R activity, while the posterior-most digit is by the absence of Gli3-R (Ahn and Joyner, 2004; Figure 1.4). However, later on it was proposed that, in addition to the Gli3-R gradient, the ratio of the Gli3-A to Gli3-R also determines limb digit patterning (Wang et al., 2007).

Meanwhile, a model based on the temporal expansion of SHH signal exposed cells was proposed by Harfe et al. (2004) in mouse. According to this model, it is not only the concentration of SHH exposure but also its duration that determines digit identity *i. e* both the spatial and temporal requirement of SHH signaling for AP patterning. Digit1 is patterned independent of SHH signaling since these cells are not at all exposed to SHH. Its development depends on Sal-like 4 (SAll4), T-box 5 (TBX5) and Hox transcriptional regulators (Montavon et al., 2008). Digit4 and digit5 contain SHH-descendants that were exposed to higher level of SHH

signaling for longer duration (autocrine signaling). Digit2 is exclusively formed from cells exposed to lower SHH signal through diffusion (long-range signaling), while, digit3 contains half of the cells that are exposed to high level SHH (but lesser than digit4) and remaining half cells that encountered SHH signal by diffusion (Harfe et al., 2004; Figure 1.4). Independent experiments to test the importance of duration and concentration were analysed by cyclopamine treatment in chick and genetically modified mouse, respectively. In accordance to this model, brief exposure to SHH was sufficient to specify anterior but not posterior digit and longer duration of moderate SHH exposure produced posterior digit (Scherz et al., 2007). Moreover, the fate map of SHH responding cells performed by Ahn and Joyner (2004) exemplified that digit2 depends on low SHH concentration owing to diffusion is in agreement with the temporal model (Harfe et al., 2004).
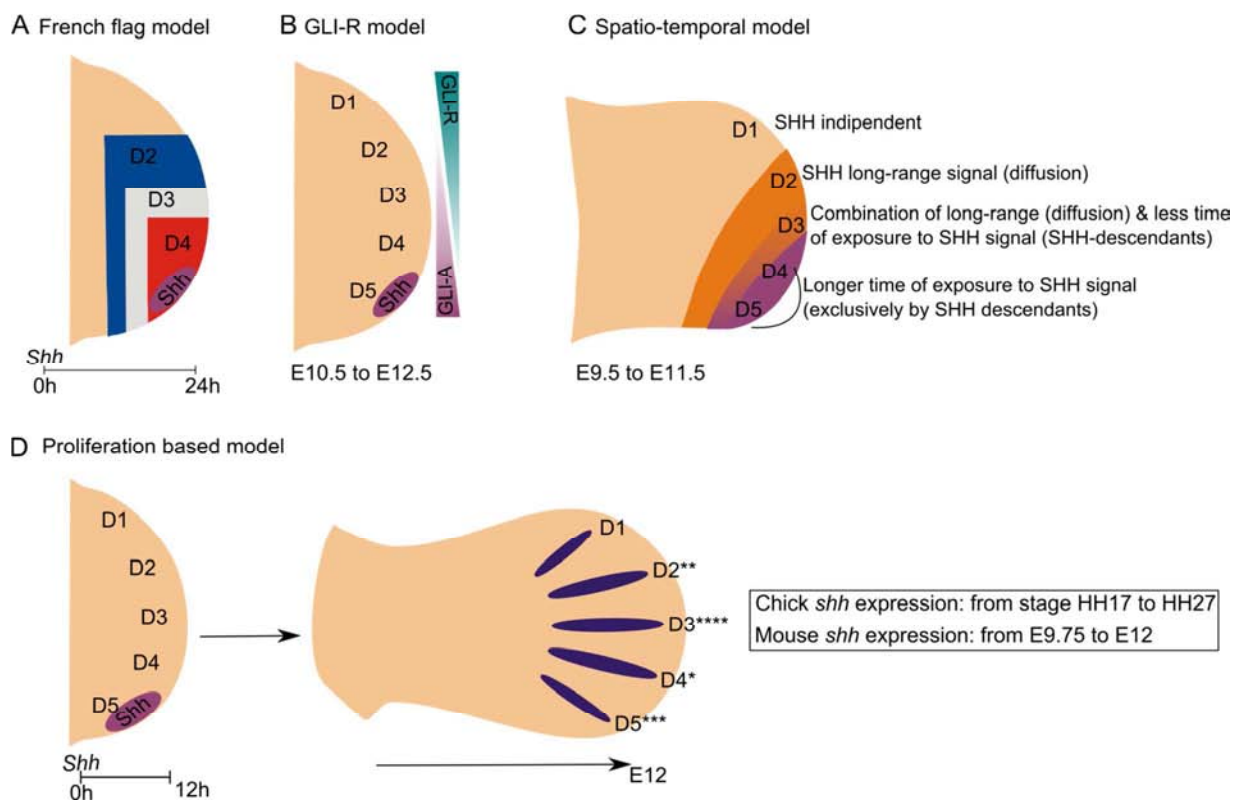
Figure 1.4: Important models explaining AP patterning. (A) The French flag model was proposed to explain chick wing digit patterning. Each colour of the flag represents different threshold concentrations established by the ZPA produced SHH through its diffusion across the limb mesenchyme. Eventually this spatial gradient will pattern each of the chick forelimb digits and this occurs within 24h of *shh* induction in the ZPA (Wolpert, 1969). **(B)** AP patterning based on the anterior-posterior Gli-R gradient. The anterior digit (D1) is specified purely by high Gli-R function and

the most posterior digit (D5) is specified because of the total absence of Gli-R in this domain. The intermediate digits are patterned by various levels of Gli-R at that position. The opposing Gli-R and Gli-A gradients derived by SHH signaling will specify the intermediate digits D2, D3 and D4 (Ahn and Joyner, 2004). The nonprocessed Gli3 also functions as an activator in vivo (Wang et al., 2007). **(C)** AP patterning is specified not only by SHH concentration but also by the duration of exposure to SHH signal. As per this model, SHH descendants derived from SHH expressing cells endow a gradient of SHH signaling across the AP limb mesenchyme. Thus, D1 is SHH independent; D2 is specified by cells that were exposed exclusively to long-range SHH signaling (low concentration) by diffusion; D3 is specified by a combination of cells exposed to low SHH concentration by long-range diffusion and by SHH descendants that were derived from former *shh*-expressing cells shortly after *shh* expression; D4 and D5 are specified solely by SHH-descendants derived from cells that expressed *shh* for progressively longer duration of time (Harfe et al., 2004). **(D)** SHH is not only needed for AP digit patterning but also for distal mesenchymal cells proliferation. As soon as *shh* is induced in mouse (E9.75), it patterns the AP axis within the first 12h. After this initial phase, SHH is necessary for survival and proliferation of the mesenchymal cells which is crucial for proper expansion of the early specified cells to form digit primordia after cessation of *shh* expression (E12). This expansion occurs in the order of D4, D2, D5 and D3 (indicated by asterisk in the scheme) (Zhu et al., 2008). AP patterning models are reviewed in Zeller et al. (2009). All limbs are represented anterior on top and proximal side to the left.

The post translational modifications of SHH protein by the addition of cholesterol and palmitate moieties (Mann and Beachy, 2004), regulate its long-range signaling. Inactivation of these modifications results in opposing effects, where, inhibition of cholesteration increases its diffusion (Li et al., 2006) while prevention of palmitoylation caused reduced diffusion (Chen et al., 2004). In fact, higher diffusion enabled the formation of polydactylus of anterior digit (digit2), further emphasising its patterning is dependent on long-range SHH signaling (Li et al., 2004; Harfe et al., 2004).

Patterning of the limb distal mesenchyme by SHH is also linked with cell proliferation. This function of SHH was illustrated by Towers et al. (2008) in chick and Zhu et al. (2008) in mouse limb. When cyclopamine was used in chick to inhibit SMO and thus all the signal transductions downstream of SHH, along with reduced limb field, only the anterior digits (digit2 & 3) were formed. But, when they used cell proliferation inhibitors, the reduced limb field formed posterior digits at the expense of the anterior ones since *shh* expression was maintained. This suggests that SHH signaling is ensuring proliferation of distal mesenchymal cells to have enough cells for the formation of each digit primordia as a part of AP patterning mechanism (Francis-West and Hill, 2008; Towers et al., 2008). In the same year, a genetic study in mouse, inhibited *shh* expression

at different stages of development and analysed the resulted digit patterns to assess the role of SHH in distal patterning (Zhu et al., 2008; Figure 1.4). Emphasising the role of SHH in mesenchymal cell proliferation, these set of experiments gave an unexpected order of digit formation in mouse: digit4, 2, 5 and 3. At present, this order of digit formation is difficult to be explained (reviewed in Francis-West and Hill, 2008). It has been suggested that SHH specifies digit pattern at very early stages, within around 12h of its induction in the ZPA and subsequently SHH signaling is necessary for cell cycle propagation and cell survival to ensure enough cells for the formation of digit primordia (Zhu et al., 2008).

1.1.3.3. Digit formation

Several lines of evidence suggest that BMP signaling is necessary for AP patterning and to determine digit identity and shape by inducing interdigital cell death (Robert, 2007). The involvement of BMP signaling in autopod formation was demonstrated by (Kawakami et al., 1996), by co-expressing dominant negative *Brk2* and *Brk3* (*BmpR1b* and *BmpR2*) in chick limb which displayed truncated forelimbs with complete absence of ulna and autopod, comparable with *shh* null mutant mouse limbs. Moreover, *Bmp2* and *Bmp7* are considered to be expressed as the consequence of SHH signalling (Laufer et al., 1994; Chiang et al., 1996; Yang et al., 1997) unlike *Bmp4*. Indeed, consistent with the role of BMPs in proper autopod formation, individual inactivation of *Bmp4* and *Bmp7* or *BmpR1a* displayed polydactyly or truncated autopod, respectively (Luo et al., 1995; Selever et al., 2004; Ovchinnikov et al., 2006). Apart from this first phase where BMPs are required for autopod formation, BMP signaling also has a second phase in which it renders digit identity from the secondary signaling centers, the inter-digital domain (Dahn and Fallon, 2000; Drossopoulou et al., 2000). The ability of graded BMP signaling across the posterior to anterior autopod has been implicated in digit specification where high levels of BMP signaling was implicated in the specification of posterior digits (Dahn and Fallon, 2000). More molecular data and insight to this particular function of BMP signaling was added by Suzuki et al (2007) in chick embryo. These authors show that a small group of sub ridge mesenchymal cells at each digital level escape the influence of the AER and start to express *sox9*, the early chondrogenic marker and eventually *BmpR1b*, denoting the phalanx-forming region. As a consequence, the intracellular mediators of BMP signaling, SMAD1/5 and 8 are phosphorylated and reach certain threshold of SMAD activity at these domains. Each digit in chick hindlimb is

specified by distinct SMAD activity in the phalanx-forming region with highest activity for digit3, lowest for digit1 and digit2 and 4 with intermediate activity (Suzuki et al., 2008).

BMP signaling is an inducer of cell death and crucial for interdigital apoptosis that shapes the digit. Inhibition of BMP signaling either by dominant negative BMP receptors or by its antagonists creates soft tissue syndactyly in limb (Zou and Niswander, 1996; Merino et al., 1999). However, whether this is a direct or an indirect effect through other signaling pathways was analysed by (Pajni-Underwood et al., 2007) where they inactivated the AER-expressed *BmpR1a* either alone or in combination with *fgf8* and *fgf4* and demonstrated that inter digital cell death is caused by BMP signaling regulated AER-FGFs. But, a previous study showed that interdigital cell death is regulated by the convergence of FGF- and BMP-mediated signaling pathways (Montero et al., 2001). (Hernandez-Martinez et al., 2009) showed that both FGF and RA are crucial for interdigital cell death, the former as negative and the later as positive regulators. They also found that BMP signaling is required only in chick for interdigital cell death and not in mouse. Many previous reports are in agreement with the cell death inducing nature of RA signaling as application of RA in inter-digital domain accelerated cell death (Lussier et al., 1993; Rodriguez-Leon et al., 1999). Also, in chick it has been proposed that RA is a physiological regulator of interdigital cell death as an all-trans-RA receptor antagonist decreases interdigital cell death (Rodriguez-Leon et al., 1999). Although the RA receptor *Rarβ* deficient limbs were normal, *Rarβ/Rarγ* double mutants showed interdigital webbing (Dupe et al., 1999) supporting the role of RA signaling in interdigital cell death.

1.1.4. DORSAL-VENTRAL (DV) PATTERNING

By looking at our own arm we can observe the difference between the back and the inner side (palm) of it. This difference also exists inside the limb at the level of tissue arrangement (skeleton, muscles, tendons, blood and nerves). The DV patterning is regulated by the non-ridge ectoderm. Similar to the identification of the key signaling centers patterning the PD and AP axes of limb, the importance of ectoderm for DV axis establishment was also first identified by classical experiments in chick. When limb ectoderm was dorso-ventrally rotated 180°, the mesenchymal structures (skeleton, muscle and tendons) become inverted corresponding to the polarity of the ectoderm (MacCabe et al., 1974). DV limb axis specification in vertebrate embryos occurs through a complex, poorly understood series of epithelial-mesenchymal interactions

(Chen and Johnson, 1999). It has been suggested that the signals from the somatic mesoderm specify the dorsal fate and render it to the LPM through an inductive mechanism, whereas, the ventral fate is a default (Chen and Johnson, 2002). Subsequently, the DV polarity from the LPM is transferred to the ectoderm prior to limb bud outgrowth resulting in the expression of *wnt7a* in the presumptive dorsal limb bud ectoderm and *En-1* in the ventral limb bud ectoderm. *En-1* is induced in the ventral ectoderm by BMP signaling through BMPR1a. In the absence of WNT7a, the dorsal pattern of the distal structures is not established and the limbs appear bi-ventral (Parr and McMahon, 1995). WNT7a induces the expression of the LIM-homeodomain transcription factor *Lmx1b* specifically in the dorsal mesenchyme of the limb bud. Gain of function experiments in the chick indicated that LMX1b is sufficient to specify dorsal limb pattern in ventral limb mesenchyme (Riddle et al., 1995; Vogel et al., 1995). Subsequently, it was shown through gene targeting in the mouse that LMX1b activity is necessary to specify dorsal limb pattern (Chen et al., 1998). In mouse, lineage compartments defining the dorsal and ventral mesenchyme were identified and the dorsal compartment coincided with *Lmx1b* expression domain (Arques et al., 2007). In *En-1* knockout limbs, *wnt7a* is misexpressed in the ventral ectoderm and the distal structures develop with bi-dorsal character (Loomis et al., 1996). Loss of BMP signaling also leads to *Wnt7a* misexpression and bi-dorsal limbs (Chen and Johnson, 1999; Ahn et al., 2001; Pizette et al., 2001).

1.1.5. INTERACTIONS BETWEEN THE KEY LIMB AXES PATTERNING MOLECULES

As it has been described in previous sections, each axis is primarily patterned by different signaling molecules: the PD by AER-FGFs; the AP by ZPA-SHH and the DV by WNT7a from the dorsal ectoderm and BMP target gene En-1 in the ventral ectoderm. However, under physiological conditions, these pathways coordinate and interact with each other to organize the structure of a fully functional adult limb. Particularly, the well understood feedback loop between the ectodermal AER-FGFs and the mesodermal ZPA-SHH to maintain each other links most of the signaling pathways. Even though, this partnership was first identified by FGF bead implantation experiments (Laufer et al., 1994; Niswander et al., 1994), the need for an intermediate molecule to relay SHH signal to the AER-FGFs in order to maintain its expression was soon identified as the BMP antagonist, GREM1 through the SHH/GREM1/FGF positive loop (Zuniga et al., 1999; Michos

et al., 2004). In the absence of GREM1 the distal limb is truncated with digit loss (Michos et al., 2004). Recently, the SHH/GREM1/FGF loop was showed as a self-regulatory system that functions in three phases of limb development: initiation, propagation and termination (Benazet et al., 2009). Using computational modelling and experimental analysis these authors proposed the mechanism and duration of this module in each stage of mouse limb development. First, during limb initiation, high mesenchymal BMP signaling is necessary to initiate the expression of its own antagonist, *Grem1* around E9 stage through a fast loop that takes only about 2h (Figure 1.5). Whereas, the second phase occurs in the presence of low BMP signaling created by the inhibitory effect of GREM1 to release the natural inhibitory effect of BMPs on FGFs (Ganan et al., 1998; Pizette and Niswander, 1999). Here, SHH takes 6h to induce *Grem1* and GREM1 takes about 6h to induce AER-*fgf* expression making a total of 12h loop, making GREM1 as a node between the BMP-GREM1 and the SHH/GREM1/FGF modules (Benazet et al., 2009; Figure 1.5). The third interesting nature of the SHH/GREM1/FGF loop is its self-terminating nature where GREM1 plays a crucial role and this will be discussed in the next section (reviewed in Zeller et al., 2009).
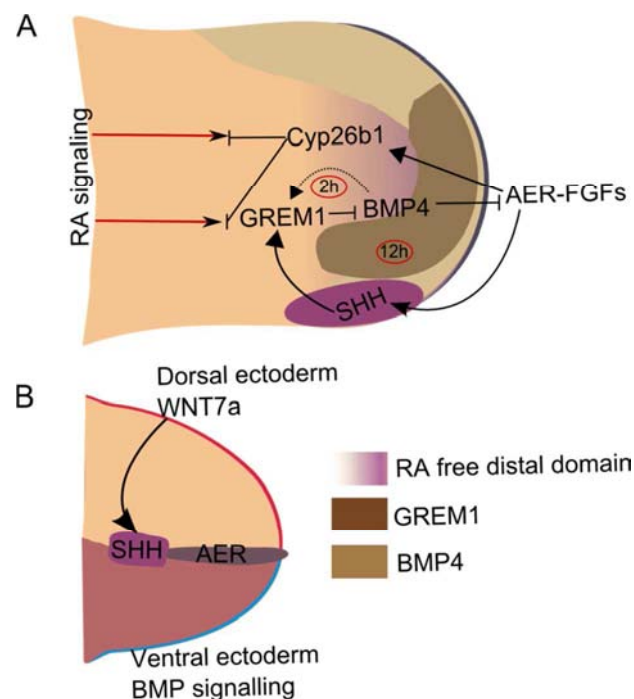

Figure 1.5: Representation of cross interactions between the key signaling pathways controlling limb development. (A) Interactions occur during limb distal propagation stage (mouse E11.5) link most of the important signaling pathways through the positive ZPA-SHH/GREM1/AER-FGF and the negative AER-FGF/Cyp26B1/RA modules.

By E9.5in mouse (stage HH17-18 in chick), BMP4 (BMP2 in chick) upregulates its own antagonist, GREM1 (high BMP signaling; fast loop of ~2h) which will inhibit BMP signaling during distal propagation stage (~until E10.5 in mouse and stage HH23 in chick). Thus, the inhibitory effect of BMPs on AER-FGFs will be relieved resulting in high AER-FGF accumulation. Meanwhile, ZPA-SHH will induce transcription of GREM1 to maintain its positive regulation to the AER-FGFs that reciprocally maintain ZPA-SHH. This whole loop functions to upregulate AER-FGFs, ZPA-SHH and mesenchymal-GREM1 in the presence of low BMP activity and takes about 12h (Benazet et al., 2009). Recently, it was identified that the high AER-FGFs maintained by the SHH/GREM1/AER-FGF loop upregulated *Cyp26b1* in the distal mesenchyme. This enables the clearance of RA from the undifferentiated zone (represented by purple gradient) and facilitates limb distal propagation (Probst et al., 2011). These loops connect the SHH, FGF, BMP and RA signaling pathways **(B)** The DV patterning molecule functioning in the dorsal ectoderm, WNT7a is also necessary for proper ZPA-SHH expression because in its absence *shh* expression is abolished (Yang and NIswander, 1995). In (A) the limb is represented anterior on top and proximal side to the left and in (B) the limb is represented dorsal to the top and proximal to the left.

This year, a new antagonistic module of AER-FGF/Cyp26B1/RA was identified and linked with the already existing SHH/GREM1/AER-FGF loop based on *shh* deficient mouse limb buds and computational simulations (Probst et al., 2011; Figure 1.5). When they made a differential screening for the genes up or down regulated in *shh* null mouse limbs, they found *Cyp26B1* to be downregulated in the distal limb while the RA responsive genes like *Meis1* and *Meis2* were upregulated with a distal expansion. Further analysis revealed that this effect is indirect through the AER-FGFs as demonstrated by *Cyp26b1* induction upon FGF4 bead implantation either in the wild type or *shh* null limb bud mesenchyme (Probst et al., 2011). This explains the indirect role of SHH in the clearance of the RA from the distal mesenchyme through the AER-FGFs to enable distal propagation through the antagonistic newly identified AER-FGF/Cyp26B1/RA module to the self-regulatory SHH/GREM1/AER-FGF positive feedback loop. These loops connect the major limb signaling pathways FGFs, RA, SHH and BMPs and provide evidence for the cooperative establishment of PD and AP patterning.

BMP signaling is necessary for initial AER induction by defining the ectodermal DV boundary (Pizette et al., 2001). However, high BMP activity during distal propagation stages has an adverse effect on the AER (Pizette and Niswander, 1999; Michos et al., 2004), emphasising a transient requirement of BMPs for the establishment of functional AER and distal outgrowth (Hayashi and McMahon, 2002). The low and persistent BMP signaling is crucial to create correct length AER which is not only important for PD patterning but also for proper AP patterning, since anteriorly extended AER can cause polydactylies (Selever et al., 2004). WNT and BMP signaling

from the non-ridge ectoderm patterns the DV axis (Chen and Johnson, 1999). Interestingly, removal of dorsal ectoderm caused loss of posterior structures and *shh* expression in the ZPA mediated by dorsal ectoderm-produced WNT7a (Yang and NIswander, 1995). Together, these experimental results indicate the connection between the patterning of limb DV, AP and PD axes.

1.1.6. TERMINATION OF OUTGROWTH

The self-terminating SHH/GREM1/FGF loop has been proposed to take different sequence to do so in chick and mouse. Manipulation of the loop components, the AER-FGF (FGF4), GREM1 or SHH just prior to the outgrowth termination stage in chick (HH27) gave different results. When either FGF4 or GREM1 was overexpressed in the posterior limb, they were able to induce the expression of *shh* or *fgf4* and *shh*, respectively. But, a SHH bead implanted in the posterior limb failed to upregulate both *Grem1* and *fgf4* expression suggesting the inability of mesenchymal cells to respond to SHH signaling in favour of Grem1 expression (Scherz et al., 2004). Moreover, cells that produce SHH are refractory to express *Grem1*. Thus SHH descendants resulted from SHH dependent cell proliferation and outgrowth create a broad domain adjacent to the ZPA that will not express Grem1. By stage HH27 in chick, cells competent to express *Grem1* become too far to receive ZPA derived SHH signaling and mark the loop termination (Scherz et al., 2004; Figure 1.6).

Verheyden and Sun (2008) identified an inhibitory AER-FGF/GREM1 loop in mouse and integrated it with the SHH/GREM1/FGF positive loop. As per their model, during the distal propagation stages of HH18-23 in chick and E9.5-10.5 in mouse, the low FGF signaling from the AER promotes *Grem1* expression through SHH´s maintenance. GREM1 in turn relay SHH signaling to the AER-FGFs and upregulate their expression. This result in the accumulation of all the three proteins: GREM1 in the mesenchyme adjacent to the AER, ZPA-SHH and AER-FGFs. When AER-FGF signaling surpasses a threshold level, it begins to inhibit *Grem1* expression more or less at stage HH23-27 in chick and E10.5-12 in mouse. Due to this inhibition and continuous growth of the distal limb mesenchyme, the *Grem1* negative domain expands pushing the *Grem1* positive domain away from the AER and the ZPA (Verheyden and Sun, 2008) triggering a sequence of termination mechanisms which take a different order in mouse and chick (Verheyden and Sun, 2008; Scherz et al., 2004; Figure 1.6). In mouse, first, *Grem1* negative domain will stop relaying

SHH signal to the AER-FGFs and permit them to fall which is followed by the ZPA-SHH and then by GREM1 (Verheyden and Sun, 2008). Whereas, in chick, the *Grem1* negative domain will be too far for the ZPA-SHH to signal and so the positive regulation of SHH on *Grem1* expression is stopped owing to the downregulation of AER-*fgfs* and finally to the ZPA-SHH (Scherz et al., 2004).
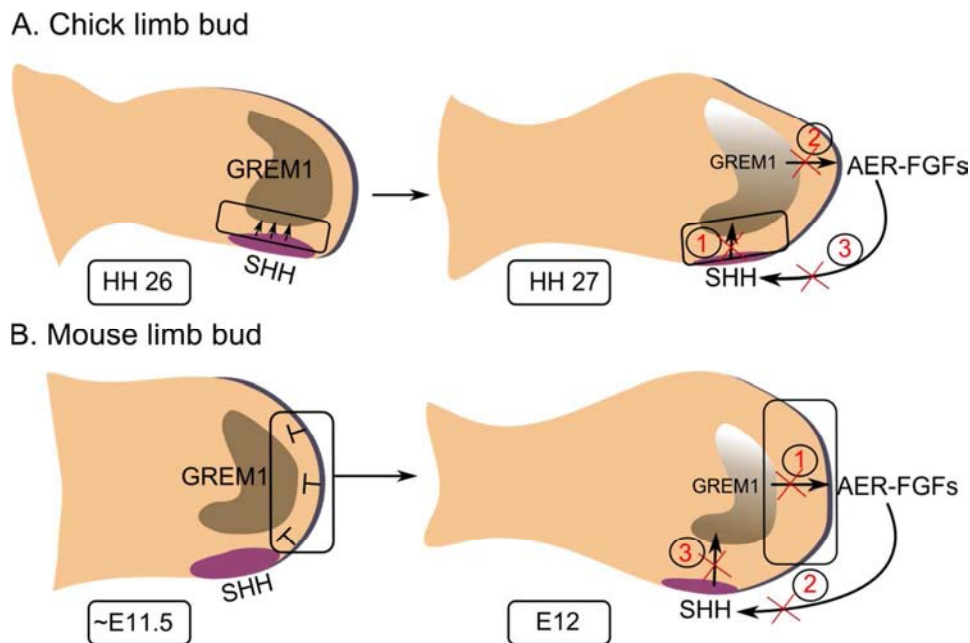
Figure 1.6: Outgrowth termination mechanisms in chick and mouse. (A) In chick, before *shh* expression ceases at stage HH27, *Grem1* expression domain is displaced anteriorly from the ZPA due to SHH dependent cell proliferation of its descendants. Thus, *Grem1* will no longer be upregulated upon SHH signaling and it starts to reduce. The reduction of GREM1 leads to a release of BMP inhibition that in turn will downregulate AER-*fgfs* and consequently ZPA-*shh* expression by stage HH27 (Scherz et al., 2004). **(B)** In mouse, between stage E10.5-12 the continuously upregulated AER-FGFs through the SHH/GREM1/AER-FGF loop will surpass a threshold level above which it starts to inhibit *Grem1* expression. As a result, GREM1 domain will be proximally displaced, that makes it difficult to maintain AER-FGFs. In addition, GREM1 domain will also be pushed anteriorly to receive inductive signals from ZPA-SHH. This leads to the overall fall of AER-*fgfs* first and then for the sequential loss of ZPA-*shh* and mesenchymal-*Grem1* expressions (Verheyden and Sun, 2008). All limbs are represented anterior on top and proximal side to the left.

1.2. TEMPORAL CONTROL

The central question in developmental biology is how a group of undifferentiated progenitor cells undergo differentiation in a timely and co-ordinated manner to create an entire

living being. What mechanisms give the notion of time for the formation of either definite or transient structures? There must be an endogenous oscillatory process functioning during embryogenesis. Now, we know that cells "can count time" through their molecular clock which was discovered in 1997 (Palmeirim et al., 1997) in the presomitic mesoderm (PSM). This work was considered to be a 20th century milestone in developmental biology (Skipper, 2004) and opened a new field of research (Andrade et al., 2007).

1.2.1. SOMITOGENESIS

After fertilization, the embryo undergoes repeated cleavage to form the blastoderm, which in the chick is located on the top of a cavity named blastocoel, which separates it from the yolk. Soon, the blastoderm splits apart to form two layers: the upper epiblast and the lower hypoblast. This is followed by the formation of a triangular thickening at the junction between the extraembryonic tissue and the posterior epiblast, the Koller sickle, and an extension of it towards the anterior region of the embryo gives rise to the primitive streak (PS). At the level of the PS, epiblast cells rapidly proliferate and start to invaginates inward giving rise to a trilayered embryo, as a consequence of the process of gastrulation. At the rostral end of the fully extended PS, a small thick structure known as the Hensen´s node (HN) arises. It is considered as the embryonic organizer and establishes the left-right asymmetry either by monociliary leftward movements or by cellular rearrangements towards the left side which eventually establish asymmetric gene expression (Levin, 2005; Raya and Izpisua Belmonte, 2006; Gros et al., 2009). While the epiblast cells ingress through the PS, they acquire positional information (Schoenwolf et al., 1992). Cells that ingress earlier form more anterior structures compared to cells ingressing later. FGF signaling through FgfR1c (Chuai et al., 2006) has been implicated in PS cell movement where anterior FGF4 has been demonstrated as a chemo attractant and posterior FGF8 as repellent (Yang et al., 2002). As gastrulation occurs, the HN begins to regress caudally until it reaches the posterior end of the embryo at stage HH12 in chick embryo. Thus the addition of cells added by ingression through the PS no longer occurs, but gastrulation continues from the tailbud (Figure 2.2). The PS and the tailbud have similarities at the level of gene expression and morphogenic movements (Catala et al., 1995; Cambray and Wilson, 2007).

The presomitic mesoderm (PSM) tissue is generated during gastrulation, and arranges itself in two bands flanking the embryo axial structures, neural tube and notochord. Somitogenesis is

the process of the formation of somites, the transient metameric units of the vertebrate embryo. Somites form in pairs as epithelial blocks pinching off from the anterior-most PSM in an anterior to posterior sequence, beginning immediately after the otic vesicle. The specialised feature of somitogenesis is its species conserved periodicity and total number. In chick, for every 90 min one pair of somites is formed until the total of 52 pairs is reached. In mouse and zebrafish, it takes 120 min and 30 min, respectively, to make a pair of somites. However, there could be a variation in this standard time to form the first and last few pairs of somites. For instance, recently it was demonstrated to take about 150 min to form the last pair of somites in chick (Tenin et al., 2010). In order to uniformize the process of somitogenesis between species and for better scientific clarity, somites are represented by roman numbers based on their AP position in the embryo, in a way that the forming somite is considered as S0 and presumptive somites starting caudally adjacent to somite S0 are represented with negative roman numbers (S-I, S-II etc.), while the completely formed somites beginning from the somite placed immediately rostral to S0 are mentioned by positive roman numbers (SI, SII…etc) (Christ and Ordahl, 1995; Pourquie and Tam, 2001) (Figure 2.2). Moreover the number of somite pairs has been used as a standard way to classify chick embryo for first ~2.5 days of its development as per Hamburger and Hamilton table (Hamburger and Hamilton, 1951; Hamburger and Hamilton, 1992).

Formation of epithelial somites from the rostral PSM is a complex process which involves extensive cell movements, mesenchymal to epithelial transitions and several molecular and environmental cues (Rifes et al., 2007; Martins et al., 2009; Benazeraf et al., 2010). The PSM cells are highly dynamic and the process of somite epithelialization has been proposed to take much longer than the periodicity of somitogenesis in chick (Martins et al., 2009). The mesenchymal to epithelial transition of PSM cells involves two steps of epithelialization both of which starts medially and recruits the adjacent lateral cells (Martins et al., 2009). This kind of medial to lateral somite boundary formation where medial cells behave autonomously while the lateral cells require the medial cells for their segregation has been previously reported (Freitas et al., 2001). Ectoderm plays a crucial role in somitogenesis, as in the absence of ectoderm, PSM explants failed to form somites, (Palmeirim et al., 1998; Borycki et al., 2000) which was later shown to be due to its ability to maintain extra cellular matrix (ECM) through the production of fibronectin (Rifes et al., 2007). In fact, employing advanced imaging techniques, the requirement of the ECM in modulating cells shape, motility and differentiation status has been exemplified during

somitogenesis (Martins et al., 2009). As the mature PSM cells are incorporated into somites in the rostral PSM, the caudal growth zone replenishes the PSM with new cells allowing the embryo to elongate posteriorly and develop properly. Pourquie and co-workers implicated the posterior to anterior gradient of random cell motility relative to the ECM endowed by FGF signaling in the posterior elongation of amniote embryo (Benazeraf et al., 2010).

Somites, the transient structures will eventually differentiate into two main sub-domains: sclerotome and dermomyotome, which will further form definite structures of the vertebrate body (Figure 1.1). WNT, BMP and SHH signals exerted by the surrounding tissues, such as ectoderm, notochord, neural tube and LPM, are responsible for this differentiation. Epithelial to mesenchymal transition occurs in the ventro-medial portion of the somite to form the sclerotome which contains the precursors of the cartilage and bone, giving rise to the axial skeleton and ribs depending upon their location within the somite. The cells in the dorso-lateral side of the somite initially retain their epithelial nature and make the dermomyotome, which further divides into the dermatome and myotome during later developmental stages to derive the dermis of the back and the skeletal muscles, respectively. In fact, another sub-compartment known as the syndetome is established and maintained by the sclerotome and myotome, which give rise to the tendons (Brent et al., 2003). Although no distinct margin exists, the position of the cells in the dermomyotome and their surrounding signals determines their eventual fate. The medial dermomyotome is specified as the epaxial myotome by the floor plate and notochord produced SHH (Borycki et al., 1999). Epaxial myoptome forms the back muscles. On the other hand, WNT signaling from the ectoderm and BMP signaling from the LPM defines the hypaxial muscles of the limb, diaphragm and body wall (Chen et al., 2004; Yokoyama and Asahara, 2011). All these events should occur in sequence and in a timely manner because defects in somitogenesis cause common human developmental disorders (Turnpenny et al., 2007).

1.2.1.1. Theory and experimental evidences for Clock and wavefront concept

The prevailing classical model predicting the mechanism behind somitogenesis is the ``Clock and Wavefront model´´ proposed in 1976 (Cooke and Zeeman, 1976). This model points to an intrinsic oscillator functioning in the PSM between permissive and non-permissive phase which controls timely somite formation. The second component of this model is the wavefront

which corresponded to the clear embryonic gradient of maturation. When the clock is in the permissive phase, the wavefront moving anteriorly, will allow the maturation of PSM cells in the anterior most PSM.
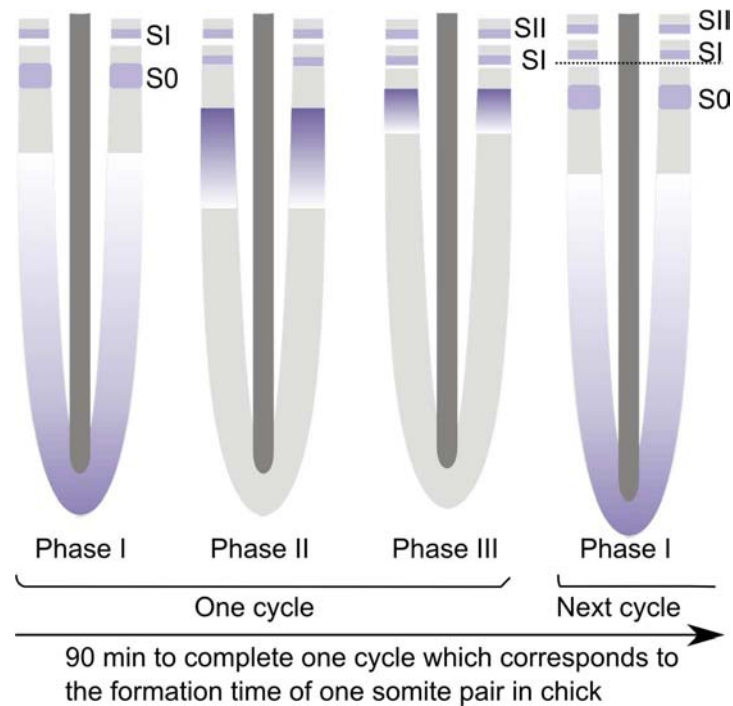
Figure 2.1: somitogenesis molecular clock. In chick, somite pairs are formed from the rostral tip of the PSM every 90 min. This periodicity is underlined by the evolutionarily conserved molecular oscillator functioning in the PSM. Here, the cyclic *hairy1* expression in chick PSM of embryos belonging to the same stage is presented as a schematic illustration. Each *hairy1* expression cycle takes 90 minutes and culminates in the complete separation of one somite pair from the anterior-most PSM (Palmeirim et al., 1997). The forming somite is represented as S0 and the somites immediately anterior to the latter are identified as SI. This kind of dynamic gene expression is observed in genes belonging to Notch, FGF and WNT signaling pathways in chick, mouse, zebrafish, etc (Krol et al., 2011). The PSM is positioned anterior on top.

The first evidence for the existence of the intrinsic clock in the PSM was provided by Palmeirim et al. (1997). These authors identified different expression patterns of the Notch target gene, *hairy1*, a member of the Hairy and enhancer of split (HES/HER) family of the basic helix loop helix (b-HLH) transcription factor, in the PSM of chick embryos belonging to the same stage.

Hairy1 expression was found to oscillate in the PSM and for sake of simplicity the variable expression patterns were grouped in three phases (Figure 2.1).

1. **Phase I**: *hairy1* is expressed in a broad caudal PSM domain along with a narrow stripe in the anterior PSM roughly corresponding to the caudal portion of the presumptive somite.

2. **Phase II**: *hairy1* transcripts become completely absent in the caudal PSM and are detected in a broader domain in the anterior PSM, while the more anterior narrow stripe is still maintained in an even narrower domain.

3. **Phase III**: Now, the presumptive somite is almost formed and the most anterior stripe of *hairy1* is restrained to its posterior region, while the other *hairy1* domain gets more anterior and thinner than in phase II. Meanwhile *hairy1* appears again in the caudal PSM representing phase I of the next cycle.

The time it takes to complete all these three phases and return to phase I is 90 min that culminate in the time to form a new pair of somite in chick (Palmeirim et al., 1997). They also showed that generation of these oscillations is an intrinsic property of the PSM tissue and is not affected by cell movement or signals coming from the posterior PSM (Palmeirim et al., 1997). Many attempts to mess the original orientation of the PSM tissue by transplantation to various locations or flip flop between them or ablation of a portion of the tissue failed to cause any alternations in its original pattern (Packard, 1978; Aoyama and Asamoto, 1988; Palmeirim et al., 1998), pointing to the robustness of segmental determination (Dubrulle et al., 2001).

Following the discovery of *hairy1* in chick PSM, many more cyclic genes in different model organisms were added to the list. However, all of them were from Notch signaling pathway, until the first WNT target gene *axin2* was found to have such oscillatory behaviour in mouse (Aulehla et al., 2003). Subsequently, many other segmentation clock genes belonging to the Notch, WNT and FGF signaling pathways were identified to have oscillatory expression in the PSM both by classical method (Andrade et al., 2007) and by microarray analysis in mouse, chick and zebrafish, (Dequeant et al., 2006; Krol et al., 2011) indicating their evolutionary conserved nature. Although previous findings suggest that the WNT signal clock genes oscillate out of phase from the Notch and FGF signaling cyclic genes in mouse (Dequéant et al., 2006), recent data from chick and zebrafish do not suggest such clear phase alterations (Krol et al., 2011). Among the 100s of cyclic genes identified by genome wide search, only HES/HER members coincided in the list of genes identified from mouse, chick and zebrafish PSM. Moreover, orthologs of HES/HER members were

also identified to present oscillations in other species suggesting their importance in the clock gene network and conservation among species (Krol et al., 2011). Jouve et al. (2002), proposed that the dynamic oscillatory gene expression is not only present in the mature PSM tissue, but also in its precursors in the PS, based on their analysis in early gastrulation stages until the formation of the first somite. To know more about the cyclic gene expression in vivo, transgenic mice that have a special construct with ubiquitinated firefly luciferase as reporter was used (Mazamisu et al., 2006). Firefly luciferase has the ability to quickly degrade (within 20 min, which corresponds to the half-life of Hes1 protein) and gets activated making it a suitable reporter protein to study the dynamic HES1 patterns. In combination with the real time bioluminescence imaging system, Mazamisu and co-workers recorded Hes1 expression for 15 hours which clearly oscillated with 2h periodicity (Masamizu et al., 2006).

Table 2.1: Comprehensive presentation of the PSM oscillatory genes belonging to the Notch, FGF and WNT signaling pathways in mouse, chick and zebrafish. Several cyclic genes have been identified in these species which represent a total of 82 in mouse, 182 in chick and 24 in zebrafish (Krol et al., 2011).

	Mouse	**Chick**	**Zebrafish**
Notch	*Lfng* (Forsberg et al., 1998)	*hairy1* (Palmeirim et al., 1997)	*deltaC* (Jiang et al., 2000)
	hes1 (Jouve et al., 2000)	*hairy2* (Jouve et al., 2000)	*her1* (Holley et al., 2000)
	hey2 (Leimeister et al., 2000)	*hey2* (Leimeister et al., 2000)	*her7* (Oates and Ho, 2002)
	hes7 (Bessho et al., 2001)	*Lfng* (McGrew et al., 1998)	*nrarp* (Wright et al., 2009)
	hes5 (Dunwoodie et al., 2002)	*nrarp* (Wright et al., 2009)	*her15, her2, her4* (Krol et al., 2011)
	nkd1 (Ishikawa et al., 2004)		
	nrarp (Dequéant et al., 2006)		
	Hey1, Id1, Efna1 (Krol et al., 2011)		
FGF	*dusp6* (Dequéant et al., 2006)	*snail2* (Dale et al., 2006)	*tbx16* (Krol et al., 2011)
	snail1 (Dale et al., 2006)	*raf1, Erk, dusp6* (Krol et al., 2011)	
	spry2 (Dequéant et al., 2006)		
	dusp4 (Niwa et al., 2007)		
	spry4 (Hayashi et al., 2009)		
	bcl2l11, egr1 (Krol et al., 2011)		
WNT	*axin2* (Aulehla et al., 2003)	*axin2, T, gpr177, rrm2* (Krol et al., 2011)	*tbx16* (Krol et al., 2011)
	dact1 (Suriben et al., 2006)		
	dkk1, sp5, myc, tnfrsf19, cyr61,shisa2 (Krol et al., 2011)		

The second component of the ``Clock and Wavefront´´ model, the Wavefront has also been experimentally proved. The first proof for the presence of a maturation front in the PSM

that provides the notion of space for somitogenesis was given by Dubrulle et al. (2001). These authors performed a series of different experiments like flip flop transplantations of PSM tissue from different locations, bead implantation and overexpression of *fgf8* in the PSM by electroporation to study the wavefront concept. First, they inverted the orientation of somites from the anterior or posterior PSM and assessed the resulted somites orientation using a caudal somatic marker, *dll1* (Notch ligand: *delta like 1*). When the PSM tissue at the level of S0 or S-I was inverted, the resulting somites were also inverted, whereas the caudal PSM tissue at the level of S-V to S-XII inversion resulted in normal somite formation. But somites S-II to S-IV presented irregular AP segregation within the abnormally formed segmental boundaries (Dubrulle et al., 2001). These set of experiments suggest that by S0, S-I level, somites have fixed AP polarity, while the caudal S-V to S-XII somites are yet to be determined. These determinations occur at the molecular level much before the morphological boundaries are formed. The ectopic boundaries and disorganized *dll1* expression observed after S-II to S-IV inversions suggest S-IV as the possible level of the determination front (DF) (Dubrulle et al., 2001). They further demonstrated this concept by placing FGF8 soaked bead at different positions in the PSM and inhibiting FGF signaling by *in-ovo* application of the FgfR1 inhibitor, SU5402. These experiments confirmed the existence of a DF in chick PSM and suggested its position at the level of S–IV after which FGF bead didn't present any effect on somitogenesis, unlike its ability to make smaller somites when implanted before somite level –IV (Dubrulle et al., 2001). The opposite was also achieved by SU5402 application simply by recruiting more cells to make bigger somites than the normal size (Dubrulle et al., 2001). These experiments reveal that FGF8 bead caused a rostral shift in the DF while SU5402 did the opposite both in chick and zebrafish, (Dubrulle et al., 2001; Sawada et al., 2001) pointing to a wavefront mechanism based of the caudo-rostral *fgf8* gradient in the PSM. This is substantiated by the fact that posterior PSM cells are maintained in an undifferentiated state by FGF signaling and they can only differentiate when they pass certain threshold level of this signal (Vasiliauskas and Stern, 2001). Soon, the proposed DF-*fgf8* gradient was illustrated to be established through mRNA decay (Dubrulle and Pourquie, 2004). Only the tail bud region of the chick and mouse embryo actively transcribes *fgf8* as viewed by the intronic probe expression and so the caudo-rostral *fgf8* gradient in the PSM is endowed by mRNA decay (Dubrulle and Pourquie, 2004). This mRNA gradient is translated into a protein gradient in the PSM that interacts with FgfR1, the only FgfR expressed in the PSM (Wahl et al., 2007), creating a graded

FGF activity. The intracellular pathways activated by FGF signaling in the PSM vary between species: chick and zebrafish PSM presents a p-Erk gradient indicating the role of Erk/MAPK signaling (Sawada et al., 2001; Delfini et al., 2005), whereas it is identified as the Akt/PI3K pathway in mouse (Dubrulle and Pourquie, 2004b).
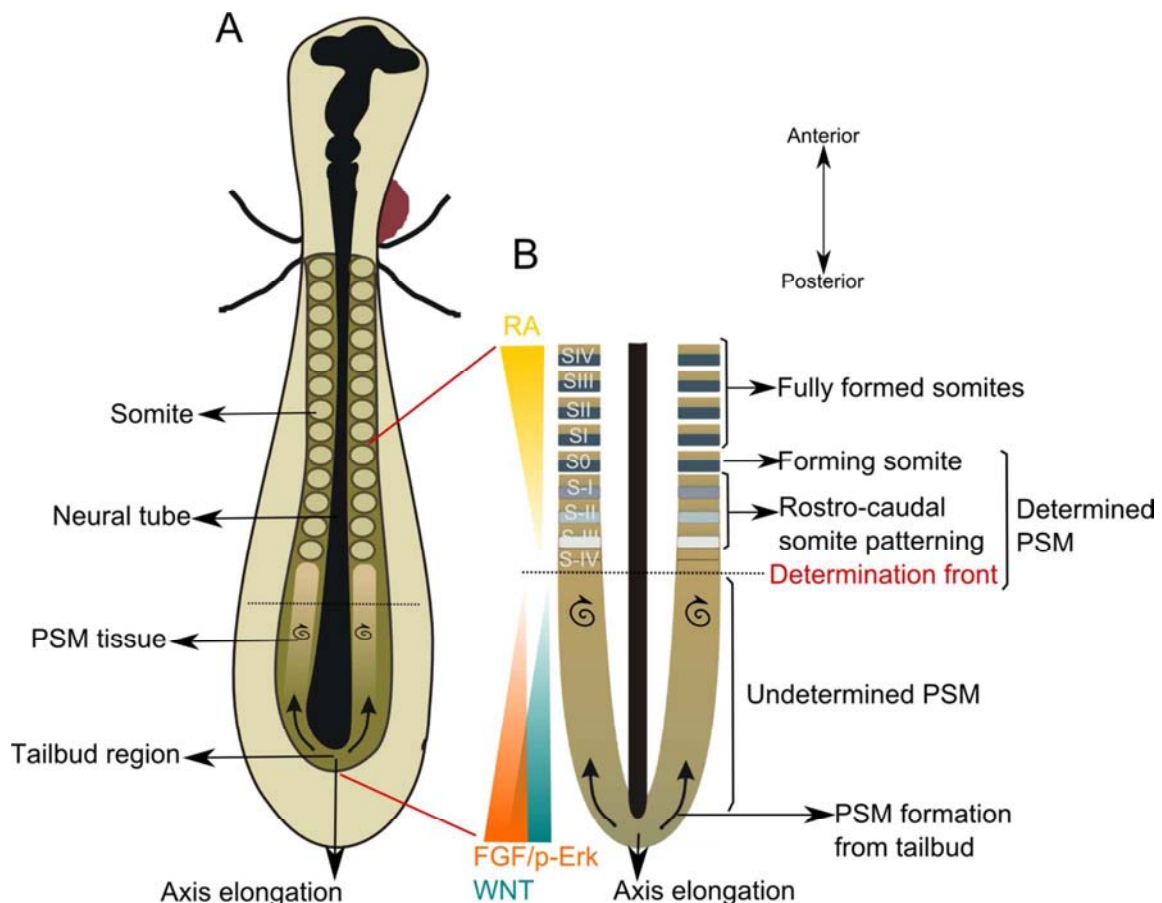
Figure 2.2: An overview of somitogenesis, molecular clock and the determination front concept. (A) Dorsal view of stage HH11 chick embryo. Epithelial Somite pairs are periodically formed from the anterior most tip of the PSM in an AP manner. As the PSM tissue is depleted by somitogenesis it will be replenished with new cells from the tailbud stem cell zone and the embryo elongates posteriorly. For proper somitogenesis to occur, the PSM cells should have the notion of time and space which are provided respectively by the molecular clock and the determination front. **(B)** Enlarged view of posterior embryo highlighting determination front (DF). The DF is positioned more or less in the two third level of the PSM by the confrontation of anterior-posterior RA and the posterior-anterior FGF (and WNT) signaling (Dubrulle et al., 2001; Diez del Corral et al., 2003; reviewed in Dequeant and Pourquie, 2008). The FGF signaling gradient is translated into p-ERK activity gradient which takes major role in positioning somite boundaries through its cooperative function with the molecular clock (Niwa et al., 2011). Rostral to the DF, the PSM tissue is molecularly determined. Here, cells undergo mesenchymal-epithelial transition and somite rostro-caudal patterning

(levels S-I to S-IV). Caudal to the DF, mesenchymal cells are maintained in an undifferentiated proliferative state by FGF and WNT signaling (Naiche et al., 2011). The forming somite is represented as S0 and the fully formed somites as SI to SIV.

The functional relevance of the graded FGF activity in chick was first tested by constitutive activation and inhibition of ERK signaling, which mimics overexpression and downregulation of FGF8 (Delfini et al., 2005). They showed that ERK activity regulates PSM cell movement and converts the FGF activity gradient into cell motility gradient which decreases towards the anterior PSM, enabling them to undergo proper somitogenesis (Delfini et al., 2005). This PSM cell motility was further confirmed by time lapse microscopy which implicated it in the caudal extension of chick embryo (Benazeraf et al., 2010).

Despite of the strong implication of FGF8 signaling in the PSM maturation front, mouse embryos lacking FGF8 in the PSM do not have any somitogenesis abnormalities (Perantoni et al., 2005). Homozygous null mutations for other FGFs expressed in mouse PSM: *fgf3, fgf5, fgf15, fgf17, fgf18* and *fgf4* also show no early somitogenesis defects or die before somitogenesis (Sun et al., 1999; Perantoni et al., 2005; Itoh and Ornitz, 2008). The functional redundancy between FGFs is well known and could be accounted for the lack of phenotypes. The ideal candidate to evade this problem is to delete FgfR1, the only FgfR expressed in the PSM (Wahl et al., 2007). When such an attempt was made (Wahl et al., 2007; Oginuma et al., 2008), somitogenesis was affected progressively, while the anterior somites formed normally.

A parallel signaling pathway working alongside of the FGF signaling to maintain the caudal PSM cells in an undifferentiated state is the WNT pathway (Aulehla et al., 2008; Dequeant and Pourquie, 2008). Manipulation of canonical WNT signaling is accompanied by loss of FGF signaling and causes shifts in the DF (Aulehla et al., 2003; Aulehla et al., 2008; Dunty et al., 2008). Thus, it is difficult to conclude whether the somitogenesis defects observed are due to the primary loss of WNT signaling or due to the secondary loss of FGF signaling.

The most recent study performed to understand the true DF signal in the PSM produced the phenotype one could expect from a DF signal loss (Naiche et al., 2011). When the DF signal is abolished from the PSM, the entire PSM tissue will lack the undifferentiating cue and differentiate prematurely. Naiche et al. (2011) applied the strategy of compound mutants to understand the actual role of FGF signaling in somitogenesis and found that the loss of *fgf8* and *fgf4* in the PSM completely disrupts the DF. Additionally, they also showed that restoration of

WNT signaling by constitutive activation of *β-catenin* in the PSM of *fgf8/fgf4* double KO mouse was unable to reverse the lost wavefront activity, proposing FGF8 and FGF4 as the sole mediators of wavefront activity (Naiche et al., 2011). According to their model, both FGF and WNT signaling reciprocally upregulate each other in the caudal PSM and maintain the cells in an undifferentiated state. But, only FGF signaling facilitated by FGF8 and FGF4 mediate the maturation front activity and position the DF at the threshold level above which cells will become determined to form somites and undergo epithelialization (Naiche et al., 2011).

Both FGF and WNT signaling gradients act from the caudal to rostral embryonic axis. The opposing gradient that runs from the rostral to caudal axis is the RA signaling whose confrontation with the maturation front is also important to position the DF (Diez del Corral et al., 2003). *Raldh2*, the RA synthesising enzyme, is expressed in the matured somites and in the anterior PSM of chick embryo. Treatment with RA agonist induces a drastic reduction or loss of *fgf8* levels, while, absence of RA signaling in the vitamin A deficient quail embryos leads to an increase in *fgf8* domain and consequent formation of smaller somites. This phenotype reflects the results obtained upon rostrally shifted DF by FGF8 bead implantation (Dubrulle et al., 2001). Moreover, FGF8 soaked beads placed in the anterior PSM were able to repress *Raldh2* expression. These results indicate that there is mutual inhibition of RA and FGF signaling pathways and this antagonism is involved in defining the position of the DF and thus somite boundary formation (Diez del Corral et al., 2003). In chick PSM, WNT8c facilitates this mutual antagonism by ensuring activation of RA signal near the DF and provides a transition switch from the FGF mediated stem zone to the RA mediated differentiation zone (Olivera-Martinez and Storey, 2007). Thus, the molecular clock and the wavefront provide PSM cells respectively with the notion of time and space, enabling proper somitogenesis. Anterior-posterior somitic compartments are determined only when cells pass a certain threshold of FGF signaling (above the DF). The region of PSM below the DF is maintained in a proliferative undifferentiated state and called the undetermined PSM. The PSM above the DF harbouring around 3 to 4 molecularly determined somites is called the determined PSM. Once cells enter the determined PSM, several changes occur: RA signaling takes over FGF signaling, anterior-posterior polarity of somites is specified at the molecular level, the clock comes to a halt and mesenchymal-epithelial transition progressively takes place, allowing morphological somite boundaries to be gradually formed (Figure 2.2).

1.2.2. THE LIMB MOLECULAR CLOCK

In 2007, after a decade of the discovery of the somitogenesis molecular clock, work from our lab reported the first evidence for the existence of a molecular clock functioning in the limb distal mesenchyme. Palmeirim and co-workers identified the cyclic expression of the Hairy/Enhancer of split (HES) family gene *hairy2* in the chondrogenic precursor cells with a 6h periodicity (Pascoal et al., 2007; Figure 2.3).
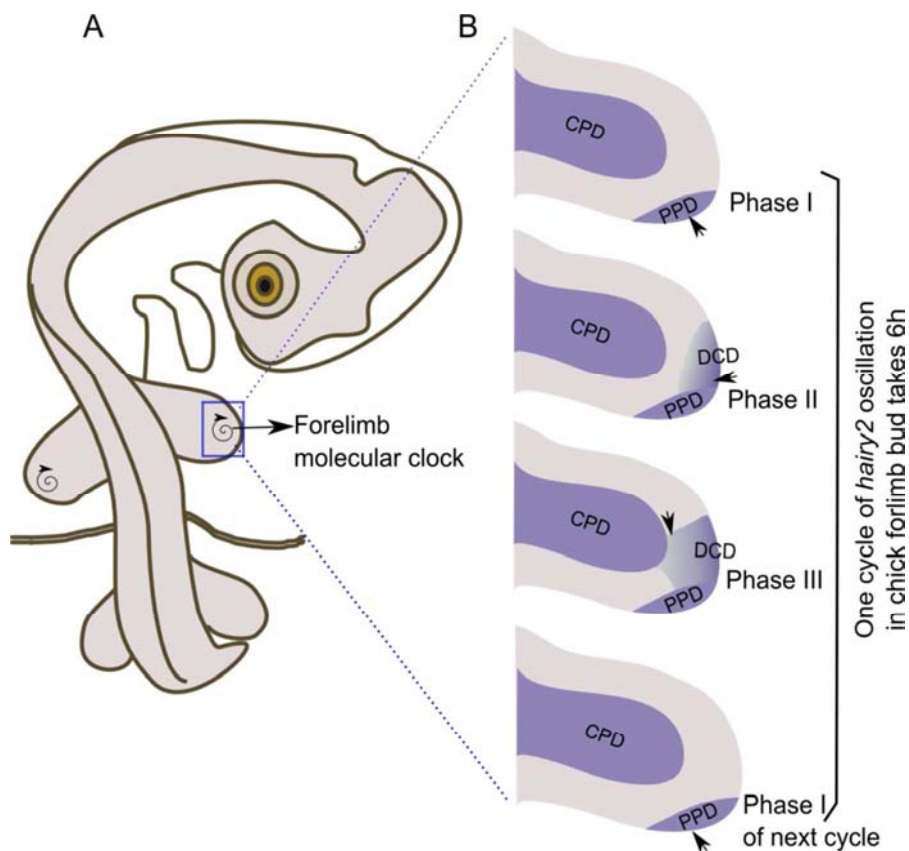
Figure 2.3: Limb molecular clock. (A) Dorsal view of stage HH24 chick embryo showing *hairy2* mRNA based molecular clock in the distal mesenchyme of forelimb bud. **(B)** Schematic representation of dynamic *hairy2* expression in forelimb buds belonging to the same stage embryo (HH24). Each illustration depicts different phases of *hairy2* expression. *hairy2* is always expressed in the central mesenchymal domain (CPD) and the posterior distal limb encompassing the ZPA (PPD). Expression of *hairy2* oscillates only in the distal limb mesenchyme (DCD). During Phase I it is detected only in the PPD (arrow in PhaseI); in Phase II, its expression also shows an anterior expansion until the two third of the distal limb mesenchyme (arrow in PhaseII) and in Phase III, *hairy2* is additionally expressed in the region between the central mesenchymal domain and the distal domain of Phase II (arrow in PhaseIII). After these phases, the expression again goes back to Phase I of the next cycle. Together, it takes 6h for *hairy2* to complete all the three phases and enter into the next cycle (Pascoal et al., 2007). For every two such oscillations a new limb bone

element is laid down (chick forelimb second phalanx; Pascoal et al., 2007). All limbs in B are positioned anterior on top and proximal to the left.

The expression profile of *hairy2* showed that this gene is expressed during limb initiation stage and continues to be expressed later in its development until stage HH32. However, dynamic expression patterns in forelimb buds belonging to same stage embryos were prominent from stage HH20-HH28 (Pascoal et al., 2007b). Variable levels of *hairy2* transcripts were observed between the central distal limb mesenchyme and the ZPA in stage HH20-22 and in HH27 and HH28, whereas this dynamic domain was displaced and widened in stage HH23-26 limb buds between the central distal mesenchyme and the AER. Interestingly, these domains correspond to the location of chondrogenic precursor cells during limb development (Saunders, 1948; Vargesson et al., 1997). In order to determine *hairy2's* oscillation period, surgically ablated right wing buds from stage HH24-HH26 embryos were fixed immediately, while the embryo with the left wing bud was reincubated for different time intervals. These experiments demonstrated that *hairy2* in stage HH24-HH26 chick wing buds oscillates with a 6h time period (Pascoal et al., 2007). Furthermore, these authors experimentally showed that the second phalanx of chick wing takes 12h to form, based on the expression of the joint marker *gdf5*. They also proposed a model where they postulate that cells in the distal limb mesenchyme (chondrogenic precursor cells) are undergoing several *hairy2* cycles of expression and for every 12h a limb bone element is laid down from two subpopulation of cells that underwent n and n+1 cycles of *hairy2* oscillations each with 6h (Pascoal et al., 2007).

1.2.3. CLOCK IN NEURAL PROGENITORS AND STEM CELLS

The experiments performed in 2002 showed that the administration of single serum shock to stationary cultured cells could induce cyclic production of both *hes1* mRNA and Hes1 protein in several mouse derived cell lines, such as myoblasts, fibroblasts, neuroblastoma and teratocarcinoma cells. The observed oscillations occurred with a 2h period, corresponding to the periodicity of cyclic gene expression observed in mouse PSM. These findings lead the authors to postulate that *hes1* oscillations occur in many cell types and that the molecular clock originally identified in the PSM could be a widespread mechanism regulating time in many biological systems (Hirata et al., 2002).

The first evidence for oscillatory gene expression in the neural progenitors located in the telencephalon of mouse embryos came from *hes1* mRNA and Hes1 protein oscillations (Shimojo et al., 2008). In these cells, *hes1* oscillations are not downstream of Notch signaling but driven through JAK-STAT pathway, which has been proposed previously to be involved in neural progenitor maintenance (Kamakura et al., 2004). Interestingly, JAK-STAT pathway has been demonstrated to activate *hes1* oscillations also in cultured fibroblasts (Yoshiura et al., 2007). Since, Notch signaling is not implicated in neural progenitor *hes1* expression, the oscillations are not synchronized between cells and show variable periods, making their detection difficult by classical methods. Shimojo et al. (2008) used real-time imaging technique which was already utilized to visualize *hes1* oscillations in mouse PSM (Mazamisu et al., 2006). The dynamic expression was reasoned to provide enough Hes1 to maintain the neural progenitor cells in an undifferentiated pluripotent state and block their progression through cell cycle, while low Hes1 allows the cells that are in the G1-phase to progress through cell cycle (Shimojo et al., 2008). Hes1 maintains neural progenitor cells in a proliferative state and allows them to differentiate into diverse cell types in an organized manner (Kageyama et al., 2007).

Recently, *hes1* oscillations were identified in ESC with 3-5h duration (Kobayashi et al. 2009). Contrary to what has been observed in neuronal progenitors, in ESC Hes1 is necessary for differentiation. ESC with high and low Hes1 levels differentiates into mesodermal and neural fate, respectively (Kobayashi et al., 2009). Furthermore, cyclic expression of *hes1* has also been described in mesenchymal stem cells derived from human umbilical cord blood with 5h periodicity by quantative PCR analysis (William et al., 2007).

1.2.4. SIGNALING PATHWAYS REGULATING CLOCK GENE OSCILLATIONS

Clock genes that belong to Notch, FGF and WNT signaling pathways have been identified so far. However, only HES/HER gene members, considered as the effectors of Notch signaling (Fisher and Caudy, 1998; Rida et al., 2004), fall into the category of common cyclic genes in the PSM of mouse, chick and zebrafish (Krol et al., 2011). Each of these pathways has its own as well as interlinked functions in regulating the somitogenesis clock. However, a constant hunt to identify the true driving force which is responsible for inducing oscillatory gene expression is a key area of research in developmental biology (Aulehla and Pourquie, 2008).

Notch signaling and the molecular clock

Notch signaling is an intercellular communication pathway mediated by direct cell-cell interactions between the Notch receptors (Notch 1-4) and their ligands (Delta or Serrate1 & 2/Jagged1 & 2), which results in the proteolytic cleavage of the intracellular domain of Notch (NICD) by multiprotein complexes containing Presinilin1/ Presinilin2 (Fortini, 2002). This allows the translocation of NICD into the nucleus where it activates the transcription of its target genes (like HES genes) in association with DNA-binding transcription factor RBPJk (Kageyama et al., 2007). HES gene regulations are extensively studied in order to understand the molecular mechanism underlying their cell intrinsic oscillatory transcription. Auto-regulatory negative feedback loops and short half-life of HES genes mRNA and protein have been accounted for their dynamic expression. Accordingly, the half-life of *hes1* mRNA and protein was first identified by Kageyama and co-workers as ~24min and ~22min respectively, (Hirata et al., 2002) owing to *hes1* dynamic expression. The mechanism for the short half-life of mRNA and proteins is distinct. The 3´untranslated region (3´-UTR) of *hes1* gene might be responsible for the short half-life of *hes1* mRNA as it has been previously reported for xenopus *hairy2* mRNA stability (Davis et al., 2001; Hirata et al., 2002). The short half-life of HES1 protein is endowed by protein degradation mediated by ubiquitin-proteasome pathway (Hirata et al., 2002). The self-inhibitory property of HES1 protein by binding to its own promoter (Sasai et al., 1992; Takebayashi et al., 1994) in combination with its short life span can generate *hes1* mRNA and protein oscillations (Hirata et al., 2002). When HES1 protein was constitutively activated by introducing an expression vector into C3H10T1/2 cells, *hes1* mRNA synthesis was repressed by HES1´s autoregulating activity. On the other hand, when *de novo* HES1 protein synthesis was inhibited by cycloheximide treatment, *hes1* mRNA levels enormously increased due to the absence of HES1 to repress its promoter. Under both conditions, *hes1* mRNA failed to oscillate in the cell lines and in mouse PSM, strongly indicating the requirement of periodic degradation and synthesis of HES1 protein for *hes1* mRNA and protein oscillations (Hirata et al., 2002).

Soon after this finding, a dual module negative feedback loop functioning between HES7, Lfng (Lunatic fringe is a Notch target gene encoding glycosyltransferase that modulates Notch signaling) and Notch activity was documented by Bessho et al. (2003). In mouse PSM, HES7 protein inhibits its own promoter and Lfng promoter as revealed by the mutual exclusive domains of *hes7* and *Lfng* mRNA to that of HES7 (Bessho et al., 2003; Chen et al., 2005). Both

hes7 mRNA and HES7 protein are short lived, applying the same mechanisms as that of *hes1* such as the 3´UTR and proteosome mediated degradation, respectively (Chen et al., 2005; Bessho et al., 2003). In order to validate the importance of the short half-life (~22min) of HES7 in its periodic expression, mutant mice with longer half-life (~30min) were generated and these mice exhibited severe segmentation defects and no *hes7* oscillations (Hirata et al., 2004).

Since Lfng is an intermediate component of the dual module negative feedback loop, its inhibition or overexpression perturbs somitogenesis (Evrard et al., 1998; Zhang and Gridley, 1998; Dale et al., 2003; Serth et al., 2003). However, constitutive expression of this gene in chick and mouse PSM provided different results. In chick, *Lfng* cyclic expression in the PSM was abolished suggesting that overexpressed Lfng inhibits Notch activity and eventually its target genes, whereas in mouse, *Lfng* and *hes7* were still dynamically expressed in the posterior PSM irrespective of constitutive Lfng accumulation, questioning the mechanism proposed in chick. Periodic Notch activity predicted by Dale et al. (2003) was experimentally proved in mouse where the authors showed that the oscillations of NICD in the posterior PSM come to a halt in the anterior PSM by Mesp2 (Meso1 in chick) induced *Lfng* expression (Morimoto et al., 2005). Interestingly, two distinct regulatory sequences controlling *Lfng* expression in the posterior (region I) and anterior (region II) regions of the PSM (Saga and Takeda, 2001) were identified and their functional relevance in somitogenesis has also been dissected (Cole et al., 2002; Morales et al., 2002; Shifley et al., 2008). Gene oscillations in region I and II have distinct roles in skeleton development. Disruption of cyclic *Lfng* expression in region I of PSM arrested oscillatory Notch activity and produced defective thoracic and lumbar skeleton, suggesting that dynamic Notch activity in region I is dispensable for sacral and tail skeletal development (Shifley et al., 2008). But, total loss of Notch activity by *presinilin1/ presinilin2* double KO totally abolished cyclic gene expression and somite formation (Ferjentsik et al., 2009), demonstrating the essential role of Notch signaling for vertebrate axial skeleton development.

However, PSM specific-RBPjk or *Lfng* mutants present *hes7* oscillations in the posterior PSM (Niwa et al., 2007) as observed in the PSM of mice constitutively expressing *Lfng* (Serth et al., 2003). Moreover, the cyclically expressed WNT signal antagonist *axin2* still displays dynamic expression in the PSM of mice constitutively expressing NICD in the entire PSM (Feller et al., 2008). These observations argue against Notch signaling as the pacemaker of segmentation clock (Aulehla and Pourquie, 2008). But, several lines of data from mouse, chick and zebrafish point to

a role of Notch signaling in synchronizing gene oscillations in the PSM. In fact, notch signaling is a potential candidate to synchronize cells, since cell-cell communication is a basic requisite for this signaling (Fortini, 2002).
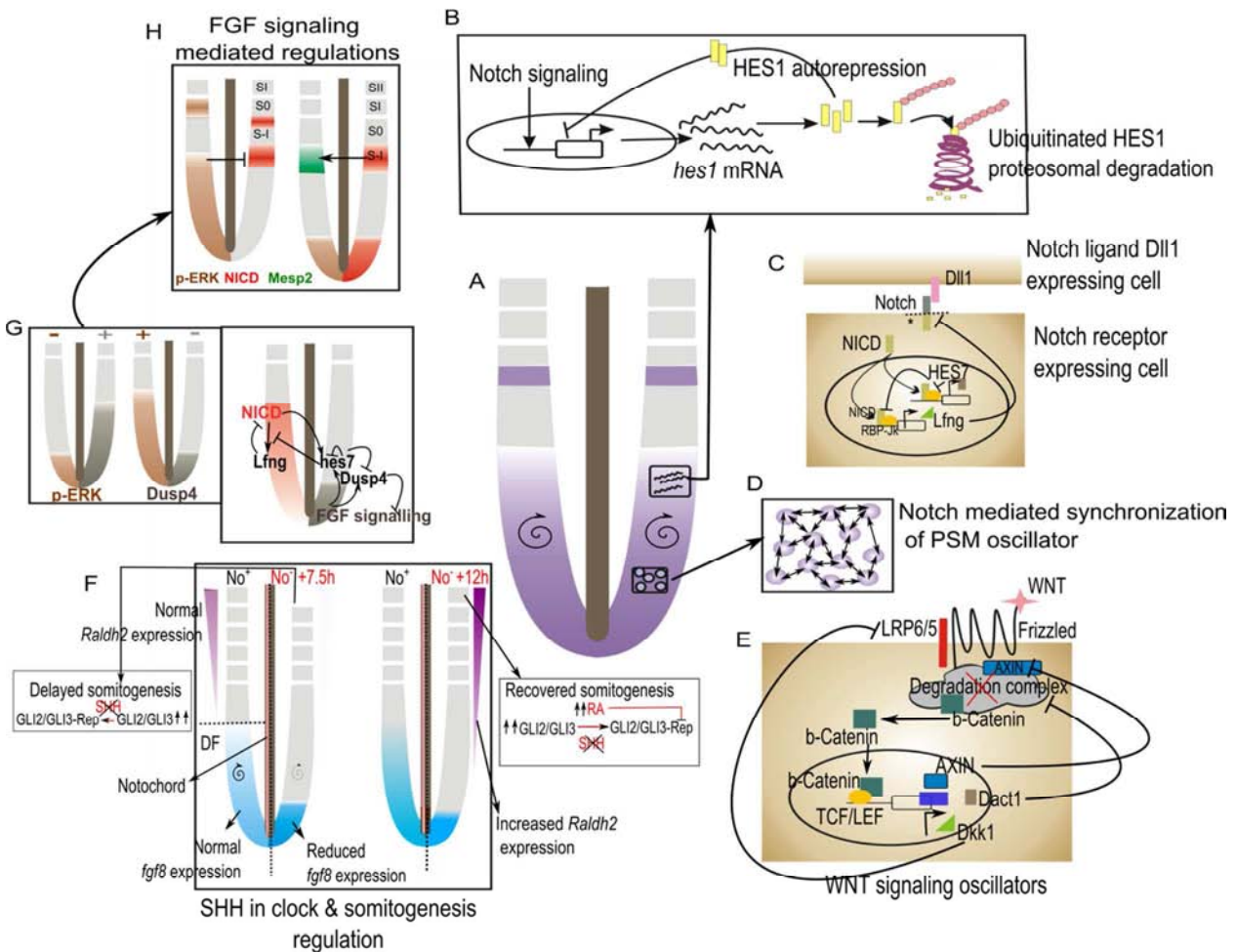
Figure 2.4: Somitogenesis molecular clock regulations. (A) Representation of mouse PSM presenting *hes1* gene expression. **(B)** Scheme mentioning the short half-life of HES1 protein and its autoregulatory capacity by binding to its own promoter. HES1 protein is ubiquitinated and degraded by proteosomal complexes in about 22 min and since it can repress its own expression this mechanism would generate oscillations of *hes1* mRNA and HES1 protein (reviewed in Kageyame et al., 2007). **(C)** The Notch-Hes7-Lfng loop functioning as the driver of gene oscillations in the PSM. Upon ligand binding, NICD is cleaved (asterisk) and translocated into the nucleus where along with RBP-Jk, it transcribes the target genes such as *hes7* and *Lfng*. HES7, repress its own and Lfng promoter periodically due to its short half-life. This generates oscillations of both *hes7* and *Lfng* expression. Lfng being the negative regulator of Notch signalling, Notch activity also oscillates in the PSM (Bessho et al., 2003, reviewed in Kageyama et al., 2007b). **(D)** Cell-cell contact is crucial for Notch signalling to occur and it serves as a mechanism to synchronize PSM cells

cyclic gene oscillations by reducing the background noise. **(E)** WNT signalling´s contribution to the oscillatory gene network. Several negative regulators of WNT signaling display oscillatory gene expression in the PSM such as, *axin2, dkk1* and *dact1*. WNT activity is reflected as a posterior-anterior gradient of β-catenin (b-catenin) in the PSM. This b-catenin gradient is implicated in determining the position of DetF (Aulehla et al., 2008; reviewed in Dequeant and Pourquie, 2008). **(F)** SHH mediated regulation of clock gene expression and somitogenesis in chick PSM. In the absence of the SHH source, the notochord (No$^-$), somitogenesis is delayed with perturbed *hairy2* and *Lfng* expression (dotted spiral arrow in the side of the PSM No$^-$+7.5h). No$^-$ PSM also has reduced *fgf8* (represented by blue gradient. Compare the gradient between the control and the No$^-$ side of the PSM) and increased *Gli2/Gli3* expression. After 9-12h of incubation in the absence of the No (No$^-$), somitogenesis is recovered with high RA activity provided by elevated *Raldh2* expression (Resende et al., 2010). The ability of RA to inhibit Gli-R activity has been proposed as the mechanism for somitogenesis recovery **(G)** Signaling interactions between FGF and Notch. FGF signalling (grey shade) in the posterior PSM initiates *dusp4* and *hes7* expression which is propagated/ maintained in the anterior PSM by Notch signalling (red shade) through the already mentioned loops in (C). Since, Dusp4 (grey shade) is a negative regulator of FGF signalling, FGF activity in the form of p-ERK (brown shade) also oscillates in the PSM (Niwa et al., 2007). **(H)** FGF activity (brown shade) and Notch activity (red shade) cooperate to form somites. Both p-ERK and NICD display different patterns of oscillation. NICD has a band propagation pattern while p-ERK has an on-off pattern of oscillations. Downregulation of p-ERK at S-I level is crucial for periodic somite boundary formation by Notch induced *Mesp2* expression. Thus, NICD oscillations periodically to mark a group of synchronized PSM cells in the anterior PSM which are released from the PSM by the process of somitogenesis by p-ERK oscillations (Niwa et al., 2011).

Generating gene oscillations is an intrinsic property of not only the PSM tissue but also the individual PSM cells (Palmeirim et al., 1997; Masamizu et al., 2006). In agreement, real-time bioluminescence imaging technique demonstrated the presence of out of synchrony *hes1* oscillations in dissociated PSM cells, where the cells presented a varying period and amplitude of *hes1* cycles, emphasizing the necessity of cell-cell contact for synchronized oscillations (Masamizu et al., 2006). The same was true in chick PSM (Maroto et al., 2005), where pieces of PSM tissue were able to perform *hairy1* oscillations, while dissociated cells were unable to maintain synchronous oscillations. Delta1 mediated synchronization of *hes1* cycles are evident by the periodic oscillations observed in mouse cell lines exposed to Delta1 expressing cells that otherwise present out of synchrony expression (Hirata et al., 2002). Consolidated reports about Notch signaling in synchronous oscillations came from zebrafish. Salt-and-pepper expression pattern of the zebrafish cyclic gene *deltaC* in Notch mutants suggests a role for Notch signaling in synchronizing gene oscillations between neighbouring PSM cells (Jiang et al., 2000). The curious observation of unaffected anterior somites and the deformed posterior somites in most of the

Notch component mutants might be due to desynchrony of oscillations between the PSM cells. Although cells begin their initial cyclic expression normally, they cannot maintain the oscillations in the absence of proper Notch signaling owing to abnormal posterior somitogenesis (Dequeant and Pourquie, 2008). Many other studies in zebrafish, either using genetic or chemical inhibition of Notch signaling or mathematical modelling suggested that DeltaC-Notch intercellular interaction synchronize PSM cells oscillations by reducing their internal noise (Horikawa et al., 2006; Giudicelli et al., 2007; Riedel-Kruse et al., 2007; Dequeant and Pourquie, 2008). Notch signaling in zebrafish somitogenesis has been solely assigned to synchronize oscillations of neighbouring cells (Ozbudak and Lewis, 2008). More recently, disruption of Delta-Notch coupling delayed zebrafish segmentation clock by extending its periodicity and revealed an additional role of Notch signalling in clock period regulation (Herrgen et al., 2010).

FGF signaling and the molecular clock

FGF signaling components have also been identified to be a part of the somitogenesis molecular oscillator in chick, mouse and zebrafish (Dequéant et al., 2006; Krol et al., 2011). At least in mouse, Notch and FGF components oscillate in phase (Krol et al., 2011) suggesting a link between these pathways. Consistent with this, conditional KO of *fgf8/fgf4* in mouse PSM before the onset of somitogenesis affected *Lfng* expression (Naiche et al., 2011), as reported before in PSM specific-*FgfR1* KO mice (Niwa et al., 2007; Wahl et al., 2007). Moreover, Niwa et al. (2007) also showed that FGF signaling is necessary to initiate the expression of *dusp4* and *hes7* in the posterior PSM which is mandatory for their dynamic expression in the anterior PSM. Soon after its initiation by FGFs, HES7 starts to inhibit its own expression (Bessho et al., 2001) and *dusp4´*s expression through its autoregulatory repressor activity and generates their oscillations in the posterior PSM (Niwa et al., 2007). HES7 oscillations generated in this manner are essential for *Lfng* oscillation (Bessho et al., 2003). Together Niwa et al (2007) proposed a model saying that FGF signal initiates *hes7* expression as well as oscillation (HES7 induced) in the posterior PSM which is propagated and maintained in the anterior PSM by Notch signaling, implementing FGF signaling as the base for HES7 generated oscillations (Bessho et al., 2003). On the contrary, FGF components (*dusp6, spry2, snail1*) didn't oscillate in *presenilin1/ presenilin2* double mutant mouse lacking NICD indicating that Notch signaling is necessary for FGF component oscillations (Ferjentsik et al., 2009). However, the finding of Niwa et al. (2007)   was supported by an

observation in zebrafish where FGF-induced *her13.2* expression is necessary for the oscillation of *her1, her7* and *deltaC* (Kawamura et al., 2005), the three molecules considered as the pacemaker of zebrafish PSM oscillator (Dequeant and Pourquie, 2008). Dusp4, being a negative regulator of FGF signaling, also generates oscillatory FGF activity endowed by ERK phosphorylation in mouse PSM (Niwa et al., 2007). Further, FGF induced oscillatory Ras/ERK activity and dynamic p-ERK´s capacity to induce periodic *hes1* mRNA and protein expression is also reported (Nakayama et al., 2008; Niwa et al., 2011) suggesting a p-ERK dependent novel oscillatory mechanism. Controversial evidence for both positive and negative effects of FGF signal inhibition on other pathway gene oscillations is accumulating. Chemical inhibitors of FgfR1 failed to perturb Notch target gene expression in mouse and chick (Dubrulle et al., 2001; Niederreither et al., 2002; Delfini et al., 2005; Gibb et al., 2009), whereas Wahl et al. (2007) observed a quick disruption of WNT target gene *axin2* and a slow but abrogated *Lfng* expression in mouse FgfR1 mutants. Despite the constitutive expression of *Dusp4* in *hes7* mutants, *axin2* still presents dynamic expression, ruling out the possibility of FGF/Dusp4 signaling to be the pacemaker of gene oscillations (Niwa et al., 2007; Hirata et al., 2004).

WNT signaling and the molecular clock

Few WNT cluster genes, such as *axin2* (Aulehla et al., 2003), *dkk1, dact1* and *c-myc* (Dequéant et al., 2006) oscillate in mouse PSM. Surprisingly, none of the chick orthologs (*axin2, dac1* and *nkd1*) are rhythmically expressed in chick PSM (Gibb et al., 2009). But, for the first time, genome-wide analysis identified new putative cycling genes of WNT components in chick: *axin2, T, gpr177* (wnt less) and *rrm2* and zebrafish: *tbx16* PSM (Krol et al., 2011). As it has been already described, in *hes7,* RBPjk and NICD gain of function mutants, *axin2* presents a dynamic expression pattern, suggesting no link between Notch signaling and WNT targets (Hirata et al., 2004; Feller et al., 2008; Ferjentsik et al., 2009). But, when Notch signaling is completely abrogated from the PSM by generating *presenilin1/presenilin2* double KO mutants, *axin2* oscillations were abolished (Ferjentsik et al., 2009) indicating that Notch signaling is operating upstream of WNT targets. On the contrary, *wnt3a* hypomorphic mouse mutants (*vestigial tail* (*vt*) with less *wnt3a* expression in the tailbud) display downregulated *dll1 and notch1* expression as well as present non-dynamic *Lfng and hes7* expression in the posterior PSM (Aulehla et al., 2003; Niwa et al., 2007). This perturbation of Notch target genes in *vt* mutants indicates that WNT

signaling is upstream of Notch. Combining these two signals, Gibb et al. (2009) observed reciprocal regulation of Notch and WNT pathways upon each other's components since, chemical inhibition of any of these pathways disrupted both component genes, suggesting a mutual interaction between Notch and WNT signaling in chick as it has been previously reported in mouse PSM (Ishikawa et al., 2004). In fact, identification of *nrarp* and *nkd1* whose cyclic expression is regulated by both Notch and WNT signaling supports this notion. While the transcription of *nkd1* and *nrarp* requires WNT signal, their oscillatory expression needs Notch signaling in mouse (Ishikawa et al., 2004; Dequeant et al., 2006; Sewell et al., 2009). However, this is not the case in chick and zebrafish, in which *nrarp* expression is only Notch-dependent (Wright et al., 2009).

WNT3a in the posterior PSM is a key ligand for WNT/β-catenin signaling. Similar to the mRNA decay based gradient of FGF8 in the PSM, WNT3a also establishes a posterior-anterior protein gradient in the PSM that is translated into its mediator, the β-catenin protein gradient (Aulehla et al., 2008). Constitutively stabilized β-catenin in mouse PSM restored *Lfng* oscillations in *FgfR1* mutants (Aulehla et al., 2008) which is otherwise absent (Wahl et al., 2007), suggesting that WNT signaling is functioning downstream of FGF signal. But, this is not the case after restoration of canonical WNT signaling in *fgf8/fgf4* double mutant KO mouse (Naiche et al., 2011). Moreover, stabilized β-catenin does not abrogate neither WNT nor Notch target gene oscillations (Aulehla et al., 2007), questioning the possibility of a WNT/β-catenin based clock pacemaker.

SHH regulates the pace of the clock and timely somite formation

The long-time perception of somitogenesis and the underlying molecular clock´s independent operation from the axial structures (neural tube and notochord) was revisited by Resende et al. (2010). They found a strong requirement of the notochord and SHH produced therein for the timely formation of somites and for proper oscillations of the clock genes (*hairy2* and *Lfng*) in chick PSM. When the PSM was isolated from its SHH source, the notochord, only 3-4 somites were formed at a normal pace and further somitogenesis was perturbed. Further analysis has revealed that this is due to a delay in somitogenesis and the periodicity of the clock gene *hairy2* expression. This phenotype was recapitulated upon SHH signal inhibition and rescued by exogenous SHH supplementation accounting notochord-SHH in the timely formation

of somites (Resende et al., 2010). The clock periodicity was altered to 2h 45min-3h in the absence of SHH, instead of the regular 90min (Resende et al., 2010). In the absence of notochord, *fgf8* expression in the tailbud was downregulated while *Raldh2, Gli2* and *Gli3* were upregulated, suggesting a possible role of SHH in determining the position of the DF and involvement of Gli´s in SHH mediated delayed somitogenesis (Resende et al., 2010). Interestingly, this delay in somitogenesis recovered automatically after 9h of incubation with a concomitant increase in *Raldh2* expression. Accordingly, exogenous RA supplementation rescues notochord ablation effects on somitogenesis. In the end, the authors propose a model where the absence of SHH upon notochord ablation upregulates *Gli2/Gli3* in the PSM, which will be processed to the respective repressor forms. High Gli-R activity inhibits molecular clock oscillations and causes a delay in somitogenesis. Upon longer (9h) incubation without SHH source, *fgf8* expression is downregulated in the caudal PSM and enables expanded *Raldh2* expression facilitating the recovery of somitogenesis rate. This should be through the previously described functions of RA to modulate Gli-R activity and *Gli2* transcription (Goyette et al., 2000; Ribes et al., 2009). Overall, this work provides evidence for the role of SHH in DF establishment by warranting the absence of Gli3-R in the PSM and so ensuring the tempo of somitogenesis (Resende et al., 2010).

1.2.5. INTEGRATED CLOCK AND WAVEFRONT IN THE PSM

During somitogenesis, the temporal periodicity provided by the PSM molecular oscillator is translated into the segmental blocks by the posterior-anterior graded wavefront activity. The wavefront is established by the posterior-anterior graded WNT and FGF signaling in the PSM (Dubrulle et al., 2001; Sawada et al., 2001; Aulehla et al., 2007; Dunty et al., 2008), both of which also have their components expressed in a rhythmic manner in mouse, chick and zebrafish, integrating the wavefront and the clock (Aulehla et al., 2003; Dale et al., 2006; Dequeant et al., 2006; Niwa et al., 2007; Krol et al., 2011). Since many of these oscillating genes are modulators of the pathway, negative feedback mechanisms cause periodic pulses of FGF or WNT activity in the PSM (Niwa et al., 2007; Niwa et al., 2011; Aulehla and Pourquie, 2010). Initiation of *hes7* and *dusp4* expression in the posterior PSM by FGF signaling in combination with the autoregulatory effect of HES7 generates *hes7, Lfng, dusp4* and FGF activity (p-ERK) oscillations. These initial oscillations are maintained/propagated by Notch signaling in the anterior PSM (Niwa et al., 2007;

Niwa et al., 2011) making a link between the wavefront FGF signaling and the clock oscillations. Even though, HES7 drives the oscillations of NICD and p-ERK, they present different dynamics: NICD propagates as a band from the posterior PSM to S0 level and p-ERK displays an on/off oscillatory pattern in the posterior PSM to S-II level (Niwa et al., 2011). It is shown that at the DF level, the clock slows down (Niwa et al., 2011) and the graded FGF/WNT signaling regress allowing the expression of *mesp2* and subsequent somite boundary formation (Aulehla and Pourquie, 2010; Niwa et al., 2011). Expression of *mesp2* is positively and negatively regulated by oscillatory Notch signaling and regressing FGF/WNT signaling, allowing a periodic and permissive state for *mesp* expression, respectively (Oginuma et al., 2008; Aulehla and Pourquie, 2010). The concomitant requirement of band propagation and on-off dynamics of Notch and FGF signaling activity in the anterior PSM is shown to be necessary for periodic *mesp2* expression at the S-I level (Niwa et al., 2011). These authors have shown that NICD oscillations in the anterior PSM are 1.5 fold slower compared to the posterior PSM. This enables a sharp segregation of NICD positive cells in the rostral PSM that are freed by the off phase of FGF signaling which allows *mesp2* expression at this level. Lfng mediated PSM cell synchrony is necessary for sharp segregation of Hes7 and NICD domains in the middle and anterior PSM (Niwa et al., 2011). This finding is interesting because FGF signaling (FgfR1-FGF4/FGF8) has been shown to be the sole mediator in positioning DF and acts upstream of WNT and Notch pathways to regulate clock gene oscillations (Wahl et al., 2007; Naiche et al., 2011).

Although Naiche et al. (2011) excluded WNT signaling from being the mediator of DF activity, compelling evidence suggests a role for WNT/β-catenin signaling in axis elongation, determining the size of oscillatory field and PSM maturation (Aulehla et al., 2007). The importance of the posterior-anterior gradient of β-catenin protein was studied by selectively deleting or stabilizing β-catenin in mouse PSM. Early deletion for β-catenin resulted in severe axis truncation with few abnormally formed anterior somites. Constitutively stabilized β-catenin produced embryos with no significant morphological somite boundaries along the axis except for four irregular anterior somites in some cases (Aulehla et al., 2007). Thus, β-catenin, the mediator of WNT signaling in mouse PSM cause axis truncation upon deletion and form longer PSM with delayed maturation upon stabilization, proposing a possible role for graded β-catenin in establishing DF. Under the influence of β-catenin, WNT and NOTCH signal dependent oscillatory genes present dynamic expression for an extended period of time and the somite boundary

defining gene *mesp2* expression was shifted anteriorly (Aulehla et al., 2007). This suggests that β-catenin maintains clock oscillations and its regression in the anterior PSM is necessary to slow down the clock and for the induction of *mesp2* expression (Aulehla et al., 2007) as it has been shown for FGF/p-ERK signaling (Niwa et al., 2011).

2. AIMS AND THESIS LAYOUT

The vertebrate limb is a structure that develops from the lateral plate mesoderm (LPM) and the myotome. Myotome cells give rise to the muscle components while lateral plate cells produce the segmented skeletal portions of the limb which grow in three dimensions to make a complete arm or leg. Somites are transient segmented structures that develop from the presomitic mesoderm (PSM) and organize the segmental pattern of vertebrate embryo. They eventually give rise to the vertebrae, ribs, dermis of the dorsal skin, skeletal muscles of the back and the skeletal muscles of the body wall and limbs. One of the important features of somitogenesis (formation of somites) is the evolutionarily conserved species specific periodicity and its underlying molecular clock. In 2007, a limb *hairy2* based molecular clock with 6h periodicity that is reminiscent to the somitogenesis clock was identified by our lab. This finding raised the possibility of establishing similarities between the limb development and somitogenesis. Although, vertebrate limb and somites differ in morphology and in their embryonic development, they share many common features.

GLOBAL AIM

The work developed throughout this thesis is aimed at finding similarities between limb development and somitogenesis and to constitute new parallelisms.

SPECIFIC AIMS

To attain our goal, we pursued the following specific aims:

1. To establish the putative role of the AER-FGFs and ZPA-SHH in the expression of the limb molecular clock gene *hairy2*

The limb molecular clock gene *hairy2* has been reported to be dynamically expressed in the distal limb mesenchyme that is in close proximity to the major limb signalling centers the AER

and the ZPA whose secreted morphogens are the FGFs and the SHH, respectively. In the recent past, FGF and SHH signalling have been reported to control the expression of *HES* genes in many systems. We intended to study the putative role of the limb signalling centers and their main signalling molecules in *hairy2* expression. This was essentially done by a series of ablation and bead implantation experiments. The results were assessed at the level of mRNA and protein expression.

2. To determine if a wavefront is travelling along the distal limb mesenchyme.

Our second approach to reach the primary aim of this thesis is to determine if a similar mechanism to the PSM wavefront could be functioning during forelimb development. To address this question, we altered the limit of the two primary signalling molecules of limb PD axis development, FGF8 and RA in the limb field. The effect caused by these manipulations was detected by measuring the size of limb bone elements and by analysing the alterations caused in the expression pattern of important genes.

3. To determine the functional relevance of the limb molecular clock.

hairy2 is the only limb molecular clock gene identified so far. *hairy2* mRNA is oscillating in the distal limb mesenchyme corresponding to the chondrogenic precursor cells and interestingly its expression ceases in the differentiating cartilage. This expression suggests a role for *hairy2* in limb bone patterning. Hence, we went to study the functional relevance of *hairy2* in limb development. We utilized the retrovirus mediated limb mesenchymal delivery of *hairy2* gene and siRNA to address this task.

THESIS LAYOUT

The present PhD thesis is organized into six different chapters. In **Chapter I**, just before the Aim of this thesis work, a General introduction describing the important molecular events occur during vertebrate limb development and somitogenesis has been presented. The review of literature cited in this section will be utilized to establish literature based parallelisms in later chapters. **Chapter II** presents the first article published from the scope of this work in a peer reviewed journal: ``Comprehensive analysis of fibroblast growth factor receptor expression patterns during chick forelimb development´´. In **Chapter III**, the research manuscript entitled: ``Limb hairy2 expression is a temporal and spatial output of AER/FGF and ZPA/SHH signaling´´

which has been submitted to a peer reviewed journal is attached. Materials and methods and unpublished/preliminary results from the on-going work concerning the limb wavefront, Hairy2 functional relevance and signaling pathways regulating limb *hairy2* expression are organized in **Chapter IV**. A compendium of the most relevant discussion on the parallelisms between limb and trunk development that has been established from this PhD work and the literature reviewed in Chapter I are presented in the form of a general discussion in **Chapter V.** All the major conclusions drawn from this work is presented as a model along with the future perspectives in **Chapter VI**. In the end of the thesis all the references from the entire write up are presented in alphabetical order.

CHAPTER II: FIBROBLAST GROWTH FACTOR RECEPTOR EXPRESSION PATTERNS DURING CHICK FORELIMB DEVELOPMENT

The results presented in this chapter were published in an international peer reviewed journal:

THE INTERNATIONAL JOURNAL OF
DEVELOPMENTAL
BIOLOGY
www.intjdevbiol.com

Comprehensive analysis of fibroblast growth factor receptor expression patterns during chick forelimb development

CAROLINE J. SHEEBA[1], RAQUEL P. ANDRADE[1], DELPHINE DUPREZ[2] and ISABEL PALMEIRIM*[,3,4]

[1]Life and Health Sciences Research Institute (ICVS), School of Health Sciences, University of Minho, Braga, Portugal,
[2]Biologie Moléculaire et Cellulaire du Développement, Université Pierre et Marie Curie, Paris, France, [3]Regenerative Medicine Program, Departamento de Ciências Biomédicas e Medicina, Universidade do Algarve and [4]Institute for Biotechnology and Bioengineering, Centro de Biomedicina Molecular e Estrutural, Universidade do Algarve, Faro, Portugal

ABSTRACT Specific interactions between fibroblast growth factors (Fgf1-22) and their tyrosine kinase receptors (FgfR1-4) activate different signalling pathways that are responsible for the biological processes in which Fgf signalling is implicated during embryonic development. In the chick, several Fgf ligands *(Fgf2, 4, 8, 9, 10, 12, 13* and *18)* and the four *FgfRs (FgfR 1, 2, 3* and *4)* have been reported to be expressed in the developing limb. The precise spatial and temporal expression of these transcripts is important to guide the limb bud to develop into a wing/leg. In this paper, we present a detailed and systematic analysis of the expression patterns of *FgfR1, 2, 3* and *4* throughout chick wing development, by *in situ* hybridisation on whole mounts and sections. Moreover, we characterize for the first time the different isoforms of *FGFR1-3* by analysing their differential expression in limb ectoderm and mesodermal tissues, using RT-PCR and *in situ* hybridisation on sections. Finally, isoform-specific sequences for *FgfR1IIIb, FgfR1IIIc, FgfR3IIIb* and *FgfR3IIIc* were determined and deposited in GenBank with the following accession numbers: GU053725, GU065444, GU053726, GU065445, respectively.

KEY WORDS: *Fgf, FgfRs, limb, chick*

The developing chick limb grows out as a protrusion of mesenchymal cells from the lateral plate mesoderm and adjacent somites. Cells from the lateral plate mesoderm form cartilage and connective tissues, such as muscle sheaths, tendons and ligaments. Meanwhile, myogenic precursor cells delaminate from the lateral part of the somites, migrate to the limb bud, colonise the dorsal and ventral limb regions and activate the myogenic program to differentiate into multinucleated myotubes, thus generating the definitive limb skeletal muscles (Christ and Brand-Saberi, 2002; Duprez, 2002; Buckingham *et al.* 2003). The mesenchyme of the limb bud is enveloped by an ectodermal jacket, whose distal tip forms a specialised epithelial structure, the apical ectodermal ridge (AER) (Todt and Fallon, 1984). Mesenchymal cells directly under the AER remain undifferentiated and populate the so-called undifferentiated zone (Tabin and Wolpert, 2007). Condensation of the cartilage elements proceeds in a proximal to distal direction based on cells' temporal and positional values, which could be provided by the reported limb molecular clock (Pascoal *et al.* 2007a; reviewed in Pascoal and Palmeirim, 2007; Tabin and Wolpert, 2007).

During development, changes occur along the three limb bud axes - anterior-posterior (AP), dorsal-ventral (DV) and proximal-distal (PD) - conducted by three distinct signalling centres, the zone of polarizing activity (ZPA), the dorsal (non-ridge) ectoderm and the AER, respectively (reviewed in Towers and Tickle, 2009). ZPA activity is mediated by the diffusible molecule Sonic hedgehog (Shh) (reviewed in Towers and Tickle, 2009). The DV axis is specified by the signalling molecule Wnt-7a and the transcription factor Lmx1b, which are expressed in the dorsal limb ectoderm and dorsal mesenchyme, respectively (Parr and McMahon, 1995; Chen *et al.* 1998). *Wnt-7a* expression is repressed in the ventral ectoderm by Engrailed1, a target of Bmp signalling (Loomis *et al.* 1996). The AER drives PD limb outgrowth (Saunders, 1948) and its activity is mediated by several fibroblast growth factor (Fgf) family members (Niswander *et al.* 1993; Fallon *et al.* 1994), whose

Abbreviations used in this paper: AER, apical ectodermal ridge; Fgf, fibroblast growth factor; FgfR, Fgf receptor; ZPA, zone of polarizing activity.

*****Address correspondence to:** Isabel Palmeirim. IBB-Institute for Biotechnology and Bioengineering, Centro de Biomedicina Molecular e Estrutural, Universidade do Algarve, Campus de Gambelas, 8005-135 Faro, Portugal. Fax: +35-128-980-0076. e-mail: imesteves@ualg.pt - web: http://www.cbme.ualg.pt

2   *C.J. Sheeba et al.*

sequential contribution to PD limb growth over time has been recently reported (Mariani *et al.* 2008). Fgfs comprise several structurally related polypeptides, many of which have been described to be expressed in the developing chick limb (Fallon *et al.* 1994; Savage and Fallon, 1995; Crossley *et al.* 1996; Ohuchi *et al.* 1997; Munoz-Sanjuan *et al.* 1999; Ohuchi *et al.* 2000; Havens *et al.* 2006). The expression of *Fgf4, 8* and *9* is restricted to the AER, *Fgf10, 12, 13* and *18* are expressed in the limb mesenchyme and *Fgf2* is expressed both in the ectoderm, including the AER, and in the mesenchyme. Fgf4 is also expressed in muscle from E6 (Edom-Vovard *et al.* 2001a) and Fgf8 in tendons from E8 (Edom-Vovard *et al.* 2001b). Fgf4 and 8, however, are indispensable for limb development, since targeted deletion of *Fgf4* and *Fgf 8* in the AER generated limbless mice (Sun *et al.* 2002; Boulet *et al.*, 2004). AER-derived Fgfs signal to the underlying mesenchyme, which is evidenced by the distal to proximal gradient of the Fgf8 effector *Mkp3* (Pascoal *et al.* 2007b), maintaining the subjacent mesoderm in an undifferentiated, proliferative state (Tabin and Wolpert, 2007).

Fgf signalling is implicated in many biological processes during development, such as differentiation, proliferation (Prykhozhij and Neumann, 2008), survival, migration, adhesion, apoptosis and chemotaxis (reviewed in Bottcher and Niehrs, 2005). All Fgfs mediate their cellular responses by binding to and activating appropriate Fgf receptors (FgfRs), which belong to a family of cell surface receptor tyrosine kinases. FgfRs contain an extracellular Fgf binding domain composed of three immunoglobulin-like domains, a transmembrane domain and an intracellular tyrosine kinase domain. There are four known FgfRs and among these, FgfR1-3 can generate alternatively spliced isoforms (reviewed in Eswarakumar *et al.* 2005) that display different ligand specificity (Ornitz *et al.* 1996; Zhang *et al.* 2006). Ligand binding in the presence of heparan sulfate proteoglycans leads to receptor dimerisation and activation of downstream intracellular signalling cascades, such as Ras-MAP kinase, PI3 kinase/Akt and PLC gamma/PKC (reviewed in Dailey *et al.* 2005). When mutated or misexpressed, Fgfs and their receptors cause morphogenic disorders affecting limb formation and can
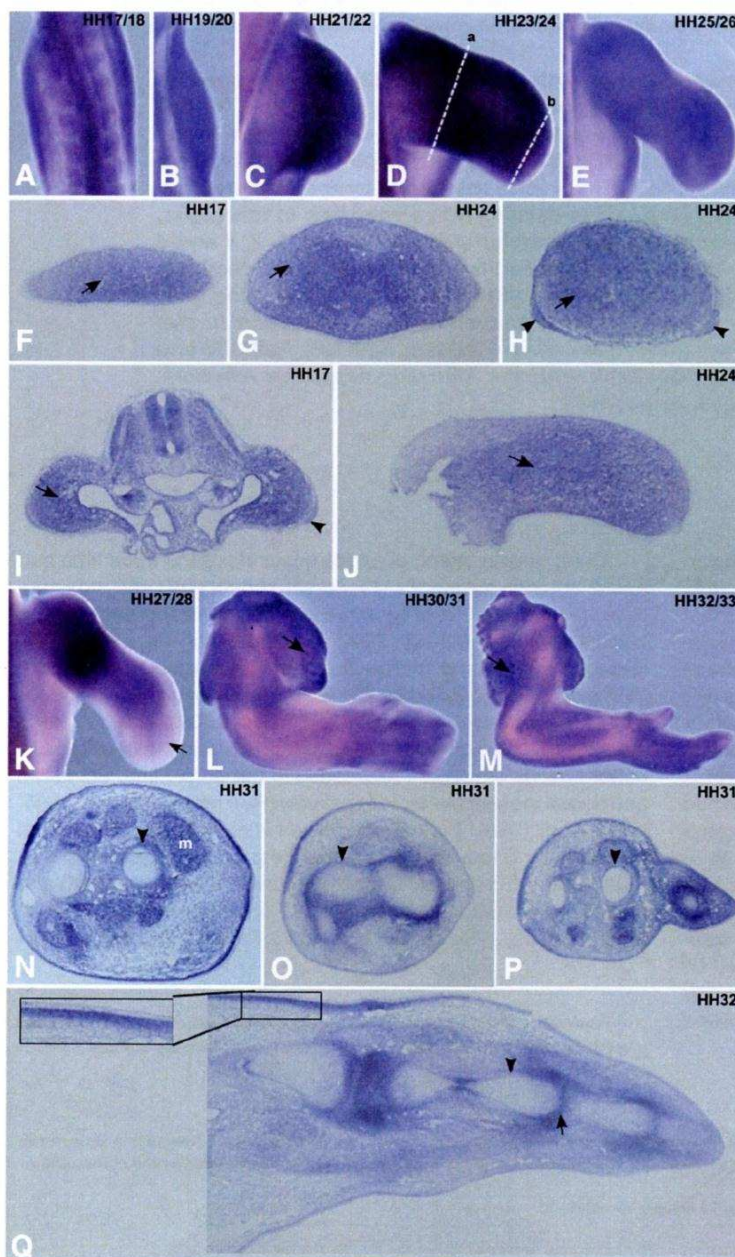

Fig. 1. *FgfR1* expression pattern during chick forelimb development. *Chick wings at HH17-33 stages were processed for* in situ *hybridisation in whole-mounts (A-E, K-M) and in transversal/longitudinal sections (F-J, N-Q) using a probe for non isoform-specific chick FgfR1. (A-E)* In situ *hybridisation in whole-mount limbs for FgfR1 showed a generalized expression in limb mesenchyme. (F-H) Transverse sections of limb buds at HH17 and HH24 (G: proximal, H: distal, represented in (D) as (a) and (b), respectively) show FgfR1 expression in the limb mesenchyme (arrows), and in the ectoderm of the distal limb (H, arrowheads). (I,J) Longitudinal limb sections at HH17 and HH24 show FgfR1 expression in the limb mesenchyme (arrows), and in the AER of HH17 limb bud (I, arrowhead). (K)* In situ *hybridisation in whole-mount limbs at HH27/28 stage show decreased nFgfR1 expression in the distal limb mesenchyme (arrow). (L,M) FgfR1 expression is observed in developing feather buds of the body wall (arrows). (N-P) Transverse sections of forelimb at stage HH31 show FgfR1 expression in perichondrium (arrowheads) and in muscles (m). (Q)* In situ *hybridisation in longitudinal limb sections at HH32 shows that FgfR1 transcripts are observed in the perichondrium (arrowhead) and in the future interphalangic joints (arrow). The inset in (Q) shows an upregulation of FgfR1 expression in the mesenchyme close to the proximal ectoderm. (A-E, K-M) are dorsal views of whole-mount limbs. (F-H, N-P) Transverse sections are oriented such that left – posterior, right – anterior, top – dorsal and bottom – ventral. (I,J,Q) longitudinal limb sections are positioned such that left – proximal and right – distal. Embryonic stages of the limbs are mentioned in the upper right corner of the pictures.*

also lead to cancer (reviewed in Wilkie *et al.* 2002; Eswarakumar *et al.* 2005).

The expression pattern of *FgfR1-4* on sections during chick limb development has been previously reported to some extent (Marcelle *et al.* 1995; Szebenyi *et al.* 1995; Eloy-Trinquet *et al.* 2009). Nevertheless, as our knowledge on the importance of Fgf signalling in limb development increased considerably over the last decade, a more detailed description of the spatial and temporal distribution of all *FgfRs* became compulsory. Moreover, very little is known about FGFR isoform-specific expression during limb development. Although there are studies available for the expression pattern of *FgfR2IIIb* and *FgfR2IIIc* isoforms (Lizarraga *et al.* 1999; Havens *et al.* 2006), knowledge on the expression of the *FgfR1* and *FgfR3* isoforms is lacking, in both chick and mouse. We hereby report

comprehensive expression analyses of *FgfR1-4* and IIIb and IIIc isoforms of *FgfR1-3* during chick forelimb bud development, from stage HH17 to HH33 (Hamburger and Hamilton, 1951), using RT-PCR and *in situ* hybridisation on whole mount and sections.

Results

This work presents a comprehensive analysis of the expression patterns of *FgfR1-4* during chick forelimb development in stages HH17 through HH33 by *in situ* hybridization. For each receptor, a non isoform-specific probe was used allowing an overall visualization of expression spatial distribution. Subsequently, we analysed the expression of the IIIb and IIIc isoforms of *FgfR1-3* by RT-PCR and *in situ* hybridisation on sections.

FgfR1 *expression*

Between stages HH17 and HH26, *FgfR1* is expressed along the entire PD axis of the chick limb bud (Fig. 1A-E). Transverse and longitudinal section analyses show that *FgfR1* transcripts are present mainly in the mesenchyme (Fig. 1 F-J, arrows) and are absent from the enveloping ectoderm in the proximal part of the limb. In the distal limb, however, *FgfR1* is also observed in sections in the distal ectoderm, including the AER (Fig. 1 H,I, arrowhead). At stage HH26, when cartilage differentiation is in progress, *FgfR1* transcripts are detected throughout the limb, although in a slightly graded proximal to distal distribution (Fig. 1E, data not
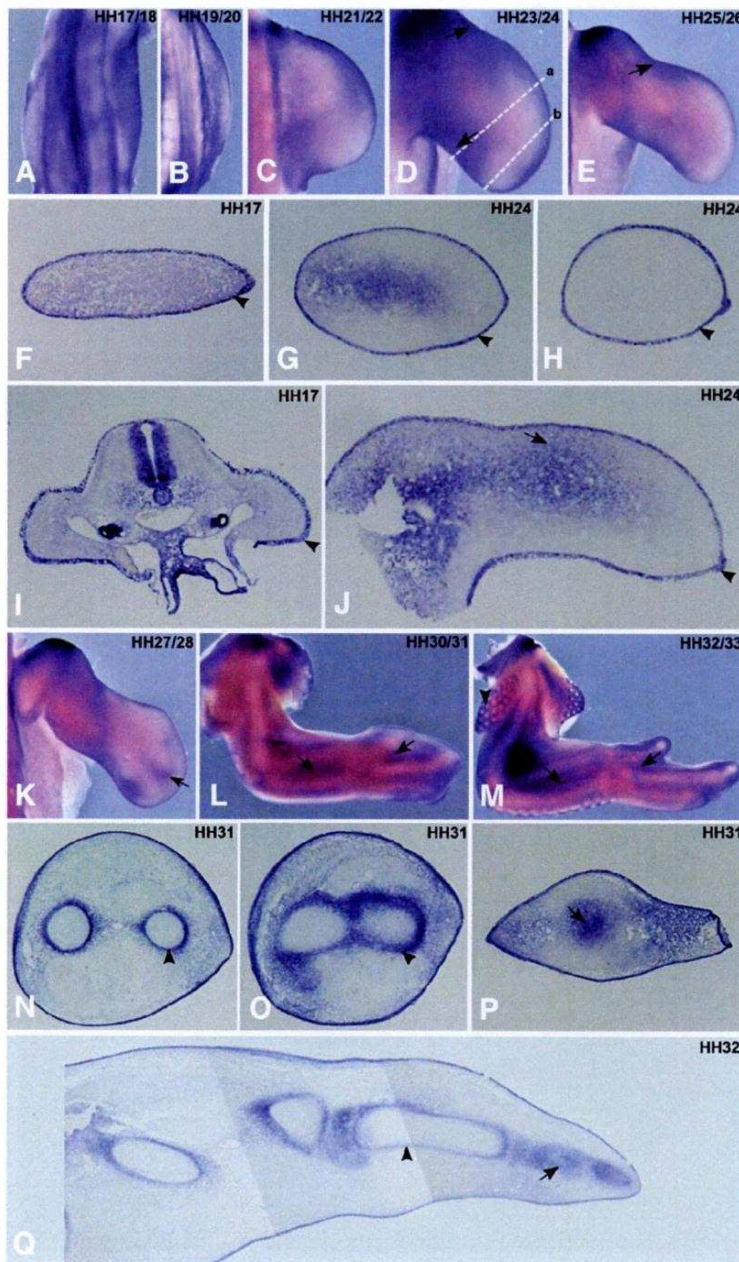

Fig. 2. *FgfR2* expression pattern during chick forelimb development. *Chick wings at HH17-33 stages were processed for* in situ *hybridisation in whole-mounts* **(A-E, K-M)** *and transverse/longitudinal sections* **(F-J, N-Q)** *using a probe for non isoform specific chick FgfR2.* **(A-E)** In situ *hybridisation in whole mount limbs using the FgfR2 probe showed its presence in the limb ectoderm, including the AER.* **(F-H)** *Transverse limb sections (G: proximal, H: distal, represented in* **(D)** *as (a) and (b), respectively) confirm the ectodermal expression of FgfR2 (arrowheads), although a faint proximal/posterior mesenchymal expression could also be observed at HH24 (G, arrow).* **(I,J)** *Longitudinal limb sections at HH17 and HH24 show FgfR2 expression in the ectoderm (arrowheads) including the AER and also in the mesenchyme (arrow).* **(K-M)** In situ *hybridisation in whole-mount limbs show FgfR2 expression in between the zeugopod skeletal elements and in the interdigital zones (arrows) and around the feather buds in the body wall (M, arrowhead).* **(N-P)** *Transverse sections of forelimb at stage HH31 show FgfR2 expression in perichondrium (arrowheads) and in the entire distal cartilage element (arrow).* **(Q)** In situ *hybridisation in longitudinal limb sections at HH32 show FgfR2 expression in distal cartilage elements (arrow) and in perichondrium in more proximal cartilage elements (arrowhead).* **(A-E, K-M)** *are dorsal views of whole-mount limbs.* **(F-H, N-P)** *transverse sections are oriented such that left – posterior, right – anterior, top – dorsal and bottom – ventral.* **(I,J,Q)** *longitudinal limb sections are positioned such that left – proximal and right – distal. Embryonic stages of the limbs are mentioned in the upper right corner of the pictures.*

4   *C.J. Sheeba et al.*

shown). Moreover, longitudinal sections revealed stronger expression in the perichondrium compared to the mesenchymal tissue (data not shown). At HH27, *FgfR1* expression decreases prominently in the distal limb mesenchyme and becomes restricted to more proximal regions (Fig. 1K, arrow). *In situ* hybridisation of stage HH31 or HH32 forelimbs show that *FgfR1* is observed in the perichondrium and in the prospective interphalangic joints (Fig. 1 N-Q, arrowheads and 1Q, arrow, respectively). In addition, *FgfR1* expression is also observed in muscles (Fig. 1 N,m), tendons (Fig. 1N) and in feather buds of the body wall (Fig. 1 L,M arrows). Interestingly, *FgfR1* is strongly expressed in a thin layer of mesenchymal cells juxtaposed the limb ectoderm, with a higher signal in the dorsal regions (Fig. 1 N-Q and 1Q, inset) which fades gradually towards the distal limb.

FgfR2 *expression*

FgfR2 transcripts are strongly detected in the entire ectodermal cell layer covering limb mesenchymal cells, including the AER (Fig. 2). This is clearly evidenced in the transverse and longitudinal limb sections (Fig. 2 F-J, arrowhead). Additionally, *FgfR2* transcripts can be observed in the proximal regions of stage HH23-26 limbs, including the anterior and posterior limb margins (Fig. 2 D,E,G,J, arrow). From stage HH27 onwards, *FgfR2* mRNA is observed in between the two zeugopod skeletal elements and in the interdigital domains (Fig. 2 K,L,M arrow) and surrounding feather buds of the body wall (Fig. 2M, arrowhead). Section analyses showed that *FgfR2* expression prefigures the distal developing chondrogenic elements (Fig. 2 P,Q, arrow), and was observed in the perichondrium of the more proximal cartilage elements (Fig. 2 N,O,Q, arrowhead).

Fig. 3. *FgfR3* expression pattern during chick forelimb development. *Chick wings at HH17-33 stages were processed for* in situ *hybridisation in whole-mounts* **(A-E, K-M)** *and transverse/longitudinal sections* **(F-J, N-Q)** *using a probe for non isoform specific chick* FgfR3. **(A-E)** In situ *hybridisation in whole mount limbs at stages HH19-24 show* FgfR3 *expression in the more proximal part of limb buds (B-D, arrows) and in forming cartilage elements* **(E)** *of the humerus (h), radius (r) and ulna (u) at HH25/26 stages. Faint* FgfR3 *expression was also observed in the anterior mesenchyme underlying the ectoderm (D, arrowhead).* **(F-H)** *Transverse (G:proximal, H:distal, represented in D as a and b, respectively) and* **(I,J)** *longitudinal limb sections at stage HH19 and HH24 shows the specific mesenchymal expression of* FgfR3 *(arrows).* **(K-M)** In situ *hybridisation in whole-mount limbs at HH27 to HH33 shows a* FgfR3 *expression in interdigital domains (arrows), in addition to digit cartilage elements (d2, d3 and d4).* FgfR3 *expression is also observed around the feather buds in the body wall (arrowhead).* **(N-Q)** *During limb stages HH31/32* FgfR3 *is expressed in the ectoderm (asterisk & inset) and also in the cartilage elements (arrows) and perichondrium (arrowhead).* **(A-E, K-M)** *are dorsal views of whole-mount limbs.* **(F-H, N-P)** *transverse sections are oriented such that left – posterior, right – anterior, top – dorsal and bottom – ventral.* **(I,J,Q)** *longitudinal limb sections are positioned such that left – proximal and right – distal. Embryonic stages of the limbs are mentioned in the upper right corner of the pictures.*

FgfR3 *expression*

FgfR3 transcripts were first detected in limb buds at stage HH19, where they are clearly restricted to the most proximal mesoderm (Fig. 3 B-J, arrow). This expression pattern is maintained until stage HH24. However, low levels of *FgfR3* expression in the mesenchyme underlying the anterior ectoderm towards the distal part of the limb could also be observed (Fig. 3D, arrowhead). *FgfR3* mRNA was never detected neither in the ZPA nor in the AER and the underlying distal mesenchyme (Fig. 3 A-J), although it could be detected in the proximal mesoderm (Fig. 3J, arrow). From HH25 stage, *FgfR3* is strongly expressed in all the
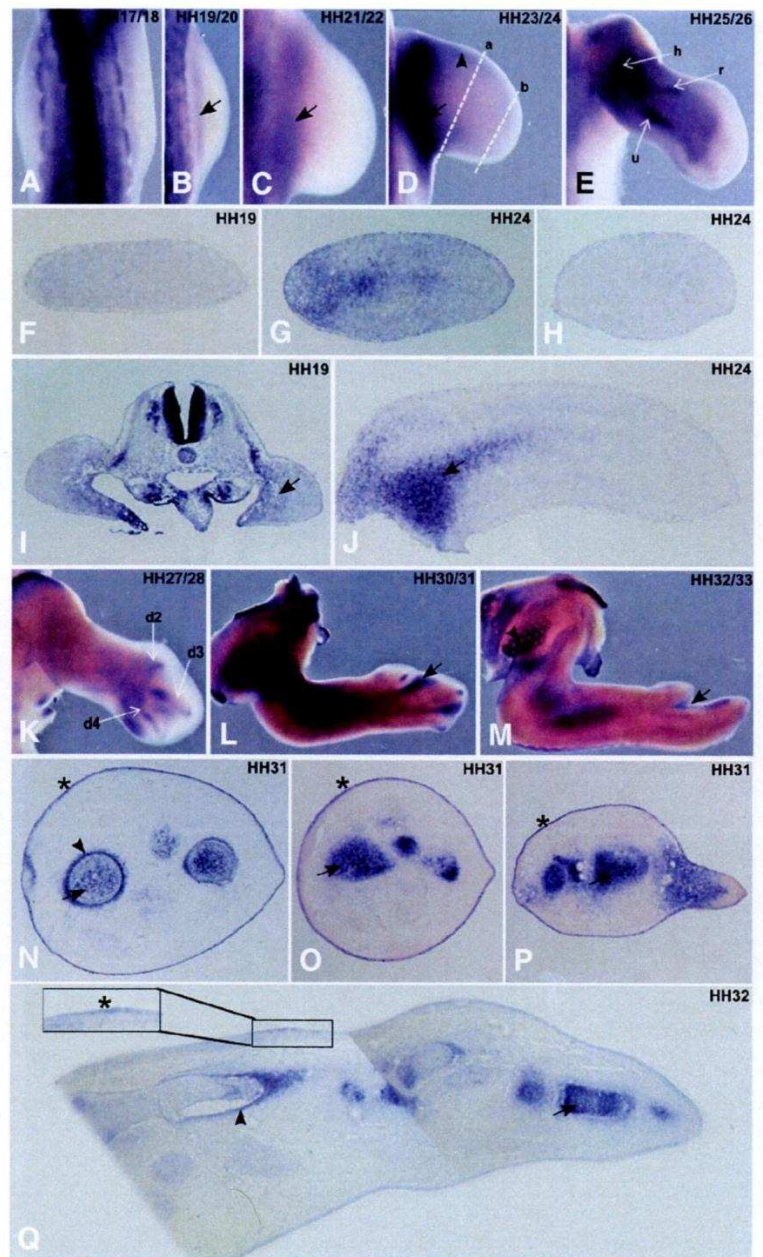
Fig. 4. RT-PCR evaluation of the differential expression of *FgfR1-3* IIIb and IIIc isoforms in the forelimb ectoderm and mesoderm. *FgfR1-3 isoform-specific expression was evaluated by RT-PCR using total RNA extracted from segregated ectoderm (Ec) and mesoderm (Mes) tissues from stage HH24 forelimbs. FgfR1IIIb, FgfR1IIIc and FgfR3IIIb are found in both ectoderm and mesenchyme. FgfR2IIIb is exclusively expressed in the ectoderm, while FgfR2IIIc and FgfR3IIIc are only expressed in the mesenchyme.*

forming cartilage elements (Fig. 3 E,K) and can also be observed in interdigital zones (Fig. 3 L,M, arrow). Sections of HH32 limbs revealed specific expression of *FgfR3* in muscles (Fig. 3N), distal cartilage elements (Fig. 3 N-Q, arrow) and in the perichondrium (Fig. 3 N,Q, arrowhead). Interestingly, *FgfR3* is also faintly expressed in the ectoderm at this stage of limb development (Fig. 3 N-Q, asterisk and inset).

Isoform-specific expression patterns of FgfRs 1-3

We employed the same experimental approach as Shin *et al.* (2005) to detect the presence of the specific IIIb and IIIc isoforms of *FgfR1-3* in segregated ectoderm and mesoderm tissues of stage HH24 limb buds. RT-PCR analysis clearly revealed that *FgfR2IIIb* is exclusively expressed in the limb ectoderm, while *FgfR2IIIc* and *FgfR3IIIc* are only found in limb mesenchyme (Fig. 4). These results strongly imply that the *FgfR2* ectodermal staining observed in Fig. 2 is due to *FgfR2IIIb* isoform expression. Conversely, *FgfR2* mesodermal staining is a result of *FgfR2IIIc* expression. Since *FgfR3IIIc* can only be detected in the limb mesoderm by RT-PCR (Fig. 4), we can clearly state that at stage HH24 the faint *FgfR3* ectodermal staining observed by *in situ* hybridization (Fig. 3G) is solely due to the *FgfR3IIIb* isoform expression. However, RT-PCR also detected this splice variant

in the mesenchyme (Fig. 4), so detailed *FgfR3* isoform-specific expression patterns in the limb mesenchyme are missing. The same stands for *FgfR1* isoforms, since both are detected by RT-PCR in ectoderm and mesoderm (Fig. 4).

To further elucidate the expression patterns of *FgfR1* and *FgfR3* isoforms, *in situ* hybridization probes were prepared using the amplification products obtained upon RT-PCR performed on total RNA extracted from HH24 whole chick embryos, using the primers previously described (Shin *et al.* 2005). The amplicon sequences were determined and deposited in GenBank with the following accession numbers: *FgfR1IIIb*-GU053725; *FgfR1IIIc*- GU065444; *FgfR3IIIb*- GU053726; *FgfR3IIIc*-GU065445.

In situ hybridization of *FgfR1IIIb* and *FgfR1IIIc* isoforms on limb sections (Fig. 5) consistently showed fainter staining compared to the non isoform-specific '*FgfR1* probe. Very subtle differences could be found for the spatial distribution of both isoforms in the limb tissues: *FgfR1IIIb* consistently marked the ectoderm stronger than the *FgfR1IIIc* isoform (Fig. 5 A,B,C,D, arrows) and, in stage HH31 limb sections, *FgfR1IIIc* presents stronger expression in the perichondrium than the other variant (Fig. 5 B,D, arrowhead).

At stage HH24, *FgfR3IIIb* is expressed throughout the entire limb and the *FgfR3IIIc* isoform is expressed in the proximal mesenchyme (Fig. 5 E,G, arrow), which is in accordance to the RT-PCR results (Fig. 4). In later developmental stages (HH30), *FgfR3IIIc* transcripts are predominantly detected in and around the cartilage, unlike the faint expression of *FgfR3IIIb* (Fig. 5

Fig. 5. Section *in situ* hybridization analyses of *FgfR1IIIb*, *FgfR1IIIc*, *FgfR3IIIb* and *FgfR3IIIc* expression patterns. *Chick wings at HH24 and HH30/31 stages were processed for transversal/longitudinal paraffin section in situ hybridisation using the isoform-specific sequences previously obtained as probes (GenBank accession numbers GU053725, GU065444, GU053726, GU065445). FgfR1IIIb presents stronger expression in the ectoderm than FgfR1IIIc; see arrows in **(A-D)**, while FgfR1IIIc transcripts could be detected in the perichondrium; see arrowhead in **(D)** unlike FgfR1IIIb. FgfR3IIIc is expressed in the proximal limb of stage HH24; see arrow in **(G)**, and in the cartilage elements at stage HH30; arrow in **(H)**, unlike FgfR3IIIb **(E,F)**. At stage HH30, both FgfR3IIIb and IIIc are expressed in the ectoderm; see asterisks in **(F,H)**.*
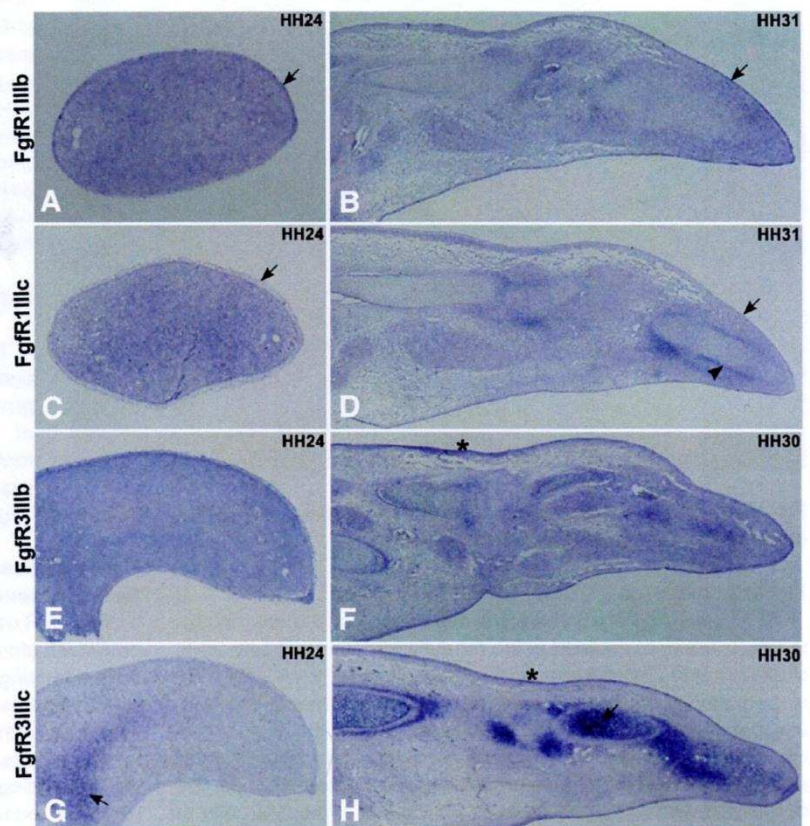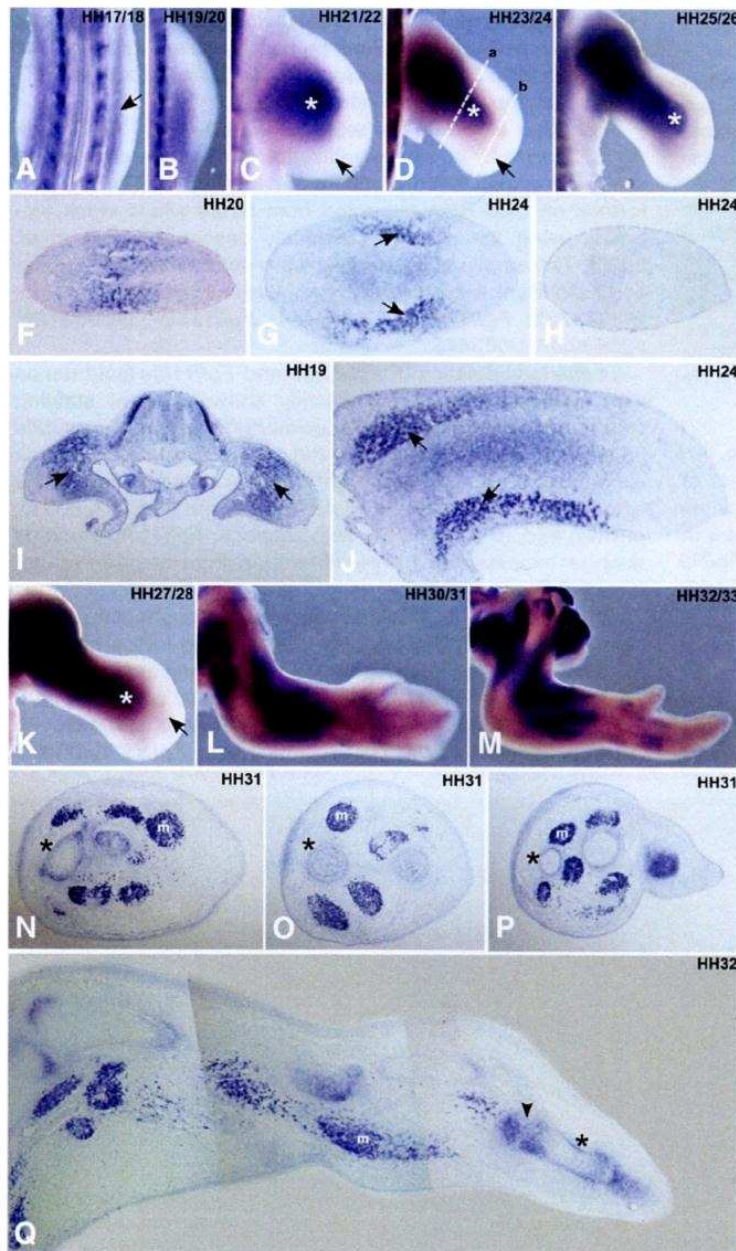
6   *C.J. Sheeba et al.*

Fig. 6. *FgfR4* expression pattern during chick forelimb development. *Chick wings at HH17-33 stages were processed for in situ hybridisation in whole-mounts* **(A-E, K-M)** *and transverse/longitudinal sections* **(F-J, N-Q)** *using a probe for non isoform specific chick* FgfR4. **(A-E)** *In situ hybridisation in whole-mount limbs shows limb* FgfR4 *expression at HH17* (*A, arrow*). *There is no FgfR4 expression in the AER and ZPA (C,D, arrows), while* FgfR4 *expression is observed in muscle masses (asterisks; also in K).* **(F-H)** *Transverse sections of HH20 and HH24 limbs (G: proximal, H: distal, represented in (D) as (a) and (b), respectively) reveal* FgfR4 *expression in the dorsal and ventral muscle masses (G, arrows).* **(I,J)** *Longitudinal sections of HH19 and HH24 limbs indicate* FgfR4 *expression in muscle precursors (I, arrows) and then in dorsal and ventral muscle masses (J, arrows).* **(K-M)** *In situ hybridisation experiments in whole mount limbs at HH27 to HH33 show an absence of FgfR4 expression in distal limb mesenchyme (K, arrow). In limb stage HH31* FgfR3 *is expressed in the perichondrium (N-P, asterisk) and in the muscle tissue (N-P, m).* **(Q)** *In situ hybridisation in longitudinal limb sections at HH32 shows* FgfR4 *expression in individualised muscles (m), in the perichondrium of distal cartilage elements (asterisk) and interphalangic joints (arrowhead).* **(A-E, K-M)** *are dorsal views of whole-mount limbs.* **(F-H, N-P)** *Transverse sections are oriented such that left, posterior; right, anterior; top, dorsal; bottom, ventral.* **(I,J,Q)** *longitudinal limb sections are positioned such that left is proximal and right is distal. Embryonic stages of the limbs are mentioned in the upper right corner of the pictures.*

al. 1995). There is no *FgfR4* expression in the AER, the underlying distal mesenchyme and in the ZPA (Fig. 6 C-E). From stage HH29 on, *FgfR4* expression is also located in limb cartilage element domains (Fig. 6 L-Q), as previously described (Marcelle *et al.* 1995). Analysis of longitudinal and cross sections at stage HH31/32 revealed that this gene is weakly expressed in the perichondrium and interphalangic joints (Fig. 6 N-Q asterisk and arrowhead, respectively), in addition to its stronger expression in individualised muscles (Fig. 6 N-Q, m).

Discussion

Fgf signalling plays an important role in many aspects of limb development, such as initiation, outgrowth and patterning (reviewed in Martin, 1998; Xu *et al.* 1999; Yu and Ornitz, 2008). In this study we performed a careful examination of the spatio-temporal expression patterns of *FgfR1-4* genes and IIIb and IIIc isoforms of *FgfR1-3* during chick wing development.

FgfR expression in the AER and in the underlying undifferentiated mesenchyme

The AER constitutes the signalling centre responsible for limb outgrowth along the PD axis. Fgfs produced by the AER signal to the underlying mesenchyme or to the neighbouring ectoderm, which express Fgf receptors and various components of the Fgf signalling pathway. Our results show that during early limb patterning events (HH17-20), *FGFR1* and *FGFR2* are expressed in the developing chick forelimb buds. *FgfR1* is the main Fgf receptor to be expressed in the undifferentiated mesenchymal cells

F,H, arrow). Moreover, both isoforms can be observed in the ectoderm at this stage (Fig. 5 F,H, asterisk).

FgfR4 *expression*

Analysis of *FgfR4* expression patterns showed that this receptor starts being expressed in the most proximal part of limb buds at stage HH17 (Fig. 6A, arrow). From stage HH21 to HH28 *FgfR4* is persistently expressed in a central mesenchymal domain, which extends distally as the limb develops (Fig. 6 C-E,K asterisk). Transverse and longitudinal section *in situ* hybridization analyses showed that this expression is most predominant in the dorsal and ventral muscle masses (Fig. 6 G,J arrow, Marcelle *et*

located in the distal part of the limb. *FgfR2* expression is also detected in the mesenchyme but not in the distal limb region. Interestingly, the distal expression of *FgfR1* is progressively lost at stages HH26-28, which correspond to the stages when distal autopod skeletal elements are being laid down. FgfR1 involvement in growth and patterning of vertebrate limbs was first evidenced by the targeted mutation of *FgfR1*, which affected autopod patterning in mice (Partanen *et al.* 1998). More recently, conditional deletion of *FgfR1* gene in mouse embryos suggested a three phase function for FgfR1: elongation of PD axis at early stages, mesenchymal cell survival at middle stages and patterning autopod at later stages (Verheyden *et al.* 2005). Supporting its role in later stages, previous studies show that mutant mouse embryos carrying a targeted deletion of the *FgfR1α (IIIc)* isoform exhibited distal truncation of limb buds which were shorter in PD axis and wider in AP axis (reviewed in Xu *et al.* 1999).

Our whole-mount analyses show that *FgfR2* is the only *FgfR* to be robustly expressed in the entire ectoderm, including the AER, throughout all stages of development. This expression pattern supports the idea that chick *FgfR2* is mediating the Fgf signal in AER formation, ectodermal cell movements towards and into the limb as well as in certain aspects of dorsoventral ectodermal polarity establishment, as already described in mice (Gorivodsky and Lonai, 2003). *FgfR2* expressed in the AER has been reported to be essential for the maintenance of this structure (Lu *et al.* 2008). These authors also reported the loss of autopod in mouse forelimb upon conditional removal of *FgfR2* from the AER bringing forth the involvement of FgfR2 in distal limb patterning. Among the two FgfR2 isoforms, FgfR2IIIb variant is implicated in mesenchymal-epithelial signalling loop in limb bud initiation (De Moerlooze *et al.* 2000), whereas the FgfR2IIIc form is associated to limb skeletal bone formation (Eswarakumar *et al.* 2002). Recently, conditional inactivation of mouse *FgfR2* from the AER and both *FgfR1* and *FgfR2* from the mesenchyme suggest that AER-Fgfs function not only as survival factors but also as regulators of mesenchymal proliferation and chondrogenic differentiation (Yu and Ornitz, 2008). Overall, *FgfR1* and *FgfR2* are involved in limb initiation and patterning.

FgfR3 and *FgfR4* are not expressed in the AER or in the underlying undifferentiated zone throughout all chick limb developmental stages.

Fgf signaling in the ZPA

The ZPA is another important limb signalling centre, which produces Shh and organizes the limb along the AP axis. It has been shown that there is a positive feed-back loop between *Shh* expressed in the ZPA and *Fgf4* expressed in the AER, which is important for limb development (reviewed in Towers and Tickle, 2009). Our whole-mount *in situ* hybridisation analyses show that *FgfR1* is the unique *FgfR* continuously expressed in the ZPA from stage HH17 to 26, suggesting that FgfR1 is involved in this regulatory loop. Accordingly, conditional inactivation of *FgfR1* in posterior limb caused reduction in *Shh* RNA levels and consequently affected digit identity (Verheyden *et al.* 2005).

FgfRs and cartilage development

Our whole-mount and section analyses showed that all four *FgfRs* are expressed during chondrogenesis in the chick wing. *FgfR1* is strongly expressed in perichondrium and in forming

joints. *FgfR1* expression in cartilage elements displays no variation along the PD axis of the limb. In contrast, *FgfR2, 3* and *4* expression in cartilage elements varies along the PD axis, being expressed in the more distal cartilage elements and becoming restricted to the perichondrium as development proceeds. Mutations in *FgfR1, 2* or *3* genes lead to human limb congenital disorders (Wilkie *et al.* 2002; Coumoul and Deng, 2003). In addition *FgfR1* and *FgfR3* have been described to take part in bone fracture repair (Nakajima *et al.* 2001; Nakajima *et al.* 2003). The involvement of *FgfR3* in chondrogenesis and its mutation in inherited defective growth of human long bones syndrome was reported earlier (Colvin *et al.* 1996; Deng *et al.* 1996; Delezoide *et al.* 1998). Recently, the involvement of Fgf signalling through FgfR3 in the commitment of pre-chondrogenic mesenchymal cells to chondrogenesis and to cartilage production was documented (Davidson *et al.* 2005). Activating *FgfR3* in mice can mimic human dwarfism (Li *et al.* 1999) and lack of *FgfR3* causes skeletal overgrowth (Colvin *et al.* 1996; Deng *et al.* 1996), indicating that FgfR3 acts as a negative regulator of bone development. The downstream pathways responsible for the negative regulation are the MAP kinase pathway that inhibits chondrocyte differentiation and the Stat1 pathway that inhibits chondrocyte proliferation (Murakami *et al.* 2004).

Our observation of *FgfR2* expression surrounding cartilage elements during limb development is in agreement with the suggestion that *FgfR2* activation elicits a lateral inhibition of chondrogenesis that limits the expansion of developing skeletal elements (Moftah *et al.* 2002). Finally, although mouse homozygous for targeted *FgfR4* mutation was normal, double homozygous disruption for both *FgfR3* and *4* showed defects in long bone growth indicating that *FgfR4* could also be a positive regulator of long bone growth (Weinstein *et al.* 1998; Lazarus *et al.* 2007).

FgfRs and muscle formation

Precursors of limb muscles orginate from the somites, migrate to the limb and undergo differentiation. In all chick limb bud stages analysed, *FgfR4* expression is observed in migrating myogenic cells, in dorsal and ventral muscle masses and then in individualised muscles, consistent with its involvement in limb myogenesis (Marcelle *et al.* 1995; Marics *et al.* 2002). FgfR4 signalling has been shown to participate in terminal skeletal muscle differentiation in the embryo and during muscle regeneration process in the adult (Marics *et al.* 2002; Yu *et al.* 2004; Zhao *et al.* 2006). However, *FgfR4* is not the only *FgfR* expressed in muscles but also *FgfR1* expression is observed (Fig. 1N), as previously described (Edom-Vovard *et al.* 2001a, b, Eloy-Trinquet *et al.* 2009). Interestingly, down-regulation of FgfR1 signalling has also been correlated with terminal myogenic differentiation (Grothe *et al.* 1996; Itoh *et al.* 1996). So, two FgfRs are associated with muscle formation, FgfR1 and 4. However, their precise role in limb myogenesis is still unclear.

FgfRs and feather development

We would also like to point out the expression of *FgfRs* in the context of feather development. Our findings that all *FgfRs* except *FgfR4* are expressed either in (*FgfR1*) or around (*FgfR2* and *3*) presumptive feather buds correlates with previously reported data (Noji *et al.* 1993). Recently the importance of FgfR1 and FgfR2 in feather development was demonstrated using dominant

negative forms (Mandler and Neubuser, 2004).

Conclusions

The results obtained throughout our work are overall in accordance to what has been previously described (Szebenyi *et al.* 1995). We additionally report *FgfR1* expression in the distal ectoderm, including the AER and *FgfR3* in the ectoderm of late limb developmental stages (HH31). The expression patterns of the different *FgfRs* are consistent with their involvement in different steps of limb development, such as early limb bud formation, outgrowth and patterning. *FgfR* expression is also linked with the differentiation process of various cell types including, cartilage, muscle and feathers. Finally, we have analysed, for the first time, the expression of the different isoforms of *FgfR1* and *FgfR3* (*FgfR1IIIb, FgfR1IIIc, FgfR3IIIb* and *FgfR3IIIc*). The results obtained highlight the importance of the epithelial-mesenchymal tissue interactions operating during limb development. The relative affinity of each FgfR isoform to the different limb Fgfs has been previously described (Ornitz *et al.* 1996; Zhang *et al.* 2006), and our FgfR expression profiles evidence a trend in that the ectodermal-expressed isoforms, such as FgfR2IIIb, respond to mesenchyme-produced Fgfs (Fgf10), while FgfR isoforms found in the mesoderm preferentially react to ectodermal-derived Fgfs. This is particularly evident for FgfR2IIIc and FgfR3IIIc which recognize Fgf2,4,8,9 and Fgf2,8,9, respectively.

Materials and Methods

Eggs and embryos

Fertilised chick (*Gallus gallus*) eggs obtained from commercial sources were incubated at 38°C in a 49% humidified atmosphere and staged according to the Hamburger and Hamilton (HH) classification (Hamburger and Hamilton, 1951).

In situ *hybridisation probes*

Non isoform-specific chick FgfR1-4 probes were kindly provided by Dr. Guojun Sheng (Nakazawa *et al.* 2006). *In situ* hybridisation probes for FgfR1-3 IIIb and IIIc isoforms were generated by amplifying portions of these genes by reverse transcription and polymerase chain reactions (RT-PCR) using the isoform-specific primers previously described in Sinh *et al.* (2005). The DNA fragments generated were cloned into the pCR®II-TOPO® vector (Invitrogen, USA) and plasmid DNA was isolated. The constructs were confirmed upon sequencing. Digoxigenin-labelled RNA probes were synthesized using linearised plasmids, according to standard procedures.

In situ *hybridisation of whole-mount embryos and tissue sections*

Embryos were fixed overnight at 4°C in a solution of 4% formaldehyde with 2 mM EGTA in PBS at pH 7.5, rinsed in PBT (PBS, 0.1% Tween 20), dehydrated in methanol and stored at −20°C. Whole mount *in situ* hybridisation was performed as previously described (Henrique *et al.* 1995).

Paraffin sections were prepared as follows: stage HH32 chick wings were collected in PBS and fixed at 4°C over night in a solution of 60% ethanol, 30% formaldehyde and 10% acetic acid. The following day, limbs were dehydrated in series of ethanol with a final step of xylene. Finally, they were incubated in paraffin at 70°C for 30 min, placed in the desired orientation and left to solidify. Longitudinal limb sections of 10 μm were made using Microm HM325 on SuperFrost Plus (Menzel-Glaser) slides and allowed to dry at 37°C overnight. *In situ* hybridisation on paraffin sections was performed as described previously (Tozer *et al.* 2007).

RNA extraction from limb tissues and RT-PCR reactions

Stage HH24 chick fore-limbs were submitted to pancretin-mediated digestion until the ectoderm detached freely from the mesoderm. The reaction was stopped by the addition of goat serum solution (Invitrogen). The ectoderm was isolated from the mesoderm and both tissues were collected separately for RNA isolation using the RNeasy Mini Kit Protect (Qiagen, Germany). Total mRNA quantification was done by spectrophotometry (NanoDrop Technologies, Inc., USA). Total RNA was digested with DNAse RNAse-Free (Promega, USA) according to manufacturer's instructions. Purified RNA was reverse transcribed using SuperScript™ II Reverse Transcriptase (Invitrogen), and a PCR reaction was performed employing the FgfR isoform-specific primer pairs described by Shin *et al.* (2005).

Imaging

Embryos processed for *in situ* hybridisation were photographed in PBT/0.1% azide, using an Olympus DP71 digital camera coupled to an Olympus SZX16 stereomicroscope equipped with Cell^B program. Vibratome and paraffin limb sections were photographed using an Olympus DP70 camera coupled to an Olympus BX61 microscope.

References

BOTTCHER, R.T. and NIEHRS, C. (2005). Fibroblast growth factor signaling during early vertebrate development. *Endocr Rev* 26: 63-77.

BOULET, A.P., MOON, A.M., ARENKIEL, B.R. and CAPECCHI, M.R. (2004). The roles of Fgf4 and Fgf8 in limb bud initiation and outgrowth. *Dev Biol* 273: 361-372.

BUCKINGHAM, M., BAJARD, L., CHANG, T., DAUBAS, P., HADCHOUEL, J., MEILHAC, S., MONTARRAS, D., ROCANCOURT, D. and RELAIX, F. (2003). The formation of skeletal muscle: from somite to limb. *J Anat* 202: 59-68.

CHEN, H., LUN, Y., OVCHINNIKOV, D., KOKUBO, H., OBERG, K.C., PEPICELLI, C.V., GAN, L., LEE, B. and JOHNSON, R.L. (1998). Limb and kidney defects in Lmx1b mutant mice suggest an involvement of LMX1B in human nail patella syndrome. *Nat Genet* 19: 51-55.

CHRIST, B. and BRAND-SABERI, B. (2002). Limb muscle development. *Int J Dev Biol* 46: 905-914.

COLVIN, J.S., BOHNE, B.A., HARDING, G.W., MCEWEN, D.G. and ORNITZ, D.M. (1996). Skeletal overgrowth and deafness in mice lacking fibroblast growth factor receptor 3. *Nat Genet* 12: 390-397.

COUMOUL, X. and DENG, C.X. (2003). Roles of FGF receptors in mammalian development and congenital diseases. *Birth Defects Res C Embryo Today* 69: 286-304.

CROSSLEY, P.H., MINOWADA, G., MACARTHUR, C.A. and MARTIN, G.R. (1996). Roles for FGF8 in the induction, initiation, and maintenance of chick limb development. *Cell* 84: 127-136.

DAILEY, L., AMBROSETTI, D., MANSUKHANI, A. and BASILICO, C. (2005). Mechanisms underlying differential responses to FGF signaling. *Cytokine Growth Factor Rev* 16: 233-247.

DAVIDSON, D., BLANC, A., FILION, D., WANG, H., PLUT, P., PFEFFER, G., BUSCHMANN, M.D. and HENDERSON, J.E. (2005). Fibroblast growth factor (FGF) 18 signals through FGF receptor 3 to promote chondrogenesis. *J Biol*

Chem 280: 20509-20515.

DELEZOIDE, A.L., BENOIST-LASSELIN, C., LEGEAI-MALLET, L., LE MERRER, M., MUNNICH, A., VEKEMANS, M. and BONAVENTURE, J. (1998). Spatio-temporal expression of FGFR 1, 2 and 3 genes during human embryo-fetal ossification. *Mech Dev* 77: 19-30.

DE MOERLOOZE, L., SPENCER-DENE, B., REVEST, J., HAJIHOSSEINI, M., ROSEWELL, I. and DICKSON, C. (2000). An important role for the IIIb isoform of fibroblast growth factor receptor 2 (FGFR2) in mesenchymal-epithelial signalling during mouse organogenesis. *Development* 127: 483-492.

DENG, C., WYNSHAW-BORIS, A., ZHOU, F., KUO, A. and LEDER, P. (1996). Fibroblast growth factor receptor 3 is a negative regulator of bone growth. *Cell* 84: 911-921.

DUPREZ, D. (2002). Signals regulating muscle formation in the limb during embryonic development. *Int J Dev Biol* 46: 915-925.

EDOM-VOVARD, F., BONNIN, M.A. and DUPREZ, D. (2001a). Misexpression of Fgf-4 in the chick limb inhibits myogenesis by down-regulating Frek expression. *Dev Biol* 233: 56-71.

EDOM-VOVARD, F., BONNIN, M.A and DUPREZ, D. (2001b). Fgf8 transcripts are located in tendons during embryonic chick limb development. *Mech Dev* 108: 203-206.

ELOY-TRINQUET, S., WANG, H., EDOM-VOVARD, F. and DUPREZ, D. (2009). Fgf Signaling Components Are Associated With Muscles and Tendons During Limb Development. *Dev Dyn* 238: 1195-1206.

ESWARAKUMAR, V.P., LAX, I. and SCHLESSINGER, J. (2005). Cellular signaling by fibroblast growth factor receptors. *Cytokine Growth Factor Rev* 16: 139-149.

ESWARAKUMAR, V.P., MONSONEGO-ORNAN, E., PINES, M., ANTONOPOULOU, I., MORRISS-KAY, G.M. and LONAI, P. (2002). The IIIc alternative of Fgfr2 is a positive regulator of bone formation. *Development* 129: 3783-3793.

FALLON, J.F., LOPEZ, A., ROS, M.A., SAVAGE, M.P., OLWIN, B.B. and SIMANDL, B.K. (1994). FGF-2: apical ectodermal ridge growth signal for chick limb development. *Science* 264: 104-107.

GORIVODSKY, M. and LONAI, P. (2003). Novel roles of Fgfr2 in AER differentiation and positioning of the dorsoventral limb interface. *Development* 130: 5471-5479.

GROTHE, C., BRAND-SABERI, B., WILTING, J. and CHRIST, B. (1996). Fibroblast growth factor receptor 1 in skeletal and heart muscle cells: expression during early avian development and regulation after notochord transplantation. *Dev Dyn* 206: 310-317.

HAMBURGER, V. and HAMILTON, H.L. (1951). A series of normal stages in the development of the chick embryo. *J Morphol* 88: 49-92.

HAVENS, B.A., RODGERS, B. and MINA, M. (2006). Tissue-specific expression of Fgfr2b and Fgfr2c isoforms, Fgf10 and Fgf9 in the developing chick mandible. *Arch Oral Biol* 51: 134-145.

HENRIQUE, D., ADAM, J., MYAT, A., CHITNIS, A., LEWIS, J. and ISH-HOROWICZ, D. (1995). Expression of a Delta homologue in prospective neurons in the chick. *Nature* 375: 787-790.

ITOH, N., MIMA, T. and MIKAWA, T. (1996). Loss of fibroblast growth factor receptors is necessary for terminal differentiation of embryonic limb muscle. *Development* 122: 291-300.

LAZARUS, J.E., HEGDE, A., ANDRADE, A.C., NILSSON, O. and BARON, J. (2007). Fibroblast growth factor expression in the postnatal growth plate. *Bone* 40: 577-586.

LI, C., CHEN, L., IWATA, T., KITAGAWA, M., FU, X.Y. and DENG, C.X. (1999). A Lys644Glu substitution in fibroblast growth factor receptor 3 (FGFR3) causes dwarfism in mice by activation of STATs and ink4 cell cycle inhibitors. *Hum Mol Genet* 8: 35-44.

LIZARRAGA, G., FERRARI, D., KALINOESKI, M., OHUCHI, H., NOJI, S., KOSHER, R. A. and DEALY, C. N. (1999). FGFR2 signaling in normal and limbless chick limb buds. *Dev Genet* 25 (4): 331-338.

LOOMIS, C.A., HARRIS, E., MICHAUD, J., WURST, W., HANKS, M. and JOYNER, A.L. (1996). The mouse Engrailed-1 gene and ventral limb patterning. *Nature* 382: 360-363.

LU, P., YU, Y., PERDUE, Y. and WERB, Z. (2008). The apical ectodermal ridge is a timer for generating distal limb progenitors. *Development* 135: 1395-1405.

MANDLER, M. and NEUBUSER, A. (2004). FGF signaling is required for initiation of feather placode development. *Development* 131: 3333-3343.

MARCELLE, C., WOLF, J. and BRONNER-FRASER, M. (1995). The *in vivo* expression of the FGF receptor FREK mRNA in avian myoblasts suggests a role in muscle growth and differentiation. *Dev Biol* 172: 100-114.

MARIANI, F.V., AHN, C.P. and MARTIN, G.R. (2008). Genetic evidence that FGFs have an instructive role in limb proximal-distal patterning. *Nature* 453: 401-405.

MARICS, I., PADILLA, F., GUILLEMOT, J.F., SCAAL, M. and MARCELLE, C. (2002). FGFR4 signaling is a necessary step in limb muscle differentiation. *Development* 129: 4559-4569.

MARTIN, G.R. (1998). The roles of FGFs in the early development of vertebrate limbs. *Genes Dev* 12: 1571-1586.

MOFTAH, M.Z., DOWNIE, S.A., BRONSTEIN, N.B., MEZENTSEVA, N., PU, J., MAHER, P.A. and NEWMAN, S.A. (2002). Ectodermal FGFs induce perinodular inhibition of limb chondrogenesis *in vitro* and *in vivo* via FGF receptor 2. *Dev Biol* 249: 270-282.

MUNOZ-SANJUAN, I., SIMANDL, B.K., FALLON, J.F. and NATHANS, J. (1999). Expression of chicken fibroblast growth factor homologous factor (FHF)-1 and of differentially spliced isoforms of FHF-2 during development and involvement of FHF-2 in chicken limb development. *Development* 126: 409-421.

MURAKAMI, S., BALMES, G., MCKINNEY, S., ZHANG, Z., GIVOL, D. and DE CROMBRUGGHE, B. (2004). Constitutive activation of MEK1 in chondrocytes causes Stat1-independent achondroplasia-like dwarfism and rescues the Fgfr3-deficient mouse phenotype. *Genes Dev* 18: 290-305.

NAKAJIMA, A., NAKAJIMA, F., SHIMIZU, S., OGASAWARA, A., WANAKA, A., MORIYA, H., EINHORN, T.A. and YAMAZAKI, M. (2001). Spatial and temporal gene expression for fibroblast growth factor type I receptor (FGFR1) during fracture healing in the rat. *Bone* 29: 458-466.

NAKAJIMA, A., SHIMIZU, S., MORIYA, H. and YAMAZAKI, M. (2003). Expression of fibroblast growth factor receptor-3 (FGFR3), signal transducer and activator of transcription-1, and cyclin-dependent kinase inhibitor p21 during endochon-dral ossification: differential role of FGFR3 in skeletal development and fracture repair. *Endocrinology* 144: 4659-4668.

NAKAZAWA, F., NAGAI, H., SHIN, M. and SHENG, G. (2006). Negative regulation of primitive hematopoiesis by the FGF signaling pathway. *Blood* 108: 3335-3343.

NISWANDER, L., TICKLE, C., VOGEL, A., BOOTH, I. and MARTIN, G.R. (1993). FGF-4 replaces the apical ectodermal ridge and directs outgrowth and pattern-ing of the limb. *Cell* 75: 579-587.

NOJI S, KOYAMA E, MYOKAI F, NOHNO T, OHUCHI H, NISHIKAWA K and S., T. (1993). Differential expression of three chick FGF receptor genes, FGFR1, FGFR2 and FGFR3, in limb and feather development. *Prog Clin Biol Res* 383B: 645-654.

OHUCHI, H., KIMURA, S., WATAMOTO, M. and ITOH, N. (2000). Involvement of fibroblast growth factor (FGF)18-FGF8 signaling in specification of left-right asymmetry and brain and limb development of the chick embryo. *Mech Dev* 95: 55-66.

OHUCHI, H., NAKAGAWA, T., YAMAMOTO, A., ARAGA, A., OHATA, T., ISHIMARU, Y., YOSHIOKA, H., KUWANA, T., NOHNO, T., YAMASAKI, M. *et al.* (1997). The mesenchymal factor, FGF10, initiates and maintains the outgrowth of the chick limb bud through interaction with FGF8, an apical ectodermal factor. *Develop-ment* 124: 2235-2244.

ORNITZ, D.M., XU, J., COLVIN, J.S., MCEWEN, D.G., MACARTHUR, C.A., COULIERI, F. O., GAO, G. and GOLDFARB, M. (1996). Receptor Specificity of the Fibroblast Growth Factor Family. *J Biol Chem* 271: 15292-15297.

PARR, B.A. and MCMAHON, A.P. (1995). Dorsalizing signal Wnt-7a required for normal polarity of D-V and A-P axes of mouse limb. *Nature* 374: 350-353.

PARTANEN, J., SCHWARTZ, L. and ROSSANT, J. (1998). Opposite phenotypes of hypomorphic and Y766 phosphorylation site mutations reveal a function for Fgfr1 in anteroposterior patterning of mouse embryos. *Genes Dev* 12: 2332-2344.

PASCOAL, S. and PALMEIRIM, I. (2007). Watch-ing out for chick limb development. *Int Comp Biol* 47: 382-389.

PASCOAL, S., CARVALHO, C.R., RODRIGUEZ-LEON, J., DELFINI, M.C., DUPREZ, D., THORSTEINSDOTTIR, S. and PALMEIRIM, I. (2007a). A molecular clock operates during chick autopod proximal-distal outgrowth. *J Mol Biol* 368: 303-

10   *C.J. Sheeba et al.*

309.

PASCOAL, S., ANDRADE, R.P., BAJANCA, F. and PALMEIRIM, I. (2007b). Progressive mRNA decay establishes an mkp3 expression gradient in the chick limb bud. *Biochem Biophys Res Commun* 352: 153-157.

PRYKHOZHIJ, S.V. and NEUMANN, C.J. (2008). Distinct roles of Shh and Fgf signaling in regulating cell proliferation during zebrafish pectoral fin development. *BMC Dev Biol* 8: 91.

SAUNDERS, J.W., JR. (1948). The proximo-distal sequence of origin of the parts of the chick wing and the role of the ectoderm. *J Exp Zool* 108: 363-403.

SAVAGE, M.P. and FALLON, J.F. (1995). FGF-2 mRNA and its antisense message are expressed in a developmentally specific manner in the chick limb bud and mesonephros. *Dev Dyn* 202: 343-353.

SHIN, M., WATANUKI, K. and YASUGI, S. (2005). Expression of Fgf10 and Fgf receptors during development of the embryonic chicken stomach. *Gene Exp Patterns* 5: 511-516.

SUN, X., MARIANI, F.V. and MARTIN, G.R. (2002). Functions of FGF signalling from the apical ectodermal ridge in limb development. *Nature* 418: 501-508.

SZEBENYI, G., SAVAGE, M.P., OLWIN, B.B. and FALLON, J.F. (1995). Changes in the expression of fibroblast growth factor receptors mark distinct stages of chondrogenesis *in vitro* and during chick limb skeletal patterning. *Dev Dyn* 204: 446-456.

TABIN, C. and WOLPERT, L. (2007). Rethinking the proximodistal axis of the vertebrate limb in the molecular era. *Genes Dev* 21: 1433-1442.

TODT, W.L. and FALLON, J.F. (1984). Development of the apical ectodermal ridge in the chick wing bud. *J Embryol Exp Morphol* 80: 21-41.

TOWERS, M. and TICKLE, C. (2009). Growing models of vertebrate limb development. *Development* 136: 179-190.

TOZER, S., BONNIN, M.A., RELAIX, F., DI SAVINO, S., GARCIA-VILLALBA, P.,

COUMAILLEAU, P. and DUPREZ, D. (2007). Involvement of vessels and PDGFB in muscle splitting during chick limb development. *Development* 134: 2579-2591.

VERHEYDEN, J.M., LEWANDOSKI, M., DENG, C., HARFE, B.D. and SUN, X. (2005). Conditional inactivation of Fgfr1 in mouse defines its role in limb bud establishment, outgrowth and digit patterning. *Development* 132: 4235-4245.

WEINSTEIN, M., XU, X., OHYAMA, K. and DENG, C.X. (1998). FGFR-3 and FGFR-4 function cooperatively to direct alveogenesis in the murine lung. *Development* 125: 3615-3623.

WILKIE, A.O., PATEY, S.J., KAN, S.H., VAN DEN OUWELAND, A.M. and HAMEL, B.C. (2002). FGFs, their receptors, and human limb malformations: clinical and molecular correlations. *Am J Med Genet* 112: 266-278.

XU, X., WEINSTEIN, M., LI, C. and DENG, C. (1999). Fibroblast growth factor receptors (FGFRs) and their roles in limb development. *Cell Tissue Res* 296: 33-43.

YU, K., XU, J., LIU, Z., SOSIC,D., SHAO,J., OLSON, E.N., TOWLER, D.A. and ORNITZ, D.M. (2003). Conditional inactivation of FGF receptor 2 reveals an essential role for FGF signaling in the regulation of osteoblast function and bone growth. *Development* 130: 3063-3074.

YU, S., ZHENG, L., TRINH, D.K., ASA, S.L. and EZZAT, S. (2004). Distinct transcriptional control and action of fibroblast growth factor receptor 4 in differentiating skeletal muscle cells. *Lab Invest* 84: 1571-1580.

ZHANG, X., IBRAHIMI, O.A., OLSEN, S.K., UMEMORI, H., MOHAMMADI, M. and ORNITZ, D.M. (2006). Receptor specificity of the fibroblast growth factor family. The complete mammalian FGF family. *J Biol Chem* 281: 15694-15700.

ZHAO, P., CARETTI, G., MITCHELL, S., MCKEEHAN, W.L., BOSKEY, A.L., PACHMAN, L.M., SARTORELLI, V. and HOFFMAN, E.P. (2006). Fgfr4 is required for effective muscle regeneration *in vivo*. Delineation of a MyoD-Tead2-Fgfr4 transcriptional pathway. *J Biol Chem* 281: 429-438.

Chapter III: Limb molecular clock´s dependence on major limb signaling centers

Results presented in this chapter constitute a manuscript that is submitted to a peer reviewed journal:

Limb *hairy2* expression is a temporal and spatial output of AER/FGF and ZPA/SHH signaling

Caroline J. Sheeba, Raquel P. Andrade and Isabel Palmeirim.

Classification: Biological Sciences, Developmental Biology

Limb *hairy2* expression is a temporal and spatial output of AER/FGF and ZPA/SHH signaling

Caroline J Sheeba[1,2], Raquel P. Andrade[1,2] and Isabel Palmeirim[3§]

Addresses:

[1]Life and Health Sciences Research Institute (ICVS), School of Health Sciences, University of

Minho, Braga, Portugal

[2]ICVS/3B's - PT Government Associate Laboratory, Braga/Guimarães, Portugal

[3]IBB-Institute for Biotechnology and Bioengineering, Centro de Biomedicina Molecular e

Estrutural, Universidade do Algarve, Campus de Gambelas, Faro, Portugal

[§]**Corresponding author**: ipalmeirim@gmail.com; phone +351289244481; Fax: +351289800076

ABSTRACT

Embryo limb development is governed by the combined action of the limb signaling centers AER and ZPA. These influence the distal limb mesenchyme through the production of the FGF and SHH morphogenes, respectively. Graded AER/FGF signaling promotes proximal-distal (PD) limb outgrowth and patterning, while a gradient of ZPA-produced SHH activity patterns the anterior-posterior (AP) axis. The distal limb mesenchyme has been reported to present oscillatory expression of the *hairy2* gene, a component of the embryonic molecular clock (EC) operating in somitogenesis. The EC gene expression is strictly dependent on FGF and SHH-mediated regulation in the presomitic mesoderm. In the present work, we evaluated the dependence of limb *hairy2* expression on AER/FGF and ZPA/SHH signaling in the chick wing. We report that *hairy2* expression results from the cooperative action of both AER/FGF and ZPA/SHH signaling, mediated by Erk/Akt and Gli3 activation, respectively. FGFs act as instructive signals on *hairy2* and present a short-range and short-term mode of action. Moreover, FGFs can only induce *hairy2* expression when the tissue is in a permissive state, previously established by ZPA/SHH signaling, which acts on *hairy2* in a long-term and long-range fashion. Overall, our work evidences that *hairy2* is an output of coordinated ZPA/SHH and AER/FGF signaling in both space and time, which suggests that *hairy2* could be coupling limb outgrowth and patterning along AP and PD limb axes.

INTRODUCTION

Multiple human congenital disorders present limb malformations, with significant implications on individual health and overall life quality. The developmental biology field has greatly contributed to elucidate the mechanisms underlying human developmental disorders, significantly improving diagnosis and treatment of these conditions (Grzeschik, 2002). Short-limbed dwarfism, Apert and Greig syndromes are examples of such cases, where mutations in genes crucial for limb development (*fgfr3, fgfr2* and *gli3*, respectively) result in short and/or malformed limbs (Grzeschik, 2002; Eswarakumar et al., 2005).

Crosstalk between several key signaling pathways, such as FGF, RA and SHH is essential for correct limb bud initiation, outgrowth and patterning (Zeller et al., 2009). The limb develops along three orthogonal axes: anterior-posterior (AP), proximal-distal (PD) and dorsal-ventral (DV), orchestrated by key molecules produced in the limb signaling centres. The AP axis is governed by the zone of polarizing activity (ZPA), located at the posterior distal margin of the limb bud, through the production of Sonic Hedgehog (SHH). A ZPA-derived SHH gradient is established from the posterior to anterior limb tip, and regulates Gli activity levels essential for correct AP digit specification (Zeller et al., 2009).

The apical ectodermal ridge (AER) formed by an ectoderm thickening at the distal tip of the limb bud, drives development along the limb PD axis. Fibroblast growth factors (FGFs) mediate AER activity, as beads soaked in different FGFs are able to rescue limb truncations caused by AER ablation (Niswander et al., 1993; Fallon et al., 1994). Distal-to-proximal AER-derived FGF signaling is counteracted by an opposing proximal–to-distal gradient of Retinoic Acid (RA), from very early stages of development. As a result, limb bud cells positioned along the limb PD axis are under the influence of two opposing gradients, which underlie the Two-Signal Model proposed to explain the intricate PD patterning of the developing limb (Mercader et al., 2000; Tabin and Wolpert, 2007; Mariani et al., 2008). According to this model, the counteracting gradients of RA and FGF signaling activities overlap in the early limb bud, due to the tissue's reduced dimensions. Over time, proximal-RA and distal-FGF gradients become increasingly separated as the limb grows. This results in three separate domains, expressing distinct markers which denote the progenitors of the limb segments (stylopod, zeugopod and autopod). Combining *in vitro* primary culture of limb distal mesenchymal cells and the recombinant limb

approach, Cooper et al. clearly established the requirement of RA for the specification of the stylopod (proximal-most limb skeletal element) and of FGF8/WNT3a for the sequential specification of zeugopod and autopod (distal structures) (Cooper et al., 2011). A parallel study conducted by Rosello-Diez and collaborators also confirmed these results, by transplanting distal limbs to embryonic regions with differing RA content and employing recombinant limb experimental approaches (Rosello-Diez et al., 2011).

The Two Signal model does not contemplate the requirement of a time-counting mechanism for correct PD limb patterning. However, RA and FGF counteracting gradients have been described to co-operate with an embryonic molecular clock (EC) in control of somite segmentation along the embryo AP body axis, both temporally and spatially (Aulehla and Pourquie, 2010; Niwa et al., 2011). The EC has been described in several species, where cyclic expression of multiple genes belonging to the Notch, FGF and WNT signaling pathways operates (Dequeant et al., 2006; Krol et al., 2011). Cycles of *Hes1* gene expression have also been described in human mesenchymal stem cells (William et al., 2007), mouse neural progenitor cells (Shimojo et al., 2008) and, more recently, in embryonic stem (ES) cells (Kobayashi et al., 2009). Furthermore, the avian *Hes1* homolog gene *hairy2*, which is cyclically expressed during somitogenesis (Jouve et al., 2000), also presents cycles of expression in the limb distal mesenchyme, namely in chondrogenic precursor cells. Here, waves of *hairy2* expression periodically propagate along the posterior/distal to anterior/proximal axes with a 6h periodicity (Pascoal et al., 2007b; Aulehla and Pourquie, 2008).

In PSM, EC gene expression depends on FGF, RA and SHH (Aulehla and Pourquie, 2010; Resende et al., 2010). The distal limb mesenchyme, where *hairy2* is cyclically expressed, is in close proximity with the FGF-producing AER and the ZPA, a SHH source. Studies on how each one of these morphogens contributes to *hairy2* expression in the developing limb, however, have been lacking and may bring great insight to the field. Herein, we demonstrate the involvement of the two major limb signaling centers the AER and the ZPA and their signaling morphogens, FGFs and SHH, respectively, in the regulation of distal limb *hairy2* expression in the chick wing. ZPA/SHH acts as a long-term and long-range signal, creating a permissive state for *hairy2* expression along the tissue by building up a proper ratio of Gli activities, defined by Gli3A/Gli3-R$\geq$1. High levels of AER/FGF signaling, mediated by Erk and Akt pathway activation, are

instructive signals for *hairy2* expression, with short-term/short-range characteristics. Importantly, *hairy2* expression is a simultaneous readout of AER/FGF and ZPA/SHH and reflects their spatial and temporal signaling activities in the distal limb bud.

RESULTS

Limb *hairy2* expression depends on AER-derived FGF signaling

The developing limb presents distinct domains of *hairy2* expression, clearly visible from stages HH20 to HH28 (Pascoal et al., 2007b): *hairy2* is persistently expressed in the central muscle mass (Fig. 1*A*, CPD) and in the posterior/distal limb mesenchyme, including the ZPA (PPD, posterior positive domain). Contrastingly, *hairy2* transcripts are absent from the proximal posterior region (PND, posterior negative domain) and from the anterior limb (AND, anterior negative domain). In the distal-most limb mesenchyme (DCD, distal cyclic domain) *hairy2 is* cyclically expressed, with a 6h periodicity, and, for sake of simplicity, this can be represented by three distinct phases (Fig. 1*A*i-iii).

In order to evaluate if AER-derived signaling is involved in the regulation of distal limb *hairy2* expression, AER tissue was microsurgically ablated from the right-side forelimb (-AER) of stage HH22-24 chick embryos *in ovo*, while the contralateral limb was untouched (control). Complete AER ablation was confirmed upon random in situ hybridization for *fgf8* (Fig. 1*B*i,ii). Operated embryos were further incubated for 4h, after which *hairy2* expression was simultaneously evaluated in control and -AER limbs by in situ hybridization. We found that in the absence of the AER, *hairy2* expression was abolished in both the DCD and PPD, revealing a crucial role for AER signaling on *hairy2* expression in these domains (Fig. 1*B*iii,iv; n=13/13).

As FGFs are key signaling molecules produced by the AER, we sought to interrogate if the observed effect was through AER-produced FGF signaling. Beads soaked in recombinant FGF8 or FGF2 were implanted in the DCD immediately following AER ablation, and *hairy2* expression was assessed after 4h of incubation. Both FGF2 and FGF8 were able to induce *hairy2* expression around the beads (Fig. 1*B*v,vi; FGF8: n=4/5; FGF2: n=3/3), indicating the importance of FGFs for *hairy2* expression in the distal limb mesenchyme. Accordingly, treating the distal limb field with FGF inhibitor SU5402 (n=12) downregulated (n=7/12) or even abolished (n=4/12) *hairy2* expression (Fig. 1*B*vii,viii). We further assessed FGF-mediated *hairy2* regulation by implanting FGF8-soaked beads in different distal limb domains. *hairy2* expression was enhanced in DCD and PPD domains (Fig. 1*C*i-iv; DCD: n=10/12; PPD: n=9/9). FGF beads also induced ectopic *hairy2*

transcription in the *hairy2* negative domain, PND (Fig. 1*C*v,vi; n=25/27). Contrastingly, FGF8 was unable to induce *hairy2* in the AND (Fig. 1*C*vii,viii; n=20/20), even after 20h of incubation and with increased amounts of FGF8 (Fig. S1), suggesting the requirement of an additional signal which is present throughout the distal limb mesenchyme, except in the AND.

Together, our results indicate that AER-derived FGFs are absolutely required for *hairy2* expression in the PPD and DCD. Moreover, FGF can induce ectopic *hairy2* in the distal limb, suggesting that FGF plays an instructive role in *hairy2* expression. This is not so in the AND, revealing a divergence of *hairy2* regulation mechanisms operating in the posterior and anterior region of the distal limb.

Distal limb *hairy2* expression is regulated by ZPA-derived SHH

The posterior limb tissue presents high SHH levels produced by the ZPA. *hairy2* is persistently expressed in the PPD, overlapping the ZPA and is absent in the AND which is deprived of SHH signaling. These observations suggest a role for ZPA/SHH gradient in the regulation of *hairy2* expression along the AP limb axis. Accordingly, we found that distal *hairy2* expression was abrogated following 6h of *in ovo* ZPA ablation, while AER-*fgf8* was unaffected (Fig. 2*A*i-iv; *fgf:* n=4/4; *hairy2:* n=22/27), strongly suggesting the requirement of ZPA-mediated signaling for *hairy2* expression. We then replaced the ZPA by QT6 cells constitutively secreting SHH. Upon incubation, QT6-SHH was able to rescue *hairy2* (Fig. 2*A*v,vi; n=7/7), indicating that SHH is the ZPA-derived signal controlling *hairy2* expression. Supporting these results, chick forelimbs treated with the Hedgehog inhibitor cyclopamine no longer exhibited *hairy2* transcripts in the distal limb (Fig. 2*B*i,ii; n=5/6). In these conditions, SHH-target *patched1* expression was abolished while AER-*fgf8* was unaffected (Fig. S2). Finally, SHH-soaked beads positioned in the AND resulted in an anterior expansion of *hairy2* towards the bead (Fig. 2*B*iii,iv; n=11/15). These results clearly indicate that ZPA-derived SHH is essential for *hairy2* expression in the distal limb mesenchyme. However, SHH-bead in the AND induced *hairy2* only along the tissue adjacent to the AER, suggesting the involvement of AER/FGFs in this induction.

Intracellular signal transduction pathways mediating distal limb *hairy2* expression

Erk/MAPK and Akt/PI3K are two predominant intracellular pathways functioning downstream of AER/FGF signaling in the chick limb (Kawakami et al., 2003). The activation levels

of each pathway upon implantation of FGF8-soaked beads in either forelimb AND or PND were assessed by western-blot analysis, after 4.5h of incubation (Fig. 3*A,B*). Experimental and contralateral control limbs were surgically ablated and divided along the proximal-distal axis prior to protein extraction and the untreated halves were discarded. Upon FGF8-bead implantation in the PND, p-Erk levels were increased by 77% and p-Akt by 37% (Fig. 3*A*i,ii), suggesting that *hairy2* induction in the PND in response to FGF signaling (Fig. 1*C*v,vi) can be mediated by both Erk/MAPK and Akt/PI3K pathways. To further clarify these results, beads soaked in specific MAPK or PI3K inhibitors (UO126 and LY294002, respectively) were co-implanted with a FGF8-bead and *hairy2* pattern was analyzed. The tissue under the direct influence of either MAPK or PI3K inhibitors no longer exhibited ectopic *hairy2* (Fig. 3*A*iii; U0126: n=4/4; LY294002: n=5/6), further supporting an important role for Erk/MAPK and Akt/PI3K pathways in mediating FGF-induced *hairy2* expression in the posterior limb. These results suggest that the FGF instructive role on *hairy2* activation is through Erk/MAPK and Akt/PI3K pathways.

The implantation of FGF8-beads in the AND did not significantly impact Erk/MAPK or Akt/PI3K activation (Fig. 3*B*) and also failed to induce ectopic *hairy2* expression (Fig. 1*C*vii,viii). This observation indicates that the AND tissue is not competent to respond to FGF8 instructive action on *hairy2*, further suggesting the need for an additional signal. SHH is a good candidate, since it is absent from the AND and FGF8 was able to induce *hairy2* in all regions containing SHH signaling activity. Gli3 is a major signal transducer of SHH signaling, so we evaluated Gli3 activity levels by western-blot analysis, upon FGF8 treatment, as described above, or after 6h of SHH-bead implantation in the AND. In agreement with previous reports (Wang et al., 2000; Bastida et al., 2004), we found that there is higher Gli3-R activity in the anterior limb than in the posterior region (Fig. S3). The implantation of a FGF-bead in the AND further enhanced Gli3-R levels, while a SHH-bead greatly decreased the amount of Gli3-R (Fig. 4*A,B*; Fig. S3). These findings indicate that Gli3-R could be responsible for inhibiting *hairy2* expression in this limb region. The fact that FGFs induced Gli3-R form in the PND (Fig. 4*A,B*; Fig. S3) concomitantly with ectopic *hairy2* (Fig. 1*C*v,vi), shows that *hairy2* expression is not solely dependent on the presence/absence of Gli3-R, but must rely on balanced Gli3-A/Gli3-R activities.

We analyzed the correlation between the experimental conditions leading to *hairy2* expression and Gli3-A/Gli3-R levels (Fig. 4*C*). FGF8 in the PND increased the levels of Gli3-A and Gli3-R to the same extent, thus balancing the overall Gli3-A/Gli3-R ratio. Moreover, the Gli3-

A/Gli3-R ratio in the control is higher in the posterior than in the anterior limb region (Fig. 4*C*), which coincides with the presence and absence of *hairy2* expression, respectively. This suggests the existence of a Gli3-A/Gli3-R threshold for *hairy2* expression along the limb AP axis. A FGF8-bead in the AND significantly decreased the Gli3-A/Gli3-R ratio and failed to induce *hairy2* (Fig. 4*C*) On the contrary, when a SHH-soaked bead was implanted in the AND, an accumulation of Gli3-A was obtained (up to 76% increase), at the expense of Gli3-R form, as its levels drastically dropped. This resulted in high Gli3-A/Gli3-R activity (Fig. 4*C*) and ectopic *hairy2* expression (Fig. 2*B*iii,iv). Collectively, there is a straight correlation between *hairy2* expression and a Gli3-A/Gli3-R ratio equal or higher than 1. This clearly shows that SHH-mediated Gli3 activity levels regulate the tissue's ability to respond to FGF instructive signal for *hairy2* expression. Moreover, we find that FGF could only induce *hairy2* when Gli3-A/Gli3-R≥1, thus unveiling this condition as a permissive state for *hairy2* expression.

Our work suggests that limb *hairy2* expression requires a permissive state provided by ZPA/SHH signaling, defined as Gli3-A/Gli3-R≥1, as well as an instructive signal provided by AER/FGFs through Erk/MAPK and Akt/PI3K pathway activation in the developing limb bud. These data evidence the existence of a cooperative action of AER and ZPA in limb *hairy2* expression.

AER/FGF and ZPA/SHH cooperate in distal limb mesenchyme *hairy2* expression

In the above sections, we have shown that AER/FGF and ZPA/SHH are individually required for *hairy2* expression regulation in the distal limb. An interesting observation was that FGF8 could not induce ectopic *hairy2* expression in the AND (Fig. 1*C*vii,viii), while SHH expanded *hairy2* anteriorly along the AER-adjacent tissue (Fig. 2*B*iii,iv). However, SHH was no longer capable of inducing *hairy2* upon AER ablation (Fig. 5*A*i-vi; AND: n=3/3; DCD: n=4/4; PPD: n=3/3). These results indicate that ZPA/SHH is not sufficient *per se*, as AER/FGF is also necessary for *hairy2* induction. FGF beads implanted immediately upon ZPA ablation were capable of locally inducing *hairy2* expression (Fig. 5*B*i,ii; n=5/5), since this tissue is still in a permissive state due to the remaining SHH graded signaling. When FGF beads were implanted after 6h of ZPA removal, *hairy2* was no longer induced by FGF in either PND or DCD (Fig. 5*B*iii-vi PND: n=6/6; DCD: n=4/4), supporting the requirement of ZPA for FGF-induced *hairy2* expression.

Our results strongly suggest that ZPA/SHH and AER/FGF signaling are jointly required for *hairy2* expression (see also Fig. S4). To further test this concept, FGF8 and SHH beads were

concomitantly implanted in the AND. In these conditions, the levels of *hairy2* induction attained (Fig. 5*C*i,ii; n=5/5) were indistinguishable from those obtained with a SHH-bead alone (Fig. 2*B*iii,iv). But if the FGF-bead was implanted in a limb previously incubated for 6h with SHH, it now greatly induced ectopic *hairy2* in the AND (Fig. 5*C*iii,iv; n=6/6). This set of experiments shows that the AER/FGFs and ZPA/SHH act cooperatively in *hairy2* expression. Moreover, it is clear that SHH is a permissive signal, while FGFs play an instructive role on *hairy2* expression.

Different temporal and spatial requirements of AER/FGF and ZPA/SHH in the maintenance of distal limb *hairy2* expression

To further understand the dynamics of *hairy2* dependence on AER/FGF and ZPA/SHH, a detailed study of the temporal response of *hairy2* expression to the removal of each limb signaling centre was performed. In the absence of the AER, *hairy2* was down-regulated as soon as in 40min (Fig. 6*A*i-ii; n=2/2) and totally abolished after 1h of incubation (Fig. 6*A*iii-iv; n=5/5). Contrastingly, *hairy2* expression was not affected even after 2h of ZPA ablation (Fig. 6*A*v-vi; n=9/10), and cyclopamine-mediated SHH signaling inhibition for 4h also only mildly down-regulated *hairy2* expression (Fig. 6*A*ix,x; n=4/4). In fact, longer incubation periods were required for total *hairy2* depletion in the distal mesenchyme after ZPA ablation (Fig. 6*A*vii-viii; n=22/27) or cyclopamine treatment (Fig. 2*B*i,ii; n=5/6). This was not a consequence of cell death as revealed by TUNEL assay (Fig. S5). In these conditions, AER/FGF inductive signals are present as revealed by the intact *fgf8* expression detected after ZPA ablation and cyclopamine treatment (Fig. 2*A*i,ii; S2), but failed to induce *hairy2*. This further supports a role for SHH signaling in creating a permissive state for *hairy2* expression in the distal limb tissue. Together, these data evidence very different temporal responses of *hairy2* to both limb signaling centers: a short-term response to AER/FGF and a long-term response to ZPA/SHH.

To further characterize AER-mediated regulation of *hairy2* expression, we ablated solely the posterior- or anterior-AER and analyzed *hairy2* expression pattern. Partial AER ablations were randomly confirmed upon *fgf8* staining (Fig. 6*B*i,ii,ix,x). Upon posterior-AER ablation, *hairy2* was rapidly abolished in the PPD (Fig. 6*B*v,vi; n=4/4), while *shh* expression was still present (Fig. 6*B*iii,iv; n=2/2), further supporting an instructive role for FGF8 on *hairy2.* This was a spatially restricted effect, since *hairy2* expression in the DCD remained unperturbed (Fig. 6*B*vii,viii; n=2/2). Similarly, when the anterior-AER was ablated, *hairy2* was unperturbed in the posterior limb and

abolished in the DCD (Fig. 6*B*xiii-xvi; Phase1: n=2/2; Phase2: n=5/5). As expected, *shh* expression was present in these conditions (Fig. 6*B*xi,xii; n=2/2). Together, these results show a restricted spatial response of *hairy2* expression to local absence of AER signaling.

Altogether, our data propose ZPA- and AER-mediated signaling as distinct regulatory mechanisms acting on distal limb *hairy2* expression, both temporally and spatially. ZPA/SHH acts at a long-range and has a long-term permissive effect on *hairy2*, whereas the AER/FGF effect is of a short-term, short-range instructive nature.

Discussion

The limb signaling centers AER and ZPA govern *hairy2* expression

The chick limb mesenchyme displays distinct *hairy2* expression patterns (Fig. 1*A*) which are cyclically recapitulated in the sub-ridge mesenchyme (Pascoal et al., 2007b; Aulehla and Pourquie, 2008). *hairy2* transcripts are persistently present in the posterior limb encompassing the ZPA (PPD), dynamically expressed in the distal limb region (DCD) and absent in the anterior limb mesenchyme (AND). The proximity of *hairy2* expression domains to the two limb signaling centers, the AER and the ZPA, suggests their potential role in *hairy2* regulation. In fact, our results clearly show that upon AER or ZPA ablation *hairy2* was lost in the distal limb mesenchyme (Fig. 1*B*, 2*A*), evidencing an indispensable role for both AER and ZPA signaling centers in *hairy2* expression.

FGFs from the AER and ZPA-derived SHH are regulating limb *hairy2* expression

Dynamic *hairy2* expression is regulated by both FGF8 (Dubrulle et al., 2001) and SHH (Resende et al., 2010) in the presomitic mesoderm (PSM). The distal limb mesenchyme is under the influence of AER-derived FGFs and expresses appropriate FGF receptors (Sheeba et al., 2010), and it also presents PA graded ZPA/SHH signaling. We found that FGF-bead implantation could induce ectopic *hairy2* expression in the distal mesenchyme, even upon AER ablation (Fig. 1*B*). An FGF inhibitor produced the contrary effect (Fig. 1*B*), evidencing an instructive role for FGF in *hairy2* regulation in the limb. Substantiating these findings, *HES* genes have been reported to be induced by FGFs in multiple systems, such as in somitogenesis (Dubrulle et al., 2001; Kawamura et al., 2005; Niwa et al., 2007), inner ear development (Doetzlhofer et al., 2009) and neural progenitor cells (Sanalkumar et al., 2010). We further identified Erk/MAPK and Akt/PI3K as the

effectors of FGF-mediated *hairy2* regulation in the limb (Fig. 3). This result is supported by a clear correlation between FGF-mediated Erk phosphorylation and *hairy2* homolog *hes1* expression in C3H10T1/2 cells (Nakayama et al., 2008).

       The consistent absence of *hairy2* in the AND, despite of the exposure to AER/FGF signaling, indicates that FGF is not sufficient for *hairy2* expression. The *hairy2*-negative AND tissue coincides with the region of the limb that is deprived of SHH signaling (Wang et al., 2000; Harfe et al., 2004). On the contrary, *hairy2* is persistently expressed in the PPD, which presents continuous high levels of SHH (Wang et al., 2000; Harfe et al., 2004), which suggests an important role for ZPA/SHH in limb *hairy2* regulation. There are previous reports of a regulatory action of SHH on *HES* genes (Ingram et al., 2008; Wall et al., 2009; Resende et al., 2010) and *shh* null mouse limb buds present downregulation of *hes1* expression (Probst et al., 2011). Accordingly, ZPA ablation or treatment with cyclopamine abolished *hairy2*, while QT6-SHH cells replacing the ZPA, rescued *hairy2* expression throughout the distal limb (Fig. 2*A*). We further show that *hairy2* expression is mediated by fine-tuned Gli3-A/Gli3-R activity levels (Fig. 4). *hairy2* expression in the chick PSM is also proposed to be regulated by fine-tuned levels of Gli-A/Gli-R activity (Resende et al., 2010). In our experimental conditions, *hairy2* was persistently expressed when Gli3-A levels were higher than Gli3-R (Gli3-A/Gli3-R>1), *hairy2* was cyclically expressed when both Gli3 forms were present in equivalent amounts (Gli3-A/Gli3-R tending towards 1), and was absent in the limb region where Gli3-R activity prevailed (Gli3-A/Gli3-R<1). These results evidence a SHH-induced permissive state for *hairy2* expression in the distal limb that can be defined as Gli3-A/Gli3-R≥1.

       A gradient of ZPA-derived SHH signaling governs digit specification along the limb AP axis (Zeller et al., 2009). We find that the spatial distribution of *hairy2* expression recapitulates the SHH gradient, mediated by balanced Gli3 activity. Strikingly, a proper balance between the Gli3-A and Gli3-R activities have been proposed to underlie the specification of limb digit number and identity (Wang et al., 2007), which leads us to hypothesis that *hairy2* could be involved in limb AP patterning.

hairy2 expression is at the intersection of AER/FGF and ZPA/SHH signaling

       As discussed above, in the AND, FGF signaling was unable to induce *hairy2* expression, since this tissue is not in a SHH-mediated permissive state. Accordingly, when a non-permissive

state was imposed on either the PND or DCD by total deprivation of ZPA/SHH signaling, FGF-beads failed to induce *hairy2* expression (Fig. 5*B*), contrarily to what had been observed in the presence of ZPA/SHH (Fig. 1*C*). The observation that FGF-bead implantation immediately upon ZPA ablation was still capable of locally inducing *hairy2* (Fig. 5*B*), further reveals the requirement of SHH-mediated tissue permissiveness for the instructive FGF signal to act on *hairy2* expression. This was clearly shown by treating the AND with SHH to induce a permissive state on the tissue, followed by implantation of FGF beads, which now ectopically induced *hairy2* expression (Fig. 5*C*).

Furthermore, we found that SHH alone was not sufficient for *hairy2* induction, as SHH-beads were unable to induce *hairy2* upon AER ablation, in all tested limb domains (Fig. 5*A*). Moreover, *hairy2* is also not expressed in the PND, a SHH-signaling rich region, but distanced from the AER/FGF source (Fig. 1*A*). These observations clearly reveal a mutual dependency between AER/FGF and ZPA/SHH for *hairy2* induction. In fact, SHH-bead implantation in the AND, which is under AER/FGF influence, resulted in *hairy2* misexpression along the limb mesenchyme beneath the AER, indicating the requirement for a cooperative action between instructive-FGF and permissive-SHH signaling in this event. Having performed a detailed time-lapse study, we found that *hairy2* and *shh* are simultaneously induced upon FGF-bead implantation (Fig. S4). This observation strongly suggests that *hairy2* induction mechanism does not involve a relay of FGF and/or SHH molecular signals, but results from a parallel convergence of signaling pathways, in both time and space, *i.e.* both signals are required at the same time, in the same tissue. Such unique mode of combinatory requirement of FGF and SHH signaling has been previously reported for *Twist* expression (Tavares et al., 2001; Hornik et al., 2004).

Hairy2 presents distinct temporal and spatial responses to AER/FGF and ZPA/SHH

We observed a clear difference in the temporal response of *hairy2* levels to FGF and SHH signaling, strikingly consistent with what would be expected for an instructive/permissive behavior, respectively. FGF8-beads induced *hairy2* within 45 min of implantation (Fig. S4) and AER ablation significantly downregulated *hairy2* in a similar short-term fashion (Fig. 6*A*). Quite contrarily, ZPA ablation or SHH-inhibition took at least 5h to impact *hairy2* expression to the same extent (Fig. 6*A;* 2*B*), suggesting that the influence of ZPA-derived SHH signaling on *hairy2* has a long-term nature. Accordingly, the distal limb remains in a permissive state for a long

period of time even after ZPA removal, evidenced by the fact that FGF beads could induce *hairy2* when implanted immediately upon ZPA ablation and 6h were required to revert this permissiveness (Fig. 5*B*). In a parallel experiment, 6h of AND incubation with SHH were required to build up the Gli3-A/Gli3-R≥1 ratio, allowing the FGF inductive effect on *hairy2* (Fig. 5*C*). These results support the previously described memory of SHH exposure in limb mesenchymal cells (Harfe et al., 2004). They also showed that SHH-bead implantation in the anterior limb diminished Gli3-R levels only after 4-8h. Besides a similar observation, we also report a concomitant increase in Gli3-A (Fig. 4), supporting that SHH long-term permissive signaling is mediated by balanced Gli3-A/Gli3-R activities.

AER/FGF and ZPA/SHH further exerted differential regulation on limb *hairy2* expression in space in the experimental conditions tested. It has been previously reported that FGFs present a short-range mode of action due to their interaction with heparin or heparan sulfate proteoglycans (Ornitz, 2000). By performing meticulous partial AER ablations, we showed that *hairy2* is lost solely in the region adjacent to the ablation site, while unaffected in the rest of the limb (Fig. 6*B*), indicating that *hairy2* expression directly depends on juxtaposed AER/FGF tissue. Additionally, FGF-beads induced *hairy2* strictly around the bead (Fig. 1*C*), further suggesting that FGF acts as a short-range signal on *hairy2*. Contrastingly, ZPA/SHH regulates *hairy2* at a distance. It is well known that SHH patterns the limb AP axis through long-range diffusion from the ZPA (Harfe et al., 2004), mediated by Gli3 processing (Wang et al., 2000). In fact, ZPA-ablation abolished *hairy2* in the whole distal mesenchyme, and QT6-SHH cells rescued *hairy2* expression along the entire AP limb axis (Fig. 2*Avi*), indicating that SHH regulates *hairy2* at a long-range.

Altogether, *hairy2* expression in the distal limb field results from short-range/short-term instructive AER/FGF signaling in a permissive-state tissue, ensured by long-range/long-term ZPA/SHH signaling. This means that *hairy2* expression is a simultaneous readout of both limb signaling centers and reflects the temporal and spatial dynamics of AER and ZPA signaling.

Proposed model for the regulatory mechanisms underlying the distinctive patterns of *hairy2* expression in the distal limb

We describe a strict regulation of *hairy2* in limb distal mesenchyme by appropriate combination of signaling activities, which occur in a domain-dependent fashion (Fig. 7). High levels of FGF signaling emanated from the AER and a ratio of Gli3A/Gli3-R≥ 1 established by the

ZPA/SHH, defines the required conditions for *hairy2* expression. These conditions are met in the PPD, where steady expression of *hairy2* is observed. The DCD possesses moderate levels of SHH, mediated by balanced Gli-A/Gli-R activity (above, but close to 1) and high AER-FGF signal. This combination may allow the dynamic *hairy2* expression observed in the DCD. The AND contains Gli3-A/Gli3-R<1, which is a non-permissive state and defines this region as a *hairy2*-free limb domain. On the other hand, although the PND experiences high levels of ZPA/SHH signaling (Gli-A/Gli-R≥1, permissive state), it does not present *hairy2* expression due to the fact that it is distanced from the ARE/FGF source.

An inter-dependency of AER/FGFs and ZPA/SHH for limb outgrowth and patterning is well established, as a feedback loop between these two signaling centers is known to function throughout limb development (Zeller et al., 2009). To our knowledge, *hairy2* is one of the very first molecular targets laying at the intersection of both limb signaling centers, AER and ZPA, acting as readout of their spatial and temporal signaling activities. The dynamics of *hairy2* expression along both AP and PD limb axes suggests that *hairy2* may be coupling limb outgrowth and patterning in both time and space, thus underlying coordinated AP and PD limb development.

MATERIALS AND METHODS

Detailed materials and methods can be found in *SI Materials and Methods*. All experiments were performed in stage HH22-24 (Hamburger and Hamilton, 1951) forelimb buds. In situ hybridizations were performed as described (Henrique et al., 1995), using antisense digoxigenin-labeled RNA probes for *shh* (Riddle et al., 1993), *hairy2* (Jouve et al., 2000), *fgf8* (Crossley et al., 1996) and *patched1* (Marigo and Tabin, 1996). AER or ZPA were microsurgically ablated from the right wing bud *in ovo* and the contralateral limb served as control. In SHH-graft experiments, clumps of either QT6-ctrl or QT6-Shh cells (Duprez et al., 1998) were juxtaposed to the ZPA-ablated region. Beads soaked in FGF8 or FGF2 (1µg/µl; R&D Systems) or SHH (4µg/µl; R&D Systems) in PBS were implanted into the mesoderm of the right limb *in ovo*. For chemical treatments, beads were soaked in SU5402 (10mM, Calbiochem), U0126 (10mM; Calbiochem) or LY294002 (20mM; Sigma) in DMSO. Cyclopamine solution (1mg/ml, Calbiochem) was applied on the right limb. Treated embryos were re-incubated *in ovo* for different time periods. Western-blots were probed with the antibodies: p44/42 MAPK, phosphor-p44/42 MAPK, Akt, phosphor-Akt primary (Cell signaling), β-tubulin (Abcam) and Gli3 (Wang et al., 2000).

REFERENCES

1.   Grzeschik KH (2002) Human limb malformations; an approach to the molecular basis of development. *The International journal of developmental biology* 46(7):983-991.
2.   Eswarakumar VP, Lax I, & Schlessinger J (2005) Cellular signaling by fibroblast growth factor receptors. *Cytokine & growth factor reviews* 16(2):139-149.
3.   Zeller R, Lopez-Rios J, & Zuniga A (2009) Vertebrate limb bud development: moving towards integrative analysis of organogenesis. *Nature reviews. Genetics* 10(12):845-858.
4.   Fallon JF*, et al.* (1994) FGF-2: apical ectodermal ridge growth signal for chick limb development. *Science* 264(5155):104-107.
5.   Niswander L, Tickle C, Vogel A, Booth I, & Martin GR (1993) FGF-4 replaces the apical ectodermal ridge and directs outgrowth and patterning of the limb. *Cell* 75(3):579-587.
6.   Mariani FV, Ahn CP, & Martin GR (2008) Genetic evidence that FGFs have an instructive role in limb proximal-distal patterning. *Nature* 453(7193):401-405.
7.   Mercader N*, et al.* (2000) Opposing RA and FGF signals control proximodistal vertebrate limb development through regulation of Meis genes. *Development* 127(18):3961-3970.
8.   Tabin C & Wolpert L (2007) Rethinking the proximodistal axis of the vertebrate limb in the molecular era. *Genes & development* 21(12):1433-1442.
9.   Cooper KL*, et al.* (2011) Initiation of proximal-distal patterning in the vertebrate limb by signals and growth. *Science* 332(6033):1083-1086.
10.   Rosello-Diez A, Ros MA, & Torres M (2011) Diffusible signals, not autonomous mechanisms, determine the main proximodistal limb subdivision. *Science* 332(6033):1086-1088.
11.   Aulehla A & Pourquie O (2010) Signaling gradients during paraxial mesoderm development. *Cold Spring Harbor perspectives in biology* 2(2):a000869.
12.   Niwa Y*, et al.* (2011) Different types of oscillations in Notch and Fgf signaling regulate the spatiotemporal periodicity of somitogenesis. *Genes & development* 25(11):1115-1120.
13.   Dequeant ML*, et al.* (2006) A complex oscillating network of signaling genes underlies the mouse segmentation clock. *Science* 314(5805):1595-1598.
14.   Krol AJ*, et al.* (2011) Evolutionary plasticity of segmentation clock networks. *Development* 138(13):2783-2792.

15.   William DA, *et al.* (2007) Identification of oscillatory genes in somitogenesis from functional genomic analysis of a human mesenchymal stem cell model. *Developmental biology* 305(1):172-186.

16.   Shimojo H, Ohtsuka T, & Kageyama R (2008) Oscillations in notch signalling regulate maintenance of neural progenitors. *Neuron* 58(1):52-64.

17.   Kobayashi T, *et al.* (2009) The cyclic gene Hes1 contributes to diverse differentiation responses of embryonic stem cells. *Genes & development* 23(16):1870-1875.

18.   Jouve C, *et al.* (2000) Notch signalling is required for cyclic expression of the hairy-like gene HES1 in the presomitic mesoderm. *Development* 127(7):1421-1429.

19.   Aulehla A & Pourquie O (2008) Oscillating signaling pathways during embryonic development. *Current opinion in cell biology* 20(6):632-637.

20.   Pascoal S, *et al.* (2007) A molecular clock operates during chick autopod proximal-distal outgrowth. *Journal of molecular biology* 368(2):303-309.

21.   Resende TP, *et al.* (2010) Sonic hedgehog in temporal control of somite formation. *Proceedings of the National Academy of Sciences of the United States of America* 107(29):12907-12912.

22.   Kawakami Y, *et al.* (2003) MKP3 mediates the cellular response to FGF8 signalling in the vertebrate limb. *Nature cell biology* 5(6):513-519.

23.   Bastida MF, *et al.* (2004) Levels of Gli3 repressor correlate with Bmp4 expression and apoptosis during limb development. *Developmental dynamics : an official publication of the American Association of Anatomists* 231(1):148-160.

24.   Wang B, Fallon JF, & Beachy PA (2000) Hedgehog-regulated processing of Gli3 produces an anterior/posterior repressor gradient in the developing vertebrate limb. *Cell* 100(4):423-434.

25.   Dubrulle J, McGrew MJ, & Pourquie O (2001) FGF signaling controls somite boundary position and regulates segmentation clock control of spatiotemporal Hox gene activation. *Cell* 106(2):219-232.

26.   Sheeba CJ, Andrade RP, Duprez D, & Palmeirim I (2010) Comprehensive analysis of fibroblast growth factor receptor expression patterns during chick forelimb development. *The International journal of developmental biology* 54(10):1517-1526.

27.   Kawamura A, *et al.* (2005) Zebrafish hairy/enhancer of split protein links FGF signaling to cyclic gene expression in the periodic segmentation of somites. *Genes & development* 19(10):1156-1161.

28.   Niwa Y, *et al.* (2007) The initiation and propagation of Hes7 oscillation are cooperatively regulated by Fgf and notch signaling in the somite segmentation clock. *Developmental cell* 13(2):298-304.

29.   Doetzlhofer A, *et al.* (2009) Hey2 regulation by FGF provides a Notch-independent mechanism for maintaining pillar cell fate in the organ of Corti. *Developmental cell* 16(1):58-69.

30.   Sanalkumar R, *et al.* (2010) ATF2 maintains a subset of neural progenitors through CBF1/Notch independent Hes-1 expression and synergistically activates the expression of Hes-1 in Notch-dependent neural progenitors. *Journal of neurochemistry* 113(4):807-818.

31.   Nakayama K, Satoh T, Igari A, Kageyama R, & Nishida E (2008) FGF induces oscillations of Hes1 expression and Ras/ERK activation. *Current biology : CB* 18(8):R332-334.

32.   Harfe BD, *et al.* (2004) Evidence for an expansion-based temporal Shh gradient in specifying vertebrate digit identities. *Cell* 118(4):517-528.

33.   Ingram WJ, McCue KI, Tran TH, Hallahan AR, & Wainwright BJ (2008) Sonic Hedgehog regulates Hes1 through a novel mechanism that is independent of canonical Notch pathway signalling. *Oncogene* 27(10):1489-1500.

34.   Wall DS*, et al.* (2009) Progenitor cell proliferation in the retina is dependent on Notch-independent Sonic hedgehog/Hes1 activity. *The Journal of cell biology* 184(1):101-112.

35.   Probst S*, et al.* (2011) SHH propagates distal limb bud development by enhancing CYP26B1-mediated retinoic acid clearance via AER-FGF signalling. *Development* 138(10):1913-1923.

36.   Wang C, Ruther U, & Wang B (2007) The Shh-independent activator function of the full-length Gli3 protein and its role in vertebrate limb digit patterning. *Developmental biology* 305(2):460-469.

37.   Hornik C, Brand-Saberi B, Rudloff S, Christ B, & Fuchtbauer EM (2004) Twist is an integrator of SHH, FGF, and BMP signaling. *Anatomy and embryology* 209(1):31-39.

38.   Tavares AT, Izpisuja-Belmonte JC, & Rodriguez-Leon J (2001) Developmental expression of chick twist and its regulation during limb patterning. *The International journal of developmental biology* 45(5-6):707-713.

39.   Ornitz DM (2000) FGFs, heparan sulfate and FGFRs: complex interactions essential for development. *BioEssays : news and reviews in molecular, cellular and developmental biology* 22(2):108-112.

40.   Hamburger V & Hamilton HL (1951) A series of normal stages in the development of the chick embryo. *Dev. Dyn.* 195:231-272.

41.   Henrique D*, et al.* (1995) Expression of a Delta homologue in prospective neurons in the chick. *Nature* 375(6534):787-790.

42.   Riddle RD, Johnson RL, Laufer E, & Tabin C (1993) Sonic hedgehog mediates the polarizing activity of the ZPA. *Cell* 75(7):1401-1416.

43.   Crossley PH, Minowada G, MacArthur CA, & Martin GR (1996) Roles for FGF8 in the induction, initiation, and maintenance of chick limb development. *Cell* 84(1):127-136.

44.   Marigo V & Tabin CJ (1996) Regulation of patched by sonic hedgehog in the developing neural tube. *Proceedings of the National Academy of Sciences of the United States of America* 93(18):9346-9351.

45.   Duprez D, Fournier-Thibault C, & Le Douarin N (1998) Sonic Hedgehog induces proliferation of committed skeletal muscle cells in the chick limb. *Development* 125(3):495-505.

FIGURE LEGENDS

Fig. 1. AER-derived FGF signaling is required for limb *hairy2* expression

(*A*) Schematic representation of limb *hairy2* expression domains. (*Ai,ii,iii*) *hairy2* expression phases in HH24 chick forelimbs, cyclically recapitulated with a 6h periodicity (Pascoal et al., 2007b). *hairy2* is permanently present in the central positive domain (CPD) and in the posterior positive domain (PPD), overlapping the ZPA. It is not expressed in neither anterior negative domain (AND) nor posterior negative domain (PND). *hairy2* is cyclically expressed in the distal cyclic domain (DCD), presenting different intensity in each phase of expression. (*Bi,ii*) Evidence for the presence/absence of AER in control and experimental (-AER 4h) limb buds, respectively, by in situ hybridization for *fgf8*. (*Biii-viii*) Representative results of *hairy2* downregulation (DCD, arrow; PPD, arrowhead) upon AER ablation or SU5402-bead implantation in AER-containing limbs, and *hairy2* induction by FGF8-bead in the absence of AER. (*C*) *hairy2* expression observed after implantation of FGF8-beads in different limb domains. FGF8 upregulated *hairy2* in all limb domains (*C*i-vi), except the AND (*C*vii,viii). Dorsal view; anterior to the top. Beads represented by asterisks.

Fig. 2. ZPA/SHH regulates *hairy2* expression in the distal limb

(*Ai,ii*) In situ hybridization for *fgf8* and *shh* revealing ZPA ablation and unaffected AER/*fgf8* expression. (*Aiii-vi*) Distal *hairy2* expression is lost upon ZPA ablation and rescued by SHH-secreting QT6-SHH cells. (*Bi,ii*) Shh inhibition by cyclopamine abolished *hairy2* expression in the distal limb (arrowhead). (*Biii,iv*) SHH-bead implantation in the AND ectopically expanded *hairy2* expression. Dorsal view; anterior to the top. Beads represented by asterisks.

Fig. 3. Activation of Erk/MAPK and Akt/PI3K pathways mediates FGF-induced *hairy2* expression.

Immunoblots for Erk, p-Erk, Akt, p-Akt and β-tubulin (loading control) using total protein extracts from posterior (*Ai*) or anterior (*Bi*) FGF8-bead implanted limb halves and their contralateral controls, as schematically represented above each lane. (*Aii*, *Bii*) Quantification of the fold change levels obtained in FGF-treated tissues. In the posterior limb, FGF8 significantly increases both p-Erk and p-Akt levels, whereas in the anterior domain, p-Erk is only slightly elevated and p-Akt is downregulated. (*Aiii*) Inhibition of FGF8-induced *hairy2* expression upon treatment with U0126

or LY4002, MAPK and PI3K inhibitors, respectively (arrowheads depict inhibition sites). Dorsal view; anterior to the top. FGF8 beads are represented by asterisks.

Fig. 4. SHH establishes a permissive state for *hairy2* expression in the distal limb, defined by balanced Gli3-A/Gli3-R levels.

(*A*) Immunoblots for Gli3-A, Gli3-R and β-tubulin (loading control) using total protein extracts from posterior FGF8-bead (asterisks) implanted limb halves, anterior FGF8- or SHH-bead (circle) treated limb halves and their contralateral controls, as schematically represented above each lane. (*B*) Fold change in the levels of Gli3-A and Gli3-R obtained in treated tissues. FGF8 increased both Gli3-A and Gli3-R to the same extent in the posterior limb (P-FGF8), whiles it only elevated Gli3-R in the anterior domain (A-FGF8). Here, SHH greatly increased Gli3-A, downregulating Gli3-R (A-SHH). (*C*) Comparison of varying *hairy2* expression responses (+, present; -, absent) to different treatments and the underlying ratio of Gli3-A/Gli3-R levels. Note that *hairy2* was expressed only when the tissue presented Gli3-A/Gli3-R≥1 (dark line), defining the SHH-mediated permissive state for *hairy2* expression.

Fig. 5. Limb *hairy2* expression requires cooperative AER/FGF and ZPA/SHH signaling.

Representative results of *hairy2* expression obtained upon implantation of SHH-beads in AER-ablated limbs (*A*) and FGF8-beads in ZPA-ablated limbs (*B*). SHH was unable to induce *hairy2* expression upon AER ablation (*A*). Implantation of FGF8-bead immediately after ZPA ablation induced local *hairy2* expression (*Bi,ii*, arrowhead). However, after 6h of ZPA ablation FGF8 failed to induce *hairy2* (*Biii-vi*). Beads represented by asterisks. (*Ci,ii*) *hairy2* expression observed after co-implantation of FGF8 and SHH beads in the AND. Only previously observed SHH-mediated expansion of *hairy2* expression is obtained. When FGF beads were implanted following 6h of SHH treatment (*Ciii,iv*), FGF8 was capable of inducing ectopic *hairy2* expression around the bead (arrowheads). S, SHH-bead; F, FGF8-bead. Dorsal view; anterior to the top.

Fig. 6. AER/FGFs and ZPA/SHH present distinctive temporal and spatial modes of action on *hairy2* expression

(*A*) Representative results of *hairy2* expression obtained upon AER ablation, ZPA removal and cyclopamine treatment. AER ablation results in a drastic, short-term downregulation of *hairy2*

(*Ai-iv*), while removal of the ZPA (*Av-viii*) or SHH inhibition with cyclopamine (*Aix,x*) only impact *hairy2* expression in a long-term fashion. Mild effects on *hairy2* expression could be observed at earlier time points (arrows). (*B*) AER/FGF signaling is shown to act at a short-range on *hairy2*. Upon partial ablation of either the posterior-AER (*Bi-viii*) or the anterior-AER (*Bix-xvi*), *hairy2* is downregulated only in the tissue immediately adjacent to the ablation site (arrows), while *shh* expression remains in the ZPA. Partial ablations were confirmed by in situ hybridization for *fgf8* (*Bi,ii,ix,x*). Dorsal view; anterior to the top.

Fig. 7. Proposed model for the regulatory mechanisms underlying the distinctive patterns of *hairy2* expression in the distal limb

The developing distal limb is under the concomitant influence of two signaling gradients, derived from the limb signaling centers: distal-proximal AER/FGF and posterior-anterior ZPA/SHH. *hairy2* is expressed in the distal mesenchyme, adjacent to the AER and presents three distinct expression domains, positioned along the AP axis. In the posterior-most region, *hairy2* is persistently expressed, overlapping the ZPA (PPD), *hairy2* is absent from the anterior limb (AND) and is cyclically expressed in the intermediate DCD. We describe that AER/FGF, acting through Erk/MAPK and Akt/PI3K, is an instructive signal for *hairy2* induction, acting at short-range, and in a short-term fashion throughout the entire distal limb mesenchyme. However, a permissive state mediated by ZPA/SHH signaling is required for the tissue to respond to FGF inductive signal. SHH permissive signal acts at long-range and in a long-term manner, patterning *hairy2* expression along the distal limb AP axis. In fact, the PPD and DCD present a ratio of Gli3-A/Gli3-R activities which are higher or proximal to one (yellow dots), allowing sustained and oscillatory *hairy2* expression respectively. In the AND, Gli3-A/Gli3-R<1 (grey dots), thus AER/FGFs can no longer induce *hairy2*. Importantly, *hairy2* expression is a simultaneous readout of AER/FGF and ZPA/SHH and reflects their spatial and temporal signaling activities in the distal limb bud.

SI MATERIALS AND METHODS

Eggs and embryos. Fertilized *Gallus gallus* eggs were incubated at 37.8°C in a 49% humidified atmosphere and staged according to Hamburger and Hamilton (HH) classification (Hamburger and Hamilton, 1951). All the experiments have been performed in stage HH22-24 forelimb buds.

RNA probes. Antisense digoxigenin-labelled RNA probes were produced as previously described: *shh* (Riddle et al., 1993), *hairy2* (Jouve et al., 2000)*, fgf8* (Crossley et al., 1996) and *patched1* (Marigo and Tabin, 1996).

Microsurgical ablation of AER and ZPA tissue. A window was cut in the shell of incubated eggs and the vitelline membrane was carefully removed. AER or ZPA was microsurgically ablated from the right wing bud of embryos using a tungsten needle. As a control, AER or ZPA extirpated embryos were randomly selected for direct fixation and hybridization with *fgf8* or *shh*, respectively. Operated embryos were re-incubated for different time periods (as long as 22h or as less as 15-30min), collected in PBS and fixed for in situ hybridization.

TUNEL assay. Apoptosis was analyzed using the Cell Death De-tection Kit (Roche) in limb sections with or without AER or ZPA after 2h or 6h, respectively. Ablated limbs were fixed overnight in 4% para-formaldehyde (PFA) in PBS, dehydrated, imbibed in paraffin and longitudinally sliced into 6μm sections. Sections were rehydrated, permeabilized with Proteinase K treatment for less than 7.5min at room temperature, and washed in PBS. Positive control embryos were incubated with DNase at 37 °C for 30min. Embryos and explants were incubated 2-4h at 37°C with the TUNEL solution mix and washed at least three times in PBS before visualization.

Cell graft experiments. The potential effect of SHH on the molecular clock was evaluated by grafting clumps of either QT6 quail fibroblasts stably transfected with an empty vector or with a construct carrying the SHH-coding region (QT6-SHH) (Duprez et al., 1998) in the posterior margin of the limb mesenchyme following ZPA ablation. Grafted embryos were re-incubated for 4-8h and processed for in situ hybridization.

Bead implantation experiments. Heparin acrylic beads (Sigma, H5263) and Affigel blue beads (Bio-Rad) were soaked for at least 1h at room temperature in recombinant human FGF8 or FGF2 (1µg/µl; R&D Systems) and SHH (4µg/µl; R&D Systems) protein solutions in PBS, respectively. The beads were implanted in-ovo into the mesoderm of chick wing buds, in the position and for the time, desired. For all experiments, beads soaked in PBS served as control. AG1-X2 beads (Bio-Rad) were incubated in SU5402 dissolved in DMSO (10mM, Calbiochem). The MAPK inhibitor, U0126 (10mM; Calbiochem) or the PI3K inhibitor, LY294002 (20mM; Sigma) in DMSO was applied using Affigel blue beads as carrier. Respective beads soaked in DMSO served as control. Both the PBS and DMSO control beads did not have any effect on gene expressions.

In ovo treatments. As described previously (Scherz et al., 2007), 5 µl of 1mg/ml cyclopamine (Calbiochem) dissolved in 45% HBC (Sigma) in PBS was applied on top of the limb to specifically antagonize SHH signaling.

In situ hybridization and imaging. In situ hybridization was performed as previously described (Henrique et al., 1995). Limbs processed for in situ hybridization were photographed using an Olympus DP71 digital camera coupled to an Olympus SZX16 stereomicroscope.

Immunoblot analysis. We performed western blot to analyze the two important intracellular pathways namely the ErK/MAPK and Akt/PI3K downstream of FGF signaling. We also assessed Gli3 activator and repressor levels downstream of SHH signaling.

Either FGF or SHH bead implanted forelimb buds were ablated and dissected along the distal-proximal axis into two halves in cold PBS. The bead implanted portions (either anterior or posterior limb) and its respective contralateral unmanipulated control limbs were collected separately. Portions from at least 10 different limbs were collected and the protein was extracted from each pool of limbs as per Kling et al. (Kling et al., 2002). 10 µg of protein extracts from FGF bead implanted limbs and the respective controls were loaded per well of a 12% SDS-PAGE minigel, subjected to electrophoresis at 100V (room temperature) and transferred to Hybond-C extra membrane (Amersham Pharmacia Biotech, Inc., Piscataway, NJ). Blots were probed with p44/42 MAPK, phosphor- p44/42 MAPK, Akt, phosphor-Akt primary antibodies (Cell signaling) over night at 4°C. β-tubulin (Abcam) antibody was used to probe the blots as loading control.

Blots were incubated with anti-rabbit secondary antibody (Abcam) for 45 min at room temperature, developed with Super Signal West Femto Substrate (Pierce Biotechnology, Inc., Rockford, IL) and exposed in Chemidoc (Bio-Rad). Full length (activator) and the short form (repressor) of Gli3 were determined from protein extracts obtained from PND-FGF-bead implanted limb halves; AND-FGF or SHH-bead implanted limb halves and their respective controls as described above. 70 µg of protein extract was loaded per well in a 7% SDS-PAGE gel and the immunoblot was performed using a polyclonel antibody against Gli3 kindly gifted by Dr. Wang (Wang et al., 2000) and all procedures were carried out as described above. Each set of experiments for both FGF and SHH downstream pathways were performed twice, each treatment with the limb halves from at least 10 limbs. Bands were quantified using Quantity one (Bio-Rad), normalized with loading control (β-tubulin) and plotted in Excel file.

REFERENCES

1. Hamburger V & Hamilton HL (1951) A series of normal stages in the development of the chick embryo. *Dev. Dyn.* 195:231-272.
2. Riddle RD, Johnson RL, Laufer E, & Tabin C (1993) Sonic hedgehog mediates the polarizing activity of the ZPA. *Cell* 75(7):1401-1416.
3. Jouve C*, et al.* (2000) Notch signalling is required for cyclic expression of the hairy-like gene HES1 in the presomitic mesoderm. *Development* 127(7):1421-1429.
4. Crossley PH, Minowada G, MacArthur CA, & Martin GR (1996) Roles for FGF8 in the induction, initiation, and maintenance of chick limb development. *Cell* 84(1):127-136.
5. Marigo V & Tabin CJ (1996) Regulation of patched by sonic hedgehog in the developing neural tube. *Proceedings of the National Academy of Sciences of the United States of America* 93(18):9346-9351.
6. Duprez D, Fournier-Thibault C, & Le Douarin N (1998) Sonic Hedgehog induces proliferation of committed skeletal muscle cells in the chick limb. *Development* 125(3):495-505.
7. Scherz PJ, McGlinn E, Nissim S, & Tabin CJ (2007) Extended exposure to Sonic hedgehog is required for patterning the posterior digits of the vertebrate limb. *Developmental biology* 308(2):343-354.
8. Henrique D*, et al.* (1995) Expression of a Delta homologue in prospective neurons in the chick. *Nature* 375(6534):787-790.
9. Kling DE*, et al.* (2002) MEK-1/2 inhibition reduces branching morphogenesis and causes mesenchymal cell apoptosis in fetal rat lungs. *American journal of physiology. Lung cellular and molecular physiology* 282(3):L370-378.
10. Wang B, Fallon JF, & Beachy PA (2000) Hedgehog-regulated processing of Gli3 produces an anterior/posterior repressor gradient in the developing vertebrate limb. *Cell* 100(4):423-434.
11. Yang Y & Niswander L (1995) Interaction between the signaling molecules WNT7a and SHH during vertebrate limb development: dorsal signals regulate anteroposterior patterning. *Cell* 80(6):939-947.

Figure S1: FGF8 bead is unable to induce *hairy2* in the AND.

(i-vi) Representative results of *hairy2* expression obtained upon implantation of FGF8-bead implantation in the AND of HH23-24 forelimb buds. *hairy2* expression was never induced in the AND even upon higher dosage *(iii,iv)* and longer incubations *(v,vi)*. Dorsal view; anterior to the top. FGF8 beads are represented by asterisks.

Figure S2: Effects observed upon cyclopamine treatments are exclusively through SHH signal inhibition.

(Ai,ii) In situ hybridization for *fgf8* and *patched1* revealing unaffected AER/*fgf8* expression and impaired ZPA/SHH signal shown by *patched1* downregulation in the treated limb. Dorsal view; anterior to the top.

Figure S3: Balanced Gli3-A and Gli3-R activities are required for ZPA/SHH-mediated limb *hairy2* expression.

Fold change in the levels of Gli3-A and Gli3-R levels detected in the untreated and FGF8 or SHH treated limb tissues in reference with the posterior control limb. Note that the anterior limbs (A-Ctrl) possess higher levels of Gli3-A and Gli3-R compared to the posterior control limb (P-Ctrl). FGF8 increased both Gli3-A and Gli3-R to the same extent in the posterior limb (P-FGF8), while it only elevated Gli3-R in the anterior domain (A-FGF8) compared to A-Ctrl. Here, SHH greatly increased Gli3-A and downregulating Gli3-R (A-SHH). This mode of Gli3 activity suggests the requirement of a balanced Gli3-A and Gli3-R levels rather than the presence or absence of any one form for limb *hairy2* expression.

Figure S4: A cooperative action of FGF8 and SHH signaling is required for *hairy2* induction in the limb

FGF8 beads can expand *shh* expression proximally when implanted near the ZPA (Yang and Niswander, 1995), which coincides with the PND, where FGF8-bead induces hairy2 expression (refer Fig. 1*Cvi*). FGF8-induced ectopic *shh* expression was obtained within the time frame of 15min *(vi,viii;* 30min: n=2/2, 45min: n=3/3). *(i-iv)* Concomitantly, FGF8 also induced ectopic *hairy2* within the same time frame of 15min as observed by its expression between 30 and 45min of FGF8-bead implantation (30min: n=2/2, 45min: n=4/4). These observations strongly support the

requirement of a cooperative action of FGF8 and SHH signaling for *hairy2* expression induction in the limb. In addition this further supports the short-term action of FGF signal for *hairy2* induction. Dorsal view; anterior to the top. FGF8 beads are represented by asterisks. (1) Yang Y & Niswander L (1995) Interaction between the signaling molecules WNT7a and SHH during vertebrate limb development: dorsal signals regulate anteroposterior patterning. *Cell* 80(6):939-947.

Figure S5: Downregulation of *hairy2* expression observed after AER or ZPA ablation is not due to cell death.

Cell death was assessed by performing TUNEL assay in longitudinal limb sections with and without the AER or ZPA. (*i,iv*) Positive control limb buds treated with DNase displaying apoptosis in the entire limb mesenchyme and ectoderm. (*ii,v*) Internal control limb buds without any manipulation showing normal pattern of apoptosis in the ectoderm and the proximal limb, respectively. (*iii*) Stage HH22 limb didn't show elevated cell death in the distal limb mesenchyme after 2h of AER ablation. (*vi*) Normal level of cell death observed after 6h of ZPA ablation in stage HH23 limb. Longitudinal limb sections are positioned such that the distal side toward the right and anterior to the top.
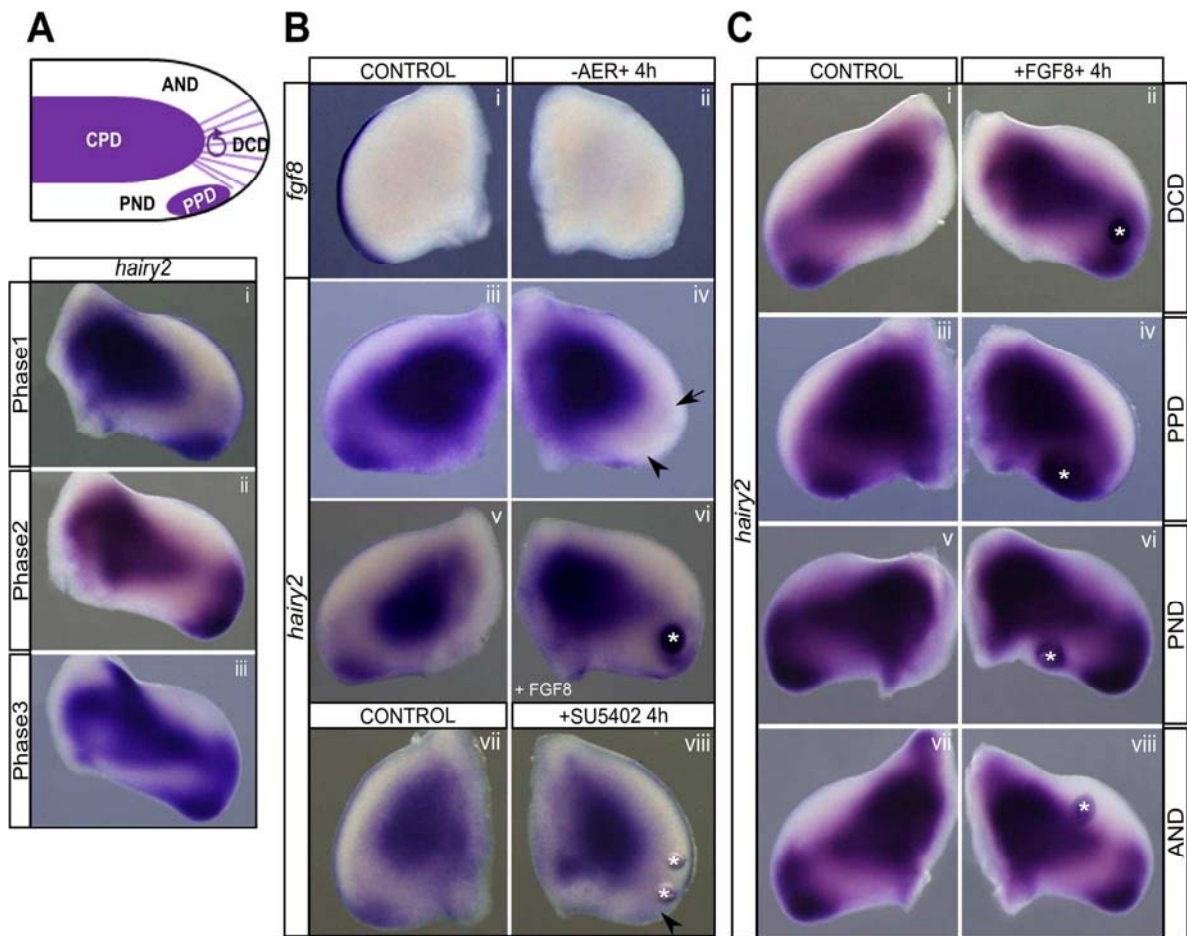
Figure 1

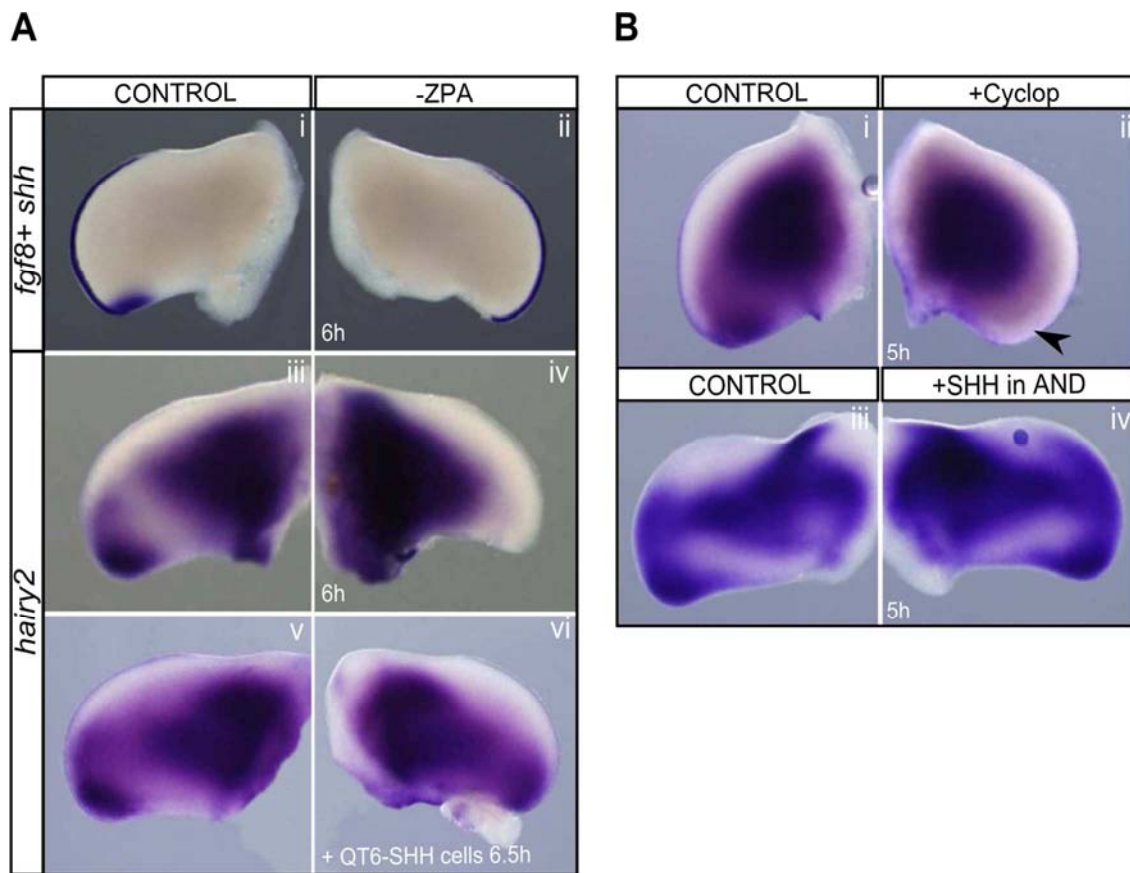**Figure 2**

Figure 3
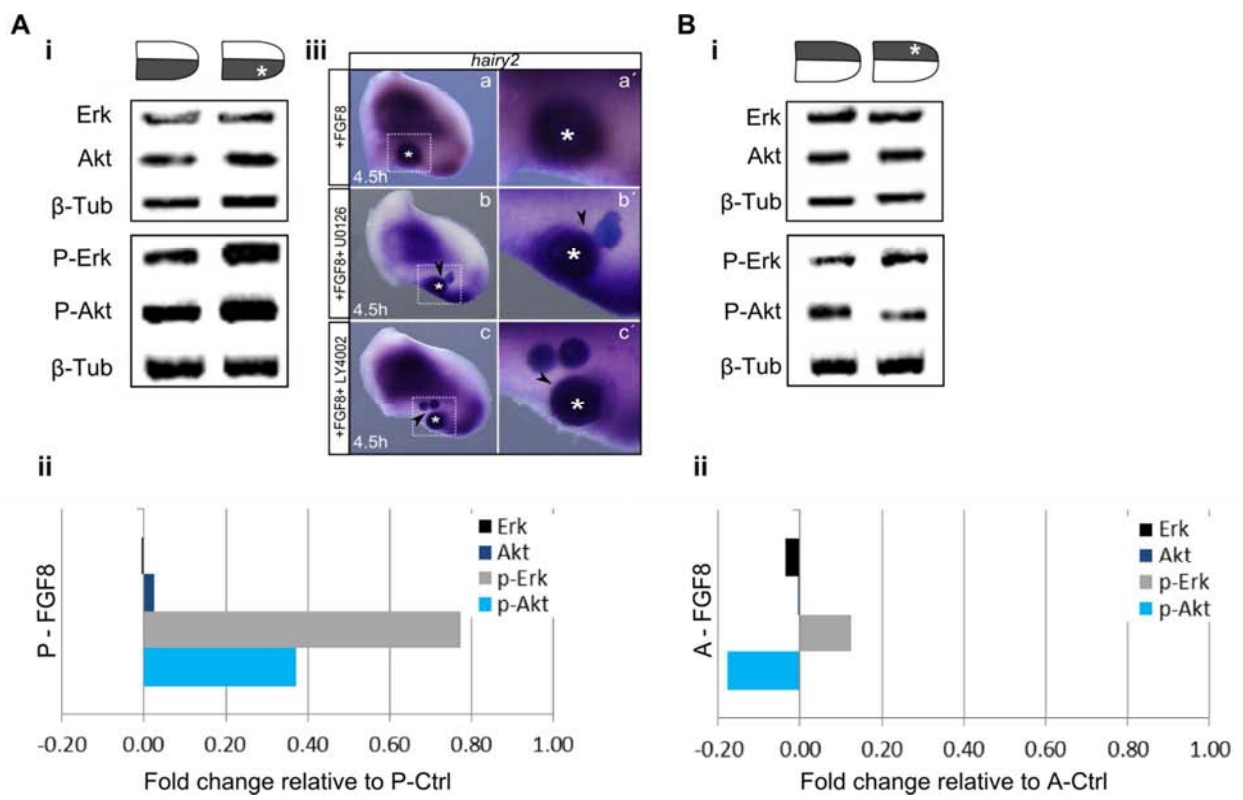
Figure 4
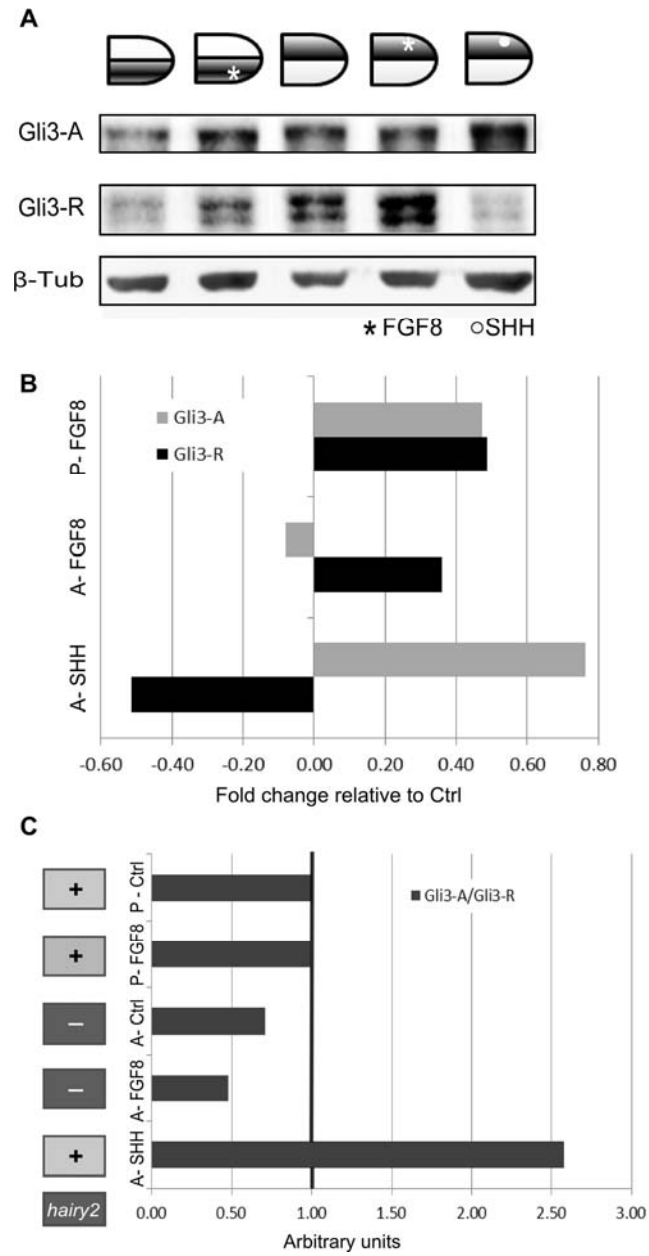
Figure 5
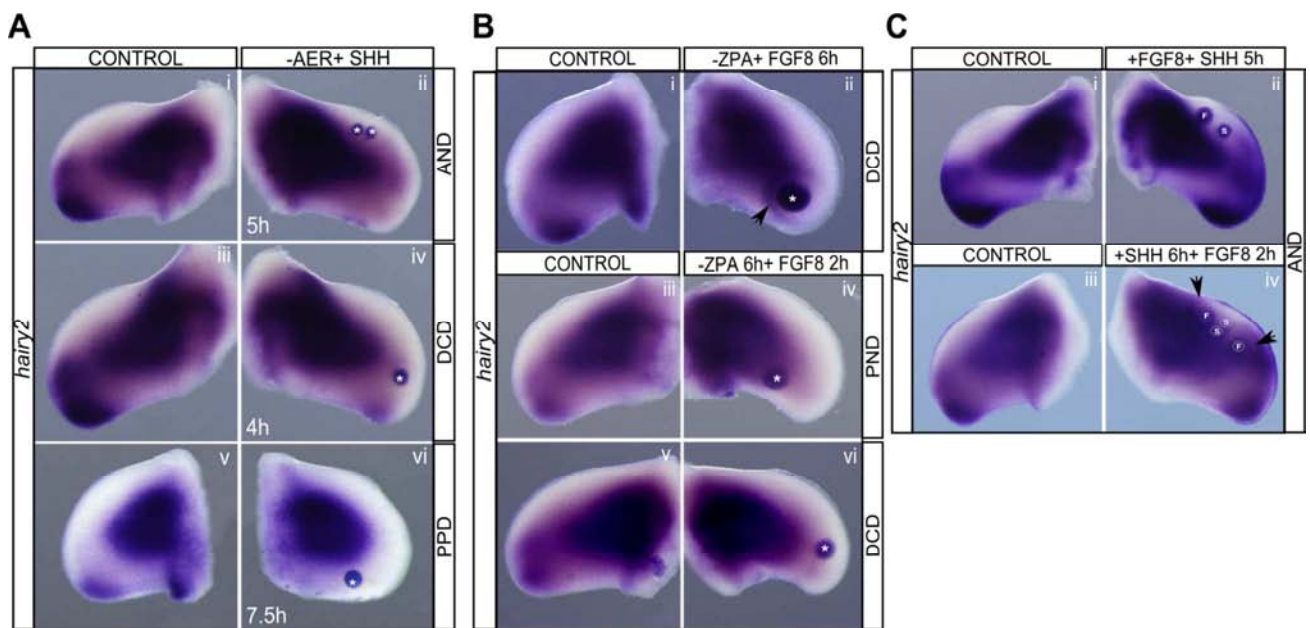
Figure 6
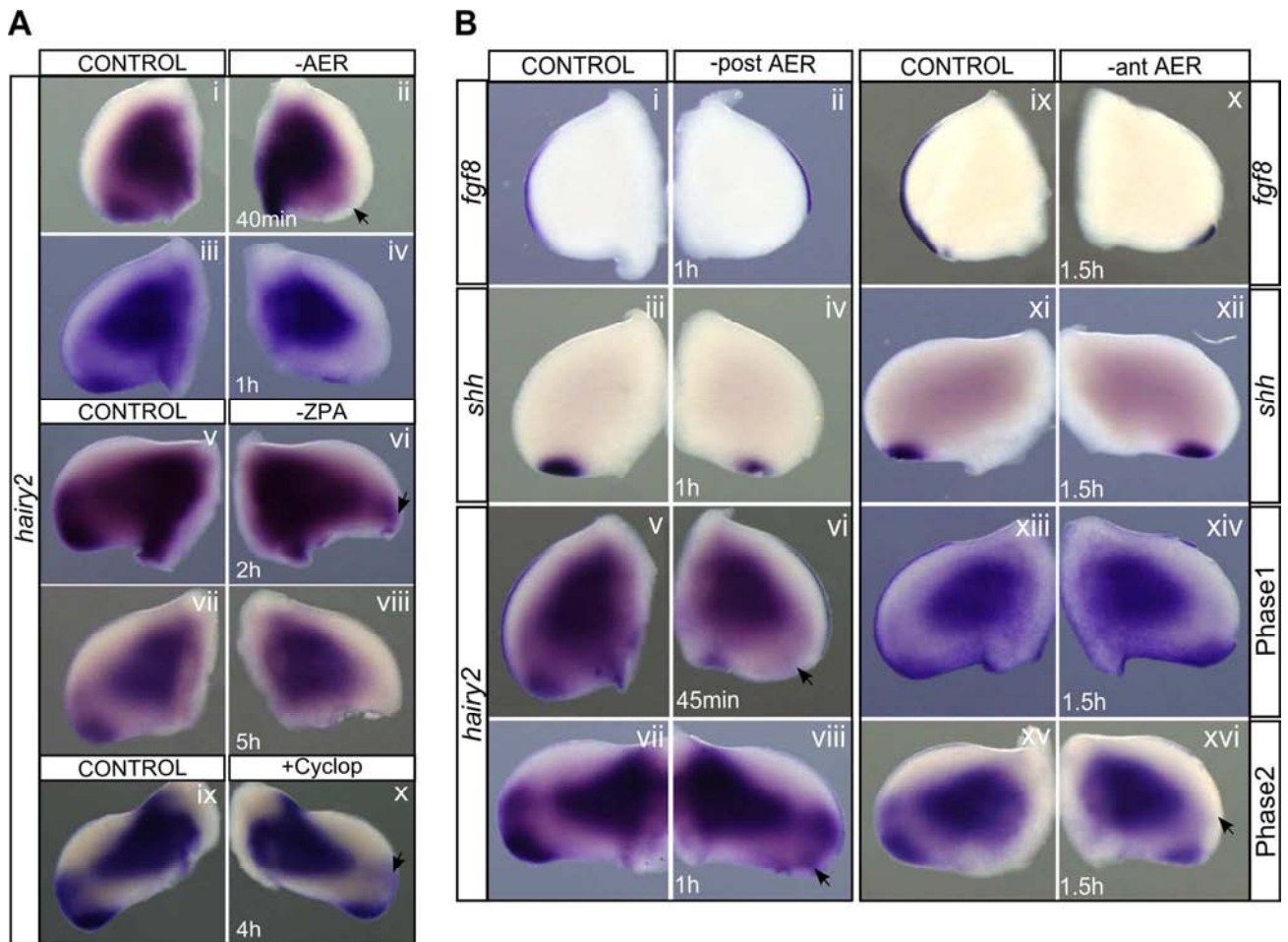
Figure 7
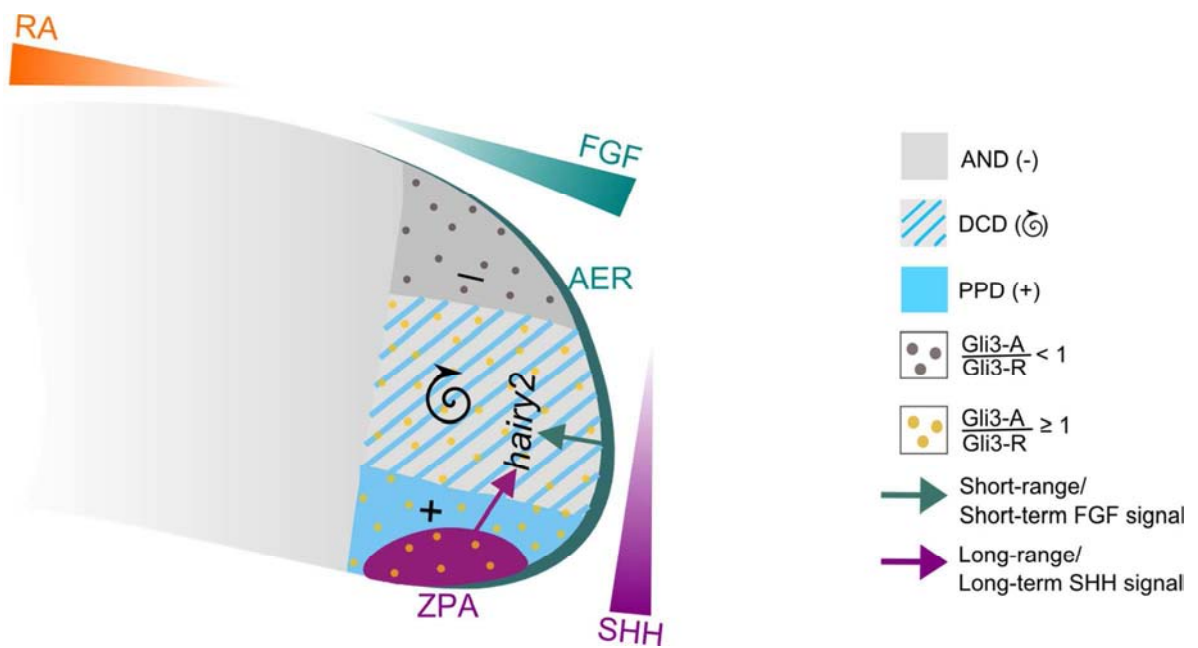
Figure S1
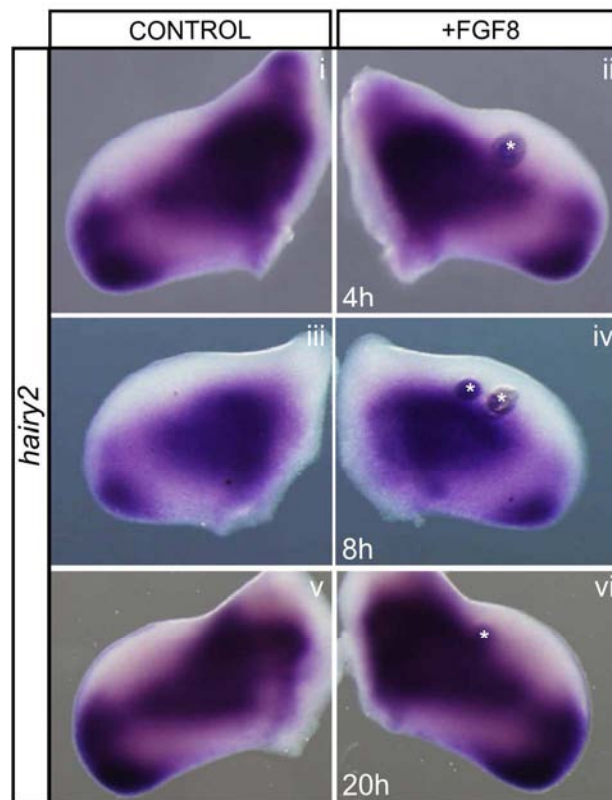
Figure S2
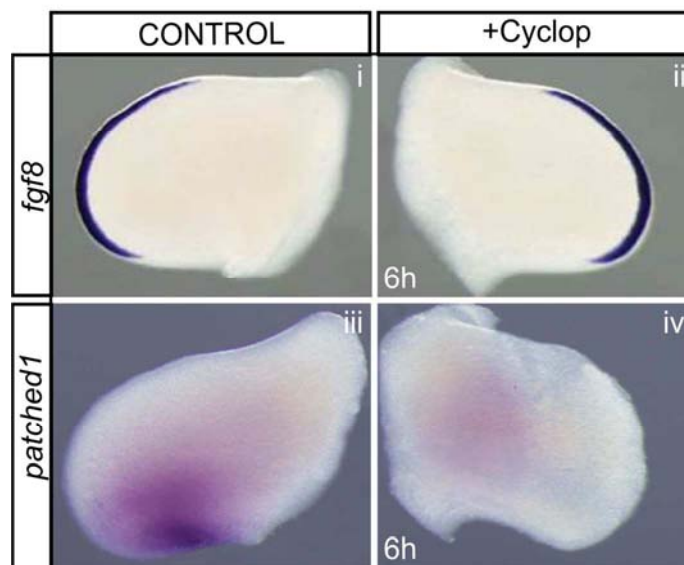
Figure S3
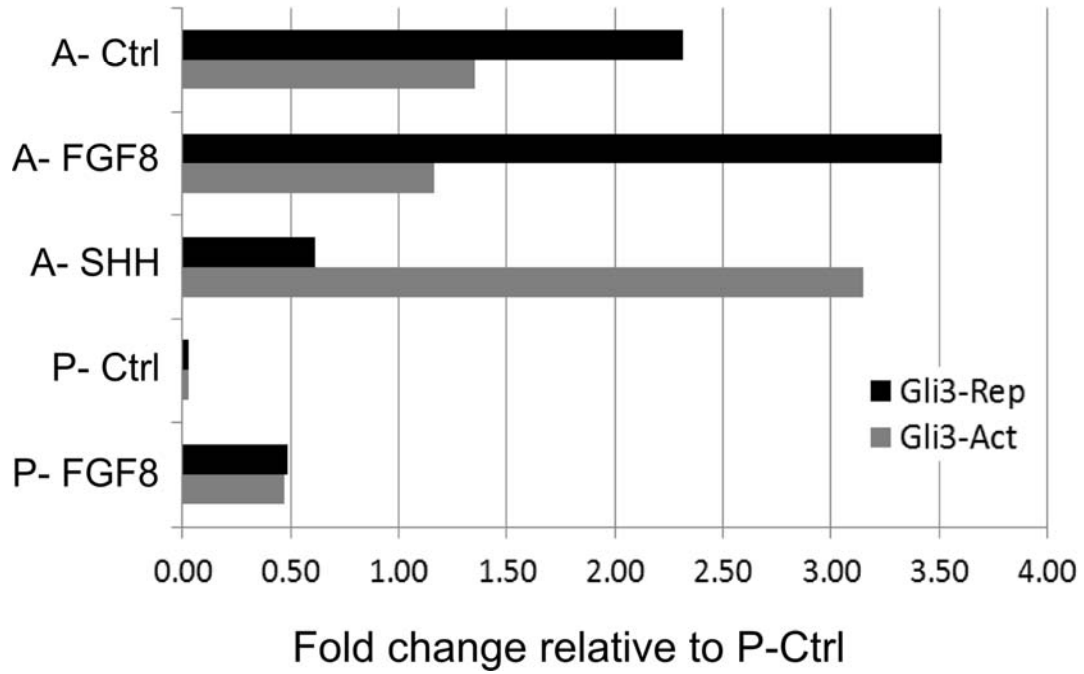
Figure S4
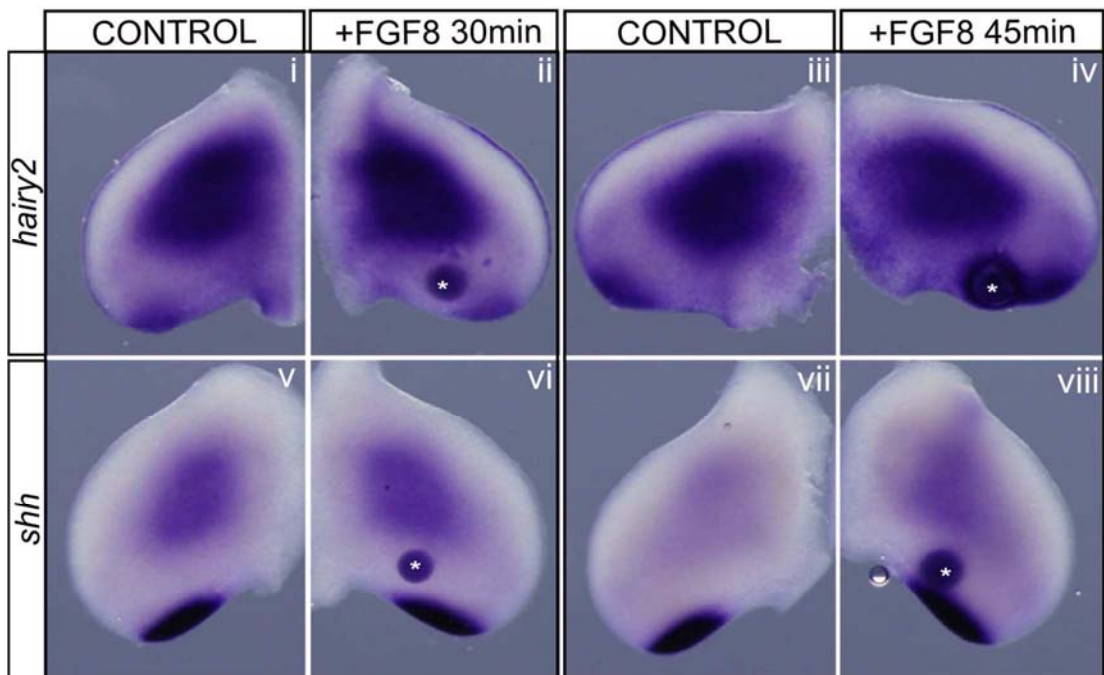
Figure S5
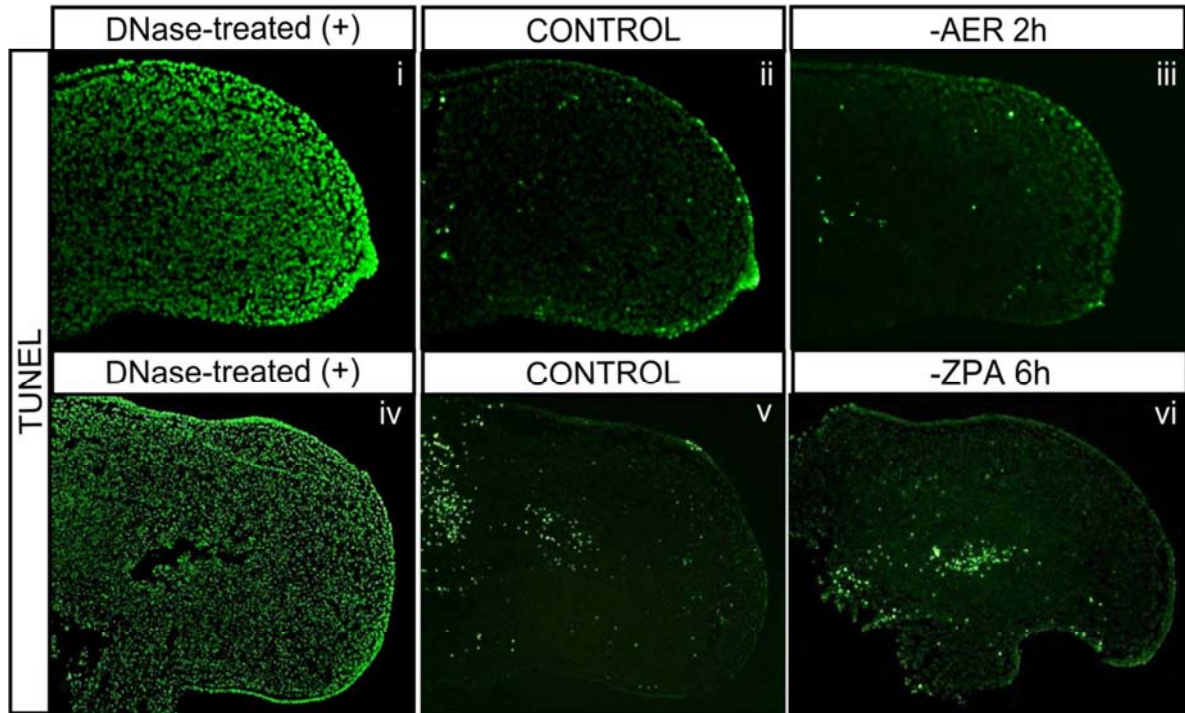
Chapter IV: Clock and wavefront concept in limb development

This chapter constitutes the unpublished and preliminary results obtained from the ongoing work:

``**Hairy2 based limb molecular clock and confronting RA and FGF signal established Determination Front underlie the limb patterning machinery**´´

Hairy2 based limb molecular clock and confronting RA and FGF signal established Determination Front underlie the limb patterning machinery

The vertebrate tetrapod limb PD axis is denoted by three limb bone elements, the proximal stylopod, middle zeugopod and the distal autopod. Growth and patterning of the PD axis has been a subject of intensive investigation for more than three decades. So far three models are proposed to explain the limb PD axis development: the PZ model, the ES model and the TS model (Towers and Tickle, 2009). At present the ``TS model´´ (Tabin and Wolpert, 2007) is prevailing with experimental evidence (Mercader et al., 2000; Roselló-Díez et al., 2011, Cooper et al., 2011). Although, this model argues against an intrinsic time counting mechanism that was proposed by the PZ model (Mackem and Lewandoski, 2011), the discovery of the limb molecular clock strongly suggests that *hairy2* oscillations provide a notion of time to the chondrogenic precursor cells (Pascoal et al., 2007). Cycles of HES gene expression are a crucial component of the somitogenesis program which functions along with the opposing FGF and RA signal based DetF in the PSM (Diez del Corral and Storey, 2004; Niwa et al., 2011). It is clear that a confronting singling gradient of AER-FGFs and flank-RA exists in the limb mesenchyme which defines the DF (Tabin and Wolpert, 2007). Thus, the limb possess *hairy2* based clock and RA/FGF signal based DF in the mesenchyme similar to the mechanisms operating in the PSM. Here, we went to analyze the function of the limb clock and limb DF during chick forelimb development. This work is still ongoing and here we present the preliminary results so far obtained from this set of experiments.

HES genes are widely considered as the target of Notch signal (Fisher and Caudy, 1998; Vasiliauskas et al., 2003; Rida et al., 2004). Co-expression of Notch receptors and its ligands (*Notch2/Serrate1*) in the distal limb mesenchyme (Pascoal and Palmeirim, 2007; Dong et al., 2010) where *hairy2* is dynamically expressed (Pascoal et al., 2007) makes Notch a plausible regulator of limb *hairy2* expression. In the light of our analysis to study limb *hairy2* regulation, we have also evaluated the role of Notch, RA and BMP signaling for its distal mesenchymal expression. Our data suggests that Notch signaling regulates *hairy2* expression more prominently in the DCD than in the PPD. By bead implantation studies, we have demonstrated RA as a positive regulator and BMP4 as an inhibitor of limb *hairy2* expression.

MATERIALS AND METHODS

Eggs and embryos

Fertilized *Gallus gallus* eggs were incubated at 37.8ºC in a 49% humidified atmosphere and staged according to Hamburger and Hamilton (HH) classification (Hamburger and Hamilton, 1951).

Bead implantation

Heparin acrylic beads (Sigma) were incubated with recombinant FGF8b (1 mg/ml; R&D Systems) or BMP4 (0.1µg/µl; R&D Systems) or Noggin (0.1µg/µl; R&D Systems) protein solutions in phosphate buffered saline (PBS). Control beads were incubated in PBS. AG1-X2 beads (Bio-Rad) were soaked in SU5402 (a drug known to specifically block the kinase activity of FGF receptors, 10mM; Calbiochem) or *all-trans* RA (5mg/ml, Sigma) or citral (20mM; SAFC) dissolved in DMSO. Control beads were incubated in DMSO. DAPT (gamma-secretase inhibitor, 2mg/ml; Calbiochem) was applied using Affigel blue beads as carrier. Same beads soaked in DMSO serves as control. Both the PBS and DMSO control beads did not have any effect on gene expression or limb bone size. Beads soaked in FGF8 and PBS was microsurgically implanted in the proximal limit of *mkp3* expression of stage HH22-23 right forelimb buds. Beads soaked in SU5402 and DMSO was implanted just underneath the AER. AGI-X2 beads with RA, citral and DMSO were implanted in the distal limit of RA signaling based on *meis1* expression. Embryos were incubated for 4-6h and processed for in situ hybridization or incubated until digit formation stages and stained for skeleton to permit cartilage analysis.

Perturbation of the limb molecular clock using retrovirus

Hairy2 cDNA and an appropriate *hairy2*-siRNA, were cloned into a RCAS(BP)A and SD1241: pRNA-H1.1/Retro (GenScript) viral expression vectors, respectively. To produce retroviral particles, O-line cells (Charles River Laboratories) were transfected with expression vectors containing the construct and the encapsulated virus released to the culture medium was harvested, concentrated by high speed ultracentrifugation and stored at -80°C until injected in the embryo (Logan and Tabin, 1998). The same procedure was also carried out using empty vectors as control. The virus solutions were injected at the level of the prospective limb field in stage HH13-15 embryos by a micro-injector (Narishige, Japan). The re-incubated embryos were

collected, fixed and analyzed for gene expression and/or for limb elements size by whole mount in situ hybridization and skeletal staining, respectively.

Whole mount in situ hybridization

Embryos or dissected limbs were fixed overnight at 4ºC in a solution of 4% formaldehyde with 2mM EGTA in PBS at pH 7.5, rinsed in PBT (PBS, 0.1% Tween 20), dehydrated in methanol series and stored at –20°C in 100% methanol. Whole mount in situ hybridization was performed as previously described (Henrique et al., 1995). Digoxigenin-labelled RNA probes for *mkp3* (Kawakami et al., 2003), *hairy2* (Jouve et al., 2000) *and sox9* were synthesized using linearized plasmids, according to standard procedures.

Skeletal staining

In brief, limbs were dissected, washed in PBS and fixed in a solution containing the cartilage specific dye Alcian blue (Sigma). This step was followed by dehydration in ethanol and Alzarine Red (Sigma) treatment (for 100ml of solution: 10mg Alzarine Red+ 1g KOH in H_2O). Then, limbs were rinsed in 80ml H_2O+ 20ml Glycerol + 1g KOH solution, until the tissue become completely transparent and finally dehydrated in a series of glycerol solution.

Imaging and statistical analysis

Embryos processed for in situ hybridization were photographed in PBT-azide (0.1%), using a Olympus DP71 digital camera coupled to a Olympus SZX16 stereomicroscope equipped with Cell^B software. Bone length was measured using image-J software and analyzed in Excel.

RESULTS

Notch signal regulates limb *hairy2* expression in a domain specific manner

To test the influence of Notch signaling in limb *hairy2* expression, we implanted beads soaked in the potent gamma-secretase inhibitor DAPT in all the three *hairy2* positive limb domains and processed the limbs for *hairy2* in situ hybridization after 5h. Our results clearly show the dependence of *hairy2* transcription on Notch signaling in the DCD (Figure 4.1iii-vi; n=12/15)

unlike the CPD where *hairy2* expression was never affected by DAPT bead implantation (Figure 4.1i,ii; n=4/4). Interestingly, DAPT beads show higher probability of abolished *hairy2* expression in the DCD compared to the PPD even when the beads were implanted in the PPD, although slight downregulation could be observed in PPD expression of *hairy2* (Figure 4.1v,vi; n=7/9) suggesting Notch is not the only regulator of *hairy2* expression in the PPD.
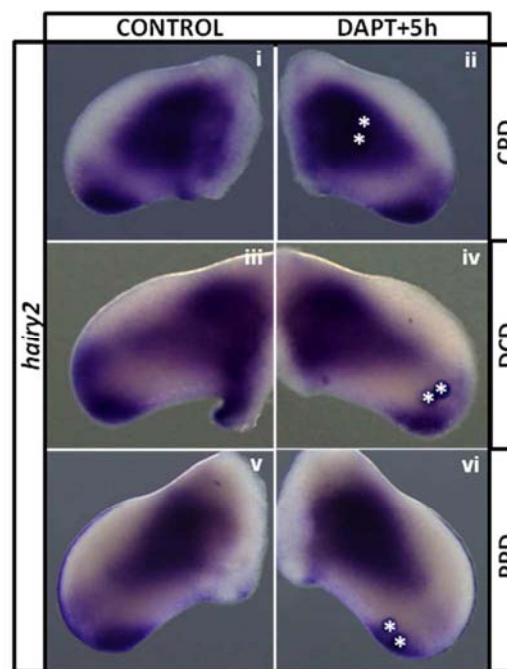
Figure 4.1: Notch signaling regulates limb *hairy2* expression in the distal mesenchyme: All the implantations were performed in stage HH23-24 chick forelimb buds (i,iii,v) Control forelimb buds without manipulations. (ii) Implantation of DAPT bead in the CPD of *hairy2* did not have any effect on its expression. (iv) DAPT bead implantation in the DCD of *hairy2*, considerably downregulated its expression in the DCD while maintaining its expression in the PPD (vi) DAPT implantation in the PPD also resulted in DCD-*hairy2* transcript´s downregulation compared to the PPD. In all images, name of the gene and the domain of manipulation are represented in the left and right side panels. All limbs are orientated anterior to the top; dorsal side facing upward. All beads are represented with a white asterisk.

RA and BMP signaling regulates limb *hairy2* expression

In mouse limb, *hes1* has been reported as a target of RA signaling (Ali-Khan and Hales, 2006). Moreover, recently our lab has evidenced a role for RA in timely somite formation and

suggested that this involves Gli2/3 activity modulation (Resende et al., 2010). Since our data in Chapter II shows that balanced Gli3-A/Gli3-R levels are crucial for *hairy2* expression, we hypothesized that RA could also play a role in *hairy2* regulation in limb. To assess this, RA-soaked beads were implanted in different distal limb domains and *hairy2* was assessed.
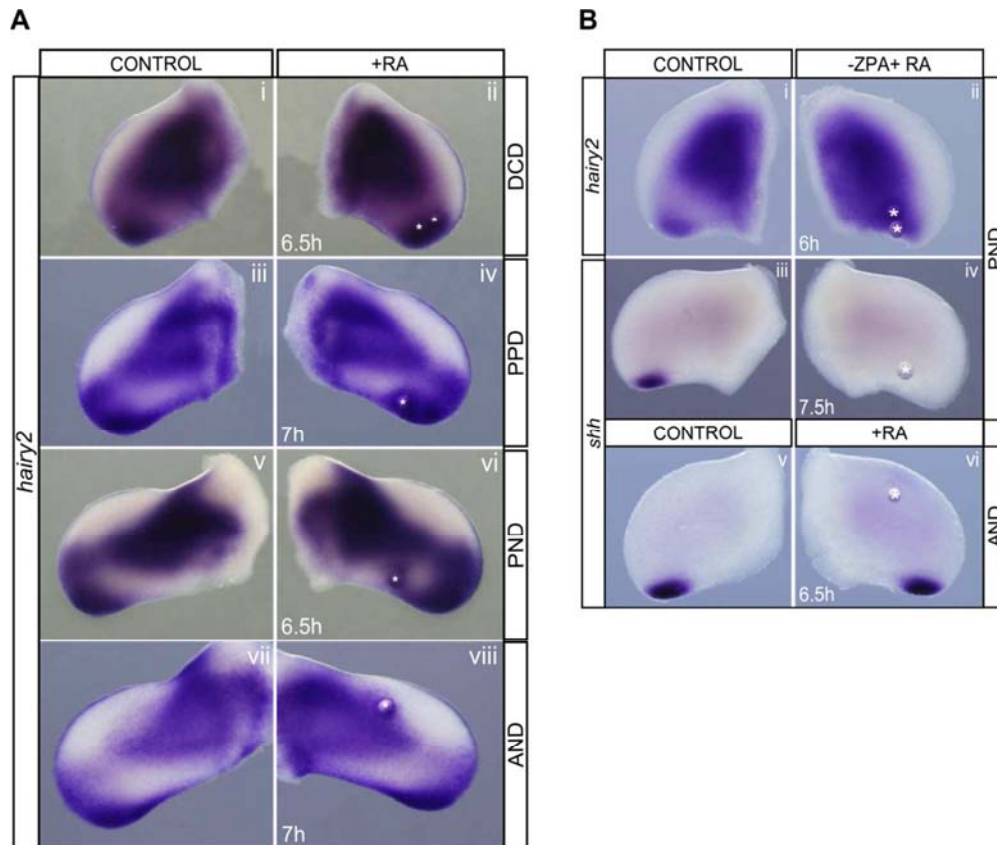
Figure 4.2: RA signaling positively regulates limb *hairy2* expression in all limb domains: (Ai-viii) RA-bead induced ectopic *hairy2* expression in the DCD, PPD, PND and AND of stage HH23-24 chick forelimb bud. (Bi,ii) RA-induced *hairy2* expression in the PND is unaffected by the absence of ZPA. (Biii-vi) RA-induced PND or AND-*hairy2* expression is not through *shh* induction. In all images, name of the gene and the domain of manipulation are represented in the left and right side panels. All limbs are orientated anterior to the top; dorsal side facing upward. All beads are represented with a white asterisk.

This manipulation resulted in *hairy2* upregulation in the DCD, PPD and PND (Figure 4.2Ai-vi; DCD: n=11/11; PPD: n=6/6; PND: n=9/9). This was independent of the ZPA, as well as of RA-mediated *shh* induction (Figure 4.2Bi-iv). Quiet strikingly to what had been observed for FGF and SHH-bead implantations in the AND (results in Chapter II shows that FGF-beads were unable to

induce ectopic *hairy2* in the AND and SHH-beads were only capable of expanding *hairy2* expression towards this tissue), RA-beads were able to locally induce ectopic *hairy2* when implanted in this limb region (Figure 5.2Avii,viii; AND: n=6/7). This *hairy2* expression is also not through RA-mediated *shh* induction (Figure 4.2Bv,vi).
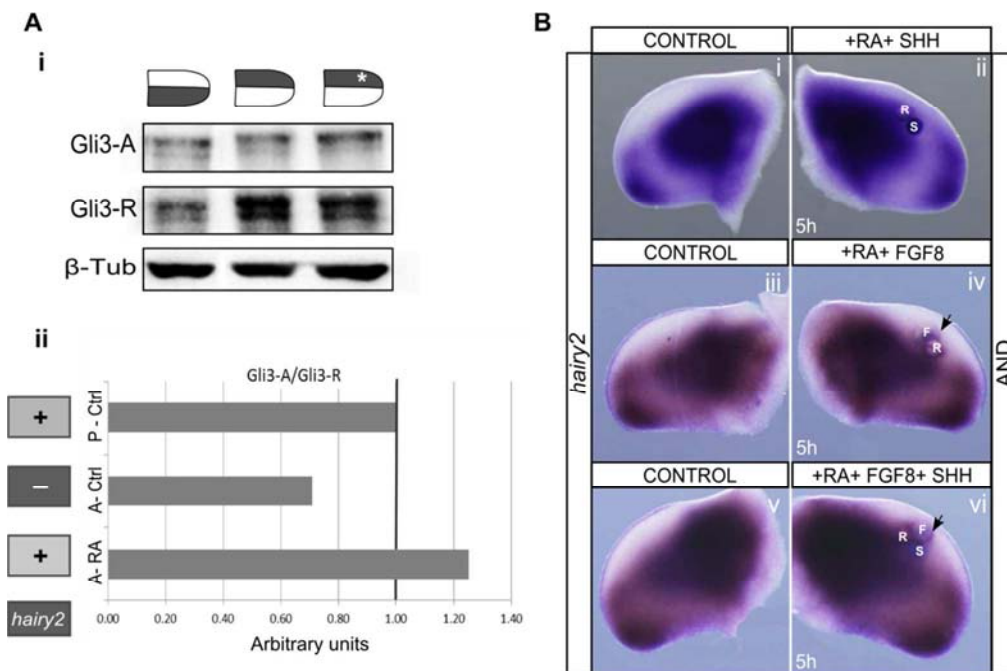
Figure 4.3: RA signaling modulates Gli3 activity and creates a permissive state for *hairy2* expression: (Ai,ii) RA-bead implantation in the AND resulted in a decrease in Gli3-R levels and increased Gli3-A. This alters the otherwise present ratio of Gli3-A/Gli3-R<1 in the AND into Gli3-A/Gli3-R≥1, building a permissive state for *hairy2* expression. (Bi,ii) RA-induced *hairy2* expression in the AND is unaffected by SHH-bead co-implantation. (Biii,iv) Co-implantation of RA and FGF8 bead in the AND enabled FGF8-bead to induce local *hairy2* expression (arrow). This effect was unaltered by SHH-bead (Bv,vi). In all images, name of the gene and the domain of manipulation are represented in the left and right side panels. All limbs are orientated anterior to the top; dorsal side facing upward. Inside the image each bead is represented as the following: RA-beads: R; SHH-bead: S; FGF8-bead: F.

In fact, in accordance with our results in chapter III, RA-bead implantation in the AND, altered the Gli3-A/Gli3-R ratio in such a way, it attains above 1 (Gli3-A/Gli3-R≥1), creating a permissive state for *hairy2* expression (Figure 4.3Ai,ii). Moreover, we also found that the ectopic *hairy2* induced in the AND by RA-bead was unaltered by co-implantation of a SHH-bead which concomitantly induced anterior expansion of *hairy2* (Figure 4.3Bi,ii; n=5/5). The presence of RA

further allowed FGF-induced ectopic *hairy2* in the AND (Figure 4.3Biii-iv; n=4/4), while FGFs alone had not been able to do so (see Fig.1Cvii,viii in chapter II). Again, SHH did not affect FGF+RA-induced *hairy2* expression (Figure 4.3Av,vii; n=5/5). Overall, RA is positively regulating *hairy2* in all the tested domains possibly by modulating Gli activity levels.

The anterior *hairy2* negative domain, AND, clearly matches the expression domain of *Bmp4* in chick limb (Geetha-Loganathan et al., 2006). Moreover, both SHH and RA signals are reported to counteract BMP4 signaling (Tumpel et al., 2002; Thompson et al., 2003; Sheng et al., 2010; Lee et al., 2011). Thus, we sought to evaluate the effect of BMP4 signaling on limb *hairy2* expression. As expected, BMP4 bead inhibited *hairy2* expression in the DCD (Figure 4.4i,ii; n=6/7). Further emphasizing the inhibitory role of BMP4 on *hairy2* was demonstrated by the FGF8-mediated ectopic local *hairy2* induction obtained upon pretreatment with a Noggin-bead (Figure 4.4iii,iv; n=5/5).
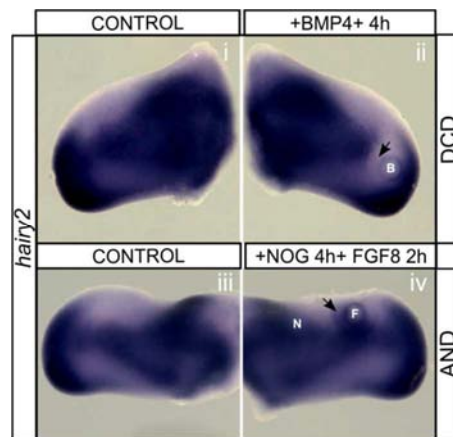
Figure 4.4: BMP4 signaling negatively regulates limb *hairy2* expression: (i,ii) BMP4-bead implantation in the DCD resulted in downregulation of hairy2 expression. (iii,iv) Pretreatment with a Noggin-bead allowed FGF8 to induce ectopic *hairy2* around the bead. In all images, name of the gene and the domain of manipulation are represented in the left and right side panels. All limbs are orientated anterior to the top; dorsal side facing upward. Inside the image each bead is represented as the following: BMP4-bead: B; FGF8-bead: F.

Collectively, our data suggest an important role for RA in limb *hairy2* regulation. RA is capable of inducing ectopic *hairy2* in the AND, possibly by counteracting BMP4-mediated inhibition and by creating a permissive state through Gli3 activity modulation. We show that BMP4 is able to repress *hairy2* and suggest that it could be one of the signaling molecules defining the limb *hairy2* AND.

Could there be a DF in limb distal mesenchyme?

Our manipulations with FGF signaling alterations were performed using recombinant FGF8 protein and FgfR1 specific inhibitor, SU5402 soaked bead implantations. As per the fate map analysis performed by Dudley et al. (2002), the zeugopod cells complete their expansion between stages HH22-HH23 at which our implantations were carried out. FGF8-bead was implanted in the proximal limit of *mkp3* expression in order to extend the limit of FGF signal proximally. This boundary expansion was evaluated by *mkp3* expression analysis which presented a proximal expansion (Figure 4.5i). Since, *mkp3* was shown to be transcribed only in the mesenchymal tissue adjacent to the AER (Pascoal et al., 2007a), SU5402 bead was implanted just beneath the AER. This resulted in downregulation of *mkp3* expression domain (Figure 4.5iv). Since we performed our implantations in the time frame of zeugopod expansion (stage HH22-HH23), we only analyzed the size of zeugopod elements: ulna and radius. Both bead- manipulations affected chondrogenesis and the size of the limb bone elements formed (Figure 4.5ii,iii,v-vii). FGF8 bead resulted in overall reduction of the limb (Figure 4.5iii- 90% of the cases). This is evident at the level of *sox9* expression, the earliest chondrogenic marker (Figure 4.5ii) and skeletal staining (Figure 4.5iii). On the contrary, bones formed after FGF signal inhibition by SU5402-bead implantations were not consistently shorter or longer, instead they produced 40% longer and 60% shorter limb bones as visualized by *sox9* expression (Figure 4.5v,vi) and skeletal staining (Figure 4.5vii).
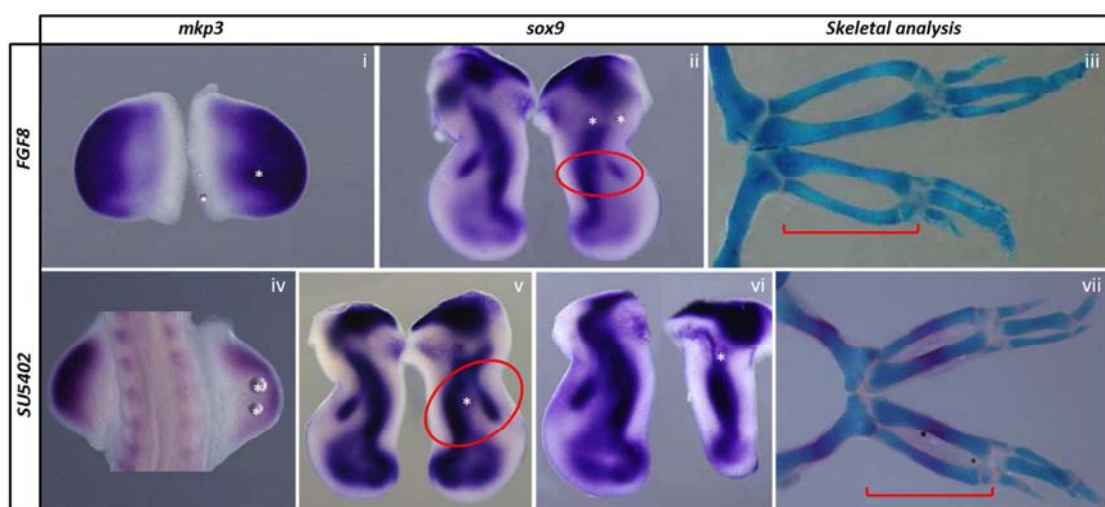

Figure 4.5: AER/FGF signaling determines limb bone size in chick forelimb. (i) *mkp3* expression pattern in the control (left) and expanded *mkp3* expression domain in the right forelimb 5h after implantation of a FGF8-soaked

bead. (ii) *sox9* expression of the FGF8-bead implanted limb and the contralateral control limb. The zeugopod size is reduced (circled in red). (iii) Bone staining performed in FGF8-bead implanted limb buds after 4 days of incubation. The overall skeletal pattern is complete and digit patterning occurred normally but bones (radius and ulna) are smaller (red bracket) compared to the control forelimb (up). (iv) *mkp3* expression is downregulated in the right forelimb 5h after incubation with an SU5402-soaked bead. (v) *sox9* expression of the SU5402 bead implanted limb showing longer zeugopod (circled in red) compared to the control. However, early implantations caused severe reduction in limb development (vi). (vii) Bone staining performed in SU5402 bead implanted limb buds after 4 days of incubation. The overall skeletal pattern is complete and digit patterning occurred normally, however the radius and ulna were slightly longer (red bracket) compared to the control forelimb (up). All beads are represented by asterisk.

The same manipulations were carried out with *all-trans* RA and citral bead to displace the limits of RA signaling. RA and FGF signals are known to have mutual inhibitory regulation in limb (Mercader et al., 2000). So, after manipulating the limits of RA signaling in limb mesenchyme, we assessed the alterations in FGF signaling boundaries through *mkp3* expression. Surprisingly, RA-bead caused proximal expansion of *mkp3* expression (Figure 4.6i) despite of the distal expansion of RA-signal as evidenced by *meis1* expression (Figure 4.6ii). Here, the limb bone elements were mostly shortened (Figure 4.6iii,iv-80%). RA-signal inhibitor, citral-beads also expanded *mkp3* expression proximally as expected (Figure 4.6v) but the limb elements were elongated in most of cases (Figure 4.6vi,vii-80%).Although, not conclusive, our preliminary results suggest that both the AER/FGF and flank-RA signals participate in limb bone size determination.
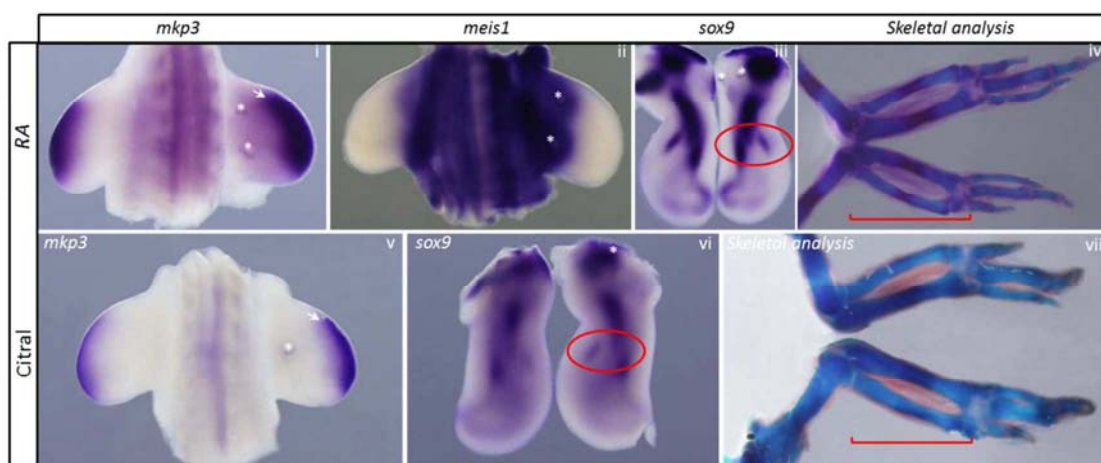
Figure 4.6: Flank-RA signaling participates in limb bone size determination. (i,v) *mkp3* expression expanded upon RA-bead or Citral-bead implantation in 5h. (ii) Expansion of *meis1* expression observed after 5h of RA-bead implantation in the distal limit of RA-signaling (iii) *sox9* expression revealing short zeugopod in the RA-bead

implanted limb (red circle) compared to the untreated control (iv) Bone staining performed in RA-bead implanted limb buds after 4 days of incubation. The overall skeletal pattern is complete and digit patterning occurred normally but radius and ulna are smaller (red bracket) compared to the control forelimb (up). (vi) *sox9* expression of the Citral-bead implanted limb showing stronger expression in the zeugopod (red circle) compared to the control. (vii) Bone staining performed in Citral-bead implanted limb buds after 4 days of incubation. The overall skeletal pattern is complete and digit patterning occurred normally, however the radius and ulna were slightly longer (red bracket) compared to the control forelimb (up). All beads are represented by asterisk.

Retrovirus production

In order to assess the functional relevance of hairy2 expression/oscillations, we wanted to downregulate or overexpress Hairy2 in the limb mesenchyme by retrovirus mediated construct delivery.
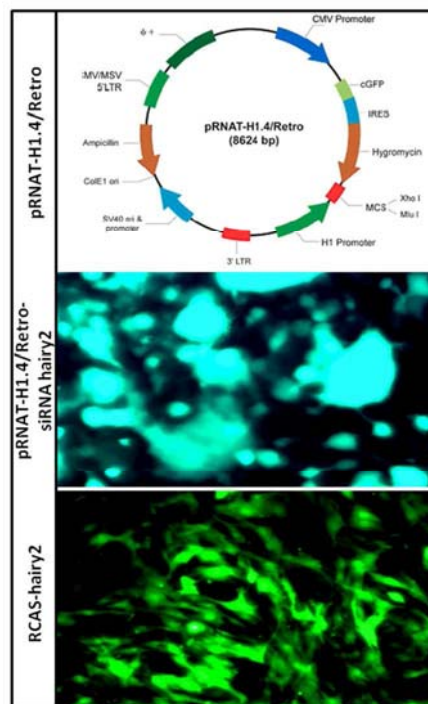
Figure 4.7: Production of retrovirus containing Hairy2 overexpression and downregulation constructs. Scheme of the pRNAT-H1.4/Retro construct used to produce siRNA for *hairy2* containing retrovirus (ii) Transfection efficiency observed in GP2-293 cells after transfecting with pRNAT-H1.4/Retro-siRNA *hairy2* construct (iii) Transfection efficiency observed in CEF cells after transfecting with RCAS BP (A) ires GFP-*hairy2* construct.

The siRNA containing retrovirus was produced by co-transfection of the GP2-293 cell lines with pVSV-G envelop and pRNAT-1.4/Retro-siRNA *hairy2* constructs (vector map is provided:

Figure 4.7i). Similarly, O-line cell lines (chick embryonic fibroblasts) were co-transfected with *hairy2* c-DNA inserted RCAS-BP(A) and pVSAFP plasmid in order to evaluate transfection efficiency. Moreover, the viral expression vector used in our study has GFP as a fusion protein with our protein of interest and so all the cells that are infected with the virus will eventually express GFP. Virus production greatly depends on the efficiency of tranfection which was evaluated by GFP expression. Transfection efficiency of the siRNA-*hairy2* containing virus and *hairy2*-possessing virus displayed high efficiency (Figure 4.7ii,iii). Thus, retroviruses containing *hairy2*-siRNA and *hairy2*-ORF have been produced and stored at -80°C. These viruses will be used for Hairy2 functional analysis.

CHAPTER V:

GENERAL DISCUSSION

5. PARALLELISMS BETWEEN LIMB DEVELOPMENT AND SOMITOGENESIS

The chief aim of this thesis is to establish parallelisms between the two distinct developmental processes the limb development and somitogenesis. While limb development has served as a wonderful paradigm to study pattern formation from a mass of mesenchymal cells (Tabin and Wolpert, 2007), somitogenesis is predominantly known for its striking species conserved periodicity underlined by PSM molecular clock (Andrade et al., 2007). The identification of a similar molecular oscillator in chick distal limb mesenchyme (Pascoal et al., 2007) suggests that many parallelisms between limb development and somitogenesis might exist. The work performed throughout this thesis has further substantiated this possibility and allowed us to establish the similarities between these two systems based on the existing literature and our work.

5.1. COMPARISON AT THE LEVEL OF MORPHOLOGY

The somites and limb are two prominent structures formed during embryogenesis. Emphasizing this, the widely used Hamburger and Hamilton method of chick embryo classification has utilized the morphological features of somite number and limb shape to characterize different developmental stages of chick embryo (Hamburger and Hamilton, 1992). The limb is a segmented structure, denoted by its PD axis specifying bone elements: the stylopod, zeugopod and autopod. This resembles the segmented pattern of the somites, formed in an AP sequence of the embryo through the process of somitogenesis. Moreover, these two structures share common mesodermal germ layer as precursors, namely, the LPM and the PSM tissues for limb bones and axial skeleton bones, respectively. The PD axis of limb development is comparable with the AP axis of vertebrate embryo in such a way that the maturation of limb bone elements and somites follows limb PD and body AP axis, respectively (Summerbell et al., 1973; Dudley et al., 2002; Christ and Ordahl, 1995). The PD sequence of limb bone determination has been determined by fate map studies as per which the proximal stylopod territory is defined between stage HH19-20; the middle zeugopod between stage HH22-23 and the distal autopod progenitors continue to expand even after stage HH26 (Dudley et al., 2002). On the other hand, in somitogenesis, somite formation relies on strict periodicity (1.5h in chick and 2h in mouse) underlined by the PSM clock (Palmeirim et al., 1997). However, there might be a slight variation

in this expected duration along the AP axis in such a way that the formation of the first somites my need less time (Tam, 1981) and the last few somites need more time (150 min) compared to the usual 90 min in chick (Tenin et al., 2010). Although, the precursor cells in both systems are provided by the mesoderm, surface ectoderm has also been demonstrated to be absolutely necessary for proper limb and somite formation (Yang and Niswander, 1995; Rifes et al., 2007).

5.2. COMPARISON AT THE LEVEL OF GENE EXPRESSION

In order to compare the expression pattern of important genes in developing limb and PSM, a stage HH24 forelimb bud, longitudinally cut along the AP axis without splitting it into two separate pieces is compared with a the caudal part of stage HH13 embryo containing the PSM, tail bud and the last few somites (Figure 5.1).

5.2.1. PARALLELISMS IN RA SIGNALING COMPONENTS

The two principal signaling gradients known to pattern the limb mesenchyme and the PSM are the RA and FGFs. RA can be visualized either through mRNA expression of its synthesizing enzyme, *Raldh2* or by assessing its activity. *Raldh2* is expressed at the limb flank which is comparable with its expression in the anterior PSM immediately posterior to the recently formed somite (Swindell et al., 1999; Blentic et al., 2003; Diez del Corral et al., 2003). This pattern of expression was further confirmed by RA activity visualized in transgenic mice having RA signaling responsive element (RARE) driven by a reporter promoter construct. This analysis revealed that RA activity is present in the proximal forelimb region, somites and the anterior most PSM while absent from the distal limb mesenchyme, posterior PSM and tail bud (Rossant et al., 1991; Mic et al., 2004). However, *Raldh2* expression at later developmental stages (from stage HH21) in chick tailbud has been recently reported (Tenin et al., 2010) which is similar to its late expression observed in stage HH25-27 distal limb mesenchyme (Berggren et al., 2001). On the other hand, the RA degrading enzyme, *Cyp26* has the opposing gradient in both systems: in the PSM *Cyp26A1* is expressed in the tail bud (Sakai et al., 2001) and in the limb, it is expressed in the distal limb mesenchyme with a mild variation in chick and mouse. In mouse, *Cyp26B1* is initially expressed in the outer epithelium and then also in the distal mesenchyme (MacLean et

al., 2001), whereas, in chick, *Cyp26A1* is always expressed in the ectoderm (Swindell et al., 1999; Blentic et al., 2003) and *Cyp26B1* in the distal mesenchyme (Reijntjes et al., 2003).

5.2.2. PARALLELISMS IN FGF SIGNALING COMPONENTS

Other crucial factor functioning in an opposing gradient to that of RA in both the limb as well as in the PSM is the FGFs. Being a growth factor, it is required to maintain the stemness of the limb distal mesenchyme and the tail bud cells of an embryo. Facilitating this function, *fgf8* is expressed in the distal most structure of limb, the AER (Crossley et al., 1996) and in the prospective PSM (P-PSM) region (Dubrulle et al., 2001). In the PSM, the tailbud transcribed *fgf8* establishes a caudo-rostral gradient based on mRNA decay (Dubrulle and Pourquie, 2004). However, in the limb, the distal-proximal FGF signaling gradient is not formed by graded *fgf8* expression itself, since *fgf8* is solely expressed in the entire AER, but, its effector *mkp3* has a distal-proximal mesenchymal gradient (Kawakami et al., 2003). Interestingly, this gradient of *mkp3* is also established through mRNA decay (Pascoal et al., 2007a), the same mechanism which produces *fgf8* gradient in the caudal PSM. In this mode of establishment, the limb *mkp3* and the PSM *fgf8* are only transcribed in the mesenchymal tissue adjacent to the AER and in the tailbud, respectively. Due to continuous proliferation and outgrowth, cells that actively produce these molecules are progressively displaced either proximally or rostrally resulting in a gradient of limb-*mkp3* and PSM-*fgf8* mRNA expression (Dubrulle and Pourquie, 2004; Pascoal et al., 2007a). FGF signaling gradient created in this manner has to be sensed by appropriate FgfR to activate the downstream pathways. In the PSM the only FgfR to be expressed is FgfR1 (Patstone et al., 1993; Wahl et al., 2007), which is strongly expressed in the anterior PSM (Dubrulle et al., 2001). Interaction of the FGF ligand with FgfR1 in the PSM activates downstream pathways such as: Erk/MAPK in chick and zebrafish (Delfini et al., 2005; Sawada et al., 2001) or Akt/PI3K pathway in mouse (Dubrulle and Pourquie, 2004). In the limb, although FgfR1 is the predominant FgfR expressed in limb mesenchyme, other FgfRs are also expressed in distinct domains (Sheeba et al., 2010). Among them, FgfR1 and FgfR2 are the two potential receptors mediating the AER derived FGF signaling during limb initiation and patterning stages (Revest et al., 2001; Yu and Ornitz, 2008). We recently observed *FgfR1* transcripts in the AER of stage HH17 and HH24 chick limb for the first time (Sheeba et al., 2010) making it an equally important candidate as that of FgfR2 for

autocrine and paracrine FGF signaling. Consistent with the variation in downstream pathway activations observed in mouse and chick PSM, Akt/PI3K has been shown to be active in chick limb mesenchyme (Kawakami et al., 2003) and Erk/MAPK in mouse (Corson et al., 2003). However, the AER of chick limb expresses p-Erk (Kawakami et al., 2003).

5.2.3. PARALLELISMS IN WNT, BMP AND SHH SIGNALING COMPONENTS

WNT, BMP and SHH are other important signaling pathways functioning during embryo development. The P-PSM expresses *wnt3a*, which is steadily degraded, establishing a caudo-rostral PSM gradient of its transcripts by RNA decay, such as the case for *fgf8* (Aulehla et al., 2003; Aulehla and Herrmann, 2004). Upon ligand binding, β-catenin gets translocated into the nucleus and transcribes its target genes thus serves as the key mediator of canonical WNT signaling (Church and Francis-West, 2002). The PSM oriented caudo-rostral *wnt3a* mRNA gradient is translated into a β-catenin activity gradient, although β-catenin mRNA is ubiquitously expressed in the PSM (Aulehla et al., 2008). In the limb, several WNT ligands are distinctly expressed (Loganathan et al., 2005) and, similarly to *fgf8*, *wnt3a* expression is also confined to the AER tissue (Kengaku et al., 1998; Soshnikova et al., 2003). It is reported that in E10.5 mouse forelimb bud, *β-catenin* mRNA is ubiquitously expressed in the entire limb mesenchyme and ectoderm including the AER (Hill et al., 2006). However, in stage HH22 chick forelimb, *β-catenin* mRNA is expressed in a distal-proximal gradient in addition to its expression in the AER (Schmidt et al., 2004). These expression patterns support a potential equivalent role of WNT signaling in somitogenesis and limb development (Aulehla and Herrmann, 2004; Church and Francis-West, 2002).

During body axis elongation*, Bmp4* signaling is restricted to the LPM tissue through active inhibition by its antagonist Noggin, which is expressed at the LPM/PSM border ((Capdevila and Johnson, 1998; McMahon et al., 1998; Tonegawa and Takahashi, 1998). Many BMPs are expressed during limb development (Geetha-Loganathan et al., 2006). Among them, *Bmp4* presents a strong AER and anterior-mesenchymal expression (Geetha-Loganathan et al., 2006; Bastida et al., 2009). Although, *noggin* is only expressed in the ventral proximal mesenchyme (Capdevila and Johnson, 1998), the distal mesenchymal located *germlin1*, another antagonist of BMP signaling is crucial for early limb development (Zeller et al., 2009). *Bmp4* expression pattern

during somitogenesis and limb development nicely resemble each other in a way, the LPM expressed *Bmp4* in somitogenesis is comparable with its expression in the anterior limb mesenchyme (Figure 5.1).
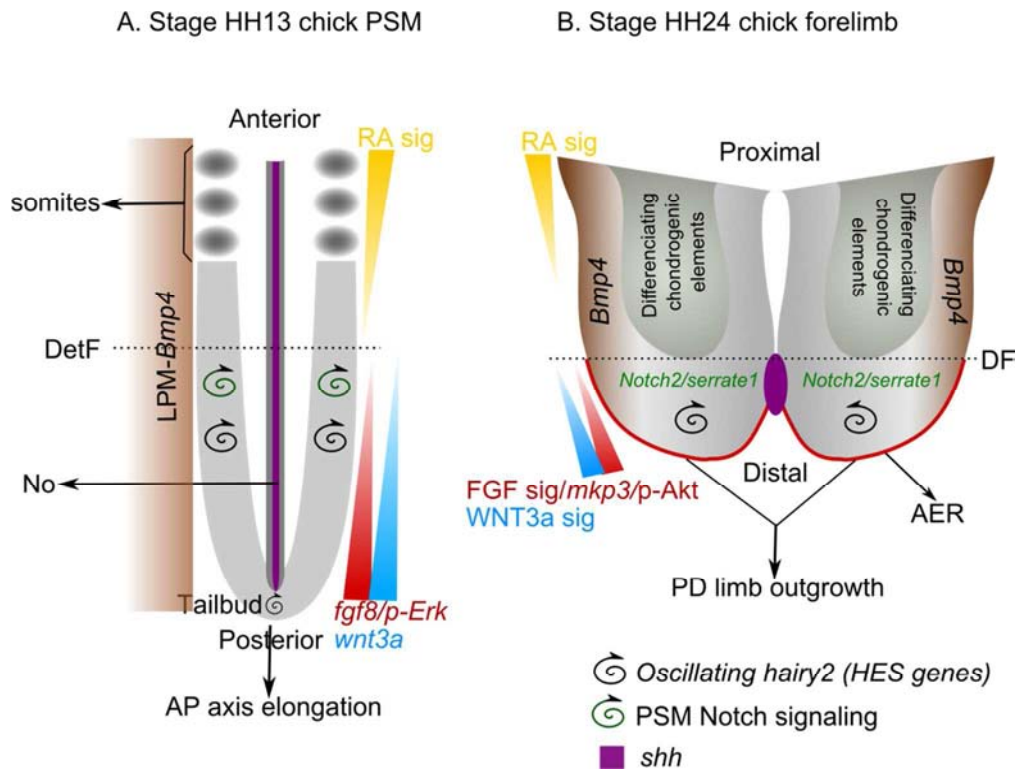
Figure 5.1.**Comparative analysis of limb development and somitogenesis at the level of morphology and gene expression. (A)** Caudal part of a stage HH13 chick embryo focusing the PSM, tail bud and the last few somite pairs. **(B)** Stage HH24 chick forelimb bud longitudinally cut through the AP boundary from the anterior until the posterior edge without splitting it into two separate pieces. The PSM is placed anterior to the top and the limb is positioned proximal to the top. The distal portion of the limb can be compared to the caudal end of the embryo. FGF8 is actively produced in the AER of the limb and in the tailbud of the growing body axis (Red graded triangles in the PSM) (Dubrule and Pourquie, 2004; Crossley et al., 1996). The FGF effector *mkp3* is expressed as a distal-proximal gradient in the limb mesenchyme (Kawakami et al., 2003) similar to the posterior-anterior *fgf8* gradient in the PSM. In both systems, a graded FGF signal is translated into an activity gradient (either p-Erk or p-Akt depending on the species and tissue) (Dubrule and Pourquie, 2004; Delfini et al., 2005; Sawada et al., 2001). The same regions are also endowed with a WNT signal gradient mainly through WNT3a and its signal transducer β-catenin (blue graded triangle). In limb, *wnt3a* is expressed only in the AER (Kengaku et al., 1998; Soshnikova et al., 2003), whereas in the PSM it is expressed in a caudal-rostral gradient (Aulehla et al., 2003). Both FGF and WNT signals keep the caudal PSM (Naichi et al., 2011) and distal limb in a undifferentiated proliferative state (ten Berge et al., 2008) and allow the structures to grow (PSM: AP direction as mentioned by axis elongation; Limb: Distal outgrowth). AP graded RA activity is a consequence of *Raldh2* expression in the somites and anterior PSM (Diez del Corral et al., 2003) which is

analogous to its flank oriented expression in limb (Mercader et al., 2000) (yellow graded triangles). *Cyp26* presents a complementary expression to that of *Raldh2* in limb and PSM (not mentioned in the figure). The opposing RA and FGF gradients establish the Differentiation Front (DF) (dashed black line) in limb at the proximal boundary of the FGF signaling and the Determination Front (DetF) in more or less the anterior one third level of the PSM (dashed black line) from where cells will be committed to be a part of a segment (limb bone or axial skeleton element). The region distal to the DF is called the undifferentiated zone (UZ) and the PSM tissue caudal to the DetF is known as the undetermined PSM. *Bmp4* is exclusively expressed in the LPM (brown bar) through noggin mediated antagonism from the lateral part of the PSM (LPM is represented only in the left side of the PSM in this schematic representation) (Tonegawa and Takahashi, 1998). In limb mesenchyme, *Bmp4* is predominantly expressed in the anterior region (brown domain) (Loganathan et al., 2006). The black spiral arrows in the PSM and limb distal mesenchyme indicate cyclic gene expression (*hairy2* in limb (Pascoal et al., 2007) and somitogenesis molecular clock genes in the PSM (Andrade et al., 2007). *hairy2* is no longer expressed in the differentiating chondrogenic cells of limb. In the PSM, the clock is functional in the PSM precursors at the tailbud (spiral arrow at the tailbud). Regulator of *HES* gene expression, Notch signaling also oscillates in the PSM (green spiral arrow). The Notch receptor (*Notch2*) and its ligand (*serrate1*) are co-localized with *hairy2* in the distal limb. ZPA in the middle of the mesenchymal limb longitudinal halves expresses *shh* (violet oval fill), while in the PSM *shh* is produced by the Notochord (No) (violet long bar in the middle of the neural tube).

shh is an important morphogen needed in all stages of limb development (Zeller et al., 2009) and it is expressed in the ZPA (Riddle et al., 1993). Although, it was long believed that somitogenesis is totally independent of the body axial structures (notochord and neural tube) recent data from our lab clearly point to the requirement of notochord and therein produced SHH (Teillet et al., 1998) for timely somite formation (Resende et al., 2010). In our comparative way of representing the limb bud and caudal embryo, *shh* expressing ZPA falls in the middle of the two limb sides and shows its resemblance to *shh* expression in the axially located notochord (Figure 5.1).

5.2.4. PARALLELISMS IN NOTCH SIGNALING COMPONENTS

The PSM molecular clock genes controlling somitogenesis are expressed in a periodic kinematic wave that propagates from the tail bud until the anterior PSM where it slows-down and finally become persistently expressed in the posterior or anterior somite compartments, as it is the case for *hairy1* and *hairy2,* respectively (Palmeirim et al., 1997; Jouve et al., 2000; Rodrigues et al., 2006). These genes oscillate with a species specific periodicity which is 90 min in

chick (Andrade et al., 2007). Ten years after the discovery of the somitogenesis molecular clock, a comparable limb molecular clock was identified, based on *hairy2* mRNA expression (Pascoal et al., 2007b). Limb clock displays *hairy2* mRNA expression cycles of 6h periodicity in the distal limb mesenchymal tissue where limb chondrogenic precursor cells are located (Vargesson et al., 1997; Pascoal et al., 2007). *HES* genes are traditionally referred as downstream effectors of Notch signaling pathway (Vasiliauskas et al., 2003; Rida et al., 2004). In the limb, *Notch1/Serrate2* (*jagged2* in mouse) receptor/ligand pair are exclusively expressed in the AER while *Notch2/Serrate1* (*jagged1* in mouse) are expressed in the distal mesenchyme and thus, could be controlling limb clock expression in the distal limb region (Pascoal and Palmeirim, 2007; Dong et al., 2010). Whereas in the PSM, *Notch1/delta1* (*dll1*) pair is co-expressed from very early stages of chick gastrulation (Caprioli et al., 2002).

The aforementioned comparisons describe the resemblances existing between limb development and somitogenesis at the level of spatial expression of key signaling molecules. How these systems could relate with each other at the functional level is compared in the next section.

5.3. PARALLELISMS AT THE FUNCTIONAL LEVEL

5.3.1. ``STEMNESS´´ OF THE DISTAL LIMB MESENCHYME AND TAILBUD

Limb development begins as a bundle of mesenchymal cells encompassed into an ectodermal hull. Eventually, this mesenchymal tissue forms all the distinct limb elements, except limb muscles and tendons, indicating the multipotent progenitor nature of the early limb mesenchyme (Dong et al., 2010). During limb outgrowth, the distal limb mesenchyme is maintained in an undifferentiated proliferative state by the AER produced FGFs and WNTs (Dudley et al., 2002; ten Berge et al., 2008; Cooper et al., 2011. One of the classical models to explain the limb PD patterning, the PZ model, proposes that the cells from the distal limb mesenchyme progressively acquire more distal positional values as they spend longer time in the distal limb (Summerbell et al., 1973) and emphasize the ability of the distal limb tissue to generate the entire limb. When endowed with right signals, the distal limb mesenchyme of early limb bud has the intrinsic ability to form the entire limb. This has been clearly demonstrated through molecular analysis of stage HH19-20 distal limb mesenchyme derived recombinant limbs

(Dudley et al., 2002; Cooper et al., 2011; Roselló-Díez et al., 2011) and limbs generated from distal limb transplantation studies (Summerbell et al., 1973; Roselló-Díez et al., 2011). However, the responsiveness of the distal most ~200μm limb mesenchymal cells (along with the AER) to the PD patterning signaling molecules is progressively lost along the limb developmental stages (Roselló-Díez et al., 2011). Due to the combinatory influence of the AER produced FGFs and WNTs, the distal limb mesenchymal cells present high proliferation compared to all other limb regions and enable the limb to grow out in the PD direction (ten Berge et al., 2008).

The tail bud region could be comparable with the distal limb mesenchyme, namely for its "stemness". As the PSM generates somites from its rostral tip, it is posteriorly replenished with new cells that ingress from the PS and tailbud (Pourquie, 2004). Here, the PS and tailbud not only serves as a route for cells to ingress during gastrulation, but also provide positional information along the AP and medio-lateral axis of somites (Selleck and Stern, 1991; Schoenwolf et al., 1992; Iimura et al., 2007), parallel to the ability of the distal limb to provide PD positional values (Summerbell et al., 1973). The positional identity possessed in the PS cells situated along its AP axis could be altered by grafting them to another location (Garcia-Martinez et al., 1997). Nevertheless, this plasticity is progressively lost as the embryo matures (Garcia-Martinez and Schoenwolf, 1992). As a consequence of the addition of new cells in the tailbud, the AP axis of the embryo elongates (Benazeraf et al., 2010).

Analogous to the limb mesenchyme´s intrinsic ability to form the entire limb in right sequence, (Summerbell et al., 1973; Dudley et al., 2002), classical experimental data has suggested the segmental autonomy and pre-pattern present in the PSM tissue (Pourquie, 2004). However, now we know that the PSM has two distinct domains: the determined rostral PSM where segmentation is determined at the molecular level and the undetermined caudal PSM where cells present segmental plasticity (Dubrulle et al., 2001).

5.3.2. THE TIME COUNTING MECHANISM OPERATING IN THE LIMB AND THE PSM

The somitogenesis molecular clock was first discovered in chick PSM based on the cyclic expression of *hairy1*, a Notch target HES family member (Palmeirim et al., 1997). Since then, a cyclic transcription behavior of many other genes from Notch, FGF and WNT pathways has been identified in different species (Andrade et al., 2007; Krol et al., 2011) and different developmental

systems (Hirata et al., 2002; William et al., 2007; Shimojo et al., 2008; Kobayashi et al., 2009) including the distal mesenchyme of chick forelimb (Pascoal et al., 2007). Six hour period pulses of *hairy2* (HES member) expression in the limb chondrogenic precursor cells underlie the limb molecular clock (Figure 2.3; Pascoal et al., 2007b; Vargesson et al., 1997). *hairy2* or its mammalian homolog *hes1* also display cyclic gene expression in the PSM (Figure 2.1; Jouve et al., 2000). The PSM oscillator provides a notion of time to the PSM cells and each oscillation (90 min in chick) culminates in a somite pair formation (Palmeirim et al., 1997; Aulehla and Pourquie, 2010). Accordingly, the limb molecular clock has also been proposed to deliver the concept of time to the chondrogenic precursor cells where *hairy2* is oscillating. Experimentally, it was demonstrated that the second phalanx of chick forelimb takes 12h to be formed and n and n+1 cycles of *hairy2* is required to make one limb bone element (Pascoal et al., 2007). This finding supports the intrinsic time counting mechanism proposed by PZ model (Summerbell et al., 1973).

5.3.3. CONFRONTING GRADIENTS OF FGF/WNT AND RA SIGNALING IN LIMB AND PSM

Another parallel mechanism operating along with the clock to control the differentiation status of the PSM and limb field is the confronting signaling gradients of RA and FGFs. In the limb, the flank region expresses *Raldh2*, an RA synthesizing enzyme and creates a proximal-distal RA signaling gradient. The distal limb domain expresses the RA catabolizing enzyme *Cyp26* which creates a RA free distal domain (Niederreither and Dolle, 2008; Probst et al., 2011). The distal limb structure, AER, produces many *fgfs* in which *fgf8* is the predominant one in terms of duration and domain occupation (Martin, 1998; Mariani et al., 2008). The distal-proximal AER/FGF8 signaling gradient is counteracted by the proximal-distal RA signaling gradient (Mercader et al., 2000; Tabin and Wolpert, 2007). These graded signaling activities correspond to the opposing gradients that are functional for somitogenesis.

In the PSM, *fgf8* is expressed in a caudo-rostral gradient, which is opposed by the rostro-caudal RA signaling gradient established by *Raldh2* expression (Diezdel Corral et al., 2003). In both systems, the graded *fgf8* signaling is a consequence of mRNA decay (Dubrulle and Pourquie, 2004; Pascoal et al., 2007b). The limb and PSM FGF8 signaling is translated into an activity gradient by phosphorylation of Erk or Akt depending on the species (Dubrulle and Pourquie, 2004; Delfini et al., 2005; Sawada et al., 2001; Kawakami et al., 2003; Corson et al., 2003), further

emphasizing their functional similarity. This activity gradient proportionally influences PSM cell movement. Cells that are located in the caudal part of the PSM (high FGF8 activity) are more dynamic compared to the slow moving cells in the anterior PSM which enable the cells above the DetF to get integrated into a somite segment (Delfini et al., 2005; Benazeraf et al., 2010). Similarly, in the chick, the distal limb mesenchyme equivalent to the caudal PSM, also presents high cell dynamics. It has been reported that the distal limb mesenchymal cells constantly change their neighbors possibly through action of the AER produced FGF2 and FGF4 (Li and Muneoka, 1999). Thus generated opposing RA and FGF gradients position the DetF between somite –IV and –V in the PSM (Olivera-Martinez and Storey, 2007). This divides the PSM into the rostral Determined Region (DR) and the caudal Undetermined Region (UR) (Dubrulle et al., 2001; Aulehla and Pourquie, 2010). Similarly, the confronting flank-RA and AER-FGF signals are patterning the PD axis of limb as proposed by the TS model (Tabin and Wolpert, 2007). Moreover, the distal mesenchyme under the direct influence of the AER derived FGFs is maintained in a undifferentiated state and defines the Undifferentiated Zone (UZ) whose proximal limit marks the Differentiation Front (DF) after which cells start their chondrogenic differentiation (Tabin and Wolpert, 2007). This entire perception resembles the PSM oriented UR and DetF. Recent studies has provided compelling evidence in support of the TS model (Mercader et al., 2000; Mariani et al., 2008; Roselló-Díez et al., 2011, Cooper et al., 2011) and argues against the presence of an internal clock (Mackem and Lewandoski, 2011). This argument against the limb autonomous mechanism is mainly based on two experiments (Mackem and Lewandoski, 2011): 1) the formation of recombinant limbs derived from stage HH18 limb mesenchymal cells cultured in the presence of WNT3a, FGF8 and RA and 2) the ectopic limbs generated from transplants of distal limb to endogenous RA containing or deprived domains (Roselló-Díez et al., 2011, Cooper et al., 2011). Although these authors have clearly proved the requirement of the opposing RA and FGF/WNT gradients for proper PD axis formation, no evidence was provided to rule out the participation of an internal clock in this process. Our results presented in previous chapters has clearly showed the indispensable requirement of AER/FGF and ZPA/SHH for proper *hairy2* expression. We have also demonstrated the ability of RA-bead to induce *hairy2*. Thus, it is most plausible that when the cells are packed inside an ectodermal hull, the ectodermally produced FGFs might be turning on *hairy2* expression in the mesenchymal cells. Since the recombinant limbs form all the three limb segments, there must have been a posterior mesenchyme

associated SHH signal functioning in the packed cells (Roselló-Díez et al., 2011, Cooper et al., 2011) which could have created a permissive state for the inductive AER/FGF signal to turn on the *hairy2* clock (as described in chapter III). Thus, an intrinsic oscillator could be providing the positional informations to the packed mesenchymal cells and facilitated their allocation to each limb segment.

Our preliminary results from displacing the limits of FGF and RA signals suggest the importance of these gradients in the determination of limb bone size (Figure 4.5; 4.6). We followed the bead implantation strategy of Dubrulle et al. (2001) to shift the limits of FGF signal either proximally or distally. This was attained as evidenced by the proximally expanded or distally confined *mkp3* expression (Figure 4.5). We only evaluated the size of the zeugopod elements (radius and ulna) since our bead implantations were performed between stage HH22-23 during which the zeugopod is established (Dudley et al., 2002). Similar to the small somites obtained in the PSM (Dubrulle et al., 2001), short limb bones (90%) were obtained upon FGF8 bead implantation (Figure 4.5). Reduction in bone size could be explained by the extended period of time the distal limb cells were under the influence of the AER/FGF signal. As it has been described that the distal limb mesenchymal cells acquire positional information based on the time they spend in the UZ (Summerbell et al., 1973) or based on the segment specific marker they express while they exit the UZ (Tabin and Wolpert, 2007), not enough cells would have exited the UZ to form proper sized zeugopod. Conversely, application of FgfR1 inhibitor (SU5402) caused bigger somites as a result of the allocation of more cells than normal to form the somites (Dubrulle et al., 2001). But our SU5402 bead implantations didn't produce consistent results concerning limb bone size (60% short and 40% long limbs), although FgfR1 is the major receptor expressed in the limb mesenchyme (Sheeba et al., 2010). This inconsistency might be due to the functional redundancy existing between FGFs and WNTs in the maintenance of the distal limb mesenchymal cells in an undifferentiated proliferative state (ten Berg et al., 2008; Cooper et al., 2011). Accordingly, the PSM-DetF is believed to be set also by WNT signaling (Aulehla et al., 2008; Aulehla and Pourquie, 2010). However, a recent study has reported that WNT and FGF signaling maintain each other in the caudal PSM while only FGF signal positions the DetF (Naiche et al., 2011). In fact in limb, several WNT members are responsible for the proper expression of *fgf8* in the AER. Among which *wnt3a* is co-expressed along with *fgf8* in the AER and shown to maintain its expression in this tissue (Kawakami et al., 2001). In addition to the maintenance of *fgf8*

expression, WNT3a is also necessary for UZ cell proliferation and it co-operates with FGF signal to begin UZ cells differentiation program (ten Berg et al., 2008). This suggests that WNT3a might indeed be positioning the DF along with FGF8 in the limb mesenchyme.

Alternatively, we pushed the limits of the proximal-RA signal either proximally or distally by implanting RA or citral beads. As expected, when RA signal limit was pushed proximally, FGF8 signal effector, *mkp3* domain expanded proximally supporting the opposing effect of RA on FGF signaling (Tabin and Wolpert, 2007). But, this mutual inhibition was not evidenced when RA bead was implanted in the distal limit of *meis1* expression (RA signal read out) since, this manipulation failed to push *mkp3* domain distally (Figure 4.6). Although citral bead implantation caused proximal expansion of *mkp3* expression, it produced longer limb elements compared to the control (Figure 4.6). This is contradicting with the short limbs formed after the proximal expansion of *mkp3* upon FGF8 bead implantation. However, these results implement FGF and RA signaling in limb bone size determination, although, more experiments are needed to derive a conclusion.

Following the patterning stages, cells begin their differentiation program, during which several changes occur at the cellular level including gene expression and cell type. In the PSM, one of the prominent gene to be expressed just before boundary formation is *Mesp2* (Evrard et al., 1998; Zhang and Gridley, 1998; Aulehla et al., 2008; Oginuma et al., 2008; Oginuma et al., 2010; Niwa et al., 2011). Moreover, mesenchymal cells maintained by FGF and WNT signals from the caudal PSM will enter epithelial transition until they form well defined epithelial somites (Dubrulle and Pourquie, 2004a; Martins et al., 2009). During limb development, when cells escape the influence of the AER-FGF/WNT signals, cell cycle is withdrawn and they start to express the early chondrogenesis marker, *sox9* and begin to differentiate in a PD sequence. In the periphery, cells that are out of FGF signaling range, but still under the influence of ectodermal WNT signal will differentiate into connective tissue (ten Berge et al., 2008).

5.4. COMPARISON OF *HES* GENE EXPRESSION REGULATIONS BETWEEN LIMB AND PSM

5.4.1. ROLE OF NOTCH SIGNALING IN HES GENE EXPRESSION

Our work with chick forelimb aiming to understand limb *hairy2* expression regulation has brought more similarities between somitogenesis and limb development. *HES* genes are

generally considered as effectors of Notch signaling (Fisher and Caudy, 1998; Rida et al., 2004). In chick forelimb, *hairy2* is expressed in three distinct domains namely CPD, DCD and PPD, being dynamically expressed in DCD and PPD (Figure 2.3). When we assessed the role of Notch signal inhibition on limb *hairy2* expression by applying DAPT beads in the two distal limb *hairy2* positive domains (Posterior Positive Domain: PPD; Distal Cyclic Domain: DCD), we obtained results that infer different degrees of *hairy2* downregulation. DAPT prominently downregulated *hairy2* in the DCD compared to the PPD (Figure 4.1) suggesting that Notch is not the only regulator of *hairy2* in the PPD. This kind of domain-specific effect of Notch signaling has been previously reported during murine neurogenesis based on Notch ligand expression patterns (Marklund et al., 2010). Actually, chick and mouse limb displays distinct domain specific expression of receptor/ligand pairs, where *Notch1/serrate2* is expressed in the AER and *Notch2/Serrate1* is expressed in the limb distal mesenchyme (Pascoal and Palmeirim, 2007; Dong et al., 2010). In the PSM, the sole dependency of *HES* genes on Notch signaling was questioned by studies where NICD nuclear partner RBP-jk was mutated. In the absence of Notch signaling, *hes7* expression was still observed in the PSM suggesting the participation of other signaling pathways in its regulation (Aulehla and Herrmann, 2004; Niwa et al., 2007; Aulehla and Pourquie, 2008). Eventually, it was identified that Notch signaling is only necessary for the anterior propagation or maintenance of *hes7* oscillations while FGF signaling initiates its oscillations in the posterior PSM (Niwa at al., 2007). Moreover, Notch based synchronization of PSM cells (through *Lfng* expression) is crucial for robust *hes7* and NICD oscillations (Niwa et al., 2011). Our results in chapter III have strongly illustrated the requirement of AER/FGF signaling for limb distal mesenchymal *hairy2* expression. Additionally, the observation that chemical inhibition of Notch signaling had profound effect on DCD-*hairy2* expression compared to the PPD is tempting us to speculate a similar role for Notch in limb *hairy2* expression. Like in the PSM, *hairy2* expression initiated by AER/FGF signaling might be propagated proximally by Notch through its involvement in cell synchronization.

5.4.2. ROLE OF FGF SIGNALING IN HES GENE EXPRESSION

Notch independent *HES* gene regulations through other signaling pathways are beginning to be uncovered in different systems (Nakayama et al., 2008; Ingram et al., 2008; Wall et al., 2009; Sanalkumar et al., 2010; Niwa et al., 2007; Gibb et al, 2009; Resende et al, 2010). Inability

of DAPT beads to completely abolish *hairy2* expression in the PPD and the close proximity of *hairy2* dynamic domain to the major limb signaling centers, the AER and the ZPA, urged us to study the involvement of AER/FGFs and ZPA/SHH in limb *hairy2* regulation. Our findings clearly show that the AER-produced FGFs and ZPA-derived SHH are absolutely required for the physiological expression of limb *hairy2* expression (Chapter III).

We found that *hairy2* expression is extremely sensitive to AER-FGF signaling. It took only less than an hour to abolish distal limb *hairy2* expression upon AER ablation or to induce *hairy2* by FGF bead implantation. In the PSM, FGF dependent *HES* gene expressions are reported and demonstrated to have significant biological value (Kawamura et al., 2005; Niwa et al., 2007). In zebrafish, *her13.2* (zebrafish HES gene member) expression is shown to be induced by FGF signaling in an Notch independent manner and Her13.2 protein is necessary for Notch mediated oscillations of *her1* and *her7* and for proper somite segmentation (Kawamura et al., 2005). Nevertheless, the initiation of Hes7 oscillation in the posterior PSM is regulated by FGF signaling and maintained in the anterior PSM by Notch signaling in mouse (Niwa et al., 2007). Hes7 is required for the cyclic expression of *hes7*, *Lfng* and periodic notch activity in mouse PSM (Bessho et al., 2003; Kageyama et al., 2007). By a series of AER ablation (anterior and/or posterior AER), bead implantation and time lapse experiments, we showed that AER-FGFs exert a short range, short-term inductive signal for *hairy2* expression in distal limb (Figure 5.2). This effect is mediated through Erk/MAPK and Akt/PI3K pathway activations. Intracellular signaling pathways downstream of FGFs such as c-Jun N-terminal kinases (JNK) (Curry et al., 2006; Sanalkumar et al., 2010) and Ras/Erk/MAPK pathways (Stockhausen et al., 2005; Nakayama et al., 2008) have been implicated in the regulation of Notch-independent *hes1* transcription. Interestingly, chick PSM presents graded p-Erk in response to FGF8 signaling (Delfini et al., 2005). Emphasizing the importance of p-Erk levels, Nakayama et al. (2008) has demonstrated a correlation between Erk phosphorylation and *hes1* expression under in vitro conditions. In limb, AER-FGFs enable ZPA-*shh* expression through Erk/MAPK pathway activation in chick forelimb (Bastida et al., 2009) making Erk phosphorylation a crucial regulatory mechanism during limb development. Our immunoblot analysis also exhibited up to 77% elevation in p-Erk levels upon FGF8 bead implantation. In addition, we also found a 37% increase in p-Akt levels and both MAPK as well as PI3K pathway inhibitors interfered with FGF8 induced ectopic *hairy2* induction. Thus, we propose that

activation of Erk/MAPK and Akt/PI3K pathways downstream of FGF signaling is necessary for limb *hairy2* expression.

5.4.3. ROLE OF SHH SIGNALING IN HES GENE EXPRESSION

The ability of SHH to regulate HES gene expression has so far been reported in very few studies (Ingram et al., 2008; Wall et al., 2009; Resende et al., 2010). In the PSM, the direct role of Notochord (No) derived SHH in timely somite formation and *hairy2* expression through *Gli2/Gli3* transcriptional modulation was recently exemplified by Resende et al. (2010). Our analysis of ZPA derived SHH signaling on limb *hairy2* regulation suggests a long-term, long-range permissive effect as revealed from the results of both ZPA ablation and ectopic SHH application experiments. Upon ZPA ablation, the complete abrogation of *hairy2* from the entire distal limb mesenchyme took around 5-6h unlike the quick response (within 1h) observed after AER ablation. Furthermore, the absence of the ZPA, situated in the posterior distal limb margin enabled downregulation of *hairy2* even from the distanced DCD. On the other hand, AER tissue ablation presented a very restricted *hairy2* expression loss, in a way only in the mesenchyme just adjacent to the ablation site. Moreover, grafting SHH secreting QT6-cells immediately after ZPA ablation rescued *hairy2* expression in the entire limb distal mesenchyme while FGF bead implantation following AER extirpation only induced local *hairy2* expression. These observations reveal a long-term, long-range nature of ZPA/SHH signaling on *hairy2* expression (Figure 5.2). The positive role of ZPA/SHH on limb *hairy2* expression is in agreement with the recent report on the transcriptome analysis of *shh* null mouse limb buds (Probst et al., 2011). In their analysis of down or upregulated genes in *shh* null mouse limb buds, *hes1* (the mouse homolog of *hairy2*) is placed among the genes that are downregulated in the absence of limb SHH signaling which supports our results.

Through western blot analysis, we further found that the ZPA/SHH-mediated balance between Gli3-A and Gli3-R determines the permissive state for limb *hairy2* expression. Based on the conditions that induced ectopic *hairy2* and therein created Gli3-A/Gli3-R ratio, we define Gli3-A/Gli3-R≥1 as the permissive state for limb distal mesenchymal *hairy2* expression. The distal limb is known to display high Gli3-R activity in the anterior than in the posterior region (Wang et al., 2000; Ahn and Joyner, 2004). Since SHH inhibits the processing of the whole Gli3 protein into its short repressor form (Wang et al., 2000), there established a posterior to anterior gradient of

Gli3-A/Gli3-R ratio. Accordingly, *hairy2* is persistently expressed in the PPD which presents higher Gli3-A/Gli3-R ratio and the anterior limb with lower Gli3-A/Gli3-R ratio is negative for *hairy2* expression. *hairy2* oscillatory domain, the DCD contains moderate SHH signaling via balanced Gli-A and Gli-R levels compared to the most posterior and anterior limb.
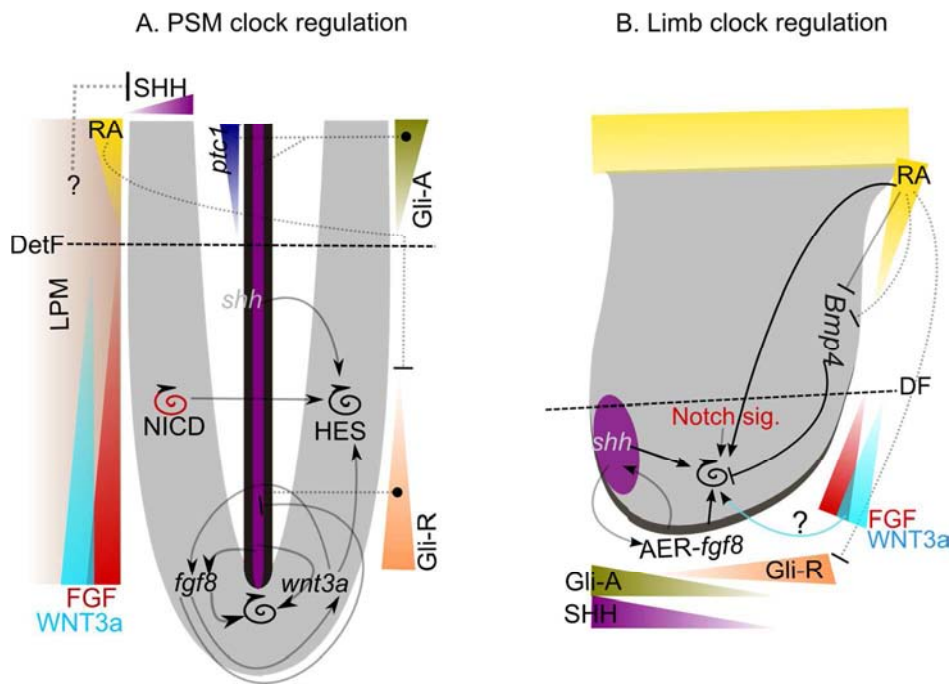
Figure 5.2. Schematic representation of PSM and limb showing multiple signaling pathways regulating *HES* gene expression. A stage HH13 chick PSM (A) and a stage HH24 chick forelimb bud (B) are placed next to each other for comparison. A well-known regulator of HES genes, Notch signaling is cyclic in the PSM (red spiral arrow) and regulates the cyclic *HES* gene expression (Bessho et al., 2003). Correspondingly in limb, the distal mesenchyme presents Notch signaling (through Notch2/Serrate1 pair) and regulates *hairy2* expression (results from the present study; Visiliauskas et al., 2003). In both systems, FGF signaling regulates *HES* gene expression: in the PSM, caudally produced FGF8 initiates *hes7,* which has essential biological functions (Niwa et al., 2007) and in the limb, AER derived FGFs exert a short range, short-term inductive signal to regulate *hairy2* expression (our result). The caudal PSM also transcribes *wnt3a* which is engaged in a positive loop with *fgf8* (Naiche et al., 2011). WNT3a also positively regulates *HES* genes in the PSM (Gibb et al., 2009). This mechanism has not yet been analyzed for limb *hairy2* (blue line with question mark). The SHH produced from the Notochord (violet bar in the middle of the neural tube) and ZPA (violet circle in the posterior-distal margin of limb) also regulates *hairy2* expression in the PSM and limb, respectively. Although SHH positively regulates *fgf8* expression in the posterior PSM (Resende et al., 2010), high FGF signaling in this region inhibits *shh* (Diezdel Corral et al., 2003; Ribes et al., 2009). This could results in elevated Gli-R accumulation in the posterior PSM (orange graded triangle in the PSM). Low level of FGF signaling above the DetF

(dashed line in the PSM), and the graded *ptc1* expression (dark blue graded triangle; Resende et al., 2010) enables SHH signaling to be active in the anterior PSM (above the DetF: violet graded triangle on top) which maintains high Gli-A gradient (green graded triangle). In fact, this region of the PSM expresses *Gli1-3* (Borycki et al., 2000; Resende et al., 2010). There might be a counteracting regulation between SHH signal in the anterior PSM and BMP4 signal from the LPM as it is observed in somite differentiation (reviewed in Stockdale et al., 2000). RA signal inhibits Gli-R activity above the DetF (Goyette et al., 2000; Resende et al., 2010). Parallel to these mechanisms, limb *hairy2* is also regulated by ZPA derived SHH in a long-range, long-term manner (our work). Limb distal mesenchyme is endowed by SHH mediated (violet graded triangle in the limb) Gli-A (green graded triangle in the limb) opposed by a Gli-R gradient (orange graded triangle in the limb) (Wang et al., 2000; Ahn and Joyner, 2004). The balance between Gli3-A and Gli3-R establish a Gli3-A/Gli3-R ratio gradient from the posterior-anterior limb which creates a permissive state defined as Gli3-A/Gli3-R≥1 for *hairy2* expression (our work). BMP4 signaling inhibits *hairy2* from being expressed in the anterior limb domain (our work). RA positively regulate *hairy2* expression in the anterior limb by neutralizing BMP4 and Gli3-R signaling (Goyeet et al., 2000; Thompson et al., 2003; Sheng et al., 2010; Lee et al., 2011). ZPA/SHH and AER/FGFs maintain each other in a positive feedback loop (Niswander et al., 1993; Fallon et al., 1994). Grey lines indicate interactions from existing literature and black lines represent interactions identified from the present work. Solid and dotted lines denotes respectively the transcriptional and activity levels of interactions. Arrows represents transcriptional activation, blunt bars represent inhibitions and dotted lines with black round ends indicates the proposed Gli-A and Gli-R gradients in the PSM (refer the text for more details).

Our study also revealed the mutual dependency of AER/FGF and ZPA/SHH for limb *hairy2* expression. This is evident from the inability of SHH-bead to misexpress *hairy2* in the absence of AER and the failure of FGF bead to act as an inductive signal when ZPA/SHH signaling was completely eliminated from the tissue. Strikingly, FGF-bead implanted in the AND that do not possess SHH signaling, never induced *hairy2* even after longer incubations. Whereas, in the presence of an imposed permissive state build by previous SHH-bead implantation in the AND, enabled FGF bead to induce *hairy2.* These experiments clearly suggest the permissive nature of ZPA/SHH signaling on hairy2 expression in chick limb.

The long term effect observed upon ZPA ablation to eliminate *hairy2* expression in the distal limb mesenchyme suggests that there might be a temporal threshold to disturb the well-established GLI-A/GLI-R ratio in this limb region. In fact, Harfe et al. (2004) found that SHH bead implantation in the anterior limb require at least 4h to begin Gli3-R downregulation. Interestingly, the duration of ~5h to abolish limb *hairy2* expression after ZPA ablation closely coincides with the time of 4.5h until which normal somitogenesis rate was maintained in No ablated (No⁻) chick PSM explants (Resende et al., 2010). Although, the authors reasoned the

initial unaltered somite formation as the consequence of the predetermined somites present above the DetF, it is so suggestive that it may need around 4.5-6h to destabilize the balance between Gli-R/Gli-A ratios. While no distinct Gli-A and Gli-R gradients are reported in the PSM, indirect evidence suggests that an anterior-posterior Gli-A gradient above the DetF and a posterior-anterior Gli-R gradient in the caudal end of the PSM might exist. This speculation is derived from two previous studies (Borycki et al., 2000; Resende et al., 2010). *Gli1, Gli2* and *Gli3* are expressed in the somites and the anterior most region of the PSM (Borycki et al., 2000; Resende et al., 2010), in addition *Gli3* is also expressed in the posterior PSM (Borycki et al., 2000). Since the inhibition of *shh* by the caudal FGF signaling (Diez del Corral et al., 2003; Ribes et al., 2009) would be relieved in the anterior PSM (above the DetF), Gli1-3 proteins produced here should be in an activator form. Expression of *ptc1* in this domain supports this notion (Resende et al., 2010). The lack of *ptc1* or *ptc2* receptors (Borycki et al., 2000; Resende et al., 2010) and low/residual SHH signaling caused by high FGF activity below the DetF might generate a posterior-anterior Gli3 based repressor gradient in the posterior PSM. However, this hypothesis needs to be verified experimentally.

5.4.4. POSSIBLE ROLE OF RA AND BMP4 SIGNALS ON HES GENE EXPRESSION

In developing mouse limb, *hes1* has been identified as a target of RA-signaling (Ali-Khan and Hales, 2006). Our bead implantation studies performed in all limb domains including the AND (PPD, DCD, PND and AND) revealed RA as a positive regulator of limb *hairy2* expression (Figure 4.2). Results from immunoblot analysis suggest that a permissive condition (Gli3-A/Gli3-R≥1) was created in the AND, upon RA-bead implantation (Figure 4.3). In agreement, RA signaling has been reported to inhibit Gli3-R activity (Goyette et al., 2000) and it rescued somitogenesis delay caused by the absence of Notochord/SHH signals in the PSM (Resende et al., 2010). Yet another interesting observation in our study is the local ectopic *hairy2* expression induced around FGF-bead that was co-implanted with a RA-bead in the AND.

The AND also coincides with the intense expression of *Bmp4* in chick wing bud (Geetha-Loganathan et al., 2006). Thus we went to analyze the effect of BMP4 signaling on *hairy2* expression. As expected, BMP4-bead inhibited *hairy2* expression in the DCD (Figure 4.4). Moreover, implantation of FGF-bead in the AND following a Noggin-bead also enabled FGF-bead

to induce local *hairy2* expression (Figure 4.4). This clearly suggests BMP4 as a negative regulator of limb *hairy2* expression. From the literature, it is known that both the RA and SHH signaling could inhibit BMP4 activity. Thus in the AND, BMP4 might have been neutralized by RA signal as shown in other systems (Thompson et al., 2003; Sheng et al., 2010; Lee et al., 2011). Similarly, SHH also inhibits Bmp4 expression in the anterior limb upon implantation of SHH-soaked bead (Tumpel et al., 2002). Thus the ectopic *hairy2* expression brought in the AND by the application of either RA or SHH-bead could have been a combinatory inhibition of both Gli3-R and BMP4 activities. During somitogenesis, *Bmp4* is expressed in the LPM tissue and it is inhibited from being expressed in the PSM by *noggin* expressed in the lateral PSM (IM) (Tonegawa and Takahashi, 1998; Capdevila and Johnson, 1998). When *Bmp4* expression in the LPM was inhibited by Noggin misexpression, ectopic somites were formed by respecification of LPM into PSM tissue (Tonegawa and Takahashi, 1998). This proposes the possible inhibition of clock genes by BMP4 signaling in the PSM, although this phenomenon was not evaluated in this study.

The limb also exhibits mutual antagonism between ZPA-SHH and BMP signals. Recently, Bastida et al. (2009) revealed the necessity of BMP signal mediated inhibition for the confinement of *shh* transcripts to the ZPA. SHH signaling also inhibits BMP signal through *Grem1* induction (Zuniga et al., 1999; Michos et al., 2004) which is an integrated component of the ZPA/SHH-AER/FGF positive feedback loop. In parallel, we postulate that a mutual inhibition between anterior PSM-SHH and LPM-BMP4 signals might exist similar to the one implemented in somite differentiation (Stockdale et al., 2000).

Although, the above mentioned RA- mediated regulation of *hairy2* expression might not be functional during stage HH22-24 (the stage frame of this study), at early stages, RA could be co-operatively regulating *hairy2* along with the inductive AER/FGF signal (Figure 5.3). The presumptive limb mesenchyme expresses *Raldh2, Bmp4* and *hairy2* at stage HH14-HH15 (Swindell et al., 1999; Berggren et al., 2001; Blentic et al., 2003; Nimmagadda et al., 2005; Pascoal et al., 2007b) and the nascent limb is pre-patterned by high Gli3-R activity in the anterior mesenchyme before *shh* is initiated at stage HH17 (Marigo et al., 1996; Schweitzer et al., 2000; te Welscher et al., 2002). The entire early limb mesenchyme displays *hairy2* transcripts despite of the presence of its inhibitory signals, BMP4 and Gli3-R. This co-expression might be due to the joint role of flank-RA signals capacity to suppress BMP4 and Gli3-R mediated *hairy2* inhibition and AER/FGF *hairy2* inductive signal. At the early stages of limb development both the AER/FGF and

flank-RA signals influence the nascent limb mesenchyme (Tabin and Wolpert, 2007). Once *shh* is initiated at stage HH17, opposing gradients of Gli-A and Gli-R will be established in the limb mesenchyme (Wang et al., 2000; Ahn and Joyner, 2004; Harfe et al., 2004). Concurrently, from stage HH18 onwards, *hairy2* shows posterior-positive and anterior-negative limb domains (Pascoal et al., 2007). The co-existence of *hairy2* in the presumptive and nascent limb along with its inhibitory signals (BMP4 and Gli3-R) and its domain distinction after ZPA-*shh* establishment validates our finding of the involvement of AER/FGF, ZPA/SHH and RA signals in limb *hairy2* expression.
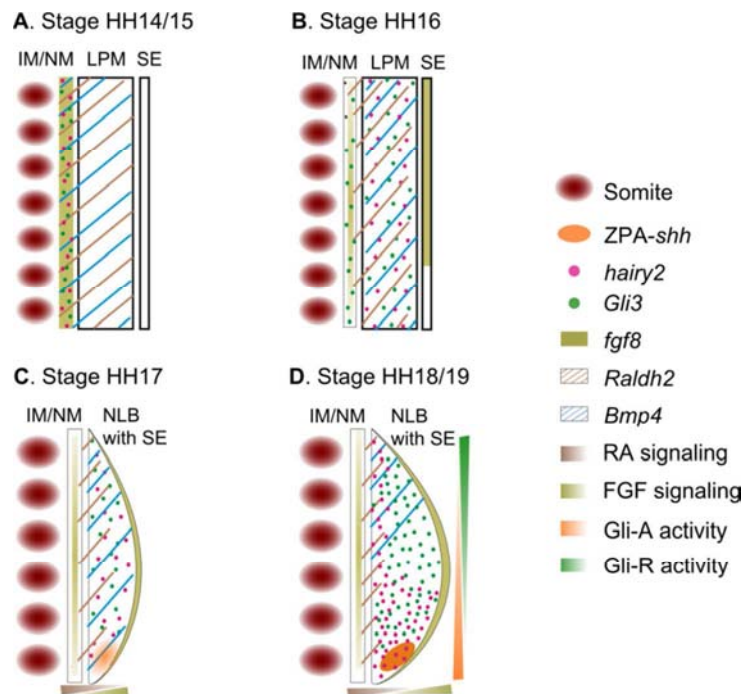
Figure 5.3: Possible role of RA signaling mediated *hairy2* regulation at limb initiation stages. (A) Scheme representing somite level 14-20 of a stage HH14/15 chick embryo. Here, the Intermediate mesoderm (IM)/Nephrogenic mesoderm (NM) exhibit the expression of *hairy2* (Pascoal et al., 2007b), *Gli3* (Gaisha ID: 42Q) and *fgf8* (Crossley et al., 1996). *Bmp4* (Nimmagadda et al., 2005) and *Raldh2* (Swindell et al., 1999; Blentic et al., 2003) are expressed both in the IM and in the LPM. The SE and the posterior mesenchyme are yet to express *fgf8* and shh, respectively, at this stage (Crossley et al., 1996). (B) Scheme representing somite level 14-20 of a stage HH16 chick embryo. By this stage of development, *fgf8* is already expressed in the SE (partially); *hairy2* is expressed in the LPM but not in the IM (Pascoal et al., 2007b) and *Gli3* occupies the LPM in addition to its IM expression. *Raldh2* and *Bmp4* are maintained in the same domains (Blentic et al., 2003; Bastida et al., 2009). *shh* is yet to be expressed in the posterior mesenchyme (Crossley et al., 1996). (C) Scheme representing somite level 15-20 of a stage HH17 chick

embryo. Three important changes occur at this stage: a visible nascent limb bud (NLB) is formed; *fgf8* expression spreads to the entire SE and the posterior mesenchyme begins to express *shh* (Crossley et al., 1996). *Bmp4* transcripts inhabit the entire limb mesenchyme (Bastida et al., 2009). *Raldh2* expression begins to withdraw proximally (Swindell et al., 1999; Berggren et al., 2001; Blentic et al., 2003) but, the entire limb mesenchyme will be under the influence of confronting RA and FGF signaling (reviewed in Tabin and Wolpert, 2007). *hairy2* still occupies the whole of the limb mesenchyme (Pascoal et al., 2007b) (D) Scheme representing somite level 15-20 of a stage HH18/19 chick embryo. Expression of *shh* gets stronger in the ZPA (Crossley et al., 1996) and *Gli3* is still expressed in the entire limb mesenchyme (Marigo et al., 1996; Schweitzer et al., 2000). Presence of SHH signaling will establish opposing gradients of Gli-A and Gli-R across the AP axis (Wang et al., 2000; Harfe et al., 2004; Ahn and Joyner, 2004). Concomitantly, *hairy2* display domain specificity: the anterior limb domain that is free of its transcripts and a posterior positive domain encompassing the ZPA (Pascoal et al., 2007b). By now, *Bmp4* expression is anteriorized (Geetha-Loganathan et al., 2006; Bastida et al., 2009); *Raldh2* expression is proximilized (Swindell et al., 1999; Blentic et al., 2003) and the PD axis controlling flank-RA and AER/FGF signals begins to get apart gradually (reviewed in Tabin and Wolpert, 2007). Panel of each color representing different molecule/signals is provided in the right side of the scheme. This scheme is derived based on the existing literature and our results on the RA signal-mediated *hairy2* regulation.

All the aforementioned experiments with DAPT bead implantation, AER and ZPA ablation did not alter *hairy2* expression in the CPD suggesting that an independent mechanism other than those described here takes part in the regulation of CPD-*hairy2* expression. Overall, we show that limb distal mesenchymal *hairy2* is positively regulated by multiple signaling pathways, namely: Notch, AER/FGFs, ZPA/SHH and RA, whereas this gene is negatively regulated by BMP4 and Gli3-R activities suggesting an immense similarity with HES gene regulation in the PSM in which all these signaling pathways are also implicated (Figure 5.2).

CHAPTER VI: CONCLUSIONS & FUTURE PERSPECTIVES

6.1. MAIN CONCLUSIONS

In this thesis, we have established parallelisms between limb development and somitogenesis at the level of their morphology, gene expression patterns and gene function, using the findings of our work and existing literature. We have primarily studied the signaling pathways regulating the expression of limb molecular clock gene, *hairy2,* in the distal mesenchyme. The main achievements derived from this study are listed below.

1. We have identified the involvement of the two renowned limb signaling centres, the AER and ZPA, and their key mediators, the FGFs and SHH, for limb *hairy2* expression.

2. We have determined that the activation of Erk/MAPK and Akt/PI3K pathways in response to FGF signaling and SHH-mediated Gli3-A/Gli3-R balance is vital for *hairy2* expression.

3. We further demonstrated AER/FGF as a short-term, short-range inductive signal and ZPA/SHH as a long-term, long-range permissive signal of limb *hairy2* expression.

4. We showed that the permissive state of Gli3-A/Gli3-R≥1 built by ZPA/SHH is crucial for the AER/FGF instructive signal to induce *hairy2*. Similarly, in the absence of AER/FGF signal ZPA/SHH cannot induce *hairy2* expression.

5. We have demonstrated RA as a positive regulator of limb *hairy2* expression and BMP4 as a negative regulator.

6. We suggest that RA mediated *hairy2* induction is possibly through counteracting BMP4 and Gli3-R activities as previously described in other systems (Goyette et al., 2000; Thompson et al., 2003; Sheng et al., 2010; Lee et al., 2011). We propose that this mechanism might be facilitating *hairy2* expression in the presumptive and nascent limb during early stages of limb development.

7. Thus, each domain of limb *hairy2* is defined by the combinations of different signals: the PPD is defined by high SHH signal-mediated Gli3-A/Gli3-R≥1 ratio (higher than one) and high FGF signal; DCD by moderate SHH signaling (balanced GLI-A and GLI-R levels presenting Gli3-A/Gli3-R≥1 tending towards 1) and high FGF signaling; finally AND by less SHH signaling-mediated Gli3-A/Gli3-R≥1 (less than 1) and high BMP4 activity.

8. We show that the regulation of *hairy2* by AER/FGF and ZPA/SHH is not a relay but a convergence. Thus *hairy2* functions as a temporal and spatial readout of the AER/FGF and ZPA/SHH signaling.

9.   Finally, we propose that Hairy2 might be acting as a node that co-ordinates patterning along the limb PD and AP axis through its strict transcriptional regulation by both the PD pattern instructor AER-FGF and AP axis organizer ZPA-SHH signals.

It is interesting that the positive regulator of *hairy2*, ZPA/SHH inhibits Gli3 processing into its repressor form (our results; Wang et al., 2000; Harfe et al., 2004; Bastida et al., 2004) and inhibits *Bmp4* transcription (Tumpel et al., 2002; Bastida et al., 2004) as well as its activity through *Grem1* expression (Zuniga et al., 1999; Michos et al., 2004). On the other hand, the negative regulator of *hairy2*, Gli3-R, positively regulates BMP4 signaling directly (Bastida et al., 2004) or through *Grem1* inhibition (Lallemand et al., 2009). All the interactions specified above are summarized in Figure 6.1.
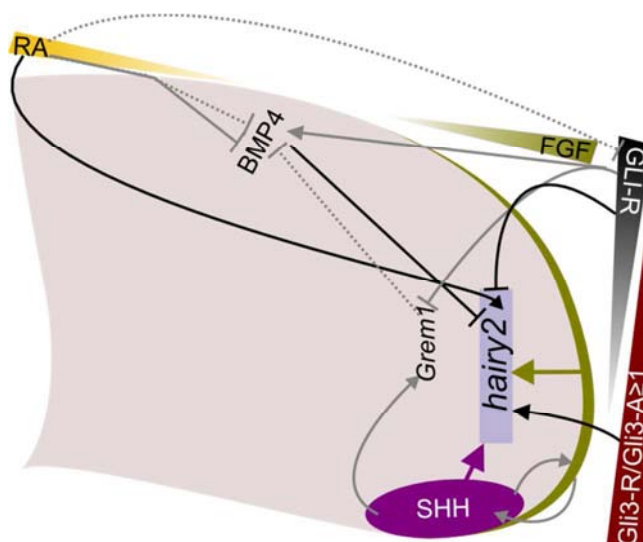
Figure 6.1: Schematic representation of signaling network regulating limb *hairy2* expression. Stage HH23 chick forelimb bud displaying the regulatory network of limb distal mesenchymal *hairy2* expression identified from our work. *hairy2* is positively regulated by AER/FGFs in a sort-term, short-range inductive manner (thick green arrow) and by ZPA/SHH in a long-term, long-range permissive fashion (represented by thick violet arrow). Inhibition of Gli3 processing proportional to ZPA/SHH signaling establishes a ratio between Gli3-A and Gli3-R along the posterior-anterior axis (maroon graded triangle). When this ratio is Gli3-A/Gli3-R≥1, the tissue is in a permissive state to express *hairy2* in the presence of the AER/FGF inductive signal. AND presents Gli3-A/Gli3-R<1 and so do not express *hairy2*. *Bmp4* expressed in the anterior limb mesenchyme negatively regulates *hairy2* and along with the Gli3-A/Gli3-R<1, it defines the AND. SHH prevent BMP4 transcription (Bastida et al., 2004; Tumpel et al., 2002) and signaling in the distal limb through *Grem1* induction, which is a BMP antagonist (Zuniga et al., 1999; Michos et al., 2004). SHH also inhibits Gli3 processing to its repressor form (our work; Wang et al., 2000; Ahn and Joyner, 2004). Gli3-R

positively regulates *Bmp4* expression (Bastida et al., 2004) and activity (Lallemand et al., 2009). Ectopic RA inhibits Gli-R activity (Goyeet et al., 2000) and BMP4 signaling (Sheng et al., 2010; Lee et al., 2011) as well as *Bmp4* transcription (Thompson et al., 2003) in the AND. Grey lines indicate interactions from existing literature all other color lines represent interactions identified from our work. Solid lines and dotted lines denote transcriptional and activity level interactions, respectively. Arrows represent transcriptional activation and blunt bars represent inhibitions.

The conclusions derived from this work clearly suggest the importance of limb *hairy2* expression through its tight regulation in the multi-potent distal limb mesenchymal cells (Dong et al., 2010) mediated by almost all the major signaling pathways. This region of the limb is very important to determine a complete limb through patterning and differentiation events (Pearse et al., 2007). The FGFs and WNTs from the AER and non-ridge ectoderm are known to maintain the juxtaposed cells in an undifferentiated state and allow them to enter their fate, once they escape their signaling influence (ten Berge et al., 2008). Being a HES family member, *hairy2* expression in the distal mesenchyme might be maintaining these cells in the undifferentiated state as proposed for neural progenitor cells (Kageyama et al., 2007). Moreover, *hairy2* regulations identified in our work suggest that Hairy2 might be coordinating limb development along PD and AP axes. During later developmental stages, HES genes take part in the formation of proper limb bone elements in terms of their size and mass (Vasiliauskas et al., 2003; Zanotti et al., 2011). In general, embryogenesis is a highly organized timely process and a mechanism that gives the notion of time to the cells is crucial for which somitogenesis is the best example. We strongly suggest that a *hairy2* based molecular clock is operating in the limb reminiscent to the PSM clock. However, whether the limb clock is purely *hairy2* based needs to be evaluated by functional studies, which is under way in our lab. Our preliminary results to assess the concept of DF in the limb suggest that the confronting gradients of RA and FGF signaling determine the size of limb bone elements.

We believe that our perception of making the parallelisms between limb development and somitogenesis has highlighted the similarities existing between these two systems at the level of gene expression and their functions. Furthermore it has provided the possibility of utilizing the knowledge from one system to the other in order to understand the systems better.

6.2. FUTURE PERSPECTIVES

Our detailed study on the parallelisms between limb and trunk development suggests that both systems can benefit from each other's literature. Some of the important concepts generated from our comparative study are presented here for future exploration.

The only identified limb clock gene, *hairy2* will be characterized better at its regulation by analyzing the role of WNTs since WNT signaling is regulating Notch target clock genes in the PSM (Gibb et al., 2009). The molecular hierarchy involved in *hairy2* regulation and intracellular pathways will also be evaluated. It has already been reported that cyclic gene expression is cell-autonomous and depends on negative auto-regulation based on ubiquitin/proteasome-mediated protein degradation and rapid mRNA depletion (Hirata et al., 2002). These mechanisms will be evaluated for Hairy2 during limb development to check whether it is operational in limb to generate *hairy2* oscillations. In fact, we expect a variation in this mechanism since the limb clock oscillates with longer periodicity. Moreover, the role of RA signaling in early limb *hairy2* expression will be thoroughly investigated, which might provide additional insights in limb initiation program.

Importantly, our ongoing work to assess the functional relevance of *hairy2* will be continued. Perturbation of *hairy2* cycles can be achieved either by constitutively producing Hairy2 protein or by abolishing its production. We are utilizing retrovirus mediated gene delivery system to express both *hairy2* coding sequence to overexpress Hairy2 and a specific *hairy2* siRNA to downregulate its expression by injecting the virus in stage HH12-14 forelimb bud mesenchyme. In somitogenesis, loss of cyclic gene expression or Notch activity has resulted in somitogenesis defects and shift in axial identities (Cordes et al., 2004; Feller et al., 2008; Ferjentsik et al., 2009). Since limb molecular clock is linked to skeletal element positional information, a careful study of limb phenotype upon *hairy2* misexpression will be performed by assessing the expression of limb segment specific markers and skeletal preparations. Special emphasis will also be given to AP axis patterning.

We also aim to assess the possibility of other Notch, FGF and WNT components known to be cyclically expressed in chick PSM for dynamic limb expression by performing in ovo microsurgery and whole-mount in situ hybridization techniques. Moreover, we aspire to assess if the limb molecular clock is a phylogenetically conserved by searching for a putative mouse limb

molecular clock. In this row, we first wish to document real time imaging of HES1 expression in mouse limb utilizing the transgenic mice containing a highly unstable luciferase reporter driven by Hes1 promoter (Masamizu et al., 2006).

Compared to somitogenesis, role of SHH and BMP signaling are better characterized in limb development. For instance, the opposing Gli-A and Gli-R activities participation in somitogenesis will be elucidated in detail. Similarly, the cross talk and mutual positive and negative loops between SHH, BMP, FGF and RA signaling may add great insights to PSM segmentation. Limb outgrowth termination mechanisms involving SHH, FGF and GREM1 can be assessed in the tailbud since *fgf8* expression is ceased after stage HH20 in chick (Tenin et al., 2010); *shh* in the No is known to positively regulate PSM-*fgf8* expression (Resende et al., 2010) and high FGF signaling inhibits *shh* (Diez del Corral et al., 2003; Ribes et al., 2009). Additionally, as it has been mentioned in the general discussion, analysis of PSM clock in the presence of ectopic RA will be performed to see if RA positively or negatively regulates *HES* genes in the PSM. This study will be carried out in PSM explants and under in-vivo conditions.

REFERENCES

Agarwal, P., Wylie, J. N., Galceran, J., Arkhitko, O., Li, C., Deng, C., Grosschedl, R. and Bruneau, B. G. (2003) 'Tbx5 is essential for forelimb bud initiation following patterning of the limb field in the mouse embryo', *Development* 130(3): 623-33.

Ahn, D. G., Kourakis, M. J., Rohde, L. A., Silver, L. M. and Ho, R. K. (2002) 'T-box gene tbx5 is essential for formation of the pectoral limb bud', *Nature* 417(6890): 754-8.

Ahn, K., Mishina, Y., Hanks, M. C., Behringer, R. R. and Crenshaw, E. B., 3rd (2001) 'BMPR-IA signaling is required for the formation of the apical ectodermal ridge and dorsal-ventral patterning of the limb', *Development* 128(22): 4449-61.

Ahn, S. and Joyner, A. L. (2004) 'Dynamic changes in the response of cells to positive hedgehog signaling during mouse limb patterning', *Cell* 118(4): 505-16.

Akita, K., Francis-West, P. and Vargesson, N. (1996) 'The ectodermal control in chick limb development: Wnt-7a, Shh, Bmp-2 and Bmp-4 expression and the effect of FGF-4 on gene expression', *Mech Dev* 60(2): 127-37.

Ali-Khan, S. E. and Hales, B. F. (2006) 'Novel retinoid targets in the mouse limb during organogenesis', *Toxicol Sci* 94(1): 139-52.

Altabef, M., Clarke, J. D. and Tickle, C. (1997) 'Dorso-ventral ectodermal compartments and origin of apical ectodermal ridge in developing chick limb', *Development* 124(22): 4547-56.

Andrade, R. P., Palmeirim, I. and Bajanca, F. (2007) 'Molecular clocks underlying vertebrate embryo segmentation: A 10-year-old hairy-go-round', *Birth Defects Res C Embryo Today* 81(2): 65-83.

Aoyama, H. and Asamoto, K. (1988) 'Determination of somite cells: independence of cell differentiation and morphogenesis', *Development* 104(1): 15-28.

Arman, E., Haffner-Krausz, R., Gorivodsky, M. and Lonai, P. (1999) 'Fgfr2 is required for limb outgrowth and lung-branching morphogenesis', *Proc Natl Acad Sci U S A* 96(21): 11895-9.

Arques, C. G., Doohan, R., Sharpe, J. and Torres, M. (2007) 'Cell tracing reveals a dorsoventral lineage restriction plane in the mouse limb bud mesenchyme', *Development* 134(20): 3713-22.

Aulehla, A. and Herrmann, B. G. (2004) 'Segmentation in vertebrates: clock and gradient finally joined', *Genes Dev* 18(17): 2060-7.

Aulehla, A. and Pourquie, O. (2008) 'Oscillating signaling pathways during embryonic development', *Curr Opin Cell Biol* 20(6): 632-7.

Aulehla, A. and Pourquie, O. (2010) 'Signaling gradients during paraxial mesoderm development', *Cold Spring Harb Perspect Biol* 2(2): a000869.

Aulehla, A., Wehrle, C., Brand-Saberi, B., Kemler, R., Gossler, A., Kanzler, B. and Herrmann, B. G. (2003) 'Wnt3a plays a major role in the segmentation clock controlling somitogenesis', *Dev Cell* 4(3): 395-406.

Aulehla, A., Wiegraebe, W., Baubet, V., Wahl, M. B., Deng, C., Taketo, M., Lewandoski, M. and Pourquie, O. (2008) 'A beta-catenin gradient links the clock and wavefront systems in mouse embryo segmentation', *Nat Cell Biol* 10(2): 186-93.

Bai, C. B., Auerbach, W., Lee, J. S., Stephen, D. and Joyner, A. L. (2002) 'Gli2, but not Gli1, is required for initial Shh signaling and ectopic activation of the Shh pathway', *Development* 129(20): 4753-61.

Bai, C. B., Stephen, D. and Joyner, A. L. (2004) 'All mouse ventral spinal cord patterning by hedgehog is Gli dependent and involves an activator function of Gli3', *Dev Cell* 6(1): 103-15.

Bandyopadhyay, A., Tsuji, K., Cox, K., Harfe, B. D., Rosen, V. and Tabin, C. J. (2006) 'Genetic analysis of the roles of BMP2, BMP4, and BMP7 in limb patterning and skeletogenesis', *PLoS Genet* 2(12): e216.

Barrow, J. R., Thomas, K. R., Boussadia-Zahui, O., Moore, R., Kemler, R., Capecchi, M. R. and McMahon, A. P. (2003) 'Ectodermal Wnt3/beta-catenin signaling is required for the establishment and maintenance of the apical ectodermal ridge', *Genes Dev* 17(3): 394-409.

Bastida, M. F., Delgado, M. D., Wang, B., Fallon, J. F., Fernandez-Teran, M. and Ros, M. A. (2004) 'Levels of Gli3 repressor correlate with Bmp4 expression and apoptosis during limb development', *Dev Dyn* 231(1): 148-60.

Bastida, M. F., Sheth, R. and Ros, M. A. (2009) 'A BMP-Shh negative-feedback loop restricts Shh expression during limb development', *Development* 136(22): 3779-89.

Baur, S. T., Mai, J. J. and Dymecki, S. M. (2000) 'Combinatorial signaling through BMP receptor IB and GDF5: shaping of the distal mouse limb and the genetics of distal limb diversity', *Development* 127(3): 605-19.

Bell, S. M., Schreiner, C. M., Goetz, J. A., Robbins, D. J. and Scott, W. J., Jr. (2005) 'Shh signaling in limb bud ectoderm: potential role in teratogen-induced postaxial ectrodactyly', *Dev Dyn* 233(2): 313-25.

Benazeraf, B., Francois, P., Baker, R. E., Denans, N., Little, C. D. and Pourquie, O. (2010) 'A random cell motility gradient downstream of FGF controls elongation of an amniote embryo', *Nature* 466(7303): 248-52.

Benazet, J. D., Bischofberger, M., Tiecke, E., Goncalves, A., Martin, J. F., Zuniga, A., Naef, F. and Zeller, R. (2009) 'A self-regulatory system of interlinked signaling feedback loops controls mouse limb patterning', *Science* 323(5917): 1050-3.

Benazet, J. D. and Zeller, R. (2009) 'Vertebrate limb development: moving from classical morphogen gradients to an integrated 4-dimensional patterning system', *Cold Spring Harb Perspect Biol* 1(4): a001339.

Berggren, K., Ezerman, E. B., McCaffery, P. and Forehand, C. J. (2001) 'Expression and regulation of the retinoic acid synthetic enzyme RALDH-2 in the embryonic chicken wing', *Dev Dyn* 222(1): 1-16.

Bessho, Y., Hirata, H., Masamizu, Y. and Kageyama, R. (2003) 'Periodic repression by the bHLH factor Hes7 is an essential mechanism for the somite segmentation clock', *Genes Dev* 17(12): 1451-6.

Bessho, Y., Miyoshi, G., Sakata, R. and Kageyama, R. (2001) 'Hes7: a bHLH-type repressor gene regulated by Notch and expressed in the presomitic mesoderm', *Genes Cells* 6(2): 175-85.

Blentic, A., Gale, E. and Maden, M. (2003) 'Retinoic acid signalling centres in the avian embryo identified by sites of expression of synthesising and catabolising enzymes', *Dev Dyn* 227(1): 114-27.

Borycki, A., Brown, A. M. and Emerson, C. P., Jr. (2000) 'Shh and Wnt signaling pathways converge to control Gli gene activation in avian somites', *Development* 127(10): 2075-87.

Borycki, A. G., Brunk, B., Tajbakhsh, S., Buckingham, M., Chiang, C. and Emerson, C. P., Jr. (1999) 'Sonic hedgehog controls epaxial muscle determination through Myf5 activation', *Development* 126(18): 4053-63.

Bouldin, C. M., Gritli-Linde, A., Ahn, S. and Harfe, B. D. (2010) 'Shh pathway activation is present and required within the vertebrate limb bud apical ectodermal ridge for normal autopod patterning', *Proc Natl Acad Sci U S A* 107(12): 5489-94.

Boulet, A. M., Moon, A. M., Arenkiel, B. R. and Capecchi, M. R. (2004) 'The roles of Fgf4 and Fgf8 in limb bud initiation and outgrowth', *Dev Biol* 273(2): 361-72.

Brent, A. E., Schweitzer, R. and Tabin, C. J. (2003) 'A somitic compartment of tendon progenitors', *Cell* 113(2): 235-48.

Cambray, N. and Wilson, V. (2007) 'Two distinct sources for a population of maturing axial progenitors', *Development* 134(15): 2829-40.

Capdevila, J. and Johnson, R. L. (1998) 'Endogenous and ectopic expression of noggin suggests a conserved mechanism for regulation of BMP function during limb and somite patterning', *Dev Biol* 197(2): 205-17.

Capdevila, J., Tsukui, T., Rodriquez Esteban, C., Zappavigna, V. and Izpisua Belmonte, J. C. (1999) 'Control of vertebrate limb outgrowth by the proximal factor Meis2 and distal antagonism of BMPs by Gremlin', *Mol Cell* 4(5): 839-49.

Capellini, T. D., Di Giacomo, G., Salsi, V., Brendolan, A., Ferretti, E., Srivastava, D., Zappavigna, V. and Selleri, L. (2006) 'Pbx1/Pbx2 requirement for distal limb patterning is mediated by the hierarchical control of Hox gene spatial distribution and Shh expression', *Development* 133(11): 2263-73.

Caprioli, A., Goitsuka, R., Pouget, C., Dunon, D. and Jaffredo, T. (2002) 'Expression of Notch genes and their ligands during gastrulation in the chicken embryo', *Mech Dev* 116(1-2): 161-4.

Carpenter, D., Stone, D. M., Brush, J., Ryan, A., Armanini, M., Frantz, G., Rosenthal, A. and de Sauvage, F. J. (1998) 'Characterization of two patched receptors for the vertebrate hedgehog protein family', *Proc Natl Acad Sci U S A* 95(23): 13630-4.

Catala, M., Teillet, M. A. and Le Douarin, N. M. (1995) 'Organization and development of the tail bud analyzed with the quail-chick chimaera system', *Mech Dev* 51(1): 51-65.

Celli, G., LaRochelle, W. J., Mackem, S., Sharp, R. and Merlino, G. (1998) 'Soluble dominant-negative receptor uncovers essential roles for fibroblast growth factors in multi-organ induction and patterning', *EMBO J* 17(6): 1642-55.

Charite, J., McFadden, D. G. and Olson, E. N. (2000) 'The bHLH transcription factor dHAND controls Sonic hedgehog expression and establishment of the zone of polarizing activity during limb development', *Development* 127(11): 2461-70.

Chen, H. and Johnson, R. L. (1999) 'Dorsoventral patterning of the vertebrate limb: a process governed by multiple events', *Cell Tissue Res* 296(1): 67-73.

Chen, H. and Johnson, R. L. (2002) 'Interactions between dorsal-ventral patterning genes lmx1b, engrailed-1 and wnt-7a in the vertebrate limb', *Int J Dev Biol* 46(7): 937-41.

Chen, H., Lun, Y., Ovchinnikov, D., Kokubo, H., Oberg, K. C., Pepicelli, C. V., Gan, L., Lee, B. and Johnson, R. L. (1998) 'Limb and kidney defects in Lmx1b mutant mice suggest an involvement of LMX1B in human nail patella syndrome', *Nat Genet* 19(1): 51-5.

Chen, J., Kang, L. and Zhang, N. (2005) 'Negative feedback loop formed by Lunatic fringe and Hes7 controls their oscillatory expression during somitogenesis', *Genesis* 43(4): 196-204.

Chen, M. H., Li, Y. J., Kawakami, T., Xu, S. M. and Chuang, P. T. (2004) 'Palmitoylation is required for the production of a soluble multimeric Hedgehog protein complex and long-range signaling in vertebrates', *Genes Dev* 18(6): 641-59.

Chiang, C., Litingtung, Y., Harris, M. P., Simandl, B. K., Li, Y., Beachy, P. A. and Fallon, J. F. (2001) 'Manifestation of the limb prepattern: limb development in the absence of sonic hedgehog function', *Dev Biol* 236(2): 421-35.

Chiang, C., Litingtung, Y., Lee, E., Young, K. E., Corden, J. L., Westphal, H. and Beachy, P. A. (1996) 'Cyclopia and defective axial patterning in mice lacking Sonic hedgehog gene function', *Nature* 383(6599): 407-13.

Christ, B. and Ordahl, C. P. (1995) 'Early stages of chick somite development', *Anat Embryol (Berl)* 191(5): 381-96.

Christ, B., Schmidt, C., Huang, R., Wilting, J. and Brand-Saberi, B. (1998) 'Segmentation of the vertebrate body', *Anat Embryol (Berl)* 197(1): 1-8.

Chuai, M., Zeng, W., Yang, X., Boychenko, V., Glazier, J. A. and Weijer, C. J. (2006) 'Cell movement during chick primitive streak formation', *Dev Biol* 296(1): 137-49.

Church, V. L. and Francis-West, P. (2002) 'Wnt signalling during limb development', *Int J Dev Biol* 46(7): 927-36.

Ciruna, B. and Rossant, J. (2001) 'FGF signaling regulates mesoderm cell fate specification and morphogenetic movement at the primitive streak', *Dev Cell* 1(1): 37-49.

Ciruna, B. G., Schwartz, L., Harpal, K., Yamaguchi, T. P. and Rossant, J. (1997) 'Chimeric analysis of fibroblast growth factor receptor-1 (Fgfr1) function: a role for FGFR1 in morphogenetic movement through the primitive streak', *Development* 124(14): 2829-41.

Cohn, M. J., Izpisua-Belmonte, J. C., Abud, H., Heath, J. K. and Tickle, C. (1995) 'Fibroblast growth factors induce additional limb development from the flank of chick embryos', *Cell* 80(5): 739-46.

Cole, S. E., Levorse, J. M., Tilghman, S. M. and Vogt, T. F. (2002) 'Clock regulatory elements control cyclic expression of Lunatic fringe during somitogenesis', *Dev Cell* 3(1): 75-84.

Colvin, J. S., White, A. C., Pratt, S. J. and Ornitz, D. M. (2001) 'Lung hypoplasia and neonatal death in Fgf9-null mice identify this gene as an essential regulator of lung mesenchyme', *Development* 128(11): 2095-106.

Cooper, K. L., Hu, J. K., ten Berge, D., Fernandez-Teran, M., Ros, M. A. and Tabin, C. J. (2011) 'Initiation of proximal-distal patterning in the vertebrate limb by signals and growth', *Science* 332(6033): 1083-6.

Cordes, R., Schuster-Gossler, K., Serth, K. and Gossler, A. (2004) 'Specification of vertebral identity is coupled to Notch signalling and the segmentation clock', *Development* 131(6): 1221-33.

Corson, L. B., Yamanaka, Y., Lai, K. M. and Rossant, J. (2003) 'Spatial and temporal patterns of ERK signaling during mouse embryogenesis', *Development* 130(19): 4527-37.

Coumoul, X., Shukla, V., Li, C., Wang, R. H. and Deng, C. X. (2005) 'Conditional knockdown of Fgfr2 in mice using Cre-LoxP induced RNA interference', *Nucleic Acids Res* 33(11): e102.

Crossley, P. H. and Martin, G. R. (1995) 'The mouse Fgf8 gene encodes a family of polypeptides and is expressed in regions that direct outgrowth and patterning in the developing embryo', *Development* 121(2): 439-51.

Crossley, P. H., Minowada, G., MacArthur, C. A. and Martin, G. R. (1996) 'Roles for FGF8 in the induction, initiation, and maintenance of chick limb development', *Cell* 84(1): 127-36.

Curry, C. L., Reed, L. L., Nickoloff, B. J., Miele, L. and Foreman, K. E. (2006) 'Notch-independent regulation of Hes-1 expression by c-Jun N-terminal kinase signaling in human endothelial cells', *Lab Invest* 86(8): 842-52.

Dahn, R. D. and Fallon, J. F. (2000) 'Interdigital regulation of digit identity and homeotic transformation by modulated BMP signaling', *Science* 289(5478): 438-41.

Dailey, L., Ambrosetti, D., Mansukhani, A. and Basilico, C. (2005) 'Mechanisms underlying differential responses to FGF signaling', *Cytokine Growth Factor Rev* 16(2): 233-47.

Dale, J. K., Malapert, P., Chal, J., Vilhais-Neto, G., Maroto, M., Johnson, T., Jayasinghe, S., Trainor, P., Herrmann, B. and Pourquie, O. (2006) 'Oscillations of the snail genes in the presomitic mesoderm coordinate segmental patterning and morphogenesis in vertebrate somitogenesis', *Dev Cell* 10(3): 355-66.

Dale, J. K., Maroto, M., Dequeant, M. L., Malapert, P., McGrew, M. and Pourquie, O. (2003) 'Periodic notch inhibition by lunatic fringe underlies the chick segmentation clock', *Nature* 421(6920): 275-8.

Davis, C. A. and Joyner, A. L. (1988) 'Expression patterns of the homeo box-containing genes En-1 and En-2 and the proto-oncogene int-1 diverge during mouse development', *Genes Dev* 2(12B): 1736-44.

Davis, R. L., Turner, D. L., Evans, L. M. and Kirschner, M. W. (2001) 'Molecular targets of vertebrate segmentation: two mechanisms control segmental expression of Xenopus hairy2 during somite formation', *Dev Cell* 1(4): 553-65.

Delaurier, A., Burton, N., Bennett, M., Baldock, R., Davidson, D., Mohun, T. J. and Logan, M. P. (2008) 'The Mouse Limb Anatomy Atlas: an interactive 3D tool for studying embryonic limb patterning', *BMC Dev Biol* 8: 83.

Delfini, M. C., Dubrulle, J., Malapert, P., Chal, J. and Pourquie, O. (2005) 'Control of the segmentation process by graded MAPK/ERK activation in the chick embryo', *Proc Natl Acad Sci U S A* 102(32): 11343-8.

Deng, C., Bedford, M., Li, C., Xu, X., Yang, X., Dunmore, J. and Leder, P. (1997) 'Fibroblast growth factor receptor-1 (FGFR-1) is essential for normal neural tube and limb development', *Dev Biol* 185(1): 42-54.

Dequeant, M. L., Glynn, E., Gaudenz, K., Wahl, M., Chen, J., Mushegian, A. and Pourquie, O. (2006) 'A complex oscillating network of signaling genes underlies the mouse segmentation clock', *Science* 314(5805): 1595-8.

Dequeant, M. L. and Pourquie, O. (2008) 'Segmental patterning of the vertebrate embryonic axis', *Nat Rev Genet* 9(5): 370-82.

Diez del Corral, R., Olivera-Martinez, I., Goriely, A., Gale, E., Maden, M. and Storey, K. (2003) 'Opposing FGF and retinoid pathways control ventral neural pattern, neuronal differentiation, and segmentation during body axis extension', *Neuron* 40(1): 65-79.

Doetzlhofer, A., Basch, M. L., Ohyama, T., Gessler, M., Groves, A. K. and Segil, N. (2009) 'Hey2 regulation by FGF provides a Notch-independent mechanism for maintaining pillar cell fate in the organ of Corti', *Dev Cell* 16(1): 58-69.

Dong, Y., Jesse, A. M., Kohn, A., Gunnell, L. M., Honjo, T., Zuscik, M. J., O'Keefe, R. J. and Hilton, M. J. (2010) 'RBPjkappa-dependent Notch signaling regulates mesenchymal progenitor cell proliferation and differentiation during skeletal development', *Development* 137(9): 1461-71.

Drossopoulou, G., Lewis, K. E., Sanz-Ezquerro, J. J., Nikbakht, N., McMahon, A. P., Hofmann, C. and Tickle, C. (2000) 'A model for anteroposterior patterning of the vertebrate limb based on sequential long- and short-range Shh signalling and Bmp signalling', *Development* 127(7): 1337-48.

Duboc, V. and Logan, M. P. (2011) 'Regulation of limb bud initiation and limb-type morphology', *Dev Dyn* 240(5): 1017-27.

Dubrulle, J., McGrew, M. J. and Pourquie, O. (2001) 'FGF signaling controls somite boundary position and regulates segmentation clock control of spatiotemporal Hox gene activation', *Cell* 106(2): 219-32.

Dubrulle, J. and Pourquie, O. (2004a) 'Coupling segmentation to axis formation', *Development* 131(23): 5783-93.

Dubrulle, J. and Pourquie, O. (2004b) 'fgf8 mRNA decay establishes a gradient that couples axial elongation to patterning in the vertebrate embryo', *Nature* 427(6973): 419-22.

Dudley, A. T., Ros, M. A. and Tabin, C. J. (2002) 'A re-examination of proximodistal patterning during vertebrate limb development', *Nature* 418(6897): 539-44.

Dunty, W. C., Jr., Biris, K. K., Chalamalasetty, R. B., Taketo, M. M., Lewandoski, M. and Yamaguchi, T. P. (2008) 'Wnt3a/beta-catenin signaling controls posterior body development by coordinating mesoderm formation and segmentation', *Development* 135(1): 85-94.

Dupe, V., Ghyselinck, N. B., Thomazy, V., Nagy, L., Davies, P. J., Chambon, P. and Mark, M. (1999) 'Essential roles of retinoic acid signaling in interdigital apoptosis and control of BMP-7 expression in mouse autopods', *Dev Biol* 208(1): 30-43.

Duprez, D., Fournier-Thibault, C. and Le Douarin, N. (1998) 'Sonic Hedgehog induces proliferation of committed skeletal muscle cells in the chick limb', *Development* 125(3): 495-505.

Eloy-Trinquet, S., Wang, H., Edom-Vovard, F. and Duprez, D. (2009) 'Fgf signaling components are associated with muscles and tendons during limb development', *Dev Dyn* 238(5): 1195-206.

Eswarakumar, V. P., Lax, I. and Schlessinger, J. (2005) 'Cellular signaling by fibroblast growth factor receptors', *Cytokine Growth Factor Rev* 16(2): 139-49.

Evrard, Y. A., Lun, Y., Aulehla, A., Gan, L. and Johnson, R. L. (1998) 'lunatic fringe is an essential mediator of somite segmentation and patterning', *Nature* 394(6691): 377-81.

Fallon, J. F., Lopez, A., Ros, M. A., Savage, M. P., Olwin, B. B. and Simandl, B. K. (1994) 'FGF-2: apical ectodermal ridge growth signal for chick limb development', *Science* 264(5155): 104-7.

Feller, J., Schneider, A., Schuster-Gossler, K. and Gossler, A. (2008) 'Noncyclic Notch activity in the presomitic mesoderm demonstrates uncoupling of somite compartmentalization and boundary formation', *Genes Dev* 22(16): 2166-71.

Ferjentsik, Z., Hayashi, S., Dale, J. K., Bessho, Y., Herreman, A., De Strooper, B., del Monte, G., de la Pompa, J. L. and Maroto, M. (2009) 'Notch is a critical component of the mouse somitogenesis oscillator and is essential for the formation of the somites', *PLoS Genet* 5(9): e1000662.

Fernandez-Teran, M. and Ros, M. A. (2008) 'The Apical Ectodermal Ridge: morphological aspects and signaling pathways', *Int J Dev Biol* 52(7): 857-71.

Fisher, A. and Caudy, M. (1998) 'The function of hairy-related bHLH repressor proteins in cell fate decisions', *Bioessays* 20(4): 298-306.

Fortini, M. E. (2002) 'Gamma-secretase-mediated proteolysis in cell-surface-receptor signalling', *Nat Rev Mol Cell Biol* 3(9): 673-84.

Francis-West, P. and Hill, R. (2008) 'Uncoupling the role of sonic hedgehog in limb development: growth and specification', *Sci Signal* 1(26): pe34.

Freitas, C., Rodrigues, S., Charrier, J. B., Teillet, M. A. and Palmeirim, I. (2001) 'Evidence for medial/lateral specification and positional information within the presomitic mesoderm', *Development* 128(24): 5139-47.

Galceran, J., Farinas, I., Depew, M. J., Clevers, H. and Grosschedl, R. (1999) 'Wnt3a-/--like phenotype and limb deficiency in Lef1(-/-)Tcf1(-/-) mice', *Genes Dev* 13(6): 709-17.

Galli, A., Robay, D., Osterwalder, M., Bao, X., Benazet, J. D., Tariq, M., Paro, R., Mackem, S. and Zeller, R. (2010) 'Distinct roles of Hand2 in initiating polarity and posterior Shh expression during the onset of mouse limb bud development', *PLoS Genet* 6(4): e1000901.

Galloway, J. L., Delgado, I., Ros, M. A. and Tabin, C. J. (2009) 'A reevaluation of X-irradiation-induced phocomelia and proximodistal limb patterning', *Nature* 460(7253): 400-4.

Galloway, J. L. and Tabin, C. J. (2008) 'Classic limb patterning models and the work of Dennis Summerbell', *Development* 135(16): 2683-7.

Ganan, Y., Macias, D., Basco, R. D., Merino, R. and Hurle, J. M. (1998) 'Morphological diversity of the avian foot is related with the pattern of msx gene expression in the developing autopod', *Dev Biol* 196(1): 33-41.

Garcia-Martinez, V., Darnell, D. K., Lopez-Sanchez, C., Sosic, D., Olson, E. N. and Schoenwolf, G. C. (1997) 'State of commitment of prospective neural plate and prospective mesoderm in late gastrula/early neurula stages of avian embryos', *Dev Biol* 181(1): 102-15.

Geduspan, J. S. and Solursh, M. (1992) 'A growth-promoting influence from the mesonephros during limb outgrowth', *Dev Biol* 151(1): 242-50.

Geetha-Loganathan, P., Nimmagadda, S., Huang, R., Scaal, M. and Christ, B. (2006) 'Expression pattern of BMPs during chick limb development', *Anat Embryol (Berl)* 211 Suppl 1: 87-93.

Gibb, S., Zagorska, A., Melton, K., Tenin, G., Vacca, I., Trainor, P., Maroto, M. and Dale, J. K. (2009) 'Interfering with Wnt signalling alters the periodicity of the segmentation clock', *Dev Biol* 330(1): 21-31.

Gibert, Y., Gajewski, A., Meyer, A. and Begemann, G. (2006) 'Induction and prepatterning of the zebrafish pectoral fin bud requires axial retinoic acid signaling', *Development* 133(14): 2649-59.

Gibson-Brown, J. J., S, I. A., Silver, L. M. and Papaioannou, V. E. (1998) 'Expression of T-box genes Tbx2-Tbx5 during chick organogenesis', *Mech Dev* 74(1-2): 165-9.

Giudicelli, F., Ozbudak, E. M., Wright, G. J. and Lewis, J. (2007) 'Setting the tempo in development: an investigation of the zebrafish somite clock mechanism', *PLoS Biol* 5(6): e150.

Globus, M. and Vethamany-Globus, S. (1976) 'An in vitro analogue of early chick limb bud outgrowth', *Differentiation* 6(2): 91-6.

Goyette, P., Allan, D., Peschard, P., Chen, C. F., Wang, W. and Lohnes, D. (2000) 'Regulation of gli activity by all-trans retinoic acid in mouse keratinocytes', *Cancer Res* 60(19): 5386-9.

Grandel, H. and Brand, M. (2010) 'Zebrafish limb development is triggered by a retinoic acid signal during gastrulation', *Dev Dyn*.

Grandel, H., Lun, K., Rauch, G. J., Rhinn, M., Piotrowski, T., Houart, C., Sordino, P., Kuchler, A. M., Schulte-Merker, S., Geisler, R. et al. (2002) 'Retinoic acid signalling in the zebrafish embryo is necessary during pre-segmentation stages to pattern the anterior-posterior axis of the CNS and to induce a pectoral fin bud', *Development* 129(12): 2851-65.

Gros, J., Feistel, K., Viebahn, C., Blum, M. and Tabin, C. J. (2009) 'Cell movements at Hensen's node establish left/right asymmetric gene expression in the chick', *Science* 324(5929): 941-4.

Grzeschik, K. H. (2002) 'Human limb malformations; an approach to the molecular basis of development', *Int J Dev Biol* 46(7): 983-91.

Guo, Q., Loomis, C. and Joyner, A. L. (2003) 'Fate map of mouse ventral limb ectoderm and the apical ectodermal ridge', *Dev Biol* 264(1): 166-78.

Hamburger, V. and Hamilton, H. L. (1951) 'A series of normal stages in the development of the chick embryo', *Dev. Dyn.* 195: 231-72.

Hamburger, V. and Hamilton, H. L. (1992) 'A series of normal stages in the development of the chick embryo. 1951', *Dev Dyn* 195(4): 231-72.

Harfe, B. D. (2011) 'Keeping up with the zone of polarizing activity: New roles for an old signaling center', *Dev Dyn* 240(5): 915-9.

Harfe, B. D., Scherz, P. J., Nissim, S., Tian, H., McMahon, A. P. and Tabin, C. J. (2004) 'Evidence for an expansion-based temporal Shh gradient in specifying vertebrate digit identities', *Cell* 118(4): 517-28.

Hasson, P., Del Buono, J. and Logan, M. P. (2007) 'Tbx5 is dispensable for forelimb outgrowth', *Development* 134(1): 85-92.

Hasson, P., DeLaurier, A., Bennett, M., Grigorieva, E., Naiche, L. A., Papaioannou, V. E., Mohun, T. J. and Logan, M. P. (2010) 'Tbx4 and tbx5 acting in connective tissue are required for limb muscle and tendon patterning', *Dev Cell* 18(1): 148-56.

Havens, B. A., Rodgers, B. and Mina, M. (2006) 'Tissue-specific expression of Fgfr2b and Fgfr2c isoforms, Fgf10 and Fgf9 in the developing chick mandible', *Arch Oral Biol* 51(2): 134-45.

Hawke, T. J. and Garry, D. J. (2001) 'Myogenic satellite cells: physiology to molecular biology', *J Appl Physiol* 91(2): 534-51.

Hayashi, S. and McMahon, A. P. (2002) 'Efficient recombination in diverse tissues by a tamoxifen-inducible form of Cre: a tool for temporally regulated gene activation/inactivation in the mouse', *Dev Biol* 244(2): 305-18.

Helms, J. A., Kim, C. H., Eichele, G. and Thaller, C. (1996) 'Retinoic acid signaling is required during early chick limb development', *Development* 122(5): 1385-94.

Henrique, D., Adam, J., Myat, A., Chitnis, A., Lewis, J. and Ish-Horowicz, D. (1995) 'Expression of a Delta homologue in prospective neurons in the chick', *Nature* 375(6534): 787-90.

Hernandez-Martinez, R., Castro-Obregon, S. and Covarrubias, L. (2009) 'Progressive interdigital cell death: regulation by the antagonistic interaction between fibroblast growth factor 8 and retinoic acid', *Development* 136(21): 3669-78.

Herrgen, L., Ares, S., Morelli, L. G., Schroter, C., Julicher, F. and Oates, A. C. (2010) 'Intercellular coupling regulates the period of the segmentation clock', *Curr Biol* 20(14): 1244-53.

Hill, T. P., Taketo, M. M., Birchmeier, W. and Hartmann, C. (2006) 'Multiple roles of mesenchymal beta-catenin during murine limb patterning', *Development* 133(7): 1219-29.

Hirata, H., Bessho, Y., Kokubu, H., Masamizu, Y., Yamada, S., Lewis, J. and Kageyama, R. (2004) 'Instability of Hes7 protein is crucial for the somite segmentation clock', *Nat Genet* 36(7): 750-4.

Hirata, H., Yoshiura, S., Ohtsuka, T., Bessho, Y., Harada, T., Yoshikawa, K. and Kageyama, R. (2002) 'Oscillatory expression of the bHLH factor Hes1 regulated by a negative feedback loop', *Science* 298(5594): 840-3.

Horikawa, K., Ishimatsu, K., Yoshimoto, E., Kondo, S. and Takeda, H. (2006) 'Noise-resistant and synchronized oscillation of the segmentation clock', *Nature* 441(7094): 719-23.

Hornik, C., Brand-Saberi, B., Rudloff, S., Christ, B. and Fuchtbauer, E. M. (2004) 'Twist is an integrator of SHH, FGF, and BMP signaling', *Anat Embryol (Berl)* 209(1): 31-9.

Hui, C. C. and Joyner, A. L. (1993) 'A mouse model of greig cephalopolysyndactyly syndrome: the extra-toesJ mutation contains an intragenic deletion of the Gli3 gene', *Nat Genet* 3(3): 241-6.

Iimura, T., Yang, X., Weijer, C. J. and Pourquie, O. (2007) 'Dual mode of paraxial mesoderm formation during chick gastrulation', *Proc Natl Acad Sci U S A* 104(8): 2744-9.

Ingram, W. J., McCue, K. I., Tran, T. H., Hallahan, A. R. and Wainwright, B. J. (2008) 'Sonic Hedgehog regulates Hes1 through a novel mechanism that is independent of canonical Notch pathway signalling', *Oncogene* 27(10): 1489-500.

Isaac, A., Rodriguez-Esteban, C., Ryan, A., Altabef, M., Tsukui, T., Patel, K., Tickle, C. and Izpisua-Belmonte, J. C. (1998) 'Tbx genes and limb identity in chick embryo development', *Development* 125(10): 1867-75.

Ishikawa, A., Kitajima, S., Takahashi, Y., Kokubo, H., Kanno, J., Inoue, T. and Saga, Y. (2004) 'Mouse Nkd1, a Wnt antagonist, exhibits oscillatory gene expression in the PSM under the control of Notch signaling', *Mech Dev* 121(12): 1443-53.

Itoh, N. and Ornitz, D. M. (2008) 'Functional evolutionary history of the mouse Fgf gene family', *Dev Dyn* 237(1): 18-27.

Jiang, Y. J., Aerne, B. L., Smithers, L., Haddon, C., Ish-Horowicz, D. and Lewis, J. (2000) 'Notch signalling and the synchronization of the somite segmentation clock', *Nature* 408(6811): 475-9.

Jouve, C., Palmeirim, I., Henrique, D., Beckers, J., Gossler, A., Ish-Horowicz, D. and Pourquie, O. (2000) 'Notch signalling is required for cyclic expression of the hairy-like gene HES1 in the presomitic mesoderm', *Development* 127(7): 1421-9.

Kageyama, R., Ohtsuka, T. and Kobayashi, T. (2007) 'The Hes gene family: repressors and oscillators that orchestrate embryogenesis', *Development* 134(7): 1243-51.

Kamakura, S., Oishi, K., Yoshimatsu, T., Nakafuku, M., Masuyama, N. and Gotoh, Y. (2004) 'Hes binding to STAT3 mediates crosstalk between Notch and JAK-STAT signalling', *Nat Cell Biol* 6(6): 547-54.

Kawakami, Y., Capdevila, J., Buscher, D., Itoh, T., Rodriguez Esteban, C. and Izpisua Belmonte, J. C. (2001) 'WNT signals control FGF-dependent limb initiation and AER induction in the chick embryo', *Cell* 104(6): 891-900.

Kawakami, Y., Ishikawa, T., Shimabara, M., Tanda, N., Enomoto-Iwamoto, M., Iwamoto, M., Kuwana, T., Ueki, A., Noji, S. and Nohno, T. (1996) 'BMP signaling during bone pattern determination in the developing limb', *Development* 122(11): 3557-66.

Kawakami, Y., Rodriguez-Leon, J., Koth, C. M., Buscher, D., Itoh, T., Raya, A., Ng, J. K., Esteban, C. R., Takahashi, S., Henrique, D. et al. (2003) 'MKP3 mediates the cellular response to FGF8 signalling in the vertebrate limb', *Nat Cell Biol* 5(6): 513-9.

Kawamura, A., Koshida, S., Hijikata, H., Sakaguchi, T., Kondoh, H. and Takada, S. (2005) 'Zebrafish hairy/enhancer of split protein links FGF signaling to cyclic gene expression in the periodic segmentation of somites', *Genes Dev* 19(10): 1156-61.

Kengaku, M., Capdevila, J., Rodriguez-Esteban, C., De La Pena, J., Johnson, R. L., Izpisua Belmonte, J. C. and Tabin, C. J. (1998) 'Distinct WNT pathways regulating AER formation and dorsoventral polarity in the chick limb bud', *Science* 280(5367): 1274-7.

Kengaku, M., Twombly, V. and Tabin, C. (1997) 'Expression of Wnt and Frizzled genes during chick limb bud development', *Cold Spring Harb Symp Quant Biol* 62: 421-9.

Kikuchi, A. (2000) 'Regulation of beta-catenin signaling in the Wnt pathway', *Biochem Biophys Res Commun* 268(2): 243-8.

Kimmel, R. A., Turnbull, D. H., Blanquet, V., Wurst, W., Loomis, C. A. and Joyner, A. L. (2000) 'Two lineage boundaries coordinate vertebrate apical ectodermal ridge formation', *Genes Dev* 14(11): 1377-89.

Kling, D. E., Lorenzo, H. K., Trbovich, A. M., Kinane, T. B., Donahoe, P. K. and Schnitzer, J. J. (2002) 'MEK-1/2 inhibition reduces branching morphogenesis and causes mesenchymal cell apoptosis in fetal rat lungs', *Am J Physiol Lung Cell Mol Physiol* 282(3): L370-8.

Kmita, M., Tarchini, B., Zakany, J., Logan, M., Tabin, C. J. and Duboule, D. (2005) 'Early developmental arrest of mammalian limbs lacking HoxA/HoxD gene function', *Nature* 435(7045): 1113-6.

Knobloch, J., Shaughnessy, J. D., Jr. and Ruther, U. (2007) 'Thalidomide induces limb deformities by perturbing the Bmp/Dkk1/Wnt signaling pathway', *FASEB J* 21(7): 1410-21.

Kobayashi, T., Mizuno, H., Imayoshi, I., Furusawa, C., Shirahige, K. and Kageyama, R. (2009) 'The cyclic gene Hes1 contributes to diverse differentiation responses of embryonic stem cells', *Genes Dev* 23(16): 1870-5.

Kraus, P., Fraidenraich, D. and Loomis, C. A. (2001) 'Some distal limb structures develop in mice lacking Sonic hedgehog signaling', *Mech Dev* 100(1): 45-58.

Krol, A. J., Roellig, D., Dequeant, M. L., Tassy, O., Glynn, E., Hattem, G., Mushegian, A., Oates, A. C. and Pourquie, O. (2011) 'Evolutionary plasticity of segmentation clock networks', *Development* 138(13): 2783-92.

Kuhl, M., Sheldahl, L. C., Park, M., Miller, J. R. and Moon, R. T. (2000) 'The Wnt/Ca2+ pathway: a new vertebrate Wnt signaling pathway takes shape', *Trends Genet* 16(7): 279-83.

Lallemand, Y., Bensoussan, V., Cloment, C. S. and Robert, B. (2009) 'Msx genes are important apoptosis effectors downstream of the Shh/Gli3 pathway in the limb', *Dev Biol* 331(2): 189-98.

Lallemand, Y., Nicola, M. A., Ramos, C., Bach, A., Cloment, C. S. and Robert, B. (2005) 'Analysis of Msx1; Msx2 double mutants reveals multiple roles for Msx genes in limb development', *Development* 132(13): 3003-14.

Laufer, E., Dahn, R., Orozco, O. E., Yeo, C. Y., Pisenti, J., Henrique, D., Abbott, U. K., Fallon, J. F. and Tabin, C. (1997) 'Expression of Radical fringe in limb-bud ectoderm regulates apical ectodermal ridge formation', *Nature* 386(6623): 366-73.

Laufer, E., Nelson, C. E., Johnson, R. L., Morgan, B. A. and Tabin, C. (1994) 'Sonic hedgehog and Fgf-4 act through a signaling cascade and feedback loop to integrate growth and patterning of the developing limb bud', *Cell* 79(6): 993-1003.

Lee, J. S., Park, J. H., Kwon, I. K. and Lim, J. Y. (2011) 'Retinoic acid inhibits BMP4-induced C3H10T1/2 stem cell commitment to adipocyte via downregulating Smad/p38MAPK signaling', *Biochem Biophys Res Commun* 409(3): 550-5.

Lettice, L. A., Heaney, S. J., Purdie, L. A., Li, L., de Beer, P., Oostra, B. A., Goode, D., Elgar, G., Hill, R. E. and de Graaff, E. (2003) 'A long-range Shh enhancer regulates expression in the developing limb and fin and is associated with preaxial polydactyly', *Hum Mol Genet* 12(14): 1725-35.

Levin, M. (2005) 'Left-right asymmetry in embryonic development: a comprehensive review', *Mech Dev* 122(1): 3-25.

Lewandoski, M. and Mackem, S. (2009) 'Limb development: the rise and fall of retinoic acid', *Curr Biol* 19(14): R558-61.

Lewandoski, M., Sun, X. and Martin, G. R. (2000) 'Fgf8 signalling from the AER is essential for normal limb development', *Nat Genet* 26(4): 460-3.

Li, C., Xu, X., Nelson, D. K., Williams, T., Kuehn, M. R. and Deng, C. X. (2005) 'FGFR1 function at the earliest stages of mouse limb development plays an indispensable role in subsequent autopod morphogenesis', *Development* 132(21): 4755-64.

Li, S. and Muneoka, K. (1999) 'Cell migration and chick limb development: chemotactic action of FGF-4 and the AER', *Dev Biol* 211(2): 335-47.

Li, Y., Zhang, H., Litingtung, Y. and Chiang, C. (2006) 'Cholesterol modification restricts the spread of Shh gradient in the limb bud', *Proc Natl Acad Sci U S A* 103(17): 6548-53.

Litingtung, Y., Dahn, R. D., Li, Y., Fallon, J. F. and Chiang, C. (2002) 'Shh and Gli3 are dispensable for limb skeleton formation but regulate digit number and identity', *Nature* 418(6901): 979-83.

Liu, N., Barbosa, A. C., Chapman, S. L., Bezprozvannaya, S., Qi, X., Richardson, J. A., Yanagisawa, H. and Olson, E. N. (2009) 'DNA binding-dependent and -independent functions of the Hand2 transcription factor during mouse embryogenesis', *Development* 136(6): 933-42.

Lizarraga, G., Ferrari, D., Kalinowski, M., Ohuchi, H., Noji, S., Kosher, R. A. and Dealy, C. N. (1999) 'FGFR2 signaling in normal and limbless chick limb buds', *Dev Genet* 25(4): 331-8.

Logan, M., Simon, H. G. and Tabin, C. (1998) 'Differential regulation of T-box and homeobox transcription factors suggests roles in controlling chick limb-type identity', *Development* 125(15): 2825-35.

Logan, M. and Tabin, C. (1998) 'Targeted gene misexpression in chick limb buds using avian replication-competent retroviruses', *Methods* 14(4): 407-20.

Logan, M. and Tabin, C. J. (1999) 'Role of Pitx1 upstream of Tbx4 in specification of hindlimb identity', *Science* 283(5408): 1736-9.

Loganathan, P. G., Nimmagadda, S., Huang, R., Scaal, M. and Christ, B. (2005) 'Comparative analysis of the expression patterns of Wnts during chick limb development', *Histochem Cell Biol* 123(2): 195-201.

Loomis, C. A., Harris, E., Michaud, J., Wurst, W., Hanks, M. and Joyner, A. L. (1996) 'The mouse Engrailed-1 gene and ventral limb patterning', *Nature* 382(6589): 360-3.

Loomis, C. A., Kimmel, R. A., Tong, C. X., Michaud, J. and Joyner, A. L. (1998) 'Analysis of the genetic pathway leading to formation of ectopic apical ectodermal ridges in mouse Engrailed-1 mutant limbs', *Development* 125(6): 1137-48.

Lu, P., Yu, Y., Perdue, Y. and Werb, Z. (2008) 'The apical ectodermal ridge is a timer for generating distal limb progenitors', *Development* 135(8): 1395-405.

Luo, G., Hofmann, C., Bronckers, A. L., Sohocki, M., Bradley, A. and Karsenty, G. (1995) 'BMP-7 is an inducer of nephrogenesis, and is also required for eye development and skeletal patterning', *Genes Dev* 9(22): 2808-20.

Lussier, M., Canoun, C., Ma, C., Sank, A. and Shuler, C. (1993) 'Interdigital soft tissue separation induced by retinoic acid in mouse limbs cultured in vitro', *Int J Dev Biol* 37(4): 555-64.

MacCabe, J. A., Errick, J. and Saunders, J. W., Jr. (1974) 'Ectodermal control of the dorsoventral axis in the leg bud of the chick embryo', *Dev Biol* 39(1): 69-82.

Mackem, S. and Lewandoski, M. (2011) 'Development. Limb cells don't tell time', *Science* 332(6033): 1038-9.

MacLean, G., Abu-Abed, S., Dolle, P., Tahayato, A., Chambon, P. and Petkovich, M. (2001) 'Cloning of a novel retinoic-acid metabolizing cytochrome P450, Cyp26B1, and comparative expression analysis with Cyp26A1 during early murine development', *Mech Dev* 107(1-2): 195-201.

Maden, M. (1982) 'Vitamin A and pattern formation in the regenerating limb', *Nature* 295(5851): 672-5.

Mahmood, R., Bresnick, J., Hornbruch, A., Mahony, C., Morton, N., Colquhoun, K., Martin, P., Lumsden, A., Dickson, C. and Mason, I. (1995) 'A role for FGF-8 in the initiation and maintenance of vertebrate limb bud outgrowth', *Curr Biol* 5(7): 797-806.

Mann, R. K. and Beachy, P. A. (2004) 'Novel lipid modifications of secreted protein signals', *Annu Rev Biochem* 73: 891-923.

Marcelle, C., Wolf, J. and Bronner-Fraser, M. (1995) 'The in vivo expression of the FGF receptor FREK mRNA in avian myoblasts suggests a role in muscle growth and differentiation', *Dev Biol* 172(1): 100-14.

Marcil, A., Dumontier, E., Chamberland, M., Camper, S. A. and Drouin, J. (2003) 'Pitx1 and Pitx2 are required for development of hindlimb buds', *Development* 130(1): 45-55.

Mariani, F. V., Ahn, C. P. and Martin, G. R. (2008) 'Genetic evidence that FGFs have an instructive role in limb proximal-distal patterning', *Nature* 453(7193): 401-5.

Marigo, V., Johnson, R. L., Vortkamp, A. and Tabin, C. J. (1996) 'Sonic hedgehog differentially regulates expression of GLI and GLI3 during limb development', *Dev Biol* 180(1): 273-83.

Marigo, V. and Tabin, C. J. (1996) 'Regulation of patched by sonic hedgehog in the developing neural tube', *Proc Natl Acad Sci U S A* 93(18): 9346-51.

Marklund, U., Hansson, E. M., Sundstrom, E., de Angelis, M. H., Przemeck, G. K., Lendahl, U., Muhr, J. and Ericson, J. (2010) 'Domain-specific control of neurogenesis achieved through patterned regulation of Notch ligand expression', *Development* 137(3): 437-45.

Maroto, M., Dale, J. K., Dequeant, M. L., Petit, A. C. and Pourquie, O. (2005) 'Synchronised cycling gene oscillations in presomitic mesoderm cells require cell-cell contact', *Int J Dev Biol* 49(2-3): 309-15.

Martin, G. R. (1998) 'The roles of FGFs in the early development of vertebrate limbs', *Genes Dev* 12(11): 1571-86.

Martins, G. G., Rifes, P., Amandio, R., Rodrigues, G., Palmeirim, I. and Thorsteinsdottir, S. (2009) 'Dynamic 3D cell rearrangements guided by a fibronectin matrix underlie somitogenesis', *PLoS One* 4(10): e7429.

Masamizu, Y., Ohtsuka, T., Takashima, Y., Nagahara, H., Takenaka, Y., Yoshikawa, K., Okamura, H. and Kageyama, R. (2006) 'Real-time imaging of the somite segmentation clock: revelation of unstable oscillators in the individual presomitic mesoderm cells', *Proc Natl Acad Sci U S A* 103(5): 1313-8.

McFadden, D. G., McAnally, J., Richardson, J. A., Charite, J. and Olson, E. N. (2002) 'Misexpression of dHAND induces ectopic digits in the developing limb bud in the absence of direct DNA binding', *Development* 129(13): 3077-88.

McMahon, J. A., Takada, S., Zimmerman, L. B., Fan, C. M., Harland, R. M. and McMahon, A. P. (1998) 'Noggin-mediated antagonism of BMP signaling is required for growth and patterning of the neural tube and somite', *Genes Dev* 12(10): 1438-52.

Mercader, N., Leonardo, E., Azpiazu, N., Serrano, A., Morata, G., Martinez, C. and Torres, M. (1999) 'Conserved regulation of proximodistal limb axis development by Meis1/Hth', *Nature* 402(6760): 425-9.

Mercader, N., Leonardo, E., Piedra, M. E., Martinez, A. C., Ros, M. A. and Torres, M. (2000) 'Opposing RA and FGF signals control proximodistal vertebrate limb development through regulation of Meis genes', *Development* 127(18): 3961-70.

Mercader, N., Selleri, L., Criado, L. M., Pallares, P., Parras, C., Cleary, M. L. and Torres, M. (2009) 'Ectopic Meis1 expression in the mouse limb bud alters P-D patterning in a Pbx1-independent manner', *Int J Dev Biol* 53(8-10): 1483-94.

Merino, R., Rodriguez-Leon, J., Macias, D., Ganan, Y., Economides, A. N. and Hurle, J. M. (1999) 'The BMP antagonist Gremlin regulates outgrowth, chondrogenesis and programmed cell death in the developing limb', *Development* 126(23): 5515-22.

Mic, F. A., Sirbu, I. O. and Duester, G. (2004) 'Retinoic acid synthesis controlled by Raldh2 is required early for limb bud initiation and then later as a proximodistal signal during apical ectodermal ridge formation', *J Biol Chem* 279(25): 26698-706.

Michos, O., Panman, L., Vintersten, K., Beier, K., Zeller, R. and Zuniga, A. (2004) 'Gremlin-mediated BMP antagonism induces the epithelial-mesenchymal feedback signaling controlling metanephric kidney and limb organogenesis', *Development* 131(14): 3401-10.

Min, H., Danilenko, D. M., Scully, S. A., Bolon, B., Ring, B. D., Tarpley, J. E., DeRose, M. and Simonet, W. S. (1998) 'Fgf-10 is required for both limb and lung development and exhibits striking functional similarity to Drosophila branchless', *Genes Dev* 12(20): 3156-61.

Minguillon, C., Del Buono, J. and Logan, M. P. (2005) 'Tbx5 and Tbx4 are not sufficient to determine limb-specific morphologies but have common roles in initiating limb outgrowth', *Dev Cell* 8(1): 75-84.

Montavon, T., Le Garrec, J. F., Kerszberg, M. and Duboule, D. (2008) 'Modeling Hox gene regulation in digits: reverse collinearity and the molecular origin of thumbness', *Genes Dev* 22(3): 346-59.

Montero, J. A., Ganan, Y., Macias, D., Rodriguez-Leon, J., Sanz-Ezquerro, J. J., Merino, R., Chimal-Monroy, J., Nieto, M. A. and Hurle, J. M. (2001) 'Role of FGFs in the control of programmed cell death during limb development', *Development* 128(11): 2075-84.

Moon, A. M. and Capecchi, M. R. (2000) 'Fgf8 is required for outgrowth and patterning of the limbs', *Nat Genet* 26(4): 455-9.

Morales, A. V., Yasuda, Y. and Ish-Horowicz, D. (2002) 'Periodic Lunatic fringe expression is controlled during segmentation by a cyclic transcriptional enhancer responsive to notch signaling', *Dev Cell* 3(1): 63-74.

Morimoto, M., Takahashi, Y., Endo, M. and Saga, Y. (2005) 'The Mesp2 transcription factor establishes segmental borders by suppressing Notch activity', *Nature* 435(7040): 354-9.

Muda, M., Theodosiou, A., Rodrigues, N., Boschert, U., Camps, M., Gillieron, C., Davies, K., Ashworth, A. and Arkinstall, S. (1996) 'The dual specificity phosphatases M3/6 and MKP-3 are highly selective for inactivation of distinct mitogen-activated protein kinases', *J Biol Chem* 271(44): 27205-8.

Naiche, L. A., Holder, N. and Lewandoski, M. (2011) 'FGF4 and FGF8 comprise the wavefront activity that controls somitogenesis', *Proc Natl Acad Sci U S A* 108(10): 4018-23.

Naiche, L. A. and Papaioannou, V. E. (2003) 'Loss of Tbx4 blocks hindlimb development and affects vascularization and fusion of the allantois', *Development* 130(12): 2681-93.

Naiche, L. A. and Papaioannou, V. E. (2007) 'Tbx4 is not required for hindlimb identity or post-bud hindlimb outgrowth', *Development* 134(1): 93-103.

Nakayama, K., Satoh, T., Igari, A., Kageyama, R. and Nishida, E. (2008) 'FGF induces oscillations of Hes1 expression and Ras/ERK activation', *Curr Biol* 18(8): R332-4.

Ng, J. K., Kawakami, Y., Buscher, D., Raya, A., Itoh, T., Koth, C. M., Rodriguez Esteban, C., Rodriguez-Leon, J., Garrity, D. M., Fishman, M. C. et al. (2002) 'The limb identity gene Tbx5 promotes limb initiation by interacting with Wnt2b and Fgf10', *Development* 129(22): 5161-70.

Niederreither, K. and Dolle, P. (2008) 'Retinoic acid in development: towards an integrated view', *Nat Rev Genet* 9(7): 541-53.

Niederreither, K., Subbarayan, V., Dolle, P. and Chambon, P. (1999) 'Embryonic retinoic acid synthesis is essential for early mouse post-implantation development', *Nat Genet* 21(4): 444-8.

Niederreither, K., Vermot, J., Schuhbaur, B., Chambon, P. and Dolle, P. (2002) 'Embryonic retinoic acid synthesis is required for forelimb growth and anteroposterior patterning in the mouse', *Development* 129(15): 3563-74.

Nimmagadda, S., Geetha Loganathan, P., Huang, R., Scaal, M., Schmidt, C. and Christ, B. (2005) 'BMP4 and noggin control embryonic blood vessel formation by antagonistic regulation of VEGFR-2 (Quek1) expression', *Dev Biol* 280(1): 100-10.

Nissim, S., Allard, P., Bandyopadhyay, A., Harfe, B. D. and Tabin, C. J. (2007) 'Characterization of a novel ectodermal signaling center regulating Tbx2 and Shh in the vertebrate limb', *Dev Biol* 304(1): 9-21.

Niswander, L. (2003) 'Pattern formation: old models out on a limb', *Nat Rev Genet* 4(2): 133-43.

Niswander, L., Jeffrey, S., Martin, G. R. and Tickle, C. (1994) 'A positive feedback loop coordinates growth and patterning in the vertebrate limb', *Nature* 371(6498): 609-12.

Niswander, L., Tickle, C., Vogel, A., Booth, I. and Martin, G. R. (1993) 'FGF-4 replaces the apical ectodermal ridge and directs outgrowth and patterning of the limb', *Cell* 75(3): 579-87.

Niwa, Y., Masamizu, Y., Liu, T., Nakayama, R., Deng, C. X. and Kageyama, R. (2007) 'The initiation and propagation of Hes7 oscillation are cooperatively regulated by Fgf and notch signaling in the somite segmentation clock', *Dev Cell* 13(2): 298-304.

Niwa, Y., Shimojo, H., Isomura, A., Gonzalez, A., Miyachi, H. and Kageyama, R. (2011) 'Different types of oscillations in Notch and Fgf signaling regulate the spatiotemporal periodicity of somitogenesis', *Genes Dev* 25(11): 1115-20.

Oginuma, M., Niwa, Y., Chapman, D. L. and Saga, Y. (2008) 'Mesp2 and Tbx6 cooperatively create periodic patterns coupled with the clock machinery during mouse somitogenesis', *Development* 135(15): 2555-62.

Oginuma, M., Takahashi, Y., Kitajima, S., Kiso, M., Kanno, J., Kimura, A. and Saga, Y. (2010) 'The oscillation of Notch activation, but not its boundary, is required for somite border formation and rostral-caudal patterning within a somite', *Development* 137(9): 1515-22.

Ohuchi, H., Nakagawa, T., Yamamoto, A., Araga, A., Ohata, T., Ishimaru, Y., Yoshioka, H., Kuwana, T., Nohno, T., Yamasaki, M. et al. (1997) 'The mesenchymal factor, FGF10, initiates and maintains the outgrowth of the chick limb bud through interaction with FGF8, an apical ectodermal factor', *Development* 124(11): 2235-44.

Ohuchi, H., Takeuchi, J., Yoshioka, H., Ishimaru, Y., Ogura, K., Takahashi, N., Ogura, T. and Noji, S. (1998) 'Correlation of wing-leg identity in ectopic FGF-induced chimeric limbs with the differential expression of chick Tbx5 and Tbx4', *Development* 125(1): 51-60.

Olivera-Martinez, I. and Storey, K. G. (2007) 'Wnt signals provide a timing mechanism for the FGF-retinoid differentiation switch during vertebrate body axis extension', *Development* 134(11): 2125-35.

Ornitz, D. M. (2000) 'FGFs, heparan sulfate and FGFRs: complex interactions essential for development', *Bioessays* 22(2): 108-12.

Ornitz, D. M., Xu, J., Colvin, J. S., McEwen, D. G., MacArthur, C. A., Coulier, F., Gao, G. and Goldfarb, M. (1996) 'Receptor specificity of the fibroblast growth factor family', *J Biol Chem* 271(25): 15292-7.

Orr-Urtreger, A., Bedford, M. T., Burakova, T., Arman, E., Zimmer, Y., Yayon, A., Givol, D. and Lonai, P. (1993) 'Developmental localization of the splicing alternatives of fibroblast growth factor receptor-2 (FGFR2)', *Dev Biol* 158(2): 475-86.

Orr-Urtreger, A., Givol, D., Yayon, A., Yarden, Y. and Lonai, P. (1991) 'Developmental expression of two murine fibroblast growth factor receptors, flg and bek', *Development* 113(4): 1419-34.

Ovchinnikov, D. A., Selever, J., Wang, Y., Chen, Y. T., Mishina, Y., Martin, J. F. and Behringer, R. R. (2006) 'BMP receptor type IA in limb bud mesenchyme regulates distal outgrowth and patterning', *Dev Biol* 295(1): 103-15.

Ozbudak, E. M. and Lewis, J. (2008) 'Notch signalling synchronizes the zebrafish segmentation clock but is not needed to create somite boundaries', *PLoS Genet* 4(2): e15.

Packard, D. S., Jr. (1978) 'Chick somite determination: the role of factors in young somites and the segmental plate', *J Exp Zool* 203(2): 295-306.

Pajni-Underwood, S., Wilson, C. P., Elder, C., Mishina, Y. and Lewandoski, M. (2007) 'BMP signals control limb bud interdigital programmed cell death by regulating FGF signaling', *Development* 134(12): 2359-68.

Palmeirim, I., Dubrulle, J., Henrique, D., Ish-Horowicz, D. and Pourquie, O. (1998) 'Uncoupling segmentation and somitogenesis in the chick presomitic mesoderm', *Dev Genet* 23(1): 77-85.

Palmeirim, I., Henrique, D., Ish-Horowicz, D. and Pourquie, O. (1997) 'Avian hairy gene expression identifies a molecular clock linked to vertebrate segmentation and somitogenesis', *Cell* 91(5): 639-48.

Park, H. L., Bai, C., Platt, K. A., Matise, M. P., Beeghly, A., Hui, C. C., Nakashima, M. and Joyner, A. L. (2000) 'Mouse Gli1 mutants are viable but have defects in SHH signaling in combination with a Gli2 mutation', *Development* 127(8): 1593-605.

Parr, B. A. and McMahon, A. P. (1995) 'Dorsalizing signal Wnt-7a required for normal polarity of D-V and A-P axes of mouse limb', *Nature* 374(6520): 350-3.

Partanen, J., Schwartz, L. and Rossant, J. (1998) 'Opposite phenotypes of hypomorphic and Y766 phosphorylation site mutations reveal a function for Fgfr1 in anteroposterior patterning of mouse embryos', *Genes Dev* 12(15): 2332-44.

Pascoal, S., Andrade, R. P., Bajanca, F. and Palmeirim, I. (2007a) 'Progressive mRNA decay establishes an mkp3 expression gradient in the chick limb bud', *Biochem Biophys Res Commun* 352(1): 153-7.

Pascoal, S., Carvalho, C. R., Rodriguez-Leon, J., Delfini, M. C., Duprez, D., Thorsteinsdottir, S. and Palmeirim, I. (2007b) 'A molecular clock operates during chick autopod proximal-distal outgrowth', *J Mol Biol* 368(2): 303-9.

Pascoal, S. and Palmeirim, I. (2007) 'Watch-ing out for chick limb development', *Integr Comp Biol* 47(3): 382-9.

Patstone, G., Pasquale, E. B. and Maher, P. A. (1993) 'Different members of the fibroblast growth factor receptor family are specific to distinct cell types in the developing chicken embryo', *Dev Biol* 155(1): 107-23.

Pautou, M. P. (1978) 'Cessation of activity of the apical ectodermic crest during morphogenesis of the acropod in the chick embryo. Histological analysis', *Arch Biol (Liege)* 89(1): 27-66.

Pearse, R. V., 2nd, Scherz, P. J., Campbell, J. K. and Tabin, C. J. (2007) 'A cellular lineage analysis of the chick limb bud', *Dev Biol* 310(2): 388-400.

Perantoni, A. O., Timofeeva, O., Naillat, F., Richman, C., Pajni-Underwood, S., Wilson, C., Vainio, S., Dove, L. F. and Lewandoski, M. (2005) 'Inactivation of FGF8 in early mesoderm reveals an essential role in kidney development', *Development* 132(17): 3859-71.

Pizette, S., Abate-Shen, C. and Niswander, L. (2001) 'BMP controls proximodistal outgrowth, via induction of the apical ectodermal ridge, and dorsoventral patterning in the vertebrate limb', *Development* 128(22): 4463-74.

Pizette, S. and Niswander, L. (1999) 'BMPs negatively regulate structure and function of the limb apical ectodermal ridge', *Development* 126(5): 883-94.

Pourquie, O. and Tam, P. P. (2001) 'A nomenclature for prospective somites and phases of cyclic gene expression in the presomitic mesoderm', *Dev Cell* 1(5): 619-20.

Power, S. C., Lancman, J. and Smith, S. M. (1999) 'Retinoic acid is essential for Shh/Hoxd signaling during rat limb outgrowth but not for limb initiation', *Dev Dyn* 216(4-5): 469-80.

Probst, S., Kraemer, C., Demougin, P., Sheth, R., Martin, G. R., Shiratori, H., Hamada, H., Iber, D., Zeller, R. and Zuniga, A. (2011) 'SHH propagates distal limb bud development by enhancing CYP26B1-mediated retinoic acid clearance via AER-FGF signalling', *Development* 138(10): 1913-23.

Rallis, C., Bruneau, B. G., Del Buono, J., Seidman, C. E., Seidman, J. G., Nissim, S., Tabin, C. J. and Logan, M. P. (2003) 'Tbx5 is required for forelimb bud formation and continued outgrowth', *Development* 130(12): 2741-51.

Raya, A. and Izpisua Belmonte, J. C. (2006) 'Left-right asymmetry in the vertebrate embryo: from early information to higher-level integration', *Nat Rev Genet* 7(4): 283-93.

Reijntjes, S., Gale, E. and Maden, M. (2003) 'Expression of the retinoic acid catabolising enzyme CYP26B1 in the chick embryo and its regulation by retinoic acid', *Gene Expr Patterns* 3(5): 621-7.

Resende, T. P., Ferreira, M., Teillet, M. A., Tavares, A. T., Andrade, R. P. and Palmeirim, I. (2010) 'Sonic hedgehog in temporal control of somite formation', *Proc Natl Acad Sci U S A* 107(29): 12907-12.

Revest, J. M., Spencer-Dene, B., Kerr, K., De Moerlooze, L., Rosewell, I. and Dickson, C. (2001) 'Fibroblast growth factor receptor 2-IIIb acts upstream of Shh and Fgf4 and is required for limb bud maintenance but not for the induction of Fgf8, Fgf10, Msx1, or Bmp4', *Dev Biol* 231(1): 47-62.

Ribes, V., Le Roux, I., Rhinn, M., Schuhbaur, B. and Dolle, P. (2009) 'Early mouse caudal development relies on crosstalk between retinoic acid, Shh and Fgf signalling pathways', *Development* 136(4): 665-76.

Rida, P. C., Le Minh, N. and Jiang, Y. J. (2004) 'A Notch feeling of somite segmentation and beyond', *Dev Biol* 265(1): 2-22.

Riddle, R. D., Ensini, M., Nelson, C., Tsuchida, T., Jessell, T. M. and Tabin, C. (1995) 'Induction of the LIM homeobox gene Lmx1 by WNT7a establishes dorsoventral pattern in the vertebrate limb', *Cell* 83(4): 631-40.

Riddle, R. D., Johnson, R. L., Laufer, E. and Tabin, C. (1993) 'Sonic hedgehog mediates the polarizing activity of the ZPA', *Cell* 75(7): 1401-16.

Riedel-Kruse, I. H., Muller, C. and Oates, A. C. (2007) 'Synchrony dynamics during initiation, failure, and rescue of the segmentation clock', *Science* 317(5846): 1911-5.

Rifes, P., Carvalho, L., Lopes, C., Andrade, R. P., Rodrigues, G., Palmeirim, I. and Thorsteinsdottir, S. (2007) 'Redefining the role of ectoderm in somitogenesis: a player in the formation of the fibronectin matrix of presomitic mesoderm', *Development* 134(17): 3155-65.

Robert, B. (2007) 'Bone morphogenetic protein signaling in limb outgrowth and patterning', *Dev Growth Differ* 49(6): 455-68.

Rodrigues, S., Santos, J. and Palmeirim, I. (2006) 'Molecular characterization of the rostral-most somites in early somitic stages of the chick embryo', *Gene Expr Patterns* 6(7): 673-7.

Rodriguez-Esteban, C., Schwabe, J. W., De La Pena, J., Foys, B., Eshelman, B. and Izpisua Belmonte, J. C. (1997) 'Radical fringe positions the apical ectodermal ridge at the dorsoventral boundary of the vertebrate limb', *Nature* 386(6623): 360-6.

Rodriguez-Esteban, C., Tsukui, T., Yonei, S., Magallon, J., Tamura, K. and Izpisua Belmonte, J. C. (1999) 'The T-box genes Tbx4 and Tbx5 regulate limb outgrowth and identity', *Nature* 398(6730): 814-8.

Rodriguez-Leon, J., Merino, R., Macias, D., Ganan, Y., Santesteban, E. and Hurle, J. M. (1999) 'Retinoic acid regulates programmed cell death through BMP signalling', *Nat Cell Biol* 1(2): 125-6.

Ros, M. A., Dahn, R. D., Fernandez-Teran, M., Rashka, K., Caruccio, N. C., Hasso, S. M., Bitgood, J. J., Lancman, J. J. and Fallon, J. F. (2003) 'The chick oligozeugodactyly (ozd) mutant lacks sonic hedgehog function in the limb', *Development* 130(3): 527-37.

Rosello-Diez, A., Ros, M. A. and Torres, M. (2011) 'Diffusible signals, not autonomous mechanisms, determine the main proximodistal limb subdivision', *Science* 332(6033): 1086-8.

Rossant, J., Zirngibl, R., Cado, D., Shago, M. and Giguere, V. (1991) 'Expression of a retinoic acid response element-hsplacZ transgene defines specific domains of transcriptional activity during mouse embryogenesis', *Genes Dev* 5(8): 1333-44.

Rubin, L. and Saunders, J. W., Jr. (1972) 'Ectodermal-mesodermal interactions in the growth of limb buds in the chick embryo: constancy and temporal limits of the ectodermal induction', *Dev Biol* 28(1): 94-112.

Saga, Y. and Takeda, H. (2001) 'The making of the somite: molecular events in vertebrate segmentation', *Nat Rev Genet* 2(11): 835-45.

Saito, D., Yonei-Tamura, S., Kano, K., Ide, H. and Tamura, K. (2002) 'Specification and determination of limb identity: evidence for inhibitory regulation of Tbx gene expression', *Development* 129(1): 211-20.

Sakai, Y., Meno, C., Fujii, H., Nishino, J., Shiratori, H., Saijoh, Y., Rossant, J. and Hamada, H. (2001) 'The retinoic acid-inactivating enzyme CYP26 is essential for establishing an uneven distribution of retinoic acid along the anterio-posterior axis within the mouse embryo', *Genes Dev* 15(2): 213-25.

Sanalkumar, R., Indulekha, C. L., Divya, T. S., Divya, M. S., Anto, R. J., Vinod, B., Vidyanand, S., Jagatha, B., Venugopal, S. and James, J. (2010) 'ATF2 maintains a subset of neural progenitors through CBF1/Notch independent Hes-1 expression and synergistically activates the expression of Hes-1 in Notch-dependent neural progenitors', *J Neurochem* 113(4): 807-18.

Sanz-Ezquerro, J. J. and Tickle, C. (2000) 'Autoregulation of Shh expression and Shh induction of cell death suggest a mechanism for modulating polarising activity during chick limb development', *Development* 127(22): 4811-23.

Sanz-Ezquerro, J. J. and Tickle, C. (2003) 'Fgf signaling controls the number of phalanges and tip formation in developing digits', *Curr Biol* 13(20): 1830-6.

Sasai, Y., Kageyama, R., Tagawa, Y., Shigemoto, R. and Nakanishi, S. (1992) 'Two mammalian helix-loop-helix factors structurally related to Drosophila hairy and Enhancer of split', *Genes Dev* 6(12B): 2620-34.

Sato, K., Koizumi, Y., Takahashi, M., Kuroiwa, A. and Tamura, K. (2007) 'Specification of cell fate along the proximal-distal axis in the developing chick limb bud', *Development* 134(7): 1397-406.

Saunders, J. (1948) 'The proximo-distal sequence of the origin of the parts of the chick wing and the role of the ectoderm', *Journal of Experimental Zoology* 108: 363-403.

Saunders, J. W. and and Gasseling, M. T. (1968) 'Epithelial-Mesenchymal Interactions', *(eds Fleischmajer, R. and Billingham, R. E.), Williams and Wilkins, Baltimore*: 78-97.

Sawada, A., Shinya, M., Jiang, Y. J., Kawakami, A., Kuroiwa, A. and Takeda, H. (2001) 'Fgf/MAPK signalling is a crucial positional cue in somite boundary formation', *Development* 128(23): 4873-80.

Scherz, P. J., Harfe, B. D., McMahon, A. P. and Tabin, C. J. (2004) 'The limb bud Shh-Fgf feedback loop is terminated by expansion of former ZPA cells', *Science* 305(5682): 396-9.

Scherz, P. J., McGlinn, E., Nissim, S. and Tabin, C. J. (2007) 'Extended exposure to Sonic hedgehog is required for patterning the posterior digits of the vertebrate limb', *Dev Biol* 308(2): 343-54.

Schmidt, M., Patterson, M., Farrell, E. and Munsterberg, A. (2004) 'Dynamic expression of Lef/Tcf family members and beta-catenin during chick gastrulation, neurulation, and early limb development', *Dev Dyn* 229(3): 703-7.

Schoenwolf, G. C., Garcia-Martinez, V. and Dias, M. S. (1992) 'Mesoderm movement and fate during avian gastrulation and neurulation', *Dev Dyn* 193(3): 235-48.

Schweitzer, R., Vogan, K. J. and Tabin, C. J. (2000) 'Similar expression and regulation of Gli2 and Gli3 in the chick limb bud', *Mech Dev* 98(1-2): 171-4.

Searls, R. L. and Janners, M. Y. (1971) 'The initiation of limb bud outgrowth in the embryonic chick', *Dev Biol* 24(2): 198-213.

Sekine, K., Ohuchi, H., Fujiwara, M., Yamasaki, M., Yoshizawa, T., Sato, T., Yagishita, N., Matsui, D., Koga, Y., Itoh, N. et al. (1999) 'Fgf10 is essential for limb and lung formation', *Nat Genet* 21(1): 138-41.

Selever, J., Liu, W., Lu, M. F., Behringer, R. R. and Martin, J. F. (2004) 'Bmp4 in limb bud mesoderm regulates digit pattern by controlling AER development', *Dev Biol* 276(2): 268-79.

Selleck, M. A. and Stern, C. D. (1991) 'Fate mapping and cell lineage analysis of Hensen's node in the chick embryo', *Development* 112(2): 615-26.

Serth, K., Schuster-Gossler, K., Cordes, R. and Gossler, A. (2003) 'Transcriptional oscillation of lunatic fringe is essential for somitogenesis', *Genes Dev* 17(7): 912-25.

Sewell, W., Sparrow, D. B., Smith, A. J., Gonzalez, D. M., Rappaport, E. F., Dunwoodie, S. L. and Kusumi, K. (2009) 'Cyclical expression of the Notch/Wnt regulator Nrarp requires modulation by Dll3 in somitogenesis', *Dev Biol* 329(2): 400-9.

Sheeba, C. J., Andrade, R. P., Duprez, D. and Palmeirim, I. (2010) 'Comprehensive analysis of fibroblast growth factor receptor expression patterns during chick forelimb development', *Int J Dev Biol* 54(10): 1517-26.

Sheldahl, L. C., Park, M., Malbon, C. C. and Moon, R. T. (1999) 'Protein kinase C is differentially stimulated by Wnt and Frizzled homologs in a G-protein-dependent manner', *Curr Biol* 9(13): 695-8.

Sheng, N., Xie, Z., Wang, C., Bai, G., Zhang, K., Zhu, Q., Song, J., Guillemot, F., Chen, Y. G., Lin, A. et al. (2010) 'Retinoic acid regulates bone morphogenic protein signal duration by promoting the degradation of phosphorylated Smad1', *Proc Natl Acad Sci U S A* 107(44): 18886-91.

Shifley, E. T., Vanhorn, K. M., Perez-Balaguer, A., Franklin, J. D., Weinstein, M. and Cole, S. E. (2008) 'Oscillatory lunatic fringe activity is crucial for segmentation of the anterior but not posterior skeleton', *Development* 135(5): 899-908.

Shimojo, H., Ohtsuka, T. and Kageyama, R. (2008) 'Oscillations in notch signaling regulate maintenance of neural progenitors', *Neuron* 58(1): 52-64.

Shubin, N., Tabin, C. and Carroll, S. (1997) 'Fossils, genes and the evolution of animal limbs', *Nature* 388(6643): 639-48.

Skipper, M. (2004) 'Time for segmentation. Nature milestones in development', *Milestone 24.Nat Rev Neurosci* 5(Suppl): S18.

Smith, J. C. (1980) 'The time required for positional signalling in the chick wing bud', *J Embryol Exp Morphol* 60: 321-8.

Soshnikova, N., Zechner, D., Huelsken, J., Mishina, Y., Behringer, R. R., Taketo, M. M., Crenshaw, E. B., 3rd and Birchmeier, W. (2003) 'Genetic interaction between Wnt/beta-catenin and BMP receptor signaling during formation of the AER and the dorsal-ventral axis in the limb', *Genes Dev* 17(16): 1963-8.

Stephens, T. D. and McNulty, T. R. (1981) 'Evidence for a metameric pattern in the development of the chick humerus', *J Embryol Exp Morphol* 61: 191-205.

Stockhausen, M. T., Sjolund, J. and Axelson, H. (2005) 'Regulation of the Notch target gene Hes-1 by TGFalpha induced Ras/MAPK signaling in human neuroblastoma cells', *Exp Cell Res* 310(1): 218-28.

Stratford, T., Horton, C. and Maden, M. (1996) 'Retinoic acid is required for the initiation of outgrowth in the chick limb bud', *Curr Biol* 6(9): 1124-33.

Stratford, T., Logan, C., Zile, M. and Maden, M. (1999) 'Abnormal anteroposterior and dorsoventral patterning of the limb bud in the absence of retinoids', *Mech Dev* 81(1-2): 115-25.

Strecker, T. R. and Stephens, T. D. (1983) 'Peripheral nerves do not play a trophic role in limb skeletal morphogenesis', *Teratology* 27(2): 159-67.

Suemori, H. and Noguchi, S. (2000) 'Hox C cluster genes are dispensable for overall body plan of mouse embryonic development', *Dev Biol* 220(2): 333-42.

Summerbell, D., Lewis, J. H. and Wolpert, L. (1973) 'Positional information in chick limb morphogenesis', *Nature* 244(5417): 492-6.

Sun, X., Lewandoski, M., Meyers, E. N., Liu, Y. H., Maxson, R. E., Jr. and Martin, G. R. (2000) 'Conditional inactivation of Fgf4 reveals complexity of signalling during limb bud development', *Nat Genet* 25(1): 83-6.

Sun, X., Mariani, F. V. and Martin, G. R. (2002) 'Functions of FGF signalling from the apical ectodermal ridge in limb development', *Nature* 418(6897): 501-8.

Sun, X., Meyers, E. N., Lewandoski, M. and Martin, G. R. (1999) 'Targeted disruption of Fgf8 causes failure of cell migration in the gastrulating mouse embryo', *Genes Dev* 13(14): 1834-46.

Suzuki, T., Hasso, S. M. and Fallon, J. F. (2008) 'Unique SMAD1/5/8 activity at the phalanx-forming region determines digit identity', *Proc Natl Acad Sci U S A* 105(11): 4185-90.

Swindell, E. C., Thaller, C., Sockanathan, S., Petkovich, M., Jessell, T. M. and Eichele, G. (1999) 'Complementary domains of retinoic acid production and degradation in the early chick embryo', *Dev Biol* 216(1): 282-96.

Szebenyi, G., Savage, M. P., Olwin, B. B. and Fallon, J. F. (1995) 'Changes in the expression of fibroblast growth factor receptors mark distinct stages of chondrogenesis in vitro and during chick limb skeletal patterning', *Dev Dyn* 204(4): 446-56.

Tabin, C. and Wolpert, L. (2007) 'Rethinking the proximodistal axis of the vertebrate limb in the molecular era', *Genes Dev* 21(12): 1433-42.

Takebayashi, K., Sasai, Y., Watanabe, T., Nakanishi, S. and Kageyama, R. (1994) 'Structure, chromosomal locus, and promoter analysis of the mouse gene encoding the mouse helix-loop-helix factor HES-1: negative autoregulation through the multiple N box elements.', *J Biol Chem* 270: 1342-1349.

Takeuchi, J. K., Koshiba-Takeuchi, K., Matsumoto, K., Vogel-Hopker, A., Naitoh-Matsuo, M., Ogura, K., Takahashi, N., Yasuda, K. and Ogura, T. (1999) 'Tbx5 and Tbx4 genes determine the wing/leg identity of limb buds', *Nature* 398(6730): 810-4.

Takeuchi, J. K., Koshiba-Takeuchi, K., Suzuki, T., Kamimura, M., Ogura, K. and Ogura, T. (2003) 'Tbx5 and Tbx4 trigger limb initiation through activation of the Wnt/Fgf signaling cascade', *Development* 130(12): 2729-39.

Tam, P. P. (1981) 'The control of somitogenesis in mouse embryos', *J Embryol Exp Morphol* 65 Suppl: 103-28.

Tarchini, B., Duboule, D. and Kmita, M. (2006) 'Regulatory constraints in the evolution of the tetrapod limb anterior-posterior polarity', *Nature* 443(7114): 985-8.

Tavares, A. T., Izpisuja-Belmonte, J. C. and Rodriguez-Leon, J. (2001) 'Developmental expression of chick twist and its regulation during limb patterning', *Int J Dev Biol* 45(5-6): 707-13.

te Welscher, P., Fernandez-Teran, M., Ros, M. A. and Zeller, R. (2002) 'Mutual genetic antagonism involving GLI3 and dHAND prepatterns the vertebrate limb bud mesenchyme prior to SHH signaling', *Genes Dev* 16(4): 421-6.

Teillet, M. A., Lapointe, F. and Le Douarin, N. M. (1998) 'The relationships between notochord and floor plate in vertebrate development revisited', *Proc Natl Acad Sci U S A* 95(20): 11733-8.

ten Berge, D., Brugmann, S. A., Helms, J. A. and Nusse, R. (2008) 'Wnt and FGF signals interact to coordinate growth with cell fate specification during limb development', *Development* 135(19): 3247-57.

Tenin, G., Wright, D., Ferjentsik, Z., Bone, R., McGrew, M. J. and Maroto, M. (2010) 'The chick somitogenesis oscillator is arrested before all paraxial mesoderm is segmented into somites', *BMC Dev Biol* 10: 24.

Theil, T., Kaesler, S., Grotewold, L., Bose, J. and Ruther, U. (1999) 'Gli genes and limb development', *Cell Tissue Res* 296(1): 75-83.

Thompson, D. L., Gerlach-Bank, L. M., Barald, K. F. and Koenig, R. J. (2003) 'Retinoic acid repression of bone morphogenetic protein 4 in inner ear development', *Mol Cell Biol* 23(7): 2277-86.

Tickle, C. (1981) 'The number of polarizing region cells required to specify additional digits in the developing chick wing', *Nature* 289(5795): 295-8.

Tickle, C. (2002) 'The early history of the polarizing region: from classical embryology to molecular biology', *Int J Dev Biol* 46(7): 847-52.

Tickle, C. (2003) 'Patterning systems--from one end of the limb to the other', *Dev Cell* 4(4): 449-58.

Tickle, C., Lee, J. and Eichele, G. (1985) 'A quantitative analysis of the effect of all-trans-retinoic acid on the pattern of chick wing development', *Dev Biol* 109(1): 82-95.

Tonegawa, A. and Takahashi, Y. (1998) 'Somitogenesis controlled by Noggin', *Dev Biol* 202(2): 172-82.

Towers, M., Mahood, R., Yin, Y. and Tickle, C. (2008) 'Integration of growth and specification in chick wing digit-patterning', *Nature* 452(7189): 882-6.

Towers, M. and Tickle, C. (2009) 'Growing models of vertebrate limb development', *Development* 136(2): 179-90.

Tumpel, S., Sanz-Ezquerro, J. J., Isaac, A., Eblaghie, M. C., Dobson, J. and Tickle, C. (2002) 'Regulation of Tbx3 expression by anteroposterior signalling in vertebrate limb development', *Dev Biol* 250(2): 251-62.

Turnpenny, P. D., Alman, B., Cornier, A. S., Giampietro, P. F., Offiah, A., Tassy, O., Pourquie, O., Kusumi, K. and Dunwoodie, S. (2007) 'Abnormal vertebral segmentation and the notch signaling pathway in man', *Dev Dyn* 236(6): 1456-74.

Vargesson, N., Clarke, J. D., Vincent, K., Coles, C., Wolpert, L. and Tickle, C. (1997) 'Cell fate in the chick limb bud and relationship to gene expression', *Development* 124(10): 1909-18.

Varjosalo, M. and Taipale, J. (2008) 'Hedgehog: functions and mechanisms', *Genes Dev* 22(18): 2454-72.

Vasiliauskas, D., Laufer, E. and Stern, C. D. (2003) 'A role for hairy1 in regulating chick limb bud growth', *Dev Biol* 262(1): 94-106.

Vasiliauskas, D. and Stern, C. D. (2001) 'Patterning the embryonic axis: FGF signaling and how vertebrate embryos measure time', *Cell* 106(2): 133-6.

Verheyden, J. M., Lewandoski, M., Deng, C., Harfe, B. D. and Sun, X. (2005) 'Conditional inactivation of Fgfr1 in mouse defines its role in limb bud establishment, outgrowth and digit patterning', *Development* 132(19): 4235-45.

Verheyden, J. M. and Sun, X. (2008) 'An Fgf/Gremlin inhibitory feedback loop triggers termination of limb bud outgrowth', *Nature* 454(7204): 638-41.

Vogel, A., Rodriguez, C. and Izpisua-Belmonte, J. C. (1996) 'Involvement of FGF-8 in initiation, outgrowth and patterning of the vertebrate limb', *Development* 122(6): 1737-50.

Vogel, A., Rodriguez, C., Warnken, W. and Izpisua Belmonte, J. C. (1995) 'Dorsal cell fate specified by chick Lmx1 during vertebrate limb development', *Nature* 378(6558): 716-20.

Wahl, M. B., Deng, C., Lewandoski, M. and Pourquie, O. (2007) 'FGF signaling acts upstream of the NOTCH and WNT signaling pathways to control segmentation clock oscillations in mouse somitogenesis', *Development* 134(22): 4033-41.

Wall, D. S., Mears, A. J., McNeill, B., Mazerolle, C., Thurig, S., Wang, Y., Kageyama, R. and Wallace, V. A. (2009) 'Progenitor cell proliferation in the retina is dependent on Notch-independent Sonic hedgehog/Hes1 activity', *J Cell Biol* 184(1): 101-12.

Wanek, N., Muneoka, K., Holler-Dinsmore, G., Burton, R. and Bryant, S. V. (1989) 'A staging system for mouse limb development', *J Exp Zool* 249(1): 41-9.

Wang, B., Fallon, J. F. and Beachy, P. A. (2000) 'Hedgehog-regulated processing of Gli3 produces an anterior/posterior repressor gradient in the developing vertebrate limb', *Cell* 100(4): 423-34.

Wang, C., Ruther, U. and Wang, B. (2007) 'The Shh-independent activator function of the full-length Gli3 protein and its role in vertebrate limb digit patterning', *Dev Biol* 305(2): 460-9.

William, D. A., Saitta, B., Gibson, J. D., Traas, J., Markov, V., Gonzalez, D. M., Sewell, W., Anderson, D. M., Pratt, S. C., Rappaport, E. F. et al. (2007) 'Identification of oscillatory genes in somitogenesis from functional genomic analysis of a human mesenchymal stem cell model', *Dev Biol* 305(1): 172-86.

Wolpert, L. (1969) 'Positional information and the spatial pattern of cellular differentiation', *J Theor Biol* 25(1): 1-47.

Wolpert, L., Tickle, C. and Sampford, M. (1979) 'The effect of cell killing by x-irradiation on pattern formation in the chick limb', *J Embryol Exp Morphol* 50: 175-93.

Wright, D., Ferjentsik, Z., Chong, S. W., Qiu, X., Jiang, Y. J., Malapert, P., Pourquie, O., Van Hateren, N., Wilson, S. A., Franco, C. et al. (2009) 'Cyclic Nrarp mRNA expression is regulated by the somitic oscillator but Nrarp protein levels do not oscillate', *Dev Dyn* 238(12): 3043-55.

Xu, B. and Wellik, D. M. (2011) 'Axial Hox9 activity establishes the posterior field in the developing forelimb', *Proc Natl Acad Sci U S A* 108(12): 4888-91.

Xu, J., Liu, Z. and Ornitz, D. M. (2000) 'Temporal and spatial gradients of Fgf8 and Fgf17 regulate proliferation and differentiation of midline cerebellar structures', *Development* 127(9): 1833-43.

Xu, X., Weinstein, M., Li, C. and Deng, C. (1999) 'Fibroblast growth factor receptors (FGFRs) and their roles in limb development', *Cell Tissue Res* 296(1): 33-43.

Xu, X., Weinstein, M., Li, C., Naski, M., Cohen, R. I., Ornitz, D. M., Leder, P. and Deng, C. (1998) 'Fibroblast growth factor receptor 2 (FGFR2)-mediated reciprocal regulation loop between FGF8 and FGF10 is essential for limb induction', *Development* 125(4): 753-65.

Yamaji, N., Celeste, A. J., Thies, R. S., Song, J. J., Bernier, S. M., Goltzman, D., Lyons, K. M., Nove, J., Rosen, V. and Wozney, J. M. (1994) 'A mammalian serine/threonine kinase receptor specifically binds BMP-2 and BMP-4', *Biochem Biophys Res Commun* 205(3): 1944-51.

Yang, X., Dormann, D., Munsterberg, A. E. and Weijer, C. J. (2002) 'Cell movement patterns during gastrulation in the chick are controlled by positive and negative chemotaxis mediated by FGF4 and FGF8', *Dev Cell* 3(3): 425-37.

Yang, Y., Drossopoulou, G., Chuang, P. T., Duprez, D., Marti, E., Bumcrot, D., Vargesson, N., Clarke, J., Niswander, L., McMahon, A. et al. (1997) 'Relationship between dose, distance and time in Sonic Hedgehog-mediated regulation of anteroposterior polarity in the chick limb', *Development* 124(21): 4393-404.

Yang, Y. and Niswander, L. (1995) 'Interaction between the signaling molecules WNT7a and SHH during vertebrate limb development: dorsal signals regulate anteroposterior patterning', *Cell* 80(6): 939-47.

Yashiro, K., Zhao, X., Uehara, M., Yamashita, K., Nishijima, M., Nishino, J., Saijoh, Y., Sakai, Y. and Hamada, H. (2004) 'Regulation of retinoic acid distribution is required for proximodistal patterning and outgrowth of the developing mouse limb', *Dev Cell* 6(3): 411-22.

Yi, S. E., Daluiski, A., Pederson, R., Rosen, V. and Lyons, K. M. (2000) 'The type I BMP receptor BMPRIB is required for chondrogenesis in the mouse limb', *Development* 127(3): 621-30.

Yokoyama, S. and Asahara, H. (2011) 'The myogenic transcriptional network', *Cell Mol Life Sci* 68(11): 1843-9.

Yoshiura, S., Ohtsuka, T., Takenaka, Y., Nagahara, H., Yoshikawa, K. and Kageyama, R. (2007) 'Ultradian oscillations of Stat, Smad, and Hes1 expression in response to serum', *Proc Natl Acad Sci U S A* 104(27): 11292-7.

Yu, K. and Ornitz, D. M. (2008) 'FGF signaling regulates mesenchymal differentiation and skeletal patterning along the limb bud proximodistal axis', *Development* 135(3): 483-91.

Zanotti, S., Smerdel-Ramoya, A. and Canalis, E. (2011) 'HES1 (hairy and enhancer of split 1) is a determinant of bone mass', *J Biol Chem* 286(4): 2648-57.

Zeller, R., Lopez-Rios, J. and Zuniga, A. (2009) 'Vertebrate limb bud development: moving towards integrative analysis of organogenesis', *Nat Rev Genet* 10(12): 845-58.

Zhang, N. and Gridley, T. (1998) 'Defects in somite formation in lunatic fringe-deficient mice', *Nature* 394(6691): 374-7.

Zhang, X., Ibrahimi, O. A., Olsen, S. K., Umemori, H., Mohammadi, M. and Ornitz, D. M. (2006) 'Receptor specificity of the fibroblast growth factor family. The complete mammalian FGF family', *J Biol Chem* 281(23): 15694-700.

Zhao, X., Sirbu, I. O., Mic, F. A., Molotkova, N., Molotkov, A., Kumar, S. and Duester, G. (2009) 'Retinoic acid promotes limb induction through effects on body axis extension but is unnecessary for limb patterning', *Curr Biol* 19(12): 1050-7.

Zhou, J. and Kochhar, D. M. (2004) 'Cellular anomalies underlying retinoid-induced phocomelia', *Reprod Toxicol* 19(1): 103-10.

Zhu, J., Nakamura, E., Nguyen, M. T., Bao, X., Akiyama, H. and Mackem, S. (2008) 'Uncoupling Sonic hedgehog control of pattern and expansion of the developing limb bud', *Dev Cell* 14(4): 624-32.

Zou, H. and Niswander, L. (1996) 'Requirement for BMP signaling in interdigital apoptosis and scale formation', *Science* 272(5262): 738-41.

Zuniga, A., Haramis, A. P., McMahon, A. P. and Zeller, R. (1999) 'Signal relay by BMP antagonism controls the SHH/FGF4 feedback loop in vertebrate limb buds', *Nature* 401(6753): 598-602.

Zuniga, A. and Zeller, R. (1999) 'Gli3 (Xt) and formin (ld) participate in the positioning of the polarising region and control of posterior limb-bud identity', *Development* 126(1): 13-21.

Zwilling, E. (1955) 'Ectoderm-mesoderm relationship in the development of the chick embryo limb bud', *J. Exp. Zool.* 128 423-441.